

The Cell Cycle and DNA Damage-dependent Regulation of Cdt1 in *Schizosaccharomyces pombe*

Marianne E. A. Shepherd

Department of Zoology

Hertford College

University of Oxford

A thesis presented for the degree of Doctor of Philosophy

Trinity Term 2012

Abstract

The Cell Cycle and DNA Damage-dependent Regulation of Cdt1 in *Schizosaccharomyces pombe*

Marianne E. A. Shepherd
Department of Zoology, Hertford College, University of Oxford
A thesis submitted for the degree of Doctor of Philosophy
Trinity Term 2012

Cdt1 is a conserved and essential eukaryotic protein that is required for the licensing step of DNA replication. In order to control replication licensing and ensure a single round of DNA replication occurs per cell cycle, Cdt1 is subject to strict regulation. In Metazoa and *S. pombe*, Cdt1 is targeted for ubiquitylation and proteolysis in S phase and after DNA damage by the $CRL4^{Cdt2}$ ubiquitin ligase. $CRL4^{Cdt2}$ is activated in Metazoa by an unusual mechanism that requires an interaction between the substrate and chromatin-loaded proliferating cell nuclear antigen (PCNA).

This study addressed the involvement of PCNA in *S. pombe* Cdt1 proteolysis. A mutational analysis was undertaken to establish whether the Cdt1-PCNA interaction is conserved in *S. pombe* and the extent to which it regulates $CRL4^{Cdt2}$-dependent turnover of the protein. *S. pombe* Cdt1 was shown to interact with PCNA *in vivo* and two variant PCNA-interacting peptide (PIP) motifs were identified in the protein. The two motifs function near-redundantly to promote both the Cdt1-PCNA interaction and the $CRL4^{Cdt2}$-dependent proteolysis of Cdt1 in S phase and after DNA damage. The mutational analysis also resulted in the characterisation of two in-frame AUG codons in the $cdt1^{+}$ reading frame. The second in-frame AUG codon was shown to be the principal initiator codon and was required to maintain wildtype Cdt1 protein levels and cell viability.

$CRL4^{Cdt2}$ is emerging as an important regulator of proteins that are involved in the control of cell cycle progression and the maintenance of genome stability. However, there are a number of outstanding questions regarding the mechanism and regulation of $CRL4^{Cdt2}$. In order to address these questions, a genomics approach was taken to identify novel genes involved in Cdt1 regulation. A screen of non-essential *S. pombe* genes identified 17 candidate genes that, when inactivated, caused up-regulation of Cdt1. Unexpectedly, deletion of genes involved in homologous recombination resulted in a Rad3-dependent up-regulation of Cdt1. Further work is required to establish the biological significance of this finding.

Acknowledgements

I would like to thank my supervisor, Dr Stephen Kearsey, for giving me the opportunity to work in his lab and for his support, guidance and expertise throughout my DPhil. Thanks also go to past and present members of the Kearsey lab, in particular to Chen Chun, Estrella and Israel for making the lab such a nice place to work and for helping me with many aspects of my project. I would also like to thank the BBSRC, which funded my studentship.

I am grateful to Dr Tim Humphrey and his lab for their collaboration on the deletion library screen. In particular to Carol Walker, Jennifer Moss and Rachel Deegan for help with the deletion library. Thanks also go to Rachel for many helpful DPhil pep talks and comments on thesis chapters. I also really appreciate the help from Simon Li with MATLAB and data analysis.

Many thanks go to all my friends and family for their support and interest in what I have been doing during my DPhil. Special thanks go to Nick for always, always being there for me and putting up with four years of my talking about yeast. Thanks to my brother Jack for his interest in my project and for help with proof-reading. The biggest thanks of all go to my Mum and Dad for their constant support and advice, which has enabled me to get where I am today.

Finally, I would like to dedicate this thesis to the memory of my aunt, Patricia Anne Hancocks. Pat was a wonderful person who encouraged and supported my education and who will always be dearly missed.

Declaration

I declare:

The work presented in this thesis is my own, with the exception of the initial cross of the *S. pombe* deletion library, which was performed by Carol Walker, and the MATLAB analysis of the *S. pombe* deletion library image dataset, which was performed by Simon Li.

No portion of this work has been previously submitted for another qualification at this, or any other university.

Signed ……..……

Marianne Shepherd

Some of the results from this thesis have been published:

Guarino, E.*, Shepherd, M. E. A.*, Salguero, I., Hua, H., Deegan, R. S. and Kearsey, S. E. (2011). Cdt1 proteolysis is promoted by dual PIP degrons and is modulated by PCNA ubiquitylation. Nucleic Acids Research, 39(14): 5978–5990.
**Joint first authors*.

Salguero, I., Guarino, E., Shepherd, M. E. A., Deegan, T. D., Havens, C. G., MacNeill, S. A., Walter, J. C. and Kearsey, S. E. (2012). Ribonucleotide reductase activity is coupled to DNA synthesis via proliferating cell nuclear antigen (PCNA). Current Biology, 22(8): 720-726.

Abbreviations

Δ	Gene deletion
ARS	Autonomously replicating sequence
ATR	Ataxia telangiectasia and Rad3-related protein
BER	Base excision repair
BiFC	Bimolecular fluorescence complementation
BIR	Break-induced replication
bp	Base pair
Cdc	Cell division cycle
CDK	Cyclin-dependent kinase
Cdt	Cdc10-dependent transcript
CFP	Cyan fluorescence protein
CHX	Cycloheximide
CKI	Cyclin-dependent kinase inhibitor
CMG complex	Cdc45/Mcm2-7/GINS complex
CRL	Cullin-RING E3 ubiquitin ligase
CSN	COP9/signalosome
DAPI	4’6’-diamidino-2-phenylindole
DCAF	Ddb1- and Cul4-associated factors
DDK	Dbf4-dependent kinase
DMSO	Dimethyl sulphoxide
DNA	Deoxyribonucleic acid
dNTP	Deoxyribonucleotide triphosphate (A, C, G or T)
DSB	Double-strand break
dsDNA	Double-stranded DNA
DT40	Chicken B cell line
EDTA	Ethylenediamine tetra-acetic acid, disodium salt
EMM	Edinburgh minimal medium
EMMG	Edinburgh minimal glutamate medium
g	Relative centrifugal force
g	Gram
G-418	Geneticin
GFP	Green fluorescence protein
GINS	Go ichi ni san
GO	Gene ontology
HO	Homothallic endonuclease
HR	Homologous recombination
HU	Hydroxyurea
Hyg	Hygromycin B
Kb	Kilobase
kDa	Kilo Dalton
l	Litre
LB	Luria-Bertani medium
log	Logarithmic phase
M	Molar
mA	Milliamp

MBF	MCB binding factor
MCB	*Mlu*1 cell cycle box
MCM	Minichromosome maintenance
mg	Milligram
ml	Millilitre
mM	Millimolar
MMS	Methyl methanesulphonate
MRN complex	Mre11/Rad32-Rad50-Nbs1 complex
NER	Nucleotide excision repair
NHEJ	Non-homologous end-joining
NLS	Nuclear localisation sequence
nmt	No message in thiamine
OD	Optical density
ORC	Origin recognition complex
ORF	Open reading frame
PBS	Phosphate-buffered saline
PCNA	Proliferating cell nuclear antigen
PCR	Polymerase chain reaction
PIP	PCNA-interacting peptide
pre-IC	Pre-initiation complex
pre-RC	Pre-replication complex
RING	Really interesting new gene
RNA	Ribonucleic acid
RNaseA	Ribonuclease A
RNR	Ribonucleotide reductase
RPA	Replication protein A
SAC	Spindle assembly checkpoint
SCF	Skp1-cullin-F box
SDW	Sterile distilled water
SRS	Substrate recognition subunit
SSB	Single-strand break
ssDNA	Single-stranded DNA
TAE	Tris acetate EDTA
TAP	Tandem affinity purification
TCA	Trichloroacetic acid
TE	Tris EDTA
TLS	Translesion synthesis
Tris	Tris(hydroxymethyl) methylamine
ts	Temperature-sensitive
UTR	Untranslated region
UV	Ultraviolet
V	Volts
WT	Wildtype
YE3S	Yeast extract with supplements
YFP	Yellow fluorescence protein
µg	Microgram
µl	Microlitre

Table of Contents

Abstract i

Acknowledgements ii

Declaration iii

Publications arising from this thesis iv

Abbreviations v

1 Introduction 1

1.1 Eukaryotic DNA replication 1

1.1.1 Assembly of the pre-replication complex at DNA replication origins 2

1.1.2 The transition to S phase and the initiation of DNA replication 11

1.1.3 The recruitment of DNA polymerases, RPA and PCNA for the elongation phase of DNA replication 19

1.1.4 The termination of DNA replication 23

1.2 Mechanisms restricting DNA replication to once per cell cycle 24

1.2.1 Periodic transcription 24

1.2.2 CDK phosphorylation 26

1.2.3 Nuclear export 27

1.2.4 Proteolysis 27

1.2.5 Inhibition of Cdt1 by geminin 29

1.2.6 The consequences of licensing factor deregulation 31

1.3 The structure and activity of $CRL4^{Cdt2}$ 33

1.4 The essential mitotic function of human Cdt1 37

1.5 Aims of this project 39

2 Materials and Methods 41

2.1 *S. pombe* methods 41

2.1.1 Growth and maintenance of *S. pombe* 41

2.1.2 The *S. pombe* strains used in this study 42

2.1.3 Genetic crosses, random spore analysis and tetrad dissection 45

2.1.4 Diploid construction 46

2.2 *Escherichia coli* methods 46

2.3 DNA methods 47

2.3.1 DNA manipulation 47

2.3.2 DNA isolation and analysis 48

2.3.3 DNA transformation 49

2.3.4 DNA sequencing 51

2.4 Plasmid construction 52

2.5 Oligonucleotide primers 53

2.6 Protein methods 53

2.6.1 Trichloroacetic acid (TCA) protein extraction 53

2.6.2 SDS-polyacrylamide gel electrophoresis (SDS-PAGE) 54

2.6.3 Western blotting 54

2.7 Microscopy methods 56

2.7.1 Light microscopy 56
2.7.2 Fluorescence microscopy 56
2.7.3 Quantitation of nuclear fluorescence intensity 58
2.8 UV method 59
2.9 Flow cytometry 59
2.10 *S. pombe* deletion library methods 60
2.10.1 Fluorescence-based screening methods 60
2.10.2 Use of the PEM-2 system to cross Cdt1-YFP into the deletion library 61

3 Characterisation of Two In-frame Methionine Codons in *S. pombe* Cdt1 62
3.1 Introduction 62
3.2 Results 63
3.2.1 The N-terminus of Cdt1 contains a putative PIP box and is required to maintain wildtype protein levels 63
3.2.2 Analysis of two in-frame methionine codons in *S. pombe* Cdt1 65
3.2.3 The second in-frame AUG codon is essential for cell viability 71
3.2.4 Analysis of wildtype Cdt1 and the Cdt1M1A and Cdt1M23A mutant proteins when overexpressed 73
3.3 Discussion 77
3.3.1 The second in-frame AUG codon is required for Cdt1 expression 78
3.3.2 A range of factors can affect translation initiation at an AUG codon 80
3.3.3 Two in-frame AUG codons could enable the expression of N-terminally distinct Cdt1 isoforms 83
3.4 Conclusions 84

4 A Role for Dual PIP Degrons in Cdt1 Proteolysis 86
4.1 Introduction 86
4.2 Results 87
4.2.1 The N-terminal 26-100 amino acids of Cdt1 are required for correct nuclear localisation and contribute to the cell cycle- and DNA damage-dependent regulation of the protein 87
4.2.2 Truncation mutations in Cdt1 indicate a second putative PIP motif contributes to the cell cycle-dependent regulation of the protein 96
4.2.3 Dual PIP degrons at positions 28 and 301 are involved in the cell cycle- and DNA damage-dependent regulation of Cdt1 102
4.2.4 Residual Cdt2-independent turnover of Cdt1 occurs in the cell cycle 110
4.2.5 Dual PIP degrons in Cdt1 are required for the protein to interact with PCNA. 113
4.3 Discussion 117
4.3.1 The limitations of large-scale deletion mutants 118
4.3.2 Dual PIP degrons promote Cdt1 proteolysis and Cdt1-PCNA interaction 119
4.3.3 The mechanism and biological significance of $CRL4^{Cdt2}$-mediated Cdt1 proteolysis 123
4.4 Conclusions 125

5 A Genome-wide Screen for Novel Genes Involved in Cdt1 Regulation 126
5.1 Introduction 126
5.2 Results 128
5.2.1 The development of a medium-throughput fluorescence-based screening method 128

5.2.2 A screen of the *S. pombe* deletion library for genes that regulate cell cycle Cdt1 levels....135
5.2.3 Identification of candidate gene deletion backgrounds with elevated Cdt1 levels 141
5.3 Discussion....149
5.3.1 *res2*$^{+}$, *yox1*$^{+}$, *ddb1*$^{+}$, *cdt2*$^{+}$ and *csn1*$^{+}$ have well recognised roles in Cdt1 regulation 152
5.3.2 *rad32*$^{+}$, *ctp1*$^{+}$, *rhp51*$^{+}$, *nse5*$^{+}$ and *nse6*$^{+}$ function in DNA repair 155
5.3.3 Defects in cell cycle progression and large-scale effects on gene expression may underlie the up-regulation of Cdt1 that is observed in *pof3*Δ, *ask1*Δ, *dad2*Δ, *dad5*Δ, *nut2*Δ, *SPAC1805.14*Δ and *SPAC824.04*Δ mutants 161
5.4 Conclusions....164

6 Analysis of Candidate Genes Involved in Cdt1 Regulation....165
6.1 Introduction....165
6.2 Results....165
6.2.1 Analysis of Cdt1 regulation in genetic backgrounds defective in DNA repair.165
6.2.2 The role of the CSN subunit Csn1 in Cdt1 regulation 186
6.2.3 Investigation into the regulation of Cdt2 and the effect of Cdt2 levels on CRL4^{Cdt2} activity....200
6.3 Discussion....207
6.3.1 The relationship between HR, cell cycle progression, checkpoint activation and Cdt1 regulation in fission yeast cells 208
6.3.2 CSN function promotes efficient CRL4^{Cdt2}-dependent Cdt1 proteolysis....214
6.3.3 The regulation of Cdt2 levels and their effect on CRL4^{Cdt2} activity....217
6.4 Conclusions....219

7 Conclusions and Further Work 220
7.1 Principal conclusions 220
7.2 PCNA is a central component of the CRL4^{Cdt2} ubiquitylation pathway....221
7.3 The biological significance of Cdt1 regulation in response to DNA damage....223

Bibliography 226

Appendices....246

CHAPTER 1

Introduction

The subject of this thesis is the cell cycle- and DNA damage-dependent regulation of Cdt1 in the fission yeast *Schizosaccharomyces pombe*. Cdt1 is a conserved and essential licensing factor that is required for DNA replication in eukaryotic cells. Cdt1 is strictly regulated in eukaryotic cells to ensure a single round of DNA replication occurs per cell cycle. This introduction provides an overview of eukaryotic DNA replication and describes the mechanisms that restrict DNA replication to once per cell cycle. In particular, regulation of Cdt1 proteolysis through the $CRL4^{Cdt2}$ pathway will be highlighted. Finally, a novel function for human Cdt1 in mitosis that is separate from its role in replication licensing will be examined.

1.1 EUKARYOTIC DNA REPLICATION

Eukaryotic DNA replication can be divided into three stages: initiation, elongation and termination. The initiation of DNA replication occurs in two discrete steps. The first step, termed licensing, occurs in late mitosis (M)/G1 phase of the cell cycle and involves assembly of the pre-replication complex (pre-RC) at DNA replication origins. The second step occurs at the onset of the DNA synthesis (S) phase of the cell cycle and involves the initiation of DNA replication in response to an increase in the activity of two protein kinases: cyclin-dependent kinase (CDK) and Dbf4-dependent kinase (DDK). CDK and DDK activity trigger the recruitment of additional proteins to the replication origin, resulting in formation of the pre-initiation complex (pre-IC)

and the initiation of DNA replication. In the elongation phase of DNA replication, bidirectional replication forks are established and DNA is synthesised through semi-conservative DNA replication. This section provides an overview of Pre-RC and Pre-IC assembly as well as the elongation and termination stages of DNA replication (Figure 1.1).

1.1.1 Assembly of the pre-replication complex at DNA replication origins

The assembly of the pre-RC and the subsequent initiation of DNA replication occur at regions of DNA termed replication origins. In the budding yeast *Saccharomyces cerevisiae*, replication origins are well defined and are termed autonomously replicating sequences (ARS) after their initial identification as DNA sequences that promote the autonomous replication of transformed DNA, without the need for chromosomal integration (Stinchcomb et al. 1979). In *S. cerevisiae*, replication origins are located in intergenic regions and are typically 100-200 base pairs (bp) in length (Nieduszynski et al. 2006). They consist of an essential ARS consensus sequence (ACS), which is a short conserved AT-rich sequence, and additional non-essential B elements that are located adjacent to the ACS (Marahrens and Stillman 1992). Although the ACS is necessary for replication origin activity it is not sufficient and additional features, such as a flanking region of helical instability and nucleosome positioning, may contribute to the determination of origin activity (Nieduszynski et al. 2006; Eaton et al. 2010). Chromatin modification may also contribute to origin activity (Nieduszynski et al. 2006).

In comparison to the replication origins of *S. cerevisiae*, the replication origins of *S. pombe* and Metazoa are less clearly defined and no essential consensus sequence has

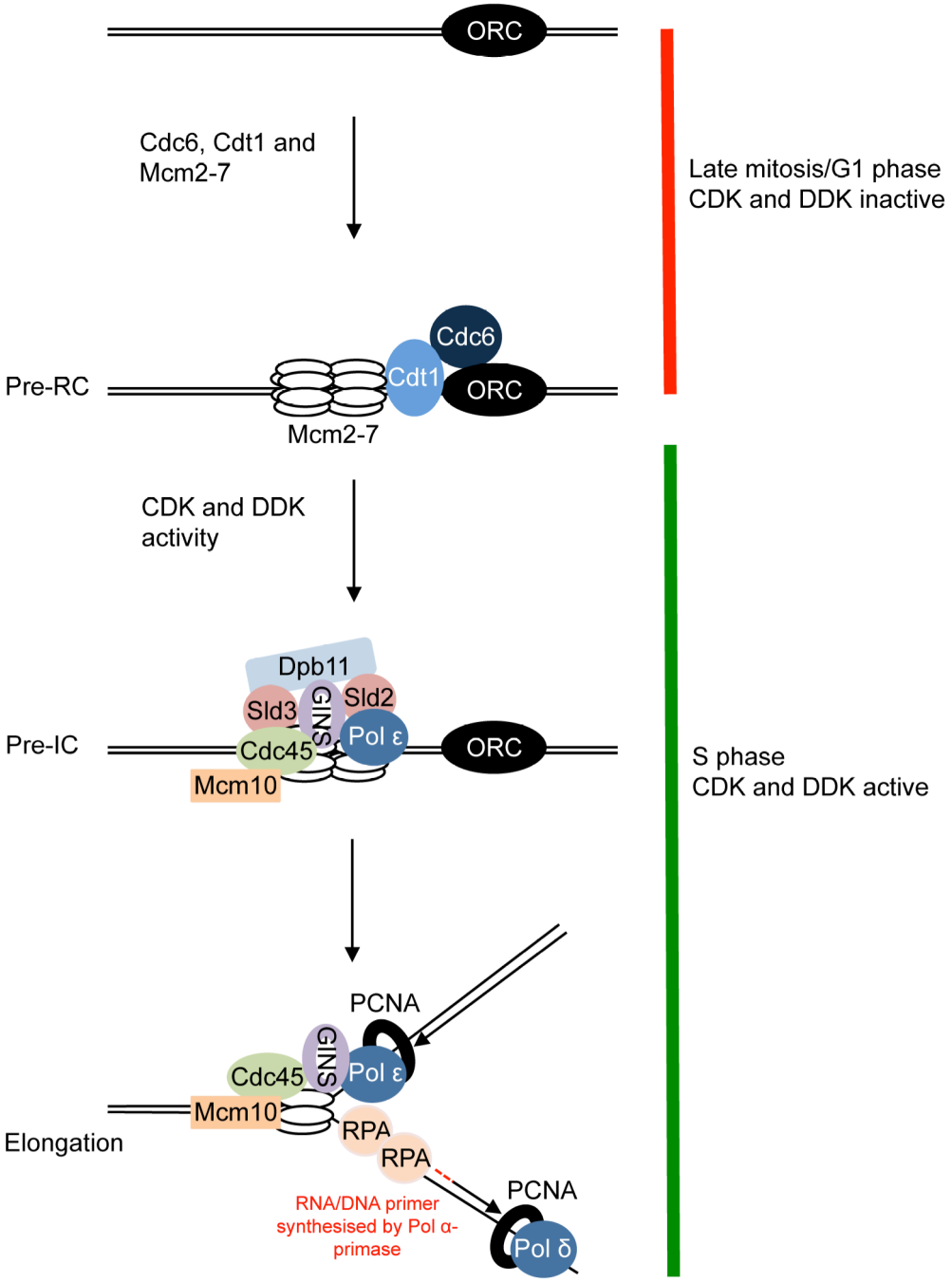


Figure 1.1 | The regulation of eukaryotic DNA replication.
The licensing, initiation and elongation stages of eukaryotic DNA replication. Licensing occurs in late M/G1 phase when CDK and DDK activity is low and involves assembly of the pre-RC at DNA replication origins. At the G1/S phase transition, an increase in CDK and DDK activity triggers the recruitment of additional factors to DNA replication origins, leading to formation of the pre-IC. Unwinding of the origin DNA results in the establishment of bi-directional replication forks and the elongation stage of DNA replication. Only one replication fork is shown in this figure. Although not included here, additional proteins have been shown to associate with eukaryotic DNA replication forks during elongation and consitute the replisome progression complex (RPC). Adapted from Labib 2010; Diffley 2011.

been identified. The replication origins of *S. pombe* are found exclusively in intergenic regions and consist of AT-rich regions of DNA, which are between 0.5 kb and 1 kb in length (Segurado et al. 2003; Hayashi et al. 2007). Although numerous features that associate with metazoan replication origins have been identified, ranging from DNA sequence elements to properties of the surrounding chromatin, none of these alone is predictive of a functional replication origin (reviewed in Mechali 2010). Recent genome-wide mapping of replication initiation events in two human cell lines has identified an enrichment of replication initiation events at genomic regions that exhibit moderate rates of transcription, CpG methylation or an open chromatin structure (Martin et al. 2011). The specification of metazoan replication origins appears to be complex and this might represent an adaption to promote DNA replication programme plasticity (reviewed in Masai et al. 2010; Mechali 2010).

The initial step in the assembly of the pre-RC is binding of the heterohexameric origin recognition complex (ORC) to DNA replication origins. ORC was initially identified and purified from budding yeast as a multiprotein complex that specifically bound to the *S. cerevisiae* ARS (Bell and Stillman 1992). Orthologues of the *S. cerevisiae ORC1-6* genes have been identified in *S. pombe* and higher eukaryotes, and Orc1-5 orthologues share a common AAA+ ATPase domain (reviewed in Duncker et al. 2009). In *S. cerevisiae*, ORC is bound constitutively to origin DNA throughout the cell cycle (Aparicio et al. 1997). Initial studies using *S. pombe* showed that ORC was also constitutively associated with chromatin throughout the cell cycle (Lygerou and Nurse 1999; Ogawa et al. 1999). However, recent chromatin-immunoprecipitation (ChIP) data suggest that ORC binds periodically to origin DNA in *S. pombe*, with a peak in late M/G1 phase (Wu and Nurse 2009). In higher eukaryotes, ORC exhibits a

similar periodic association with origin DNA, which is cell cycle regulated (Li and DePamphilis 2002; Sun et al. 2002).

Consistent with the diverse nature of eukaryotic DNA replication origins, the mechanism of ORC binding at origin DNA varies between organisms. In *S. cerevisiae*, Orc1 binds ATP and this is required for ORC association with DNA replication origins (Klemm et al. 1997). Binding of ORC to the *S. cerevisiae* ARS requires ORC subunits Orc1-5, with close contacts observed between Orc1, Orc2, Orc4 and Orc5 proteins and the origin DNA (Lee and Bell 1997). In contrast, binding of *S. pombe* ORC to origin DNA does not require ATP and is mediated exclusively by the N-terminal domain of Orc4, which contains nine AT-hook domains that interact with the AT-rich sequence of the *S. pombe* DNA replication origins (Lee et al. 2001; Chuang et al. 2002). In Metazoa, the mechanism of ORC binding at DNA replication origins is not clearly defined but it is thought to be regulated by epigenetic parameters in addition to DNA sequence elements (reviewed in DePamphilis 2005). In mammalian cells, the BAH domain of Orc1 and the activity of additional targeting proteins are implicated in promoting ORC association with origin DNA (Noguchi et al. 2006; Duncker et al. 2009). For example, the chromatin protein HMGA1a, which contains three AT-hook domains, interacts with ORC in human cells and may target it to replication origins in AT-rich heterochromatic regions (Thomae et al. 2008).

The next step in pre-RC assembly is the recruitment of Cdc6 (Cdc18 in *S. pombe*) and Cdt1 to ORC-bound origin DNA. Although Cdc6/Cdc18 and Cdt1 interact directly, it is thought that the two proteins are independently recruited to chromatin in an ORC-dependent manner (Coleman et al. 1996; Tanaka et al. 1997; Maiorano et al. 2000;

Nishitani et al. 2000; Gillespie et al. 2001; Cook et al. 2004). Cdc6/Cdc18 and Cdt1 are conserved proteins that are strictly required for the loading of the Mcm2-7 complex onto DNA, and hence the initiation of DNA replication, in yeast and higher eukaryotes (Coleman et al. 1996; Donovan et al. 1997; Tanaka et al. 1997; Maiorano et al. 2000; Nishitani et al. 2000; Gillespie et al. 2001; Cook et al. 2004; Randell et al. 2006). Cdc6/Cdc18 is highly related to Orc1 and contains an AAA+ ATPase domain (Duncker et al. 2009). As discussed in detail below, the hydrolysis of ATP by Cdc6 is essential for its licensing function (Randell et al. 2006). The stable loading of Mcm2-7 onto DNA completes pre-RC formation and it is generally thought that ORC, Cdc6 and Cdt1 are dispensable for subsequent steps of DNA replication (Hua and Newport 1998; Rowles et al. 1999; Maiorano et al. 2000; Nishitani et al. 2000).

The Mcm2-7 complex is a heterohexamer composed of six essential and distinct subunits, each of which contains an AAA+ ATPase domain and is highly conserved within the Eukaryota (reviewed in Bochman and Schwacha 2009). Recent single-particle electron microscopy (EM) analysis of the structure of the *Drosophila melanogaster* Mcm2-7 complex indicates that it forms a ring-shaped structure with the N- and C-terminal domains of each subunit aligned (Costa et al. 2011). Interestingly, on its own, the Mcm2-7 complex exists in two states: one is a ring with approximate six-fold symmetry, while the other is an open ring with discontinuity between the Mcm2 and Mcm5 subunits (Costa et al. 2011). The propensity of Mcm2-7 to form an open ring structure may facilitate its loading onto origin DNA. Mcm2-7 functions as the DNA helicase during eukaryotic DNA replication, following its association with auxiliary factors Cdc45 and the GINS complex (Moyer et al. 2006; Pacek et al. 2006; Ilves et al. 2010). The GINS complex is a heterotetramer

comprising Sld5, Psf1, Psf2 and Psf3 and the name is derived from the Japanese for five, one, two and three (*G*o, *I*chi, *N*i, *S*an) (Takayama et al. 2003). The purified *Drosophila* Cdc45/Mcm2-7/GINS (CMG) complex exhibits helicase activity *in vitro* (Moyer et al. 2006; Ilves et al. 2010).

Of the various eukaryotic organisms studied, the licensing reaction of *S. cerevisiae* has been characterised in the most detail. It serves as a useful model and is described below, together with key similarities and differences that have been noted between the licensing reaction of *S. cerevisiae* and other eukaryotes. *S. cerevisiae* is unusual in that Cdt1 and the Mcm2-7 complex are excluded from the nucleus outside of late mitosis/G1 phase and the nuclear accumulation of both Cdt1 and Mcm2-7 in late mitosis is interdependent (Tanaka and Diffley 2002). *S. cerevisiae* Cdt1 and Mcm2-7 interact as a heteroheptamer, which is recruited to ATP-bound ORC and Cdc6 at origin DNA through direct interactions between Cdt1 and Orc6 (Randell et al. 2006; Chen et al. 2007; Remus et al. 2009). Experiments using *Xenopus* egg extracts suggest that the sequential binding of Cdc6 followed by Cdt1 to chromatin is important for a functional licensing reaction (Tsuyama et al. 2005). In fission yeast and Metazoa, it has not been definitively established whether Cdt1 and Mcm2-7 interact as a complex independently of chromatin or whether Cdt1 and Cdc6 are independently recruited to chromatin and then act cooperatively to load Mcm2-7 onto origin DNA (Nishitani et al. 2000; Cook et al. 2004).

Although the context of the Cdt1-Mcm2-7 interaction may differ between eukaryotes, an interaction between Cdt1 and Mcm2-7 forms an important component of the eukaryotic licensing reaction. The C-terminal regions from a broad range of

eukaryotic Cdt1 orthologues exhibit extensive sequence conservation and mediate interactions with Mcm2-7 (Yanagi et al. 2002; Ferenbach et al. 2005; Takara and Bell 2011). Notably, the C-terminal region of Cdt1 adopts a conserved winged-helix-domain structure, which makes important contributions to the binding of Mcm2-7 (Jee et al. 2010; Takara and Bell 2011). It is thought that the Cdt1-Mcm2-7 interaction is mediated through a direct Cdt1-Mcm6 interaction, as this has been observed in both yeast and mammalian systems (Yanagi et al. 2002; Maki et al. 2011; Liu et al. 2012). The interaction between mouse Cdt1 and Mcm4/6/7 stimulates binding of the MCM subcomplex to DNA *in vitro*, and *in vivo* disruption of the Cdt1-Mcm6 interaction in *S. cerevisiae* and *S. pombe* inhibits Mcm2-7 loading at replication origins, demonstrating the critical importance of this interaction in the eukaryotic licensing reaction (You and Masai 2008; Maki et al. 2011; Liu et al. 2012).

In vitro reconstitution of the Mcm2-7 loading reaction using purified *S. cerevisiae* proteins indicates that single Cdt1•Mcm2-7 heptamers are cooperatively loaded to assemble a double Mcm2-7 hexamer on the origin DNA (Evrin et al. 2009; Remus et al. 2009). The double Mcm2-7 hexamer is arranged with a head-to-head configuration, with the C-terminal AAA+ ATPase domains of each Mcm2-7 subunit located on the outer end of each hexamer (Remus et al. 2009). Biochemical and EM analysis of the double Mcm2-7 hexamer suggests it is topologically linked to DNA as it contains a central channel through which double-stranded (ds) DNA can pass (Evrin et al. 2009; Remus et al. 2009). A recent model has sought to explain how a double Mcm2-7 hexamer might be loaded onto DNA in *S. cerevisiae* (Takara and Bell 2011). The authors propose that Orc6 interacts with two Cdt1 molecules through two independent Cdt1 binding sites, located in the N- and C-terminus of the Orc6 protein.

Interactions between the Cdt1 binding sites in Orc6 and two distinct origin recruitment regions in Cdt1 result in the association of two oppositely orientated Mcm2-7 complexes with the pre-RC. The loading of double MCM hexamers onto origin DNA has also been observed in *Xenopus* egg extracts and is thought to represent a conserved feature of eukaryotic DNA licensing (Gambus et al. 2011).

In contrast to the ORC subunits Orc1-5, the Orc6 protein is evolutionarily the least conserved between eukaryotic organisms (Duncker et al. 2009). This has implications for the extent of conservation of the Cdt1-Orc6 interaction that has been described in the *S. cerevisiae* licensing reaction. *In vitro* reconstitution of the licensing reaction using *Xenopus* purified proteins suggested that Orc6 is not essential in this process (Gillespie et al. 2001). However, human Orc6 is required for *in vitro* pre-RC assembly and for DNA replication *in vivo* (Prasanth et al. 2002; Thomae et al. 2011). A structural study of the human Cdt1-Mcm6 complex has suggested that two Cdt1 molecules, each interacting with a Mcm2-7 complex, may not be accommodated by one Orc6 molecule (Liu et al. 2012). Therefore, it appears that the precise mechanism by which head-to-head loading of double Mcm2-7 hexamers onto DNA is achieved and the extent to which this mechanism is conserved between eukaryotes is unclear.

After the origin recruitment of Cdt1•Mcm2-7 heptamers, ATP hydrolysis by Cdc6 is required for the stable loading of Mcm2-7 complexes onto DNA (Randell et al. 2006; Takara and Bell 2011). Cdc6 hydrolyses ATP in a manner that is dependent on ORC and origin DNA (Randell et al. 2006). This event promotes Cdt1 release from the origin, suggesting its association with the pre-RC is transient, and eventually leads to dissociation of Cdc6 as well (Randell et al. 2006). Subsequent ATP hydrolysis by

ORC permits repeated cycles of Mcm2-7 loading to occur (Bowers et al. 2004). The loading of multiple Mcm2-7 complexes at a single DNA replication origin has also been observed in *Xenopus* egg extracts (Edwards et al. 2002). The *S. cerevisiae* double MCM hexamer is mobile on DNA and once loaded, it may slide away from the origin to enable repeated cycles of MCM loading (Remus et al. 2009). The functional significance of loading an excess of MCM complexes onto DNA is unclear but it may be important during replication stress to promote replication restart at stalled forks (Remus et al. 2009).

In vitro reconstitution of the licensing reaction using purified *S. cerevisiae* proteins indicates that DNA, ORC, Cdc6, Cdt1, Mcm2-7 and ATP are sufficient for the loading of Mcm2-7 onto DNA (Kawasaki et al. 2006; Remus et al. 2009). However, additional proteins have been shown to participate in the licensing reaction of higher eukaryotes. Mcm9 is a member of the Mcm2-9 protein family, which is present in vertebrates but absent in yeast (Lutzmann et al. 2005). A study using *Xenopus* egg extracts has suggested that Mcm9 might be an important component of the pre-RC in higher eukaryotes (Lutzmann and Mechali 2008). The protein interacts directly with Cdt1, is recruited to chromatin in an ORC-dependent manner and is required for Mcm2-7 loading onto DNA and subsequent DNA replication (Lutzmann and Mechali 2008). In human cells, two additional proteins have been implicated in pre-RC formation: HBO1 (human acetylase binding to ORC1) histone acetylase and the chromatin-remodelling factor SNF2H (sucrose nonfermenting 2 homologue) (Miotto and Struhl 2008; Sugimoto et al. 2011). Both HBO1 and SNF2H interact with Cdt1 and associate with replication origins in G1 phase in human cells, in a Cdt1-dependent manner (Miotto and Struhl 2008; Sugimoto et al. 2011). Furthermore,

HBO1 histone acetylase activity and SNF2H promote Mcm2-7 loading onto DNA (Miotto and Struhl 2010; Sugimoto et al. 2011). It is proposed that the coordinated action of HBO1 and SNF2H may regulate chromatin structure to promote efficient Mcm2-7 chromatin loading (Sugimoto et al. 2011).

1.1.2 The transition to S phase and the initiation of DNA replication

The G1/S phase transition is marked by an increase in the activity of two protein kinases: CDK and DDK. CDK and DDK phosphorylate multiple targets and trigger the recruitment of additional factors to replication origins, including Sld2, Sld3, Dpb11, Mcm10, DNA polymerase ε (Pol ε), Cdc45 and GINS, to form the pre-IC complex. The stable association of Mcm2-7, Cdc45 and GINS within the tertiary CMG complex results in activation of the Mcm2-7 helicase, origin unwinding and the establishment of bidirectional replication forks capable of initiating semi-conservative DNA replication (reviewed in Remus and Diffley 2009; Labib 2010).

1.1.2.1 The CDK and DDK protein kinases

CDKs are serine/threonine protein kinases that act as key regulators of eukaryotic cell cycle progression. The catalytic activity of a CDK is dependent on a cyclin regulatory subunit and distinct cyclin-CDK complexes assemble at different cell cycle stages. The cyclin regulatory subunits undergo a cycle of synthesis and proteolysis during the cell cycle, which results in periodic activation of the CDK. *S. pombe* has a single CDK, Cdc2, which associates with one of four cyclin subunits; Cig1, Cig2, Puc1 or Cdc13 to regulate cell cycle progression (reviewed in Moser and Russell 2000). In *S. pombe* cells, the G1/S phase transition is mediated by the activity of Cdc2-Cig2 (Mondesert et al. 1996). However, there is some overlap in the function of the *S.*

pombe cyclins as Cdc13 can mediate S phase onset in a *cig1*Δ *cig2*Δ double mutant (Fisher and Nurse 1996). In *S. cerevisiae*, the *cdc2*$^{+}$ orthologue is *CDC28* and the Cdc28 protein regulates cell cycle progression through interactions with the G1-specific cyclins (Cln1-3) and the B-type cyclins (Clb1-6). An interaction between Cdc28 and Clb5/6 regulates S phase onset and DNA replication (Schwob and Nasmyth 1993). In contrast to yeast, mammalian cells have four CDKs (Cdk1, 2, 4 and 6) that interact with four classes of cyclins (cyclin A, B, D and E) to regulate cell cycle progression (reviewed in Malumbres and Barbacid 2005). Cdk2-cyclin E and Cdk2-cyclin A are important regulators of the G1/S phase transition and S phase progression respectively but other CDKs are thought to be able to compensate for Cdk2 activity as Cdk2-null mice are viable, indicating Cdk2 is not essential for mitotic cell division (Ortega et al. 2003).

DDK is a serine/threonine protein kinase that comprises a Cdc7 catalytic subunit and a regulatory Dbf4 subunit and is essential for the initiation of DNA replication in eukaryotic cells (reviewed in Masai and Arai 2002). Cdc7-Dbf4 was initially identified in *S. cerevisiae* but orthologues of both proteins are present in *S. pombe* and higher eukaryotes (Hartwell 1973; Masai et al. 1995; Sato et al. 1997; Brown and Kelly 1998; Roberts et al. 1999; Jares et al. 2004). In fission yeast, the Cdc7 and Dbf4 orthologues are Hsk1 and Dfp1 respectively (Masai et al. 1995; Brown and Kelly 1998). Analogous to CDK regulation by cyclins, the catalytic activity of Cdc7 is dependent on an interaction with Dbf4 (Jackson et al. 1993). Cdc7 levels are constant throughout the cell cycle but Dbf4 levels oscillate due to periodic synthesis and proteolysis, generating an increase in Cdc7-Dbf4 kinase activity from late G1 phase

through to mitosis (Jackson et al. 1993; Takeda et al. 1999; Weinreich and Stillman 1999).

1.1.2.2 The phosphorylation of multiple targets by CDK and DDK promotes assembly of the pre-IC

Cdc7-Dbf4 acts locally at replication origins to promote their activation throughout S phase (Dowell et al. 1994; Bousset and Diffley 1998; Donaldson et al. 1998). The main phosphorylation target of Cdc7-Dbf4 is the Mcm2-7 complex. Mcm2-7 was first implicated as a Cdc7-Dbf4 target following analysis of the budding yeast *mcm5-bob1* mutant, which bypassed the cellular requirement for Cdc7 and Dbf4 (Hardy et al. 1997). Subsequent experiments in human, *S. pombe* and *S. cerevisiae* systems have demonstrated that Cdc7-Dbf4 phosphorylates the MCM subunits Mcm2, Mcm4 and Mcm6 (Masai et al. 2000; Masai et al. 2006; Sheu and Stillman 2006). In particular, Cdc7-Dbf4 targets the N-terminal tails of the MCM 2/4/6 subunits, which contain conserved clusters of serine/threonine residues (Masai et al. 2006; Sheu and Stillman 2006). Phosphorylation of the Mcm2-7 complex by Cdc7-Dbf4 promotes its interaction with replication factors, such as Cdc45, which are essential for the initiation and elongation of DNA replication (Masai et al. 2006; Sheu and Stillman 2006). In addition, work using *S. cerevisiae* suggests that Cdc7-Dbf4-dependent phosphorylation of Mcm4 may promote DNA initiation by relieving an inhibitory activity specific to the N-terminus of Mcm4 (Sheu and Stillman 2010).

In *S. cerevisiae*, a minimal set of CDK targets that are essential for the initiation of DNA replication have been defined and consist of Sld2 and Sld3 (Zegerman and Diffley 2007). The CDK-dependent phosphorylation of Sld3 and Sld2 mediates their

interaction with the N- and C-terminal pairs of BRCT repeats in Dpb11 respectively (detailed in Figure 1.2, page 17) (Tanaka et al. 2007; Zegerman and Diffley 2007). Dpb11 orthologues are present in fission yeast (Rad4/Cut5) and Metazoa (TopBP1/Mus101/Cut5) and all orthologues contain a series of BRCT repeats, although the precise number of repeats varies between the eukaryotic groups, with yeast Dpb11/Rad4/Cut5 containing four and mammalian TopBP1 containing eight (reviewed in Garcia et al. 2005). BRCT repeats often function as phosphoprotein-binding domains and in *S. cerevisiae*, phosphorylation-dependent interactions between Sld2, Sld3 and Dpb11 are essential for pre-IC assembly (Tanaka et al. 2007; Zegerman and Diffley 2007; Muramatsu et al. 2010). Although Sld2, Sld3 and Dpb11 are required for DNA replication initiation, they are not incorporated into the replisome for subsequent DNA synthesis; the main function of these three proteins appears to be the recruitment of Cdc45 and GINS to replication origins (reviewed in Labib 2010).

A *SLD3* orthologue is present in *S. pombe* (*sld3*$^{+}$) and the protein is essential for DNA replication in both budding and fission yeast (Kamimura et al. 2001; Nakajima and Masukata 2002). In *S. pombe* and *S. cerevisiae*, Sld3 interacts with Cdc45 and is required for the recruitment and maintenance of Cdc45 at replication origins (Kamimura et al. 2001; Nakajima and Masukata 2002). Owing to poor sequence conservation, the identification of *SLD3* orthologues in higher eukaryotes has not been straightforward. However, there is evidence that a TopBP1-interacting protein, which was initially identified in *Xenopus* but is conserved in other vertebrate species, may represent a Sld3 counterpart. The protein is named Treslin (*T*opBP1-interacting, *r*eplication-*s*timulating prote*in*) and it is important for DNA replication in *Xenopus*

egg extracts and human cells (Kumagai et al. 2010). Treslin interacts with TopBP1 in a Cdk2-dependent manner and is required for Cdc45 recruitment to chromatin in *Xenopus* egg extracts (Kumagai et al. 2010). In addition to Treslin, a further Cdk2 target protein that is required for the initiation of DNA replication has been identified in vertebrates (Balestrini et al. 2010). GEMC1 (geminin coiled-coil containing protein 1) interacts with TopBP1, Cdk2-cyclin E and Cdc45 and is important for the chromatin loading of Cdc45 (Balestrini et al. 2010).

The *S. pombe* orthologue of *SLD2* is *drc1*$^{+}$ and the Dcr1 protein is a phosphorylation target of Cdc2 that interacts with Rad4/Cut5 in a phosphorylation-dependent manner (Noguchi et al. 2002). The CDK-dependent phosphorylation of Sld2/Drc1 is essential for DNA replication and cell viability in both *S. pombe* and *S. cerevisiae* (Masumoto et al. 2002; Noguchi et al. 2002). In higher eukaryotes, the RecQ4 DNA helicase has been identified as a Sld2 orthologue, based on homology between N-terminal region of RecQ4 and the yeast Sld2/Drc1 proteins (Sangrithi et al. 2005; Matsuno et al. 2006). RecQ4 is essential for DNA replication in mammalian cells and *Xenopus* egg extracts (Sangrithi et al. 2005; Matsuno et al. 2006). In *Xenopus* egg extracts, RecQ4 is recruited to chromatin during DNA replication initiation and maximal recruitment of the protein requires pre-RC formation and CDK activity (Sangrithi et al. 2005; Matsuno et al. 2006). Furthermore, RecQ4 has been demonstrated to interact with TopBP1/Cut5 in *Xenopus* egg extracts in a phosphorylation-dependent manner (Matsuno et al. 2006).

A recent study using *S. cerevisiae* has elucidated the mechanism by which CDK-dependent phosphorylation of Sld2 and Sld3 promotes assembly of the pre-IC

(Muramatsu et al. 2010). Phosphorylation of Sld2 promotes its interaction with Dpb11 and this event stimulates the formation of a novel, fragile complex that comprises Sld2, Dpb11, Pol ε and the GINS tetramer (Figure 1.2). This complex interacts off-chromatin and has been named the pre-loading complex (pre-LC). The authors propose that CDK-dependent phosphorylation of Sld3, which is present at replication origins with Cdc45, promotes an association between Sld3 and Dpb11, thereby recruiting the pre-LC to replication origins. In this way, the pre-LC serves to deliver the GINS tetramer to DNA replication origins and in turn, promotes assembly of the CMG complex.

1.1.2.3 The Cdc45/Mcm2-7/GINS (CMG) helicase

The process of pre-IC formation results in the stable association of Cdc45 and GINS with Mcm2-7 at DNA replication origins. As discussed in Section 1.1.1, biochemical evidence from *Xenopus* and *Drosophila* systems demonstrates that this tertiary CMG complex exhibits ATP-dependent DNA helicase activity (Moyer et al. 2006; Pacek et al. 2006; Ilves et al. 2010). Cdc45 and GINS recruitment to Mcm2-7 is therefore proposed to activate the Mcm2-7 helicase, leading to origin unwinding and the establishment of active bidirectional replication forks. Precisely how an interaction with Cdc45 and GINS converts Mcm2-7 into an active helicase, and the mechanism of the active CMG DNA helicase is unclear. Two models of MCM helicase activity appeared plausible in light of the observation that pre-RC formation involved the loading of head-to-head double MCM hexamers onto dsDNA (Evrin et al. 2009; Remus et al. 2009; Takara and Bell 2009; Gambus et al. 2011). In the “twin-pump” model, the double MCM hexamers remain physically coupled and simultaneously pump dsDNA towards the hexamer interface, where it is extruded as single-stranded

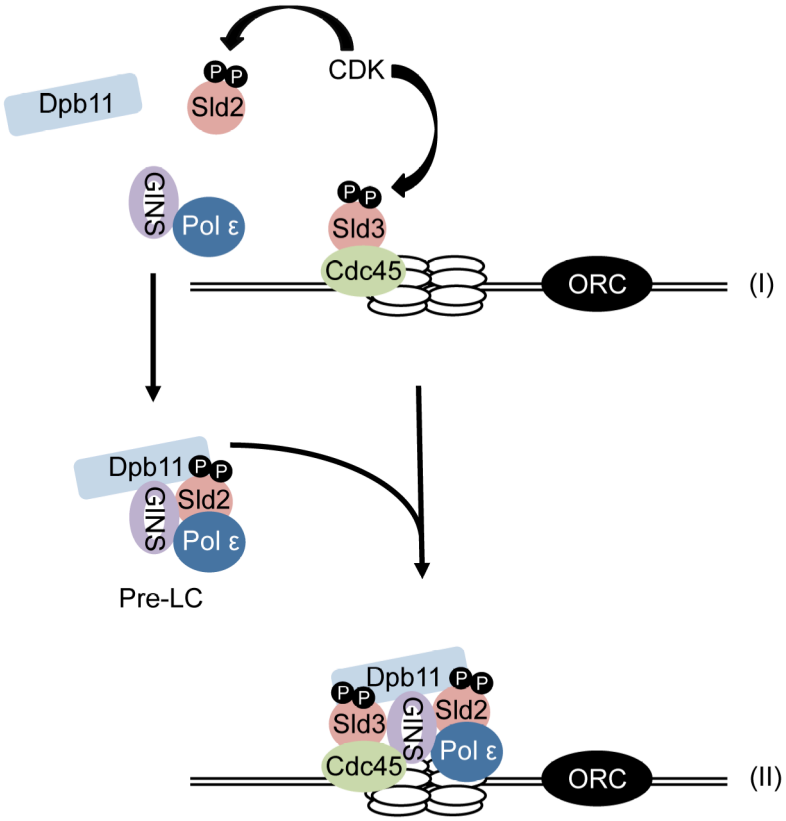


Figure 1.2 | CDK-dependent formation of the pre-LC at the onset of S phase.
CDK-dependent phosphorylation of Sld2 promotes formation of a fragile complex off-chromatin, termed the pre-loading complex (pre-LC), which contains Pol ε, GINS, Dpb11 and Sld2. Phosphorylation of Sld3 at the replication origin by CDK may promote an association between Dpb11 and Sld3, thereby recruiting the pre-LC to replication origins for the initiation of DNA replication. Adapted from Araki et al. (2010).

(ss) DNA. In the "ploughshare" model, the two MCM hexamers separate after the initiation of replication and translocate in opposite directions on the DNA; dsDNA is forced through the central channel of the hexamer towards a protein pin, which separates the two strands as they exit the complex (Takahashi et al. 2005; Takara and Bell 2009).

Recent data have cast doubt on both of these models. An elegant single-molecule study has demonstrated that Mcm2-7 helicases uncouple during DNA replication, arguing against the twin-pump model (Yardimci et al. 2010). The twin-pump model predicts that DNA is pumped towards the double MCM hexamer. To test this prediction, single molecules of DNA were tethered at each end and the constrained template was exposed to *Xenopus* egg extracts to examine whether DNA replication could occur. The constrained DNA template underwent efficient DNA replication by pairs of diverging forks, arguing in favour of a model where MCM hexamers uncouple during DNA replication. Structural studies of the CMG complex, using purified *Drosophila* proteins, suggest that Cdc45 and GINS bind to the periphery of Mcm2-7 (Costa et al. 2011). ATP-binding by the CMG complex stimulates a conformational change that restricts the central Mcm2-7 channel and generates a second channel at the periphery on Mcm2-7, bounded by Cdc45 and GINS. The authors argue that the placement of Cdc45 and GINS to the side of Mcm2-7 is inconsistent with the ploughshare model. Although the exact model is unclear, it is likely that the two channels present in the CMG complex contribute to the separation of the duplex DNA molecule (Botchan and Berger 2010; Costa et al. 2011).

1.1.3 The recruitment of DNA polymerases, RPA and PCNA for the elongation phase of DNA replication

In response to MCM complex activation and origin unwinding, addition proteins are recruited to the nascent replication forks to form the replisome; a multi-component enzymatic machine that mediates DNA replication. The ssDNA produced by the DNA helicase activity of the CMG complex is bound by replication protein A (RPA), a heterotrimeric ssDNA-binding protein that is highly conserved between eukaryotic organisms (reviewed in Wold 1997). RPA is essential for DNA replication in eukaryotic cells; it interacts with components of the replisome and has a role in stabilising and protecting ssDNA at the replication forks (Heyer et al. 1990; Wold 1997; Szuts et al. 2003). Essential to DNA replication in eukaryotic cells are three DNA polymerases: Pol α-primase, Pol ε and Pol δ (reviewed in Garg and Burgers 2005). Pol α-primase is a heterotetrameric enzyme comprising DNA polymerase and DNA primase catalytic subunits; it initiates DNA replication on both the leading and lagging strands by synthesis of a short RNA/DNA primer (reviewed in Garg and Burgers 2005; Johansson and MacNeill 2010). Polymerase switching from Pol α-primase to the processive Pol ε or Pol δ permits extended DNA synthesis. Pol ε and Pol δ are high fidelity DNA polymerases with intrinsic 3' to 5' exonuclease proofreading activity and are thought participate in DNA synthesis on the leading- and lagging-strand templates, respectively (Pursell et al. 2007; Nick McElhinny et al. 2008).

An additional and essential component of the replisome is proliferating cell nuclear antigen (PCNA). PCNA is a conserved eukaryotic protein and a member of the DNA sliding clamp family, which confer high processivity on the replicative polymerases

(Kelman and O'Donnell 1995). Crystallographic studies indicate that three PCNA monomers associate to adopt a ring-shaped structure that is able to encircle dsDNA (Krishna et al. 1994). Topological linking of the PCNA ring to DNA enables it to tether the replicative polymerases to the DNA template for extended DNA synthesis; the orientation and charge of 12 α-helices lining the central channel of PCNA enable it to slide along the DNA template to perform its sliding clamp function (Krishna et al. 1994). PCNA is loaded onto DNA by a five-protein clamp loader complex, termed replication factor C (RFC), which opens and closes the PCNA ring around DNA in an ATP-dependent manner (reviewed in O'Donnell and Kuriyan 2006). RFC loads PCNA onto DNA at primer-template junctions; binding of the RFC-PCNA complex at these regions is thought to displace Pol α-primase and result in recruitment of Pol ε or Pol δ for extended DNA synthesis (Garg and Burgers 2005). PCNA has been shown to increase the processivity of both *S. cerevisiae* Pol ε and Pol δ in an *in vitro* replication assay (Chilkova et al. 2007). Pol ε is more processive than Pol δ in the absence of PCNA and the ability of PCNA to stimulate the processivity of each polymerase is greater for Pol δ than for Pol ε (Chilkova et al. 2007).

PCNA interacts with a wide range of replication and repair proteins, which contain a conserved PCNA-binding motif, termed the PIP (*P*CNA-*i*nteracting *p*eptide) box (reviewed in Warbrick 2000; Maga and Hubscher 2003; Moldovan et al. 2007). The consensus sequence of the PIP box is Q-x-x-Ψ-x-x-ϑ-ϑ, where 'Ψ' is a hydrophobic residue, 'ϑ' is an aromatic residue and 'x' represents any residue. PIP box-containing proteins interact at a common surface on each PCNA monomer, which suggests the association of PCNA monomers with different interaction partners is mutually exclusive and competitive (Gulbis et al. 1996; Bruning and Shamoo 2004). Additional

PCNA-interaction motifs, including the KA-box and the AlkB homologue 2 PCNA interacting motif (APIM) have been defined (Xu et al. 2001; Gilljam et al. 2009). The ability of PCNA to interact with a wide range of proteins at the replication fork enables it to coordinate numerous DNA replication and DNA repair processes (Moldovan et al. 2007). For example, PCNA plays an important role during Okazaki fragment maturation by interacting with and coordinating the action of Pol δ, Fen1 and DNA Ligase I at each Okazaki fragment on the lagging strand (Maga et al. 2001; Maga and Hubscher 2003).

A number of replication factors that function during chromosomal DNA replication in S phase, such as RPA, the replicative DNA polymerases and PCNA, are also involved in DNA repair and recombination pathways. The DNA repair pathways of base excision repair (BER), nucleotide excision repair (NER), mismatch repair (MMR) and double-strand break (DSB) repair by homologous recombination (HR) all comprise a DNA synthesis step. PCNA, Pol δ and/or Pol ε are implicated in mediating the DNA synthesis step of these DNA repair pathways (reviewed in Maga and Hubscher 2003; Moldovan et al. 2007). RPA has also been shown to function in a range of DNA repair pathways (reviewed in Oakley and Patrick 2010). In particular, the binding of RPA to ssDNA at resected DSBs is required for the subsequent stages of DSB repair by HR (Oakley and Patrick 2010).

A detailed study in *S. cerevisiae* of the factors required for the HR pathway of break-induced replication (BIR) has suggested that all the essential DNA replication factors, such as the three replicative polymerases and the CMG complex, are required for this repair pathway (Lydeard et al. 2007; Lydeard et al. 2010). BIR operates when only

one end of a DSB shares homology with other sequences in the genome and results in recombination-dependent establishment of a unidirectional replication fork (Lydeard et al. 2007). In general, licensing factors have not been implicated in DNA repair and consistent with this, the pre-RC components Cdc6 and ORC were not shown to be required for BIR (Lydeard et al. 2010). However, a role for Cdt1 in BIR was identified and it was suggested that Cdt1 might function to load the Mcm2-7 complex onto the BIR template DNA (Lydeard et al. 2010).

Two further replication factors that have recently been implicated in DNA repair are the Mcm2-9 protein family members Mcm8 and Mcm9 (Lutzmann et al. 2012; Nishimura et al. 2012). Mcm8 and Mcm9 are the most recently identified members of the Mcm2-9 protein family and although present in a diverse range of eukaryotes, they appear to have been secondarily lost from certain eukaryotic taxa such as yeast (Liu et al. 2009). Recent work suggests vertebrate Mcm8 and Mcm9 interact as a complex and are required for efficient HR (Lutzmann et al. 2012; Nishimura et al. 2012). The precise role of Mcm8/Mcm9 in HR is not yet clear but a study in chicken DT40 cells suggests Mcm8/Mcm9 might function as a hexameric ATPase/helicase in HR repair that has been induced by DNA interstrand crosslinks (ICLs) (Nishimura et al. 2012).

In addition to its role in the DNA synthesis step of the various repair pathways, PCNA is involved in repair pathway choice during post-replicative DNA repair (Hoege et al. 2002). In response to DNA damage, PCNA is modified at lysine 164 by either mono- or poly-ubiquitylation in yeast and humans (Hoege et al. 2002; Frampton et al. 2006). Whereas mono-ubiquitylation of PCNA promotes its

association with translesion synthesis (TLS) DNA polymerases, which mediate error-prone DNA repair, poly-ubiquitylation of PCNA promotes a poorly understood error-free lesion bypass pathway (Moldovan et al. 2007). The $CRL4^{Cdt2}$ E3 ubiquitin ligase contributes to PCNA mono-ubiquitylation in unperturbed human cells, which may be important in the response to endogenous replication stress (Terai et al. 2010).

1.1.4 The termination of DNA replication

Eukaryotic DNA replication terminates when replication forks converge. In yeast, termination zones have been described in which replication termination occurs randomly, depending on where the two replication forks converge (Zhu et al. 1992). A recent genomics approach has identified 71 chromosomal termination regions (*TERs*) in *S. cerevisiae* that occur at specific chromosomal loci (Fachinetti et al. 2010). *TERs* are associated with replication pausing elements and the type II topoisomerase Top2 appears to facilitate replication termination at these regions (Fachinetti et al. 2010). Precisely how replication forks fuse during termination and how the replisome is dismantled is unclear. Interestingly, in *Xenopus* egg extracts and human cells, a role for a novel MCM-binding protein, termed MCM-BP, has been identified in the regulation of Mcm2-7 unloading at the end of S phase (Nishiyama et al. 2011). MCM-BP is conserved in Metazoa and *S. pombe* but not *S. cerevisiae*, and it appears to replace Mcm2 in the Mcm2-7 complex, resulting in formation of an alternative $MCM^{MCM\text{-}BP}$ complex (Sakwe et al. 2007; Ding and Forsburg 2011; Li et al. 2011). The cellular function of MCM-BP is not fully understood and is thought to extend beyond the unloading of the MCM complex in late S phase as inactivation or depletion of MCM-BP has numerous detrimental consequences for *S. pombe* and human cells (Li et al. 2011; Jagannathan et al. 2012).

1.2 MECHANISMS RESTRICTING DNA REPLICATION TO ONCE PER CELL CYCLE

To ensure genome stability, it is essential that a cell replicates its genome only once per cell cycle. The restriction of licensing to the G1 phase of the cell cycle, when CDK activity is low, is a major mechanism by which eukaryotic cells ensure a single round of DNA replication. The increase in CDK activity at the G1/S phase transition, which initiates DNA replication, also acts to inhibit *de novo* pre-RC assembly and this is an important safeguard against the occurrence of genome re-replication. Eukaryotic cells employ multiple overlapping mechanisms to inhibit licensing outside of the G1 phase of the cell cycle, which are discussed in detail below. Interestingly, although the biochemical functions of the pre-RC components are relatively conserved between eukaryotic organisms, the mechanisms employed to regulate pre-RC assembly are surprisingly divergent (reviewed in Kearsey and Cotterill 2003). The importance of regulated licensing activity for correct cell growth is highlighted by comparative analysis of normal and transformed human cell lines; transformed cells exhibit overexpression and an increased chromatin-association of ORC, Cdc6, Cdt1 and MCM proteins (Di Paola and Zannis-Hadjopoulos 2012).

1.2.1 Periodic transcription

In eukaryotic cells, the transcription of certain genes encoding pre-RC components is periodic, which ensures the proteins only accumulate and are available for licensing in late M/G1 phase. In *S. pombe*, the transcription of *cdc18*$^{+}$ and *cdt1*$^{+}$ is regulated by the MBF (*Mlu*I cell cycle box [MCB] binding factor) transcription factor complex and occurs periodically in the cell cycle, with a peak in late M/G1 phase (Kelly et al. 1993; Hofmann and Beach 1994). The MBF transcription factor mediates a wave of

transcription at the G1/S phase transition in fission yeast, and is composed of Cdc10, Res1 and Res2 subunits (reviewed in Bähler 2005). A number of regulatory subunits, including Rep2, Nrm1 and Yox1 also associate with the core MBF machinery to ensure correct cell cycle-dependent transcription of MBF target genes (Nakashima et al. 1995; de Bruin et al. 2006; Aligianni et al. 2009). MBF binds to MCB motifs that are present in the promoter regions of its target genes to regulate transcription (Lowndes et al. 1992; Maqbool et al. 2003).

In *S. cerevisiae*, G1/S phase transcription is regulated by the SBF (Swi4/6-dependent cell-cycle box [SBF]-binding factor) and the MBF (*Mul*I cell-cycle box [MCB]-binding factor) transcription factor complexes, which are heterodimers composed of Swi4/Swi6 and Mbp1/Swi6 respectively (reviewed in Bähler 2005). Mapping the genomic binding sites of SBF and MBF has identified over 200 potential target genes, with substantial overlap observed in the target genes of the two transcription factor complexes (Iyer et al. 2001). The transcription of the budding yeast *CDC6* gene occurs periodically in the cell cycle with a peak in late M/G1 and is regulated by SBF and MBF (Piatti et al. 1995). The E2F transcription factors activate G1/S phase transcription in mammalian cells. E2F family proteins are bound and regulated by the retinoblastoma (RB) family proteins (pRb, p130 and p107), which act as transcriptional corepressors (reviewed in Henley and Dick 2012). In mammalian cells, E2F transcription factors regulate the transcription of Orc1, Cdc6, Cdt1 and MCM proteins (Ohtani et al. 1996; Leone et al. 1998; Ohtani et al. 1998; Yan et al. 1998; Ohtani et al. 1999; Yoshida and Inoue 2004).

1.2.2 CDK phosphorylation

Following the transition to S phase and the initiation of DNA replication, the pre-RC components become targets for CDK phosphorylation. The specific effect of CDK phosphorylation on individual pre-RC components differs between eukaryotic organisms, but the general effect is to inhibit the association of Mcm2-7 with chromatin. This is achieved both by direct inhibition of the licensing reaction and by making the pre-RC components unavailable for licensing through promoting their nuclear export or proteolysis (Section 1.2.3 and 1.2.4 respectively).

The CDK-dependent phosphorylation of ORC subunits contributes to the prevention of re-replication in yeast (Nguyen et al. 2001; Vas et al. 2001; Wuarin et al. 2002). In *S. cerevisiae*, Orc2 and Orc6 are CDK phosphorylation targets (Nguyen et al. 2001). A recent study suggests that the CDK binding and phosphorylation of Orc6 prevents the recruitment and interaction of Cdt1-Mcm2-7 complexes with Orc6, thereby inhibiting the loading of head-to-head double MCM hexamers at ORC-bound origin DNA (Chen and Bell 2011). In *S. pombe*, Orc2 is bound and phosphorylated by Cdc2-Cdc13 in G2 and M phases of the cell cycle, which contributes to the suppression of pre-RC assembly outside of G1 phase (Vas et al. 2001; Wuarin et al. 2002). CDK-dependent phosphorylation of ORC has been observed in *Xenopus* egg extracts and is thought to inhibit ORC chromatin association G2 and M phase (Rowles et al. 1999). In *Drosophila*, Orc1 and Orc2 are CDK phosphorylation targets and CDK activity appears to inhibit both the DNA binding and ATPase activity of ORC (Remus et al. 2005).

1.2.3 Nuclear export

One mechanism by which pre-RC assembly is regulated in *S. cerevisiae* is through the nuclear exclusion of Mcm2-7 and Cdt1. Cdt1 is exported from the nucleus in a CDK-dependent manner in late G1 phase (Tanaka and Diffley 2002). Both G1-CDK and S-CDK activity contribute to the nuclear exclusion of MCM proteins (Labib et al. 1999; Liku et al. 2005). Cdt1 and Mcm2-7 reaccumulate in the nucleus interdependently at the end of mitosis, when CDK activity is low, enabling the proteins to participate in the licensing reaction (Labib et al. 1999; Tanaka and Diffley 2002). CDK-dependent nuclear export of Cdc6 is observed in vertebrates and *Caenorhabditis elegans* (reviewed in Kim and Kipreos 2008). The nuclear export of Cdc6 in *C. elegans* is an important, redundant control against re-replication as co-expression of non-exportable Cdc6 with non-degradable Cdt1 induced re-replication in this organism (Kim et al. 2007). In vertebrates, the role of Cdc6 nuclear export in the control of replication licensing is unclear, as significant fractions of endogenous Cdc6 remain nuclear-localised during S phase (Kim and Kipreos 2008).

1.2.4 Proteolysis

To regulate replication licensing in eukaryotic cells, a number of pre-RC components, including Orc1, Cdc6/Cdc18 and Cdt1, are subject to ubiquitin-mediated proteolysis. In human cells, cell cycle-dependent oscillations in the level of Orc1 are observed, in contrast to Orc2-6 levels, which remain constant throughout the cell cycle (Mendez et al. 2002; Tatsumi et al. 2003). Human Orc1 is targeted for 26S proteasome-mediated degradation at the onset of S phase, following its selective ubiquitylation by the SCF^{Skp2} (*S*kp1-*c*ullin-*F* box) ubiquitin ligase (Mendez et al. 2002; Tatsumi et al. 2003). Cdc6/Cdc18 is an unstable protein in both *S. pombe* and *S. cerevisiae*. CDK-

dependent phosphorylation of Cdc6/Cdc18 at the G1/S phase transition triggers SCF-mediated ubiquitylation and degradation of the protein (Drury et al. 1997; Jallepalli et al. 1997; Kominami and Toda 1997; Jallepalli et al. 1998; Drury et al. 2000). In fission yeast, the $SCF^{Pop1/Pop2}$ ubiquitin ligase mediates the ubiquitylation of Cdc18 following Cdc2-dependent phosphorylation of the protein at the G1/S phase transition (Jallepalli et al. 1997; Kominami and Toda 1997; Jallepalli et al. 1998).

Cdt1 proteolysis occurs in S phase in *S. pombe*, *C. elegans*, *Drosophila*, *Xenopus* and mammals (Nishitani et al. 2001; Zhong et al. 2003; Arias and Walter 2005; Ralph et al. 2006; Lee et al. 2010). A conserved pathway of Cdt1 proteolysis operates in these organisms that is dependent on the $CRL4^{Cdt2}$ ubiquitin ligase (Zhong et al. 2003; Arias and Walter 2006; Jin et al. 2006; Nishitani et al. 2006; Ralph et al. 2006; Senga et al. 2006; Lee et al. 2010). $CRL4^{Cdt2}$ is a member of the cullin-RING (*r*eally *i*nteresting *n*ew *g*ene) E3 ubiquitin ligase (CRL) family and comprises a cullin scaffold (Cul4), an E2-binding RING-finger protein (Rbx1), an adaptor protein (Ddb1) and a substrate recognition subunit (Cdt2) (reviewed in Havens and Walter 2011). The structure and activity of the $CRL4^{Cdt2}$ ubiquitin ligase is discussed further in Section 1.3. An interesting feature of $CRL4^{Cdt2}$-mediated ubiquitylation of Cdt1 is that it is dependent on an interaction between chromatin-bound PCNA and Cdt1 (Arias and Walter 2006; Havens and Walter 2009). Metazoan Cdt1 interacts with PCNA via a specialised PIP box (discussed in detail in Chapter 4) and this interaction is required for the recruitment of $CRL4^{Cdt2}$ and for the subsequent ubiquitylation and proteolysis of Cdt1 (Arias and Walter 2006; Nishitani et al. 2006; Senga et al. 2006; Havens and Walter 2009; Michishita et al. 2011). The specific interaction between chromatin-bound PCNA and Cdt1 elegantly coordinates the destruction of Cdt1 with the onset of DNA

replication. Prior to the work described in this thesis, the role of a Cdt1-PCNA interaction in *S. pombe* Cdt1 regulation had not been examined.

In mammalian cells, Cdt1 is redundantly regulated in S phase by the activity of two E3 ubiquitin ligases: $CRL4^{Cdt2}$ and SCF^{Skp2} (Nishitani et al. 2006). Ubiquitylation of Cdt1 by SCF^{Skp2} occurs in S and G2 phase, following the phosphorylation of Cdt1 by cyclin A-dependent kinases (Li et al. 2003; Liu et al. 2004; Sugimoto et al. 2004; Takeda et al. 2005; Nishitani et al. 2006). Inactivation of both the $CRL4^{Cdt2}$- and SCF^{Skp2}-dependent ubiquitylation pathways is required for the stabilisation of human Cdt1 in S phase cells (Nishitani et al. 2006). Redundancy between the SCF^{Skp2} and $CRL4^{Cdt2}$ pathway in Cdt1 regulation does not appear to be conserved in *S. pombe*, *C. elegans*, *Drosophila* or *Xenopus*, leading to the suggestion that the SCF^{Skp2} regulatory pathway evolved more recently than the $CRL4^{Cdt2}$ pathway (reviewed in Kim and Kipreos 2007).

1.2.5 Inhibition of Cdt1 by geminin

An additional regulatory mechanism for Cdt1, which is present in Metazoa but not in yeast, involves the protein geminin. Geminin interacts with Cdt1 and inhibits the loading of Mcm2-7 onto chromatin (McGarry and Kirschner 1998; Wohlschlegel et al. 2000; Tada et al. 2001). Levels of geminin in the mammalian cell cycle are consistent with its role as a negative inhibitor of licensing; the protein accumulates in S, G2 and M phase but is low in G1 phase owing to its ubiquitylation by the anaphase-promoting complex (APC) at the metaphase-anaphase transition (McGarry and Kirschner 1998; Wohlschlegel et al. 2000). In *Xenopus* egg extracts, a significant proportion of endogenous geminin persists at the exit from mitosis but undergoes

inactivation via a mechanism involving geminin ubiquitylation (Hodgson et al. 2002; Li and Blow 2004).

Crystallographic studies indicate that the central region of geminin, which mediates the interaction with Cdt1, assembles into a parallel coiled-coil homodimer (Lee et al. 2004; Saxena et al. 2004). The N-terminus of this coiled-coil region makes extensive contacts with Cdt1 and it was proposed that the C-terminus of this region might prevent Cdt1 interacting with Mcm2-7 via steric hindrance (Lee et al. 2004). However, subsequent work using *Xenopus* egg extracts demonstrated Cdt1 interacted efficiently with Mcm2-7 when complexed with geminin and a geminin-Cdt1 complex was competent for replication licensing (Lutzmann et al. 2006). Therefore, it was suggested that the geminin-Cdt1 complex might switch between two functional states: one that is active and one that is inhibitory to replication licensing (Lutzmann et al. 2006). This model is supported by structural studies that indicated the human geminin-Cdt1 complex assembles into two distinct structures (De Marco et al. 2009). These include a permissive heterotrimer (comprising one Cdt1 molecule and two geminin molecules) that is able to engage in replication licensing, and an inhibitory heterohexamer (comprising two Cdt1 molecules and four geminin molecules) where key residues required for replication licensing in Cdt1 are concealed. The authors propose that the balance between these distinct geminin-Cdt1 complexes changes depending on the cell cycle stage (De Marco et al. 2009).

A positive role for geminin in the promotion of pre-RC assembly has also been described in human cells (Ballabeni et al. 2004). Complex formation between geminin and Cdt1 has been shown to protect Cdt1 from ubiquitylation and proteolysis,

enabling the protein to accumulate in G2-M phase and participate in replication licensing during the next G1 phase (Ballabeni et al. 2004). The regulation of Cdt1 activity by geminin is important to maintain the genome integrity of metazoan cells. Geminin deficiency in *Drosophila* and human cells results in partial re-replication of the genome (Mihaylov et al. 2002; Melixetian et al. 2004). In *Xenopus* egg extracts, inhibition of Cdt1 activity by geminin and replication-dependent Cdt1 proteolysis function redundantly to prevent genome re-replication (Arias and Walter 2005).

1.2.6 The consequences of licensing factor deregulation

The deregulation of licensing factor activity has severe consequences for eukaryotic cells. Loss of replication control can result in re-replication and in *S. cerevisiae* this has been demonstrated to cause gene copy number increases, which have the potential to induce genome instability (Green et al. 2010). In particular, metazoan cells are sensitive to the deregulation of Cdt1, which is consistent with the multiple, and in some instances redundant, mechanisms employed by these cells to regulate Cdt1 (reviewed in Arias and Walter 2007). There are clinical implications when the control of Cdt1 is abrogated in human cells; in a study of non-small-cell lung carcinomas, overexpression of Cdt1 was observed in 48% of tumours (Karakaidos et al. 2004) and a number of human cancer cell lines exhibit elevated Cdt1 levels (Xouri et al. 2004; Tatsumi et al. 2006). A number of studies have therefore investigated the cellular consequences of Cdt1 overexpression in mammalian cells. Cdt1 overexpression promotes DNA re-replication in human p53-negative malignant cell lines (Vaziri et al. 2003). In primary mammalian cell lines, Cdt1 overexpression does not produce overt re-replication and the ataxia telangiectasia and Rad3 related (ATR)-mediated S phase checkpoint in implicated in the suppression of re-replication (Vaziri et al. 2003;

Liu et al. 2007). Cdt1 overexpression has been shown to induce chromosomal instability in primary human cell lines, which results in aneuploidy (Tatsumi et al. 2006). It has been suggested that Cdt1 deregulation may contribute to the malignant transformation of mammalian cells by predisposing cells to re-replication and chronic genome instability (Seo et al. 2005; Tatsumi et al. 2006).

In fission yeast, constitutive overexpression of Cdt1 or overexpression of Cdt1 in G2-arrested cells does not induce re-replication (Gopalakrishnan et al. 2001; Yanow et al. 2001). However, overexpression of Cdc18 either constitutively or in G2-arrested cells does result in re-replication (Nishitani and Nurse 1995; Yanow et al. 2001). The simultaneous deregulation of Cdc18 and Cdt1 potentiates the re-replication observed when Cdc18 alone is deregulated, suggesting that the negative regulation of both proteins is important to maintain the genome integrity of fission yeast cells (Gopalakrishnan et al. 2001; Yanow et al. 2001). Interestingly, experiments in *Xenopus* egg extracts suggest that although excess Cdt1 can initiate re-replication through inappropriate origin licensing, Cdt1 activity in S phase actually represses the elongation stage of DNA replication (Tsuyama et al. 2009). This may function as a negative feedback mechanism, which operates to limit the extent of re-replication in instances where Cdt1 is inappropriately active (Tsuyama et al. 2009). Thus far, the consequences of an inappropriate increase in licensing activity have been described, however it should be noted that impaired replication licensing also has clinical implications in human cells. Loss-of-function mutations in *ORC1*, *ORC4*, *ORC6*, *CDC6* and *CDT1* have been linked to Meier-Gorlin syndrome, a type of hereditary primordial dwarfism (Bicknell et al. 2011).

1.3 THE STRUCTURE AND ACTIVITY OF CRL4^{CDT2}

As introduced in Section 1.2.4, CRL4^{Cdt2} is a member of cullin-RING E3 ubiquitin ligase family. This family of multi-subunit E3 ubiquitin ligases comprise a catalytic core and a substrate specificity module (Figure 1.3A). The catalytic core consists of a cullin family protein bound through its C-terminal domain to a RING-finger protein (ROC/Rbx1 or 2), which recruits the E2 ubiquitin-conjugating enzyme (reviewed in O'Connell and Harper 2007; Sarikas et al. 2011). There are seven cullin proteins in mammals (Cul1, 2, 3, 4a, 4b, 5 and 7) and three in fission yeast (Pcu1, 3 and 4). The N-terminus of each cullin protein binds a distinct adaptor protein, which in turn interacts with a substrate recognition subunit (SRS) (Table 1.1). The SRS confers substrate specificity on the CRL. The modular nature of the CRLs enables assembly of a large number of substrate-specific E3 ubiquitin ligases, which constitute the largest subfamily of eukaryotic E3 ubiquitin ligases (reviewed in Sarikas et al. 2011). Cul4 is the cullin component of CRL4^{Cdt2} and it mediates an interaction with Ddb1 through its N-terminus and one of the three β-propeller domains in Ddb1 (Figure 1.3B) (Angers et al. 2006). Ddb1 in turn interacts with substrate recognition subunits, termed DCAFs (*D*db1- and *C*ul4- *a*ssociated *f*actors). DCAFs are often WD40 repeat proteins and contain a conserved 'WDXR' or 'DXR' motif, which mediates the interaction with Ddb1 (Angers et al. 2006; Jin et al. 2006). Cdt2 is the DCAF for CRL4^{Cdt2} (Jin et al. 2006).

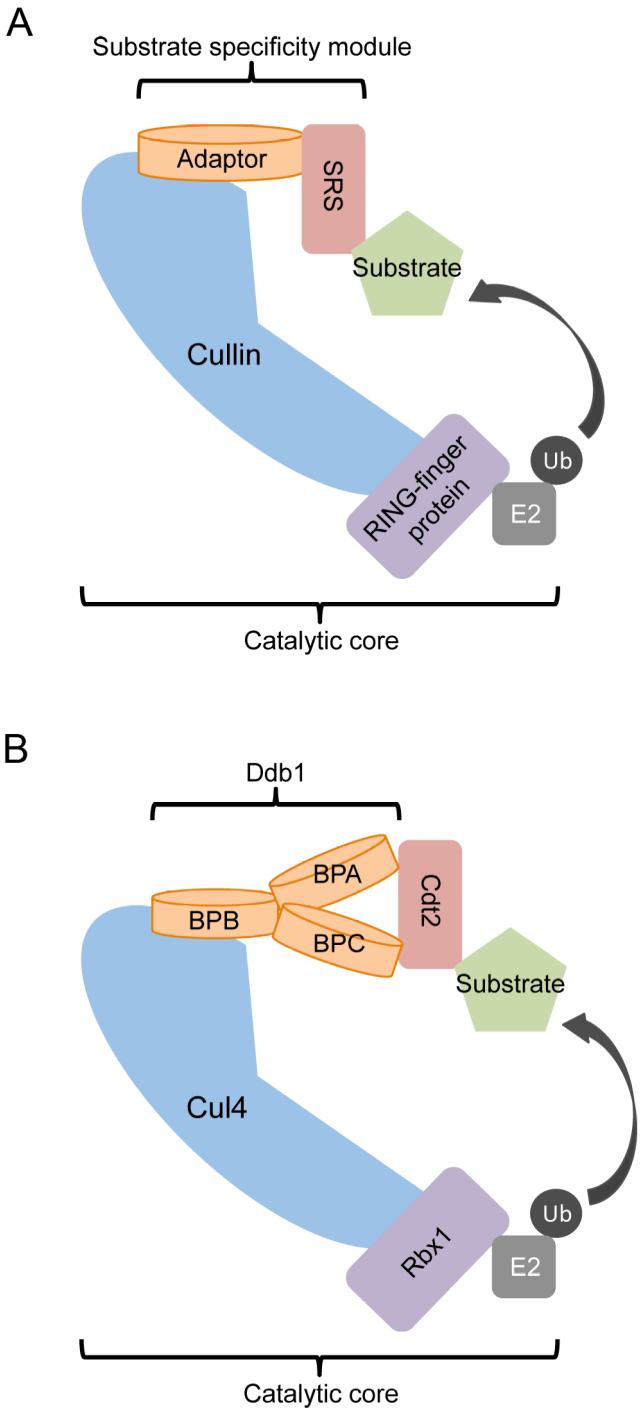


Figure 1.3 | General CRL structure and the specific architecture of CRL4^{Cdt2}.
(A) General structure of a cullin-based E3 ubiquitin ligase. The cullin scaffold interacts at its C-terminus with a small RING-finger protein (ROC/Rbx1/2), which recruits an E2 enzyme to form the CRL catalytic core. The E2 enzyme mediates transfer of ubiquitin (Ub) to the substrate. The cullin protein interacts at its N-terminus with an adaptor protein, which in turn binds a substrate recognition subunit (SRS). The SRS interacts with specific target proteins thereby conferring substrate specificity on the CRL. **(B)** The structure of CRL4^{Cdt2}. In this complex, Cul4 interacts at its N-terminus with the adaptor protein Ddb1 via one of three β-propellor (BP) domains in Ddb1. The other two β-propellor domains in Ddb1 interact with a DCAF protein, in this instance Cdt2, which acts as the SRS. Cul4 interacts at its C-terminus with the RING-finger protein ROC/Rbx1, which in turn recruits an E2 enzyme to form the catalytic core. Adapted from Abbas and Dutta (2011).

Table 1.1 | Mammalian CRL structure

Cullin protein	Adaptor	Substrate recognition subunit	RING protein
Cul1	Skp1	F-box protein	ROC1/Rbx1
Cul2	EloC/EloB	VHL-box protein	ROC1/Rbx1
Cul3	BTB protein	BTB protein	ROC1/Rbx1
Cul4a/4b	Ddb1	DCAF	ROC1/Rbx1
Cul5	EloC/EloB	SOCS-box protein	ROC2/Rbx2
Cul7	Skp1	Fbw8	ROC1/Rbx1

S. pombe Pcu1, Pcu3 and Pcu4 proteins are homologous to mammalian Cul1, Cul3 and Cul4a/4b proteins respectively. Adapted from Sarikas et al. 2011.

The E3 ubiquitin ligase activity of CRLs is modulated by covalent attachment of the ubiquitin-like Nedd8 molecule to the cullin subunit of a CRL. Conjugation of Nedd8 to a cullin (neddylation) simulates CRL ubiquitin ligase activity, possibly by inducing a conformational change in the cullin protein (Wu et al. 2000; Duda et al. 2008). Neddylation of cullin proteins is reversed (deneddylation) by COP9/signalosome (CSN), a conserved and multifunctional eight-subunit complex (Lyapina et al. 2001; Zhou et al. 2001). The deneddylation activity of CSN is associated with a conserved metalloprotease motif in the Csn5 subunit (Cope et al. 2002). Paradoxically, although CSN inhibits CRL function *in vitro*, it promotes CRL activity *in vivo* (reviewed in Cope and Deshaies 2003). The adaptor instability model has been proposed to resolve this paradox (Wee et al. 2005). This model suggests that the inhibitory activity of CSN is required to counterbalance to autocatalytic destruction of SRSs by the CRL, which if uncontrolled would render the CRL inactive. $CRL4^{Cdt2}$ interacts with components of CSN in fission yeast and the CSN complex is implicated in promoting $CRL4^{Cdt2}$ function in this organism (Liu et al. 2003; Liu et al. 2005a).

In addition to mediating the proteolysis of Cdt1 in S phase, the $CRL4^{Cdt2}$ pathway also operates after DNA damage to ubiquitylate Cdt1 and target it for degradation. $CRL4^{Cdt2}$-dependent proteolysis of Cdt1 after DNA damage is conserved and occurs in fission yeast, *Drosophila*, *Xenopus* and mammals (Higa et al. 2003; Higa et al. 2006; Jin et al. 2006; Ralph et al. 2006). PCNA is loaded onto chromatin during DNA repair and the DNA damage-dependent proteolysis of Cdt1 also requires an interaction between chromatin-bound PCNA and Cdt1 in Metazoa (Nishitani et al. 2006; Senga et al. 2006; Havens and Walter 2009). Recent work using human cells and *Xenopus* egg extracts has identified additional components that are required for Cdt1 proteolysis in response to DNA damage (Raman et al. 2011). The AAA+ ATPase p97 and its cofactor UFD1 are implicated in the unfolding of ubiquitylated Cdt1 and its extraction from PCNA/DNA for 26S proteasome-dependent degradation.

In addition to Cdt1, a number of proteins have been identified that are down-regulated in S phase and in response to DNA damage through the $CRL4^{Cdt2}$ pathway (Table 1.2). In certain instances, the timely proteolysis of $CRL4^{Cdt2}$ substrates in S phase and in response to DNA damage serves an important biological function. For example, the S phase-dependent proteolysis of Cdt1, CKI-1 and Pr-Set7/Set8 has been shown to contribute to the prevention of genome re-replication (reviewed in Havens and Walter 2011). The S phase- and DNA damage-dependent proteolysis of Spd1 in *S. pombe* is required to ensure adequate dNTP levels are maintained for replication and repair purposes (Liu et al. 2003; Moss et al. 2010). In response to DNA damage, *C. elegans* Pol η is initially protected from $CRL4^{Cdt2}$-dependent down-regulation by the Gei-17 SUMO E3 ligase (Kim and Michael 2008). This enables Pol η to perform its TLS function in early *C. elegans* embryos. However, reversal of Pol η sumoylation and

subsequent targeting of the protein by $CRL4^{Cdt2}$ is thought to be important in order to remove Pol η from the DNA template and prevent excessive error-prone synthesis (Kim and Michael 2008). $CRL4^{Cdt2}$ is therefore emerging as an important regulator of genome stability in various eukaryotic organisms. However, outstanding questions remain that relate both to the mechanism and function of $CRL4^{Cdt2}$. For example, despite extensive characterisation, the biological function of Cdt1 proteolysis after DNA damage remains uncertain.

Table 1.2 | Eukaryotic $CRL4^{Cdt2}$ substrates

Substrate	Function	Organism	Reference
Spd1	Ribonucleotide reductase (RNR) inhibitor	*S. pombe*	(Liu et al. 2003; Liu et al. 2005a)
p21	Cyclin-dependent kinase inhibitor (CKI)	Humans	(Abbas et al. 2008)
Xic1	CKI	*Xenopus*	(Kim et al. 2010a)
CKI-1	CKI	*C. elegans*	(Kim et al. 2008)
DNA polymerase (Pol) η	TLS DNA polymerase	*C. elegans*	(Kim and Michael 2008)
E2F1	Activator E2F transcription factor	*Drosophila*	(Shibutani et al. 2008)
Pr-Set7/Set8	Histone H4 methyltransferase	Humans	(Jorgensen et al. 2011)

1.4 THE ESSENTIAL MITOTIC FUNCTION OF HUMAN CDT1

Recent work has identified an essential mitotic function for Cdt1 that is independent of its role in DNA replication licensing (Varma et al. 2012). Cdt1 accumulates in G2 phase in human cells and a recent study suggests that phosphorylation of Cdt1 by the mitogen-activated protein (MAP) kinases p38 and c-Jun N-terminal kinase (JNK) is directly responsible for its stabilisation in G2 phase cells (Chandrasekaran et al. 2011). MAP kinase-dependent phosphorylation of Cdt1 inhibits $CRL4^{Cdt2}$-mediated proteolysis of Cdt1 and also reduces its replication licensing activity (Chandrasekaran

et al. 2011). The phosphorylated and low-activity Cdt1 that accumulates in G2 phase is then suitably placed to perform a mitotic role, without inducing the re-licensing of replication origins (Chandrasekaran et al. 2011; Varma et al. 2012).

It should be noted that JNK is a stress-activated MAP kinase, which has also been shown to phosphorylate human Cdt1 in response to non-genotoxic stress, in addition to during an unperturbed G2 phase (Chandrasekaran et al. 2011; Miotto and Struhl 2011). The stress-activated JNK-dependent phosphorylation of Cdt1 inhibits its interaction with HBO1 histone acetylase, resulting in dissociation of HBO1 from replication origins (Miotto and Struhl 2011). HBO1 has previously been described as a coactivator of Cdt1 during replication licensing (Miotto and Struhl 2008; Miotto and Struhl 2010). Therefore, promoting HBO1 dissociation from replication origins through JNK-mediated Cdt1 phosphorylation may serve to down-regulate replication licensing in response to non-genotoxic stress (Miotto and Struhl 2011).

The initial clue that Cdt1 might perform a mitotic function came from the observation that inhibition of Cdt1 function induced a mitotic arrest in human cells (Varma et al. 2012). The same study then demonstrated that human Cdt1 localised to kinetochores during mitosis through an interaction with the Ndc80 complex component Hec1 (Varma et al. 2012). The Ndc80 complex mediates kinetochore-microtubule (kMT) attachments to promote correct chromosome segregation during mitosis. Cdt1 localisation at the kinetochores was shown to be required for stable kMT attachment and it was proposed that binding of Cdt1 to the loop domain of Hec1 promotes a conformational change that is important for the Ndc80 complex to mediate correct kMT attachment (Varma et al. 2012). There is no evidence that the mitotic function of

Cdt1 is conserved in yeast and in *S. pombe* a different protein (Dis1/TOG) has been identified that binds to the loop domain of Hec1 to promote proper kMT attachment (Hsu and Toda 2011).

The mitotic role of Cdt1 may represent a mechanism that enables cells to coordinate mitotic exit with the licensing reaction that occurs in the next G1 phase. In this model, the spindle assembly checkpoint (SAC) might remain activated until sufficient Cdt1 had accumulated for it to perform both its mitotic function and its licensing function in the following G1 phase (Matson and Stukenberg 2012). Cdt1 is not unique in performing a function independent to its role in DNA replication in a higher eukaryote. For example, in vertebrate cells, a role for Orc6 in cytokinesis has been described (Bernal and Venkitaraman 2011), and in mammalian cells, a role for Cdc6 in the suppression of apoptosome assembly and cell death has recently been identified (Niimi et al. 2012). In addition, geminin has an established role in transcriptional regulation and the control of metazoan development (reviewed in Yoshida 2007).

1.5 AIMS OF THIS PROJECT

The correct regulation of Cdt1 is essential to maintain the genome stability of mammalian cells (Tatsumi et al. 2006). Understanding the mechanism by which Cdt1 is down-regulated in the cell cycle is of particular importance as Cdt1 overexpression is suggested to contribute to tumourigenesis and has been observed in certain human tumours and cancer cell lines (Karakaidos et al. 2004; Xouri et al. 2004; Seo et al. 2005). *S. pombe* provides an excellent model for the study of Cdt1 regulation as the $CRL4^{Cdt2}$ pathway that mediates Cdt1 proteolysis is conserved between *S. pombe* and humans. An emerging component of the $CRL4^{Cdt2}$ pathway is PCNA but the

involvement of this factor in *S. pombe* Cdt1 proteolysis has not been addressed. The first aim of this study was to establish if the Cdt1-PCNA interaction was conserved in fission yeast and to what extent it was involved in the regulation of Cdt1 proteolysis in S phase and after DNA damage. The work presented in Chapter 3 and Chapter 4 describes a mutational study of the *cdt1*$^{+}$ sequence, which was undertaken to identify regions of Cdt1 that mediate an interaction with PCNA and are required for CRL4^{Cdt2}-dependent proteolysis. The mutational analysis in Chapter 3 led to the identification of two in-frame AUG codons in the *cdt1*$^{+}$ open reading frame (ORF), which were characterised in detail owing to their unexpected effects on Cdt1 expression.

The coupling of PCNA chromatin-loading and CRL4^{Cdt2}-dependent proteolysis in S phase and after DNA damage is emerging as an important regulatory mechanism for a wide range of proteins that are involved in cell cycle progression and the maintenance of genome stability (reviewed in Havens and Walter 2011). However, a number of outstanding questions remain regarding the mechanism of CRL4^{Cdt2}. The second aim of this study was to identify novel genes involved in Cdt1 regulation, using a genomics approach. It was hoped that findings from this study would be relevant to the regulation of Cdt1 and other CRL4^{Cdt2} targets in higher eukaryotes. Chapter 5 describes the development and implementation of a genome-wide *S. pombe* deletion library screen, which was conducted in order to identify novel genes involved in Cdt1 regulation. Candidate genes of interest that were identified in this screen with elevated Cdt1 levels were characterised further and this work is presented in Chapter 6.

CHAPTER 2

Materials and Methods

General laboratory chemicals were supplied by Sigma-Aldrich, Fisher Scientific or BDH Laboratory Supplies. The media compositions used in this study are described in Appendix I. The *S. pombe* strains and plasmids used in this study are listed in Table 2.1 and Table 2.2 respectively. Further detail on plasmid and *S. pombe* strain construction is provided in Appendix II. The oligonucleotide primers used in this study are detailed in Appendix III. All centrifugations of samples in 5 ml, 15 ml and 50 ml Falcon tubes were performed in an Eppendorf 5810R centrifuge. All centrifugations of samples in Eppendorf tubes (0.6 ml, 1.5 ml and 2 ml) were performed in a Hettich Mikro 200R microcentrifuge. Centrifugations were performed at 4°C, unless otherwise stated.

2.1 *S. POMBE* METHODS

2.1.1 Growth and maintenance of *S. pombe*

Standard *S. pombe* growth and maintenance conditions were used in this study, as previously described (Moreno et al. 1991). Cells were grown in either selective minimal medium (EMM) or non-selective, nutrient-rich medium (YE3S). *S. pombe* strains were stored in the short-term as patches on appropriately-supplemented agar plates at 4°C. Long-term storage of *S. pombe* strains was achieved by freezing cells at -80°C in a 1:1 mix of YE3S and glycerol in Nunc CryoTubes™. Liquid cultures were prepared by inoculating 10 ml of medium with a single freshly grown *S. pombe*

colony. The inoculated culture was incubated overnight in a shaking water bath at the appropriate temperature, and then used to inoculate a larger culture, as appropriate. The absorbance at 595 nm (optical density, OD_{595}) was measured using an Eppendorf Biophotometer to determine the cell concentration of *S. pombe* cultures. Cell concentrations were also determined using a Sysmex F-820 cell counter. Cells were maintained in exponential growth during experiments, at a cell concentration between 2×10^6 and 1×10^7 cells/ml, corresponding to an OD_{595} of between 0.1 and 0.5.

2.1.2 The *S. pombe* strains used in this study

The *S. pombe* strains used in this study are listed below in Table 2.1.

Table 2.1 | *S. pombe* strains used in this study

Strain number	Genotype	Source
138	*ade6-M210 leu1-32 ura4-D18 h⁻*	Lab Stock
1239	*cdt1Δ::ura4+ ade6-m210 leu1-32 ura4-D18 [pREP41X-cdt1⁺] h⁻*	P. Nurse
1262	*cdt1-YFP::KanMX6 ade6-m210 leu1-32 ura4-D18 h⁻*	Lab Stock
1489	*cdt1-18myc h⁻*	Lab Stock
1540	*cdt1-TAP::KanMX6 h⁻*	Lab Stock
1590	*cdt1-YFP::KanMX6 ura4-D18 ade6 leu1-32 h⁺*	Lab Stock
1594	*cdt1-YFP::KanMX6 csn1Δ::ura4 ade6-m210 leu1-32 ura4-D18 h⁻*	Lab Stock
1615	*ddb1Δ::KanMX6 nda3-311 cdt1-18myc h⁺*	Lab Stock
1625	*972 h⁻* wildtype strain	P. Nurse
1698	*cdt2 -YFP::KanMX6 ade6-M216 ura4-D18 leu1-32 h⁺*	Lab Stock
1710	*cdt1-CFP::ura4 cdt2-YFP::KanMX6 ade6 leu1-32 ura4-D18 h⁻*	Lab Stock
1734	*cdt1-CFP::ura4 cdt2-YFP::KanMX6 nda3-311 ura4-D18 leu1-32 h⁻*	Lab Stock
1766	*spd1-TAP::KanMX6 leu1-32 ura4-D18 ade6 h⁺*	C. Lui
1769	*cdt1-YFP::KanMX6 ddb1Δ::KanMX6 h⁺*	Lab Stock
1811	*rad3Δ::ura4 ura4-D18 h⁻*	Lab Stock
1911	*rad26-YFP::KanMX6 leu1-32 ura4-D18 ade6-M210 [pREP3x-cdt1⁺] h⁺*	Lab Stock
1913	*rad26-YFP::KanMX6 leu1-32 ura4-D18 ade6-M210 [pREP3x] h⁺*	Lab Stock
1956	*cdt1-TAP::KanMX6 nda3-311 leu1-32 ura4-D18 h⁻*	Lab Stock
2009	*cdt1-YFP::Hyg ade6-M210 leu1-32 ura4-D18 mat1_m-cyhS, smt-0; rpl42::cyhR (sP56Q) h⁻*	Lab Stock
2070	*cdt1-TAP::KanMX6 nda3-311 ade6-216 leu1-32 ura4-D18 h⁻*	Lab Stock
2127	*mcm4pr::mcm4pr-cdt1(WT)-myc::KanMX6 ade6-m216 leu1-32 ura4-D18 h⁻*	This Study
2128	*mcm4pr::mcm4pr-cdt1(WT)-myc::KanMX6 cdt2Δ::ura4 ade6-m216 leu1-32 ura4-D18 h⁻*	This Study

Strain number	Genotype	Source
2144	*cdt1-TAP::KanMX6 ura4-D18 h*$^{-}$	This Study
2145	*cdt1-TAP::KanMX6 csn1*Δ*::ura4 ura4-D18 h*$^{-}$	This Study
2146	*cdt1-TAP::KanMX6 csn1*Δ*::ura4 cdc25-22 ura4-D18 h*$^{-}$	This Study
2147	*cdt1-TAP::KanMX6 cdc25-22 ura4-D18 h*$^{-}$	This Study
2149	*mcm4pr::mcm4pr-cdt1(control)-myc::KanMX6 ade6-m216 leu1-32 ura4-D18 h*$^{-}$	This Study
2227	*cdc18-YFP::ura4 ura4-D18 h*$^{+}$	Lab stock
2237	*cdt1PIP28*^{A8}*-TAP::KanMX6 nda3-311 h*$^{-}$	Lab stock
2270	*nda3-311 ura4-294 h*$^{-}$	This Study
2302	*ura4::cdt1pr-cdt1(WT)-myc::ura4 nda3-311 ura4-294 h*$^{-}$	This Study
2303	*ura4::cdt1pr-cdt1*Δ*26-100-myc::ura4 nda3-311 ura4-294 h*$^{-}$	This Study
2337	*ura4::cdtpr-cdt1(WT)-YFP::ura4 nda3-311 ura4-294 h*$^{-}$	This Study
2338	*ura4::cdt1pr-cdt1*Δ*26-100-YFP::ura4 nda3-311 ura4-294 h*$^{-}$	This Study
2339	*ura4::cdtpr-cdt1*Δ*26-100-YFP-2xNLS::ura4 nda3-311 ura4-294 h*$^{-}$	This Study
2406	*mcm4pr::mcm4pr-cdt1*Δ*100-myc::KanMX6 ade6-m216 leu1-32 ura4-D18 h*$^{-}$	This Study
2409	*cdt1*Δ*::ura4 cdt1pr::cdt1pr-cdt1-myc::KanMX6 ade6-m210 leu1-32 ura4-D18 [pREP41X-cdt1*$^{+}$*] h*$^{-}$	This Study
2410	*cdt1M23A-YFP nda3-311 ura4-294 h*$^{-}$	This Study
2421	*ura4::cdt1pr-cdt1*Δ*26-200-YFP-2xNLS::ura4 nda3-311 ura4-294 h*$^{-}$	This Study
2422	*ura4::cdt1pr-cdt1*Δ*26-300-YFP-2xNLS::ura4 nda3-311 ura4-294 h*$^{-}$	This Study
2423	*ura4::cdt1pr-cdt1*Δ*26-400-YFP-2xNLS::ura4 nda3-311 ura4-294 h*$^{-}$	This Study
2424	*ura4::cdt1pr-cdt1*Δ*390-444-YFP::ura4 nda3-311 ura4-294 h*$^{-}$	This Study
2425	*ura4::cdt1pr-cdt1(WT)-YFP::ura4 ddb1*Δ*::KanMX6 nda3-311 ura4 h*$^{-}$	This Study
2426	*ura4::cdt1pr-cdt1*Δ*26-100-YFP-2xNLS::ura4 ddb1*Δ*::KanMX6 nda3-311 ura4-294 h*$^{-}$	This Study
2427	*ura4::cdt1pr-cdt1*Δ*26-200-YFP-2xNLS::ura4 ddb1*Δ*::KanMX6 nda3-311 ura4-294 h*$^{-}$	This Study
2428	*ura4::cdt1pr-cdt1*Δ*26-300-YFP-2xNLS::ura4 ddb1*Δ*::KanMX6 nda3-311 ura4-294 h*$^{-}$	This Study
2429	*ura4::cdt1pr-cdt1*Δ*26-400-YFP-2xNLS::ura4 ddb1*Δ*::KanMX6 nda3-311 ura4-294 h*$^{-}$	This Study
2430	*ura4::cdt1pr-cdt1*Δ*390-444-YFP::ura4 ddb1*Δ*::KanMX6 nda3-311 ura4-294 h*$^{-}$	This Study
2431	*ura4::cdt1pr-cdt1*Δ*26-316-YFP-2xNLS::ura4 nda3-311 ura4-294 h*$^{-}$	This Study
2436	*cdt1M1A-YFP nda3-311 ura4-294 h*$^{-}$	This Study
2500	*ura4::cdt1pr-cdt1PIP28*^{A8} *PIP301*^{A10}*-YFP::ura4 ura4-294 nda3-311 h*$^{-}$	This Study
2507	*ura4::cdt1pr-cdt1PIP28*^{A8}*-YFP::ura4 ura4-294 nda3-311 h*$^{-}$	This Study
2513	*ura4::cdt1pr-cdt1PIP301*^{A10}*-YFP::ura4 ura4-294 nda3-311 h*$^{-}$	This Study
2535	*VN173-pcn1-KanMX6 ade6-M216 leu1-32 ura4-D18 h*$^{+}$	Lab Stock
2562	*cdt1-YFP::KanMX6 h*$^{-}$	This Study
2582	*cdt1-YFP::KanMX6 spd1*Δ*::ura4 cdt2*Δ*::ura4 nda3 ade6 leu1-32 ura4-D18 h*$^{-}$	This Study
2595	*cdt2-TAP-KanMX6 ade6 leu1-32 ura4-D18 h*$^{-}$	Lab Stock
2600	*VN173-pcn1::KanMX6 cdt1-VC155::NatMX6 ade6-M216 leu1-32 ura4-D18 h*$^{+}$	This Study
2601	*VN173-pcn1::KanMX6 cdt1-VC155::NatMX6 cdt2*Δ*::ura4 ade6-M216 leu1-32 ura4-D18 h*$^{+}$	This Study

Strain number	Genotype	Source
2602	*VN173-pcn1::KanMX6 cdt1PIP28^{A8}-VC155::NatMX6 cdt2Δ::ura4 ade6-M216 leu1-32 ura4-D18 h^{+}*	This study
2603	*VN173-pcn1::KanMX6 cdt1PIP301^{A10}-VC155::NatMX6 cdt2Δ::ura4 ade6-M216 leu1-32 ura4-D18 h^{+}*	This Study
2604	*VN173-pcn1::KanMX6 cdt1PIP28^{A8} PIP301^{A10}-VC155::NatMX6 cdt2Δ::ura4 ade6-M216 leu1-32 ura4-D18 h^{+}*	This Study
2635	*rhp55Δ::ura4 cdt1-YFP::KanMX6 ura4-D18 leu1-32 ade6 h^{+}*	This Study
2658	*spd1-TAP::KanMX6 rad3Δ::ura4 leu1-32 ura4-D18 h^{+}*	Lab Stock
2698	*spd1-TAP::KanMX6 cdt2-TAP::KanMX6 yox1Δ::KanMX6 ura4-D18 h^{-}*	This Study
2704	*spd1-TAP::KanMX6 cdt2-TAP::KanMX6 ura4-D18 h^{-}*	This Study
2711	*spd1-TAP::KanMX6 yox1Δ::KanMX6 ura4-D18 h^{+}*	This Study
2713	*spd1-TAP::KanMX6 yox1Δ::KanMX6 rad3Δ::ura4 ura4-D18 h^{+}*	This Study
2717	*cdt1-YFP::KanMX6 rhp55Δ::ura4 smt-0 ura4-D18 leu1-32 h^{-}*	This Study
2755	*spd1-TAP::KanMX6 pcn1D122A::Hyg yox1Δ::KanMX6 ura4-D18 h^{+}*	This Study
2774	*cdt1-YFP::KanMX6 rhp55Δ::ura4 ura4-D18 h^{+}*	This Study
2804	*cdt1-YFP::KanMX6 rhp51Δ::his3 his3-D1 h^{+}*	This Study
2829	*cdc18-YFP::ura4 rhp55Δ::ura4 ura4-D18 h^{+}*	This Study
2830	*cdc18-YFP::ura4 rhp55Δ::ura4 ura4-D18 h^{+}*	This Study
2831	*cdt1-CFP::ura4 cdt2-YFP::KanMX6 csn1Δ::ura4 ade6 leu1-32 ura4-D18 h^{-}*	This Study
2844	*cdt2-TAP::KanMX6 csn1Δ::ura4 ura4-D18 leu1-32 ade6 h^{-}*	This Study
2849	*cdt2-YFP::ura4 rhp51Δ::his3 his3-D1 ura4-D18 h^{-}*	This Study
2850	*cdt2-YFP::ura4 rhp51Δ::his3 his3-D1 ura4-D18 h^{-}*	This Study
2862	*ura4::cdt1pr-cdt1-YFP::ura4 ura4-294 h^{-}*	This Study
2864	*ura4::cdt1pr-cdt1 PIP28^{A8} PIP301^{A10}-YFP::ura4 ura4-294 h^{-}*	This Study
2878	*cdt2-YFP::KanMX6 cdc25-22 ura4-D18 h^{-}*	This Study
2881	*cdt2-TAP::KanMX6 csn1Δ::ura4 cdc25-22 ura4-D18 h^{-}*	This Study
2923	*cdt1-YFP::KanMX6 rad3^{ts} h^{+}*	This Study
2925	*cdt1-YFP::KanMX6 rhp55Δ::ura4 rad3^{ts} ura4-D18 h^{-}*	This Study
2928	*cdt1-YFP::KanMX6 rhp51Δ::his3 rad3^{ts} h^{+}*	This Study
3050	*cdt1-TAP::KanMX6 csn1Δ::ura4 nda3-311 leu1-32 ura4-D18 ade6 h^{-}*	This Study
3069	*cdt2-YFP::KanMX6 csn1Δ::ura4 spd1Δ::ura4 ura4-D18 leu1-32 ade6 h^{-}*	This Study
3071	*cdt2-YFP::KanMX6 csn1Δ::ura4 ura4-D18 leu1-32 ade6 h^{-}*	This Study
3075	*cdt2-TAP::KanMX6 csn1Δ::ura4 rad3^{ts} ura4-D18 leu1-32 ade6 h^{-}*	This Study
3084	*cdt1-YFP::KanMX6 csn1Δ::KanMx6 ura4-D18 leu1-32 ade6 h^{+}*	This Study
3086	*cdt1-YFP::KanMX6 csn1Δ::KanMX6 spd1Δ::ura4 ura4-D18 leu1-32 ade6 h^{-}*	This Study
3089	*cdt1-TAP::KanMx6 csn1Δ::KanMx6 rad3^{ts} ura4-D18 h^{-}*	This Study
3101	*cdt2-TAP::KanMX6 pcn1D122A::Hyg ura4-D18 h^{-}*	This Study
3111	*cdt2-TAP::KanMX6 ade6-704 leu1-32 ura4-D18 [pREP3x-cdt1-GFP] h^{+}*	This Study
3113	*cdt2-TAP::KanMX6 ade6-704 leu1-32 ura4-D18 [pREP3x] h^{+}*	This Study
3116	*cdt1-TAP::KanMX6//cdt1-TAP::KanMX6 ura4-D18//ura4-D18 leu1-32//leu1-32 ade6-m210//ade6-m216 h^{+}//h^{-}*	This study
3118	*Hyg::cdt1M23A-TAP::KanMX6//cdt1-TAP::KanMX6 ura4-D18//ura4-D18 leu1-32//leu1-32 ade6-m210//ade6-m216 h^{+}//h^{-}*	This study
3120	*Hyg::cdt1M1A-TAP::KanMX6//cdt1-TAP::KanMX6 ura4-D18//ura4-D18 leu1-32//leu1-32 ade6-m210//ade6-m216 h^{+}//h^{-}*	This study
3131	*ade6-M210 leu1-32 ura4-D18 [pREP3x-Cdt1-GFP] h^{-}*	This Study

Strain number	Genotype	Source
3133	*leu1-32 [pREP3x-cdt1M1A-GFP] h*$^{-}$	This Study
3134	*leu1-32 [pREP3x-cdt1M23A-GFP] h*$^{-}$	This Study
3135	*ura4::cdt1pr-cdt1-YFP::ura4 ddb1∆::KanMX6 spd1∆::ura4 ura4-294 h*$^{-}$	This Study
3136	*cdt1-VC155::NatMX6 ade6-M210 leu1-32 ura4-D18 h*$^{-}$	This Study
3137	*cdt1PIP28*^{A8}*-VC155::NatMX6 ade6-M210 leu1-32 ura4-D18 h*$^{-}$	This Study
3138	*cdt1PIP301*^{A10}*-VC155::NatMX6 ade6-M210 leu1-32 ura4-D18 h*$^{-}$	This Study
3139	*cdt1PIP28*^{A8} *PIP301*^{A10}*-VC155::NatMX6 ade6-M210 leu1-32 ura4-D18 h*$^{-}$	This Study
3140	*cdt1-YFP::KanMX6 rhp51∆::his3 smt-0 his3-D1 h*$^{-}$	This Study
3142	*Hyg::cdt1M1A-TAP::KanMX6 ura4-D18 leu1-32 ade6 h*$^{+}$	This study
3144	*Hyg::cdt1(WT)-TAP::KanMX6 ura4-D18 leu1-32 ade6 h*$^{-}$	This study
3147	*Hyg::cdt1(WT)-TAP::KanMX6//cdt1-TAP::KanMX6 ura4D-18//ura4-D18 leu1-32//leu1-32 ade6-m210//ade6-m216 h*$^{+}$*//h*$^{-}$	This study

2.1.3 Genetic crosses, random spore analysis and tetrad dissection

S. pombe strains of the opposite mating-type were freshly grown up and mixed together in 10 µl of sterile distilled water (SDW) on an EMMG plate, with the appropriate supplements. The cross was incubated at 25°C or 30°C (depending on the presence of temperature-sensitive alleles) for 2-3 days. The presence of asci was confirmed using light microscopy (Section 2.7.1) and progeny of the correct genotype were isolated by random spore analysis or tetrad dissection.

For random spore analysis, a loopful of a 2-3-day old cross was incubated at 30°C overnight in 1 ml of SDW containing 2 µl of *Helix Pomatia* juice (Sepracor) to break down the asci walls and kill any vegetative cells. The spores were washed once with 1 ml of 30% methanol, once with 1 ml of SDW then resuspended in 1 ml of SDW. 1:500 and 1:1000 dilutions were then made in SDW and 100 µl of each dilution was plated onto the appropriate selective media.

For tetrad dissection, a loopful of a 2-3-day old cross was suspended in 98 µl of SDW containing 2 µl of *Helix Pomatia* juice then streaked onto the side of a YE3S plate. The plate was incubated at 30°C for a least 1.5 hours and then the 4 spores were dissected using a micromanipulator (Singer Instruments, MSM). The dissected spores were incubated at an appropriate temperature until colonies became visible and then replica plated to selective media to obtain colonies of the correct genotype.

2.1.4 Diploid construction

The following protocol was used to construct an h^+/h^- sporulating diploid. An *ade6-M210* strain was crossed with an *ade6-M216* strain of the opposite mating-type on an EMMG plate and incubated at 30°C. At 8, 12 and 24 hours after setting up the cross, a loopful of the cross was streaked onto an EMM minus adenine plate and incubated at 32°C. Colonies that grew on the EMM minus adenine plate were re-streaked onto a YE (minus adenine) plate and grown at 32°C for two days. Colonies that grew on the YE plate were subsequently streaked onto a YE3S and an EMM minus adenine plate, which were incubated at 32°C, and EMMG plate, which was incubated at 30°C. The colonies that grew on the EMM minus adenine plate and that sporulated on the EMMG plate were frozen at -80°C from the YE3S plate. The h^+/h^- diploids are unstable and therefore when these strains were re-isolated from frozen stock, adenine prototrophy was always checked.

2.2 *ESCHERICHIA COLI* METHODS

The isolation of plasmid DNA from *E. coli* is described in Section 2.3.2.1 and the calcium chloride-dependent transformation of *E. coli* is described in Section 2.3.3.1. The *E. coli* strain used for the preparation of competent cells in Section 2.3.3.1 was

New England Biolabs (NEB) 5-alpha and had the genotype: *fhuA2* Δ(*argF-lacZ)U169 phoA glnV44* Φ*80*Δ (*lacZ*)M15 *gyrA96 recA1 relA1 endA1 thi-1 hsdR17* (C2988J). Liquid cultures were prepared by inoculating a single freshly grown *E. coli* colony into Luria-Bertani (LB) medium, which contained 100-150 μg/ml of ampicillin (Sigma-Aldrich) where appropriate. Liquid cultures were grown with shaking at 37°C. *E. coli* cells were stored in the short-term at 4°C on LB agar plates.

2.3 DNA METHODS

2.3.1 DNA manipulation

2.3.1.1 Restriction enzyme digest

DNA was digested using restriction enzymes and buffers supplied by NEB. Each reaction was set up as per the manufacturers instructions and generally incubated at 37°C for 2 hours, followed by heat inactivation of the enzyme and visualization of the digested DNA using gel electrophoresis.

2.3.1.2 DNA ligation

A 20 μl ligation reaction that consisted of a 1:3 ratio of digested vector DNA (~100 ng) to insert DNA, 1x T4 DNA ligase buffer and 1.5 μl T4 DNA ligase (NEB) was incubated at room temperature for 4 hours. The T4 DNA ligase was heat inactivated (10 minutes at 65°C) and 10 μl of the ligation reaction used to transform competent *E. coli* cells (Section 2.2.3.1).

2.3.1.3 Polymerase chain reaction (PCR)

PCR reactions were run on a VWR thermal cycler. Colony PCR reactions were performed by adding an amount of yeast approximately equivalent to a colony of 2 mm diameter to a 10 µl reaction containing Red Taq DNA Polymerase Mastermix (VWR) plus 0.1 µM of each forward and reverse primer. For high fidelity PCR reactions, Phusion® polymerase (NEB) was used, with the reaction conditions: 1x GC buffer, 800 µM dNTP mix, 0.5 µM forward and reverse primers, 50 ng template DNA, 3% DMSO, 0.2 mM Mg^{2+} and 1 unit (U) of Phusion® polymerase. Where Phusion® polymerase was used for colony PCR reactions, a small amount of yeast was mixed with 10 µl of 5 mg/ml Zymolyase, incubated at 37°C for 15 minutes and 2 µl of this mixture used as the DNA template in a 50 µl PCR reaction.

The standard PCR conditions used were 5 minutes at 94°C, 30 cycles of 10 seconds at 94°C, 30 seconds at 55°C, 6 minutes at 68°C and a final hold of 7 minutes at 68°C. PCR products were analysed by gel electrophoresis. Where appropriate, PCR products were purified using the QIAquick PCR Purification Kit (Qiagen), as per the manufacturer's instructions.

2.3.2 DNA isolation and analysis

2.3.2.1 Isolation of plasmid DNA from *E. coli*

For small-scale plasmid DNA preparation, a 5 ml culture of *E. coli* was grown in LB medium containing 150 µg/ml of ampicillin overnight at 37°C. Plasmid DNA was extracted using a QIAprep Spin Miniprep Kit (Qiagen), as per the manufacturer's instructions. For larger-scale plasmid DNA preparation, a 50 ml culture of *E. coli* was grown in LB medium containing 150 µg/ml of ampicillin overnight at 37°C. Plasmid

DNA was extracted using the Wizard® Plus Midiprep DNA Purification System (Promega), as per the manufacturer's instructions.

2.3.2.2 Isolation of genomic DNA from *S. pombe*

A 2 ml *S. pombe* culture was grown to saturation and genomic DNA extracted using the MasterPure™ Yeast DNA Purification Kit (Epicentre), as per the manufacturer's instructions.

2.3.2.3 DNA analysis by gel electrophoresis

DNA samples were mixed with 6x loading dye (Fermentas) and loaded onto a 1% agarose gel (VWR) made with 1x TAE (0.04 M Tris-Acetate, 0.01 M EDTA, pH 8.0) and containing 0.5 μg/ml ethidium bromide. GeneRuler™ 1 kb DNA ladder (Fermentas) was included to ascertain DNA sample size and the gel was run at 100 V for 30-40 minutes in a Submerged-Horizontal Electrophoresis System (Bio-Rad) with 1x TAE buffer. The DNA was visualized using an ultraviolet (UV, 302 nm) transilluminator and an image taken with a charge-coupled-device (CCD) camera (Alpha Innotech Corporation).

2.3.3 DNA transformation

2.3.3.1 *E. coli* calcium chloride transformation method

A 40 ml *E. coli* culture was prepared in LB medium using a 1:100 dilution from a saturated overnight culture and incubated at 37°C until the OD_{595} reached 0.5. The cells were transferred to a 50 ml Falcon tube and chilled on ice for 15 minutes then spun at 1811 *g* for 15 minutes. The cell pellet was resuspended in 20 ml of ice-cold 50

mM $CaCl_2$, and left on ice for at least 15 minutes. The cells were re-spun at 1811 *g* for 10 minutes and gently resuspended in 1 ml of ice-cold 50 mM $CaCl_2$. Competent cells could be stored at this stage by adding an equal volume of 50% glycerol and freezing at -80°C.

For transformation of competent *E. coli* cells, 50-100 ng of plasmid DNA was added to 0.2 ml of competent cells in a precooled 2 ml Eppendorf, mixed gently and left on ice for 30 minutes. The mixture was then heat-shocked in a 42°C water bath for 90 seconds and returned to ice, whereupon 1 ml of LB was added and the cells were incubated at 37°C for 1 hour. The cells were spun down at 16089 *g* for 1 minute and the supernatant was partly removed, leaving approximately 200 µl in which the transformed cells were resuspended, and then plated onto two LB agar plates containing 100 µg/ml ampicillin. The transformation plates were incubated at 37°C for approximately 16 hours and any visible colonies were subsequently restreaked to fresh LB agar plates containing 100 µg/ml ampicillin. Where appropriate, ampicillin resistant colonies from the second plate were analysed by colony PCR and restriction enzyme digestion.

2.3.3.2 *S. pombe* lithium acetate transformation method

Method from Bähler et al. (1998). A 20 ml *S. pombe* culture was grown to an OD_{595} of 0.5 in YE3S media at 32°C then centrifuged at 3220 *g* for 2 minutes and washed once with an equal volume of SDW. The cells were resuspended in 1 ml of SDW, transferred to a 2 ml Eppendorf and washed once with 1ml of 1x LiAc/TE (100 mM LiAc, 10 mM Tris-HCl pH 7.5, 1 mM EDTA pH 8.0). Cells were spun down at 1523 *g* for 1 minute and resuspended in 100 µl of 1x LiAc/TE. The cell suspension was

then mixed with 2 µl of sheared carrier DNA (10 µg/ml; Sigma-Aldrich, D7656) and 10 µl of transforming DNA and left at room temperature for 20 minutes. 260 µl of 40% polyethylene glycol (PEG)/LiAc/TE (40% PEG, 100 mM LiAc pH 8.0, 10 mM Tris-HCl pH 7.5, 1 mM EDTA pH 8.0) was then added to the cell suspension, which was mixed gently and then incubated at 30°C for 45-60 minutes. 43 µl of DMSO was then added and the cells were heat shocked in a 42°C water bath for 5 minutes. Cells were spun down at 1523 *g* for 1 minute, washed once with 1 ml of SDW, resuspended in 0.5 ml of SDW, plated onto selective media and then incubated at 32°C for 3-4 days until colonies appeared.

2.3.4 DNA sequencing

A 20 µl sequencing reaction was set up in a 0.2 µl PCR tube with 8 µl of terminator ready mix (20 µl BigDye and 30 µl 5x Sequencing Buffer; Department of Zoology, Oxford), 3.2 pmol of primer, template DNA (200-500 ng if plasmid DNA or 40 ng if linear DNA) and SDW. The sequencing PCR reaction was 35 cycles of 30 seconds at 95°C, 20 seconds at 50°C and 4 minutes at 60°C plus final storage at 4°C. PCR products were processed immediately and transferred to a 1.7 ml Eppendorf tube, containing 55 µl of SDW, 7.5 µl of 3 M NaAc (pH 5.2) and 150 µl of 100% ethanol, then left at room temperature for 15 minutes. The tube was centrifuged at 16089 *g* for 20 minutes, taking care to orientate the tubes so as the position of the DNA pellet could be judged, and the supernatant removed. The DNA pellet was washed twice with 70% ethanol and spun down at 16089 *g* for 2 minutes, enabling the supernatant to be carefully removed. The DNA pellet was then dried at room temperature in a Labcaire PCR workstation for 15 minutes and stored at -20°C until the sample was processed by the sequencing service at the Department of Zoology, Oxford.

2.4 PLASMID CONSTRUCTION

The plasmids that were used and constructed in this study are described in Table 2.2. Further detail on plasmid construction and transformation of the cloned plasmids into *S. pombe* is provided in Appendix II.

Table 2.2 | Plasmids used in this study

Number	Plasmid	Yeast marker	Source
319	pFA6a-*GFP(S65T)*	*KanMX6*	Lab stock
635	pREP3x	*LEU2*	Lab stock
699	pSMHC2+*mcm2*	*Hyg*	Lab stock
740	pSMRY2+*cdt1-YFP*	*KanMX6*	Lab stock
776	pSMRG2+*mcm4pr/cdt1(WT)-myc*	*KanMX6*	Lab stock
780	pSMRG2+*mcm4pr/cdt1(control)-myc*	*KanMX6*	This study
790	pSMRG2+*cdt1pr/cdt1(WT)-myc*	*KanMX6*	This study
798	pSMUG2+*cdt1pr/cdt1(WT)-myc*	*ura4*$^+$	This study
804	pSMUG2+*cdt1pr/cdt1Δ26-100-myc*	*ura4*$^+$	This study
808	pSMRG2+*cdt1pr/cdt1Δ100-myc*	*KanMX6*	This study
818	pSMUY2+*cdt1pr/cdt1-YFP*	*ura4*$^+$	This study
819	pSMUY2+*cdt1pr/cdt1Δ26-100-YFP*	*ura4*$^+$	This study
822	pSMUY2+*cdt1pr/cdt1Δ26-100-YFP-2x NLS*	*ura4*$^+$	This study
827	pSMUY2+*cdt1pr/cdt1Δ26-200-YFP-2x NLS*	*ura4*$^+$	This study
828	pSMUY2+*cdt1pr/cdt1Δ26-300-YFP-2x NLS*	*ura4*$^+$	This study
829	pSMUY2+*cdt1pr/cdt1Δ26-400-YFP-2x NLS*	*ura4*$^+$	This study
832	pSMUY2+*cdt1pr/cdt1Δ390-444-YFP-2x NLS*	*ura4*$^+$	This study
841	pFA6a-*VC155*	*NatMx6*	S. A. MacNeill
846	pSMUY2+*cdt1pr/cdt1M23A-YFP*	*ura4*$^+$	This study
847	pSMUY2+*cdt1pr/cdt1Δ26-316-YFP-2x NLS*	*ura4*$^+$	This study
849	pSMUY2+*cdt1pr/cdt1M1A-YFP*	*ura4*$^+$	This study
855	pSMUY2+*cdt1pr/cdt1PIP28^{A8}-YFP*	*ura4*$^+$	This study
856	pSMUY2+*cdt1pr/cdt1PIP301^{A10}-YFP*	*ura4*$^+$	This study
857	pSMUY2+*cdt1pr/cdt1PIP28^{A8} PIP301^{A10}-YFP*	*ura4*$^+$	This study
883	pFA6a-*cdt1pr/cdt1-VC155*	*NatMx6*	This study
884	pFA6a-*cdt1pr/cdt1PIP28^{A8}-VC155*	*NatMx6*	This study
885	pFA6a-*cdt1pr/cdt1PIP301^{A10}-VC155*	*NatMx6*	This study
886	pFA6a-*cdt1pr/cdt1PIP28^{A8} PIP301^{A10}-VC155*	*NatMx6*	This study
931	pSMH2+*cdt1pr/cdt1(WT)N-terminus*	*Hyg*	This study
932	pSMH2+*cdt1pr/cdt1(M1A)N-terminus*	*Hyg*	This study
933	pSMH2+*cdt1pr/cdt1(M23A)N-terminus*	*Hyg*	This study

Number	Plasmid	Yeast marker	Source
934	pREP3x-*cdt1-GFP*	*LEU2*	This study
935	pREP3x-*cdt1M1A-GFP*	*LEU2*	This study
936	pREP3x-*cdt1M23A-GFP*	*LEU2*	This study
937	pFA6a-*cdt1pr/cdt1-GFP*	*KanMX6*	This study

2.5 OLIGONUCLEOTIDE PRIMERS

Oligonucleotides primers were purchased from Sigma-Aldrich or Eurofins MWG Operon and stored at -20°C in 1x TE buffer (10 mM Tris-HCl pH 8.0, 1 mM EDTA pH 8.0). The oligonucleotide primers used in this study are detailed in Appendix III.

2.6 PROTEIN METHODS

2.6.1 Trichloroacetic acid (TCA) protein extraction

Denatured protein extracts for western blot analysis were prepared by TCA extraction (adapted from Caspari et al. 2000). Samples were kept on ice during this protocol. 15-50 ml samples of exponentially growing fission yeast cells were collected, centrifuged at 3220 *g* for 2 minutes and resuspended in 1.2 M sorbitol. Each sample was transferred to a 2 ml Eppendorf tube, re-spun at 1523 *g* for 2 minutes and the supernatant removed. Note that the cell pellet can be frozen at -80°C at this point for short-term storage. The cell pellet was resuspended in 100 µl of 20% TCA, vortexed briefly and 500 µl of acid-washed fine glass beads (Sigma-Aldrich) were added to the tube. The tube was vortexed for 5 minutes at 4°C in a Vortex-Genie 2 (Scientific Industries), followed by 1 minute resting and then a further 1 minute vortex. 900 µl of 5% TCA was added to the tube, which was vortexed briefly and 800 µl of the sample removed to a new Eppendorf tube and centrifuged at 857 *g* for 10 minutes at 4°C. The

supernatant was removed and the protein pellet was resuspended in 100-250 µl of 1x Laemmli buffer (125 mM Tris-HCl pH 6.8, 5% w/v 2-Mercaptoethanol, 2% w/v sodium dodecyl sulphate (SDS), 0.1% w/v bromophenol blue, 10% w/v glycerol), boiled for 3 minutes and re-spun at 857 *g* for 10 minutes. The protein extract-containing supernatant was transferred to a new Eppendorf tube and stored at -20°C.

2.6.2 SDS-polyacrylamide gel electrophoresis (SDS-PAGE)

Protein samples were separated on SDS-PAGE mini-gels (ATTO Corporation). A 10% running gel was made with 2.5 ml of 40% acrylamide-bis (37.5:1) (Serva), 2.5 ml of 1.5 M Tris-HCl (pH 8.7), 4.8 ml of SDW, 0.1 ml of 10% SDS, 0.1 ml of 10% ammonium persulphate (APS) and 0.01 ml of N,N,N,N-tetramethylethylenediamine (TEMED). The stacking gel was made with 0.625 ml of acrylamide-bis solution, 0.625 ml of 1 M Tris-HCl (pH 6.8), 3.5 ml of SDW, 0.05 ml of 10% SDS, 0.05 ml of 10% APS and 0.005 ml of TEMED. Protein samples were boiled for 3 minutes before being loading onto the gel, which was placed in an electrophoresis chamber (ATTO Corporation) filled with 1x running buffer (10 g/l SDS, 30 g/l Tris, 144 g/l glycine). 5-20 µl of protein sample was loaded per lane and one lane was loaded with 10 µl of Prestained Protein Marker, (broad range, 7-175 kDa; NEB). Each gel was run at 25 mA for approximately 2 hours.

2.6.3 Western blotting

The proteins separated on the SDS-PAGE mini-gels were transferred to an Immobilon-P PVDF (polyvinylidene fluoride) membrane (Millipore) by semi-dry western blotting. The PVDF membrane (8 cm x 10 cm) was immersed in 100% methanol, rinsed in SDW then equilibrated in transfer buffer (48 mM Tris-HCl, 39

mM glycine, 0.04% SDS, 10% methanol) for 2 minutes. A blotting stack was assembled on the lower plate of the semi-dry western blotting apparatus (ATTO Corporation), which consisted of the gel placed on top of the membrane and sandwiched between two triple layers of 3MM chromatography paper (Whatman), which were 8 cm x 10 cm in size and had been pre-soaked in transfer buffer. Any air bubbles were rolled out using a 15 ml Falcon tube and the proteins were transferred to the membrane by electroblotting at 16 V for 1 hour. Ponceau staining (0.1% Ponceau S, 5% acetic acid) was used to confirm protein transfer to the membrane. The membrane was rinsed twice in 1x phosphate buffered saline (PBS; 1 PBS tablet (Oxoid) per 100 ml dH_20) and then blocked in Marvel buffer (5% Marvel in 1x PBS) for 1 hour with shaking.

The membrane was incubated with the relevant antibody, diluted to an appropriate concentration in Marvel buffer, on a rotating plate. Primary antibodies were incubated with the membrane overnight at 4°C or at room temperature for 2 hours. Secondary horseradish peroxidase (HRP)-labelled antibodies were incubated with the membrane at room temperature for 3 hours, with the exception of the anti-mouse secondary antibody for α-tubulin, which was incubated at room temperature for 1 hour. A summary of information relating to the antibodies used in this study is presented in Table 2.3.

Immobilon Western Chemiluminescent HRP Substrate (Millipore) was used for chemiluminescence detection, as per the manufacturer's instructions, and the western blot was imaged using a FluorChem^{TM} 8800 imaging system (Alpha Innotech Corporation) and a CCD camera. Quantitation of band intensity in western blot

images was measured using the spot densitometry analysis tool of the FluorChem™ 8800 imaging system.

Table 2.3 | Antibodies used in this study

Antibody	Type	Dilution	Source
Peroxidase anti-peroxidase (PAP) soluble complex: recognises Protein A moiety of TAP tag.	Affinity isolated antibody, produced in rabbit	1:1000	Sigma-Aldrich, P1291
Anti-GFP	Mouse monoclonal	1:500-1:2000	Roche, 11814460001
Anti-c-Myc	Mouse monoclonal	1:1000	Sigma-Aldrich, M5546
Anti-PCNA	Mouse polyclonal	1:1000	Sigma-Aldrich, P8825
Anti-α-Tubulin	Mouse monoclonal	1:10,000-1:20,000	Sigma-Aldrich, T5168
Peroxidase labeled anti-mouse IgG	Goat monoclonal	1:10,000-1:20,000	Vector Laboratories, PI-2000

2.7 MICROSCOPY METHODS

2.7.1 Light microscopy

Fission yeast cells were visualised using the 40x objective lens of a Zeiss D.Z.Ox. microscope. *S. pombe* cells in liquid culture were viewed by applying 10 µl of culture onto a slide and placing a coverslip over the cell suspension. *S. pombe* cells grown on agar plates were viewed by mixing cells from the plate with 10 µl of SDW on the slide, using a sterile toothpick, and placing a coverslip over the cell suspension.

2.7.2 Fluorescence microscopy

S. pombe cells were viewed using the 100x objective lens of a Zeiss Axioplan 2 imaging microscope. A Hamamatsu ORCA ER camera with Micro-Manager 1.3

software (Edelstein et al. 2010) was used for image capture. Images were recorded from phase, CFP/GFP/YFP/Cherry and DAPI (4,6-diamidino-2-phenylindole, a DNA stain) channels on the microscope. Micro-Manager 1.3 was used for image analysis and Adobe Photoshop 7.0 was used to assemble the microscopy images into figures.

2.7.2.1 Cell fixation using methanol and acetone

Unless otherwise stated, this method was used to prepare cells for fluorescence microscopy. 10 ml samples of exponentially growing fission yeast cells were collected, centrifuged at 3220 *g* for 2 minutes, resuspended in ice-cold methanol and kept on ice for 10 minutes. Samples were then re-spun, resuspended in ice-cold acetone and stored at -20°C. Fixed samples were viewed within 48 hours. To view each sample, 10 µl of concentrated cells in acetone were spread evenly across a microscope slide and 10 µl of agarose mountant was applied (0.6% agarose, 0.1 M Tris-Acetate pH 8.5, 10-50 ng/ml DAPI). A coverslip was gently pressed over the sample and the slide was put at 4°C for the agarose mountant to set before being viewed under the microscope.

2.7.2.2 Septum staining with methyl blue

2 ml samples of fission yeast cells were collected, centrifuged at 1523 *g* for 2 minutes, resuspended in 70% ethanol and stored at -20°C. 10 µl of concentrated fixed cells were spread evenly across a microscope slide and 10 µl of agarose mountant containing methyl blue was applied (0.6% agarose, 0.1 M Tris-Acetate pH 8.5, 10-50 ng/ml DAPI, 0.25 mg/ml methyl blue). A coverslip was pressed gently over the sample and the slide was put at 4°C for the agarose mountant to set. Images were recorded from phase, CFP and DAPI (DNA) channels on the microscope.

2.7.2.3 Live cell fluorescence microscopy

10 ml samples of fission yeast cells were collected and concentrated by centrifugation at 3220 *g* for 2 minutes. The cell pellet was resuspended in 1 ml of YE3S containing 0.1 mM Propyl gallate and re-spun at 1523 *g* for 2 minutes. The majority of the supernatant was removed and 5 µl of the concentrated cell suspension was applied to a slide. An equal volume of 1.2 % low-melting point (LMP) agarose in YE3S/0.1 mM Propyl gallate was immediately mixed with the cell suspension on the slide. A coverslip was gently pressed over the sample and the agarose mountant was allowed to set at room temperature before the slide was viewed under the microscope.

2.7.2.4 Mitochondrion staining with MitoTracker®

MitoTracker® Red CM-H_2XRos (Invitrogen) was added to exponentially growing *S. pombe* cultures to a final concentration of 50 nM. The cultures were protected from light and incubated at 32°C with shaking for 30 minutes. 10 ml samples were collected, centrifuged at 3220 *g* for 2 minutes then washed twice with an equal volume of medium that did not contain the MitoTracker® stain. Samples were then processed for fluorescence microscopy as per the live cell protocol in Section 2.7.2.3. Mitochondria stained with MitoTracker® Red were imaged using a Zeiss Cherry (00) filter set.

2.7.3 Quantitation of nuclear fluorescence intensity

Micro-Manager 1.3 was used to quantitate nuclear YFP fluorescence intensity. A circle with a diameter of 15 pixels was centred over the nuclei of 100 cells and a mean nuclear YFP fluorescence intensity value was calculated. Background fluorescence was subtracted from this value and calculated using an average from five fluorescence

intensity measurements taken across the image field, where cells were not present. Comparative data was collected in a single session.

2.8 UV METHOD

For the UV irradiation of fission yeast cells, 100 ml of an exponentially growing culture, between an OD_{595} of 0.2-0.5, was collected and washed once with an equal volume of SDW. *S. pombe* cells were always UV irradiated in SDW to prevent the absorption of UV wavelengths by the yeast media. The cells were resuspended in 100 ml of SDW and transferred to a 140 mm petri dish (Sterilin), which was stirred rapidly and irradiated with a UV dose of 100 J/m^2, 254 nm UV (4W UV-C bulb, Sylvania, Japan), as measured with a radiometer (RS-245, UVItec). Following UV irradiation, cells were collected in new 50 ml Falcon tubes, centrifuged at 3220 *g* for 2 minutes and resuspended in the appropriate media and the relevant samples taken.

2.9 FLOW CYTOMETRY

The DNA content of individual *S. pombe* cells was measured by flow cytometry. Approximately 1 x 10^7 cells were collected and centrifuged at 3220 *g* for 2 minutes, then fixed in 1ml of 70% ethanol and stored at -20°C. To process a sample for flow cytometry, approximately 2 x 10^6 cells were added to a 5 ml Falcon tube, containing 4.5 ml of 10 mM EDTA (pH 8.0), briefly vortexed and then centrifuged at 1811 *g* for 5 minutes. The cell pellet was resuspended in 0.5 ml of 10 mM EDTA (pH 8.0) containing 0.1 mg/ml RNaseA (10 mM Tris-HCl pH 7.5, 15 mM NaCl, 10 mg/ml RNaseA; Roche Diagnostics Ltd.) and incubated at 37°C for at least 2 hours or overnight. Following the RNA digest, the cellular DNA was stained by adding 0.5 ml of 10 mM EDTA (pH 8.0) containing 2 μM Sytox Green (Invitrogen) to each 5 ml

Falcon tube. Each sample was sonicated for 10 seconds (MSE Sanyo Soniprep 150) then processed on an EPICS XL-MCL flow cytometer (Beckman-Coulter). Listmode files were analysed using WinMDI 2.8 (http://facs.scripps.edu/software.html).

2.10 *S. POMBE* DELETION LIBRARY METHODS

2.10.1 Fluorescence-based screening methods

2.10.1.1 Flow cytometry

Exponentially growing cells cultured in either YE3S or EMM media were collected live, fixed in ice-cold methanol or fixed in ice-cold methanol and acetone. Cells were washed twice in SDW then resuspended in 1 ml SDW, 0.2 ml of which was added to 4.5 ml of 10 mM Tris-Acetate (pH 8.5) in a 5 ml polystyrene Falcon tube. The tubes were inverted and centrifuged at 1811 *g* for 5 minutes, the supernatant removed and the cell pellet was resuspended in 1 ml of 0.1 M Tris-Acetate (pH 8.5). Cells were sonicated for 10 seconds and then analysed on an EPICS XL-MCL flow cytometer.

2.10.1.2 Medium-throughput fluorescence microscopy-based screening protocol

The strains to be screened were re-isolated from frozen stock by defrosted a 96-well master plate and using a multi-channel pipette to transfer 5 µl of each strain to two YE3S agar plates. The plates were incubated at 30°C for two days until yeast colonies were visible. An 8 x 6 pinned replicator was used to transfer each strain to a 96 well plate, where each well contained 150 µl of SDW. Once thoroughly mixed, the diluted cell cultures were transferred to two fresh YE3S plates and incubated overnight for 14 hours at 30°C, after which time the cells were approximately in log phase. Using a 12 well slide, a small amount of each strain was mixed with 5 µl of SDW, containing

0.1% Triton-X-100 (to reduce surface tension) in each well. The slides were left to dry, immersed in 100% ice-cold ethanol for 10 seconds, removed and left to dry for 5 minutes at room temperature. The slides were then immersed in 100% ice-cold acetone for 1 minute, removed and left to dry for 5 minutes at room temperature. The fixed cells could be stored at -20°C for several hours until ready to view. When required for viewing, each slide was mounted by applying 3 µl of agarose mountant (0.6% agarose, 0.1 M Tris-Acetate pH 8.5, 0.5 ng/ml DAPI) to each well. A 22 x 50 mm coverslip was firmly pressed over the slide, which was placed at 4°C for 5 minutes to set the DAPI/agarose mountant.

2.10.2 Use of the PEM-2 system to cross Cdt1-YFP into the deletion library

Cdt1-YFP strain 2009, containing the PEM-2 anti-diploid and mating-type selection system, was crossed to the haploid *S. pombe* deletion library in three attempts. Carol Walker performed the initial cross, using a RoTaR HDA screening robot (Singer Instruments). Correct progeny were selected on YE6S agar plus either 100 µg/ml cycloheximide to select against diploid and unmated parental cells; 200 µg/ml hygromycin B to select for Cdt1-YFP; or 200 µg/ml geneticin to select for the gene deletion. However, 27% of the *S. pombe* deletion library strains were lost during this initial cross. The missing strains were woken up by hand, transferred into a 96-well plate format and then crossed using the RoTaR HDA pinning robot. The correct progeny were selected for as above. Strains still found to be missing were crossed by hand and the final 3% that failed to cross in this third attempt were excluded from the analysis.

CHAPTER 3

Characterisation of Two In-frame Methionine Codons in *S. pombe* Cdt1

3.1 INTRODUCTION

Metazoan Cdt1 contains a conserved PIP box in the N-terminus of the protein, which mediates the interaction between Cdt1 and PCNA, and is required Cdt1 ubiquitylation by $CRL4^{Cdt2}$ (Arias and Walter 2006; Nishitani et al. 2006; Senga et al. 2006). Fission yeast Cdt1 has a partial match to the PIP box consensus sequence in the N-terminus of the protein (Figure 3.1A, page 64) but the involvement of this motif in the $CRL4^{Cdt2}$-dependent regulation of Cdt1 has not been addressed. The initial aim of this chapter was to investigate the role of this putative PIP box in Cdt1 regulation, through construction of an N-terminal truncation mutant. However, deletion of the N-terminal 100 amino acids of *S. pombe* Cdt1 resulted in a dramatic reduction in protein levels, which necessitated a change of strategy.

Subsequent investigation indicated the presence of a second in-frame methionine (AUG) codon in the $cdt1^{+}$ ORF, downstream of the documented initiator codon, which was required to maintain wildtype protein levels and cell viability (Figure 3.2, page 67). This chapter presents evidence that *S. pombe* Cdt1 is mainly expressed from the second in-frame AUG codon, which corresponds to a methionine at residue 23 of the full-length encoded protein. Establishment of the correct initiator codon in Cdt1

provided the foundations for a subsequent mutational study into the regulatory regions of the protein, which is presented in Chapter 4.

3.2 RESULTS

3.2.1 The N-terminus of Cdt1 contains a putative PIP box and is required to maintain wildtype protein levels

The N-terminus of *S. pombe* Cdt1 contains a partial match to the PIP box consensus sequence, which begins at amino acid 28 and consists only of the glutamine and the hydrophobic amino acid at positions one and four of the PIP box respectively (Figure 3.1A). Given the involvement of an N-terminal PIP box in metazoan Cdt1 proteolysis (Arias and Walter 2006; Nishitani et al. 2006; Senga et al. 2006), the N-terminal 100 amino acids of fission yeast Cdt1, which contain the putative PIP box, were deleted to determine if degradation of the protein was inhibited.

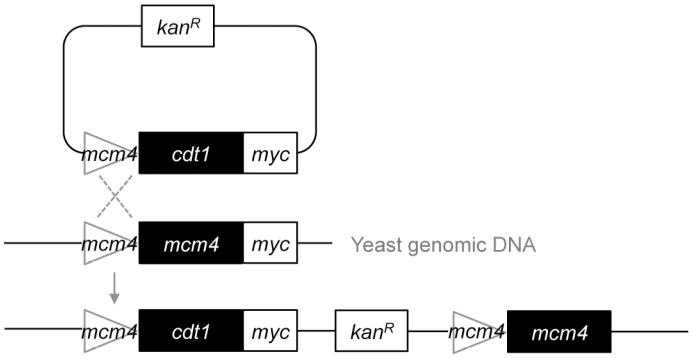
Fission yeast Cdt1 protein levels are determined by periodic expression of the gene in late M-G1 phase and proteolysis of the gene product in S phase (Hofmann and Beach 1994; Nishitani et al. 2000). To focus on the effect of the N-terminal truncation on Cdt1 proteolysis, full-length Cdt1 and the N-terminal truncation mutant were expressed from the constitutive *mcm4* promoter (Coxon et al. 1992), as opposed to the native and periodic *cdt1* promoter, for straightforward interpretation of protein levels. In brief, full-length and N-terminally truncated *cdt1* sequences were amplified as *Xho*I/*Nhe*I fragments and inserted into a *mcm4pr/cdt1(WT)-myc* plasmid to produce *cdt1(control)-myc* and *cdt1Δ100-myc* plasmids (Appendix II, 1). The *cdt1(control)* sequence differs from the *cdt1(WT)* sequence in that it lacks a 31 bp intervening sequence between the *Xho*I site and the endogenous initiator codon. The sequence

A

PIP box: QxxΨxxϑϑ

S. pombe Cdt1: ^{28}**Q**TK**L**NFSV^{35}

B



C

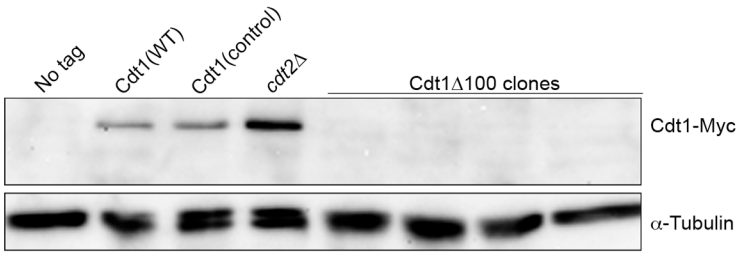


Figure 3.1 | Deletion of the N-terminal 100 amino acids of Cdt1 reduces the log phase protein level.

(A) Sequence of the putative N-terminal PIP box in *S. pombe* Cdt1 (Ψ: hydrophobic residue, ϑ: aromatic residue, x: any residue). **(B)** Plasmids containing *cdt1(WT)* (p776), *cdt1(control)* (p780) and *cdt1Δ100* (p808) sequences were integrated as a second copy at the endogenous *mcm4* promoter to produce Myc-tagged Cdt1(WT), Cdt1(control) and Cdt1Δ100 strains respectively. **(C)** Western blot analysis of exponentially growing non-tagged (138) cells, cells expressing Cdt1(WT)-Myc in wildtype (2127) or *cdt2Δ* (2128) backgrounds, and cells expressing Cdt1(control)-Myc (2149) or Cdt1Δ100-Myc (2406).

AAAATG was included downstream of the *Xho*I site in both the *cdt1(control)* and *cdt1Δ100* sequences to optimise utilisation of the initiator codon (Kozak 1986). *cdt1*$^{+}$ is an essential gene and it was unclear what effect the N-terminal truncation would have on protein function (Hofmann and Beach 1994). Therefore, the *cdt1(WT)*, *cdt1(control)* and *cdtΔ100* plasmids were integrated as a second copy at the *mcm4* promoter, in a *cdt1*$^{+}$ wildtype background (Figure 3.1B).

To examine the effect of the N-terminal truncation on Cdt1 regulation, the level of Cdt1 in cells expressing Cdt1(WT)-Myc, Cdt1(control)-Myc and Cdt1Δ100-Myc was compared by western blot analysis. Cdt1(WT) and Cdt1(control) levels were comparable, indicating that cloning the *cdt1* sequence as a *Xho*I/*Nhe*I fragment did not affect the protein level (Figure 3.1C). As expected, the level of Cdt1(WT) in the *cdt2*Δ background was higher than in the wildtype background, as Cdt1 was not ubiquitylated and degraded via the CRL4^{Cdt2} pathway (Ralph et al. 2006). Unexpectedly, in cells expressing Cdt1Δ100-Myc, no band corresponding to the truncated Cdt1 protein could be detected. Four different clones from the original *mcm4pr/cdt1Δ100-myc* transformation were analysed by western blot and none exhibited detectable Cdt1Δ100-Myc levels (Figure 3.1C). This suggests that deletion of the N-terminus of Cdt1 results in reduced gene expression and/or destabilisation of the gene product.

3.2.2 Analysis of two in-frame methionine codons in *S. pombe* Cdt1

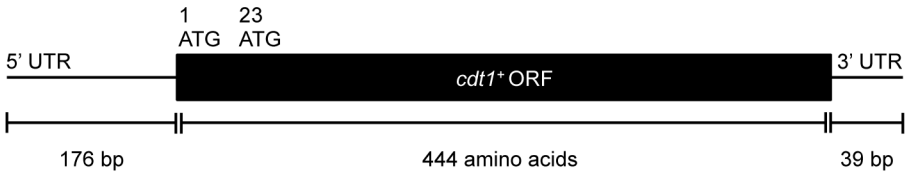
The initial paper describing Cdt1 isolated and sequenced the *S. pombe cdt1*$^{+}$ cDNA, which was 1556 bp in length and contained a single ORF of 444 amino acids, with a 5' untranslated region (UTR) of 176 bp (Hofmann and Beach 1994). Interestingly, in

addition to the described initiator codon, there is a second in-frame AUG codon that corresponds to amino acid 23 in the encoded protein (Figure 3.2A). An alignment of Cdt1 from four *Schizosaccharomyces* species indicated that the extreme N-terminus of *S. pombe* Cdt1, up to the methionine at amino acid 23 is poorly conserved (Figure 3.2B) (Heringa 1999). In light of the improved conservation of the *S. pombe* Cdt1 protein sequence downstream of methionine 23, it was speculated that the second in-frame AUG codon might represent the initiator codon. Attempting to force expression from the first in-frame AUG codon in the Cdt1Δ100 mutant (through deletion of the second AUG codon) may have been ineffective, resulting in the undetectable protein levels documented in Figure 3.1C.

To determine which in-frame AUG codon was required for Cdt1 expression, each was mutated to GCT (thereby replacing methionine with alanine in the encoded protein) and the effect of the mutation on cell cycle Cdt1 protein levels was examined. The first and second in-frame AUG codons were mutated to GCT in a *cdt1pr/cdt1-YFP* plasmid to produce *cdt1M1A* and *cdt1M23A* sequences respectively (Appendix II, 2; Figure 3.3A). As the consequence of each mutation on protein function was unclear, the wildtype, *cdt1M1A* and *cdt1M23A* sequences were integrated as a second copy at the *ura4*$^+$ locus, in a *cdt1*$^+$ wildtype background.

To analyse the effect of each mutation on the localisation and level of Cdt1, exponentially growing cells expressing Cdt1M1A-YFP or Cdt1M23A-YFP were compared to cells expressing wildtype Cdt1-YFP by fluorescence microscopy. In wildtype cells, Cdt1 was detected in the nuclei of approximately 30% of binucleate

A



B

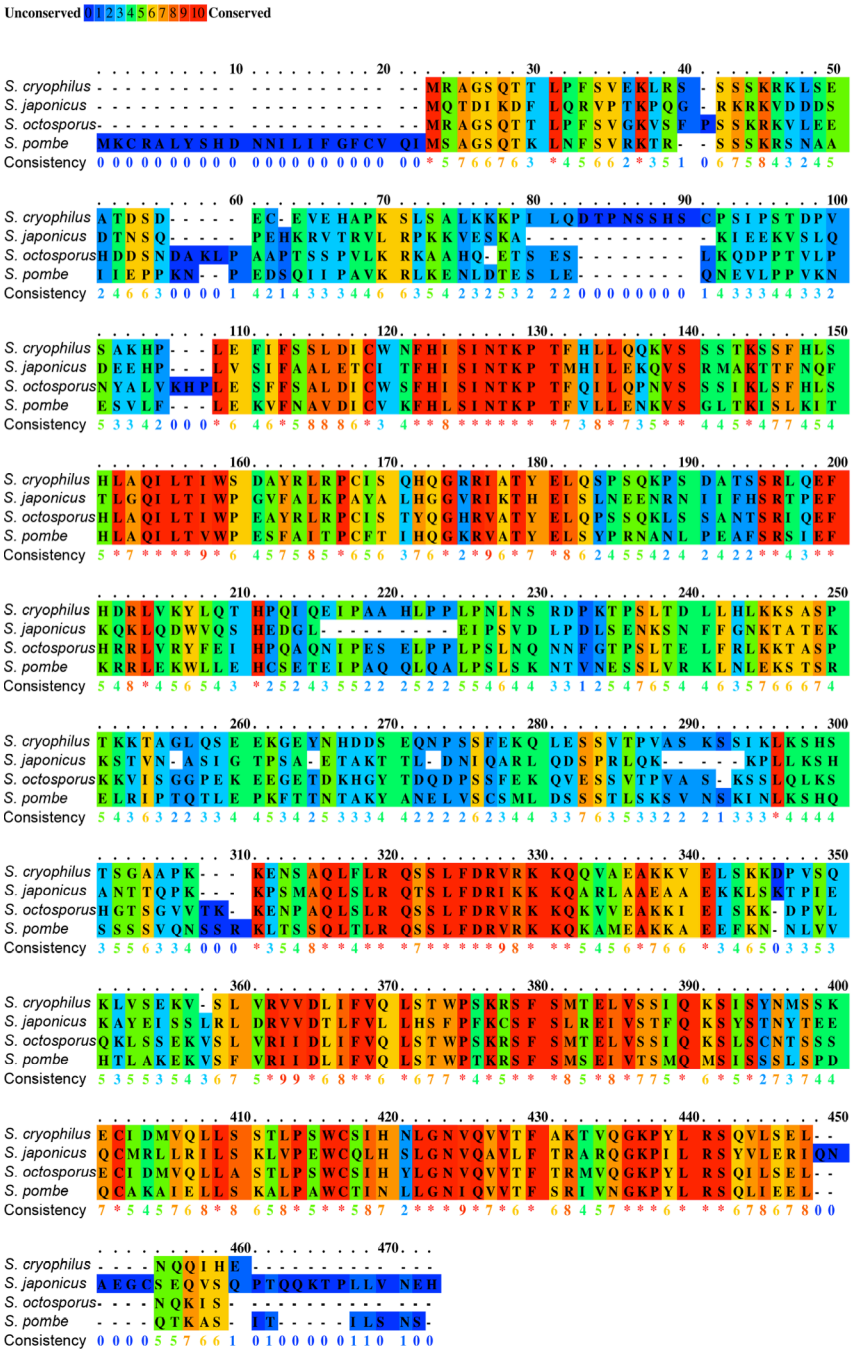


Figure 3.2 | The *cdt1*⁺ ORF contains two in-frame methionine codons.
(A) The structure of the *cdt1*⁺ cDNA, from the PomBase database (Wood et al. 2012). **(B)** A PRALINE alignment (Heringa 1999) of Cdt1 protein sequences from *S. cryophilus*, *S. japonicus*, *S. octosporus* and *S. pombe*.

A

```
Cdt1 WT   MKCRALYSHDNNILIFGFCVQIMSAGSQTKLNFSVRKTRS
Cdt1M1A   AKCRALYSHDNNILIFGFCVQIMSAGSQTKLNFSVRKTRS
Cdt1M23A  MKCRALYSHDNNILIFGFCVQIASAGSQTKLNFSVRKTRS
```

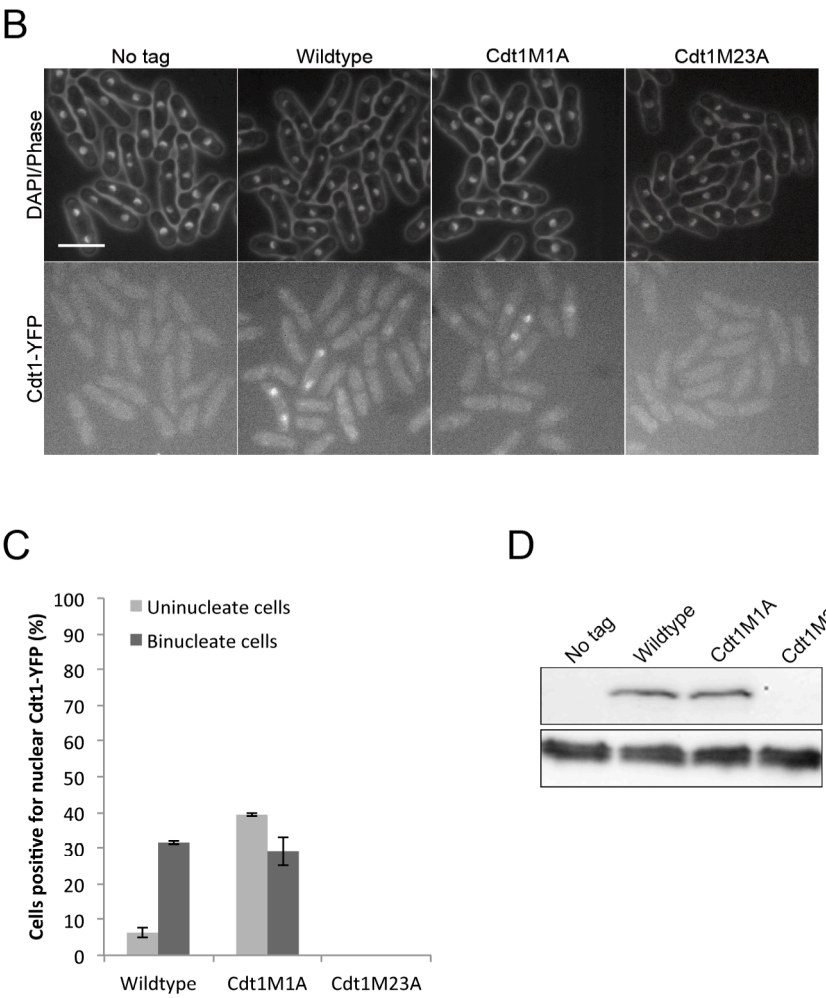


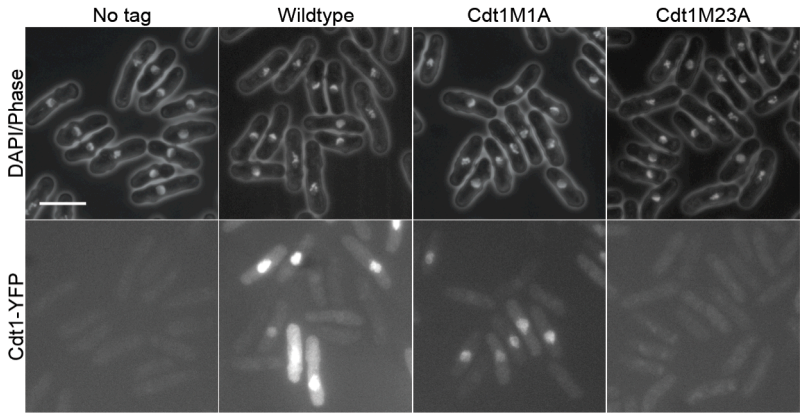
Figure 3.3 | Mutational analysis of the two in-frame AUG codons in *S. pombe* Cdt1
(A) An alignment of the N-terminus of wildtype Cdt1 with the Cdt1M1A and Cdt1M23A mutants. **(B)** Cdt1-YFP imaged in exponentially growing cells in non-tagged (2270) or wildtype (2337) strains and in Cdt1M1A (2436) or Cdt1M23A (2410) mutant strains. Scale bar: 10 μm. **(C)** The strains in (B) were analysed to determine the percentage of uninucleate and binucleate cells positive for nuclear Cdt1-YFP. At least 100 cells, from two independent experiments, were counted for each data point. Error bars: 50% of range. **(D)** Western blot analysis of Cdt1-YFP levels in exponentially growing samples of the strains described in (B).

cells (Figure 3.3B and C). A similar proportion of binucleate cells were positive for nuclear Cdt1M1A as in the wildtype strain, although Cdt1M1A was detected in the nuclei of an increased number of uninucleate (G2/early M phase cells) cells and the reason behind this was unclear (Figure 3.3B and C). In contrast, no nuclear Cdt1M23A signal was detected in any binucleate or uninucleate cells (Figure 3.3B and C). This result was confirmed by western blot analysis; no band corresponding to Cdt1M23A-YFP could be distinguished, although the Cdt1M1A-YFP protein level and size was similar to wildtype (Figure 3.3D).

To extend the observations made in exponentially growing cells, wildtype, Cdt1M1A and Cdt1M23A cells were arrested in prometaphase using the *nda3-311* mutation in β-tubulin (Hiraoka et al. 1984). At the restrictive temperature, *nda3-311* cells are unable to form a mitotic spindle and activate the spindle checkpoint, arresting in mitosis and accumulating a high level of Cdt1 due to continued transcription (He et al. 1997; Ralph et al. 2006). If a low-level of Cdt1M23A expression occurs, it is more likely to be detected under this condition than in exponentially growing cells, which are predominantly in G2 phase and therefore not actively transcribing $cdt1^{+}$ (Hofmann and Beach 1994).

To this end, *nda3-311* cells expressing YFP-tagged wildtype Cdt1, Cdt1M1A or Cdt1M23A were incubated at the restrictive temperature of 20°C for 4 hours to arrest cells in prometaphase. Fluorescence microscopy and western blot analysis indicated that wildtype Cdt1 and Cdt1M1A accumulated to a high level in the arrested cells, although unexpectedly the level of Cdt1M1A in the arrested cells was lower than wildtype Cdt1 (Figure 3.4A and B). Strikingly, no accumulation of Cdt1M23A was

A



B

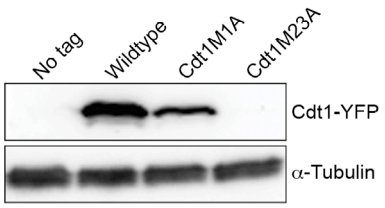


Figure 3.4 | Analysis of the Cdt1M1A and Cdt1M23A mutants in mitotically-arrested cells. **(A)** Cdt1-YFP imaged in prometaphase-arrested *nda3-311* cells in non-tagged (2270) or wildtype (2337) strains and in Cdt1M1A (2436) or Cdt1M23A (2410) mutant strains. Scale bar: 10 μm. **(B)** Western blot analysis of Cdt1-YFP levels in prometaphase-arrested samples of the strains described in (A). *nda3-311* cells were arrested in prometaphase by incubating the cultures at 20°C for 4 hours.

detected in the arrested cells (Figure 3.4A and B), suggesting that the second in-frame AUG codon is required to maintain Cdt1 protein levels.

3.2.3 The second in-frame AUG codon is essential for cell viability

Mutation of the second in-frame AUG codon to GCT dramatically reduced Cdt1 protein levels and given *cdt1*$^{+}$ is an essential gene, this reduction in protein levels might be lethal to the cell. To investigate the effect of the M1A and M23A mutation on cell viability, each mutation was introduced into a diploid strain and the viability of the haploid spores was analysed by tetrad dissection. The M1A or M23A mutation was introduced into a *cdt1pr/cdt1(N-terminus)* plasmid and integrated as a single copy at the endogenous *cdt1*$^{+}$ locus in a diploid strain (Appendix II, 3; Figure 3.5A).

Hygromycin B resistant diploid strains, which were heterozygous for the integrated *cdt1pr/cdt1(N-terminus)* plasmid were isolated, sporulated and the products of meiosis separated by tetrad dissection (Figure 3.5B). Diploid cells transformed with the *cdt1(WT)* or *cdt1M1A* sequence generally produced four viable spores, which segregated 2:2 for hygromycin B resistance to sensitivity. In contrast, diploid cells transformed with the *cdt1M23A* sequence produced a maximum of two viable spores, which were never hydromycin B resistant, indicating that the M23A mutation is lethal when introduced into fission yeast cells without a wildtype copy of *cdt1*$^{+}$.

Haploid Cdt1(WT) and Cdt1M1A cells, produced from the diploid transformation and subsequent sporulation, were analysed to determine if the single copy Cdt1M1A mutant displayed a phenotype. Western blot analysis of exponentially growing cells expressing wildtype Cdt1-TAP or Cdt1M1A-TAP suggested that the Cdt1M1A

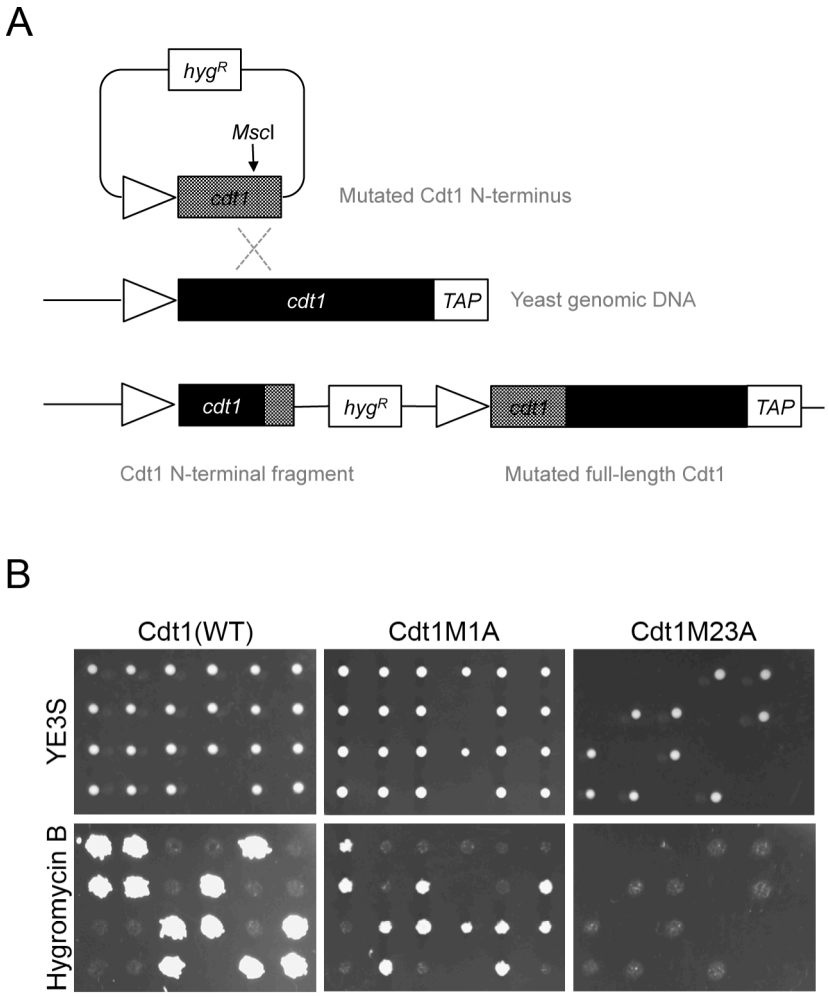


Figure 3.5 | The effect of the Cdt1M1A and Cdt1M23A mutation on cell viability.
(A) Plasmids containing *cdt1(WT)* (p931), *cdt1M1A* (p932) and *cdt1M23A* (p933) N-terminal sequences were integrated at the endogenous *cdt1*$^{+}$ locus of a diploid strain (3116) to produce TAP-tagged Cdt1(WT) (3147), Cdt1M1A (3120) or Cdt1M23A (3118) diploid strains respectively. **(B)** The diploid transformants described in (A) were sporulated and the products of meiosis separated by tetrad dissection to analyse the viability of the M1A and M23A mutation. The colonies were replica plated to YE3S agar containing 200 μg/ml hygromycin B to select for hygromycin B resistant cells that contained the integrated plasmid.

protein level and size was identical to wildtype (Figure 3.6A). Equally, the flow cytometry profiles from exponentially growing wildtype cells and the Cdt1M1A mutant were similar (Figure 3.6B). Finally, spot test analysis was used to compare the growth of the Cdt1M1A mutant with wildtype cells during normal growth conditions (Figure 3.6C 'YE3S') and following exposure to different forms of DNA damage, including UV-irradiation and treatment with the RNR inhibitor hydroxyurea (HU) or the radiomimetic bleomycin (Figure 3.6C 'UV', 'HU' and 'Bleomycin'). In each situation, growth of the Cdt1M1A mutant was indistinguishable from wildtype. The *rad3*Δ mutant was included as a positive control for cell sensitivity to DNA damage. *rad3*$^+$ is the homologue of *S. cerevisiae MEC1* and human *ATR*. It is a member of the phosphoinositide 3-kinase (PI3K) superfamily and acts as the master checkpoint regulator in *S. pombe* cells (reviewed in Melo and Toczyski 2002). The level and size of the Cdt1M1A protein and the phenotype of the Cdt1M1A mutant is therefore identical to wildtype, while the Cdt1M23A mutant is inviable. This suggests the second in-frame AUG codon represents the principal initiator codon for endogenous Cdt1 expression.

3.2.4 Analysis of wildtype Cdt1 and the Cdt1M1A and Cdt1M23A mutant proteins when overexpressed

Interestingly, non-tagged Cdt1 expressed from the thiamine-repressible *nmt1* promoter is always detected as a double band by western blot (Figure 3.7A). Based on this observation, we hypothesised that expression of Cdt1 from the *nmt1* promoter might alter the context of the first AUG codon, permitting translation initiation from both in-frame AUG codons in the *cdt1*$^+$ mRNA.

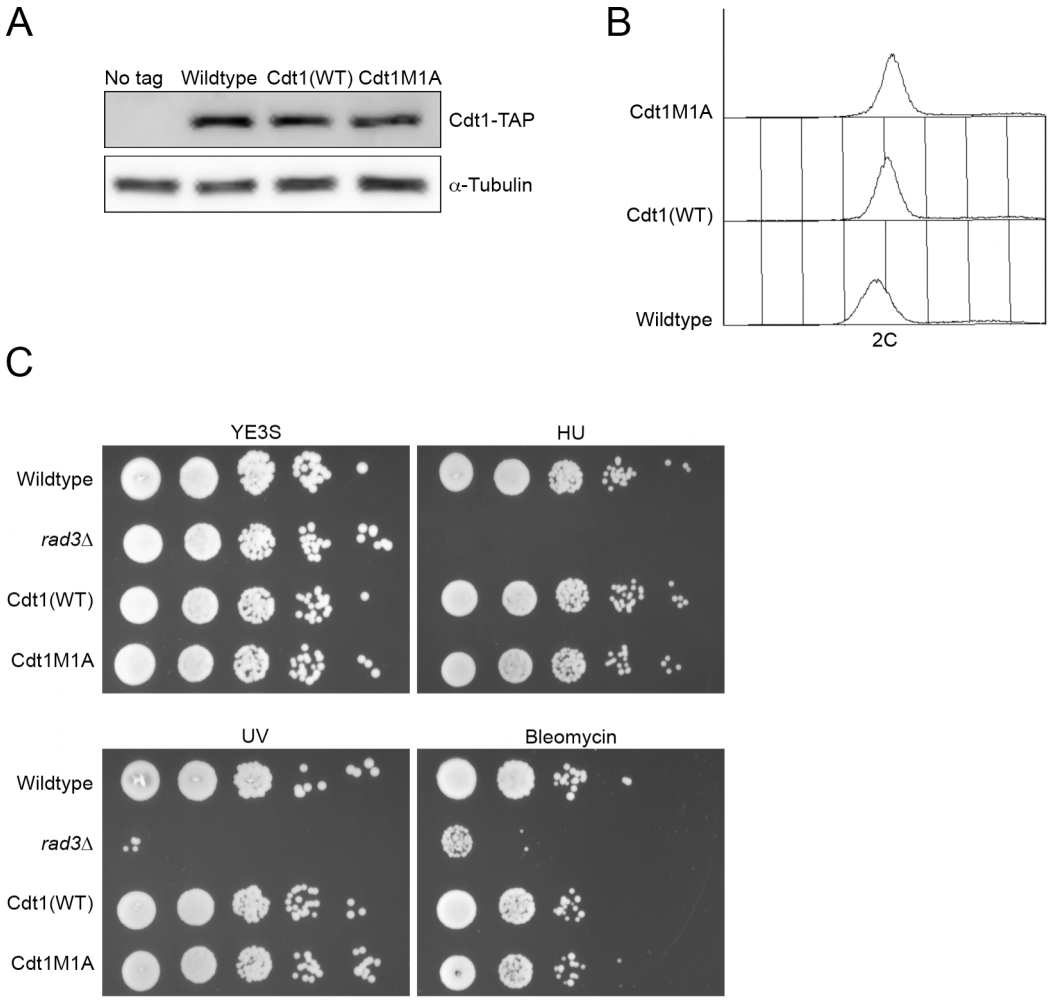


Figure 3.6 | Analysis of the Cdt1M1A mutant.
(A) Western blot analysis of Cdt1-TAP levels in exponentially growing non-tagged (138) and wild-type (1540) cells and in cells expressing Cdt1(WT) (3144) or Cdt1M1A (3142). **(B)** Flow cytometry profiles of exponentially growing wildtype (1540), Cdt1(WT) (3144) or Cdt1M1A (3142) cells. **(C)** Viability of wildtype (1625), *rad3*Δ (1811), Cdt1(WT) (3144) and Cdt1M1A (3142) cells grown at 32°C on YE3S agar or YE3S agar treated with 5 mM HU, 100 J/m^2 UV or 5 μg/ml bleomycin.

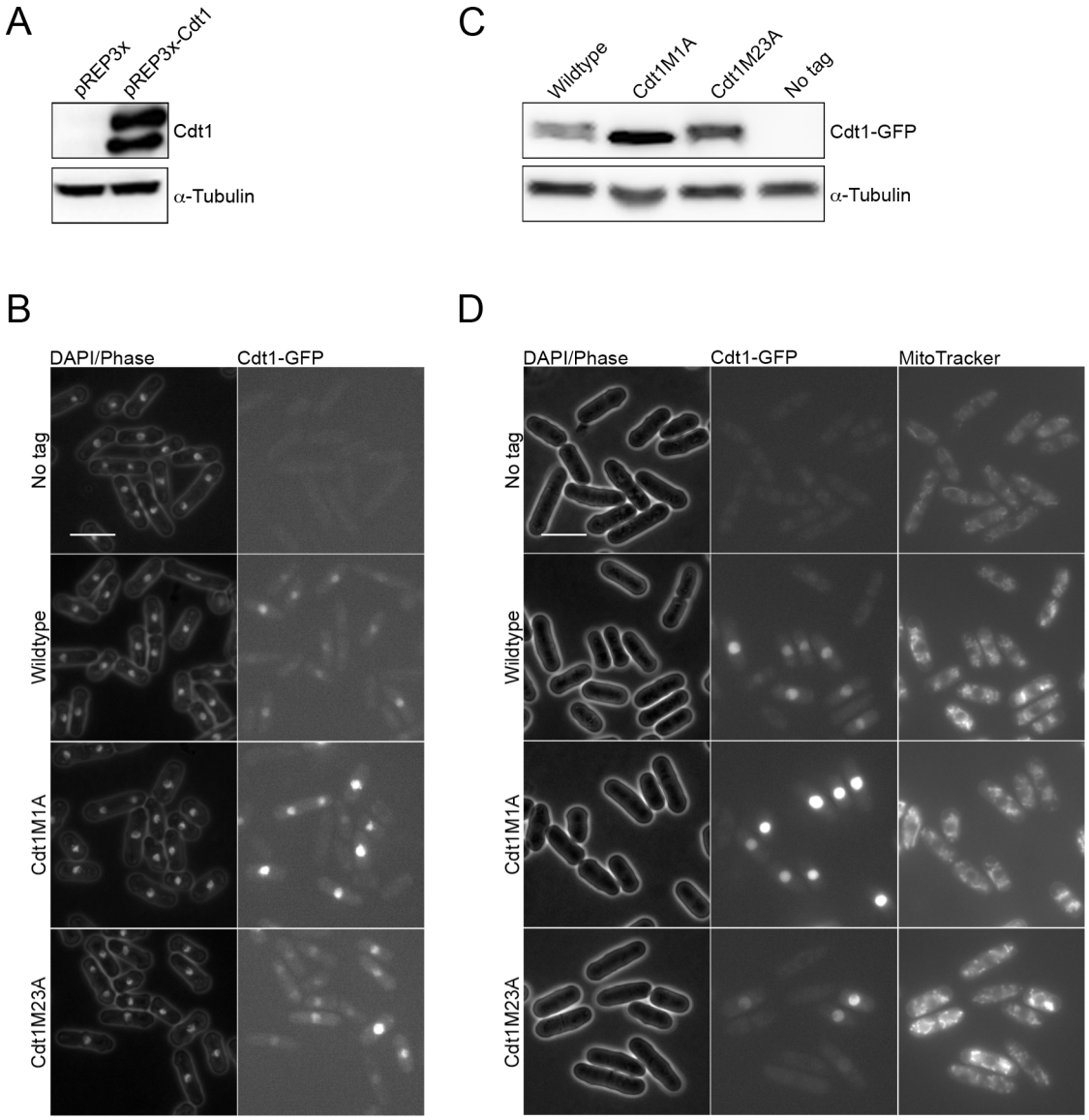


Figure 3.7 | Analysis of Cdt1 wildtype, Cdt1M1A and Cdt1M23A overexpression.
(A) Western blot analysis of control (pREP3x; 1913) and Cdt1 overexpression (pREP3x-Cdt1; 1911) strains, grown in minus thiamine medium for 24 hours. **(B)** Cdt1-GFP imaged exponentially growing cells, expressing either wildtype Cdt1-GFP (3131), Cdt1M1A-GFP (3133) or Cdt1M23A-GFP (3134) from the *nmt1* promoter on a pREP3x extrachromosomal plasmid. The strains were grown in minus thiamine medium for 15 hours to induce the *nmt1* promoter. **(C)** Western blot analysis of Cdt1-GFP levels in the strains described in (B). The strains were grown in minus thiamine medium for 15 hours. **(D)** Cdt1-GFP imaged in exponentially growing live cells, in the strains described in (B). Strains were grown in minus thiamine medium for 15 hours and stained with 50 nM MitoTracker® Red CM-H_2Xros (Materials and Methods 2.7.2.4). Scale bar: 10 μm. 10 μg/ml thiamine was used to repress the *nmt1* promoter.

To investigate whether translation initiation from the two in-frame AUG codons could occur when Cdt1 was expressed from the *nmt1* promoter, and to analyse the localisation of each Cdt1 isoform, Cdt1-GFP fusion proteins with the wildtype, M1A or M23A sequence were expressed under control of the *nmt1* promoter on a pREP3x extrachromosomal plasmid (Appendix II, 4 and 5). Cells were grown in minus-thiamine media for approximately 15 hours to induce the *nmt1* promoter and expression of wildtype Cdt1 and each methionine mutant was analysed by fluorescence microscopy and western blot (Figure 3.7B and C). Wildtype Cdt1-GFP, Cdt1M1A-GFP and Cdt1M23A-GFP were all expressed under these conditions and produced a clear nuclear signal in fixed cells (Figure 3.7B). Western blot analysis suggested that wildtype Cdt1 under control of the *nmt1* promoter migrated as a double band, and the Cdt1M1A band appeared to correspond to the smaller of the two wildtype bands (Figure 3.7C). The band that represented Cdt1M23A was indistinct; it may correspond to the larger of the two wildtype bands, which would indicate that the wildtype doublet represents translation initiation from the two in-frame AUGs. However, the similarity in size between the two Cdt1 isoforms made it difficult to accurately distinguish the two bands.

A global analysis of protein localisation in fission yeast, where each ORF was expressed under control of the *nmt1* promoter, suggested that Cdt1-YFP localised to both the nucleus and mitochondria (Matsuyama et al. 2006). Translation initiation from alternative in-frame AUG codons, enabling production of protein isoforms with different N-terminal regions, has been documented as a method to target proteins to distinct subcellular locations (reviewed in Kochetov 2008). For example, *S. pombe* DNA ligase I (Cdc17) is targeted to both the nucleus and mitochondria by alternative

expression from two in-frame AUG codons; expression from the first AUG codon produces an N-terminally extended isoform that contains a mitochondrial targeting sequence (Martin and MacNeill 2004).

Interestingly, a query of the full-length Cdt1 protein sequence using the mitochondrial targeting sequence prediction software MitoProt (Claros and Vincens 1996) indicated there was a probability of 0.65 that the N-terminus of Cdt1 supported export to the mitochondria. Based on this prediction and the Cdt1 localisation data in Matsuyama et al. (2006) it was speculated that translation initiation at the first in-frame AUG codon in the *cdt1*$^{+}$ mRNA could result in the expression of an N-terminally extended protein that was targeted to the mitochondria. To determine if colocalisation between wildtype Cdt1 and the Cdt1 methionine mutants with the mitochondria could be observed, live cells expressing Cdt1-GFP, Cdt1M1A-GFP or Cdt1M23A-GFP under control of the *nmt1* promoter were stained with the mitochondrion specific dye, MitoTracker® (Figure 3.7D). However, no colocalisation of the Cdt1 signal with the mitochondria could be detected. In conclusion, it appears that both isoforms of Cdt1 when expressed from the *nmt1* promoter, display distinct nuclear localisation.

3.3 DISCUSSION

The initial aim of this chapter was to address the involvement of a putative N-terminal PIP box in the proteolysis of fission yeast Cdt1. However, an unexpected reduction in protein levels following deletion of N-terminus of Cdt1 led to the identification and characterisation of two in-frame AUG codons in the *cdt1*$^{+}$ ORF. Characterisation of the correct initiator codon was important for a subsequent mutational study, presented in Chapter 4, which identified key regulatory regions in the protein. In this section,

three areas relating to the work presented in this chapter are discussed: the role of the second in-frame AUG codon in Cdt1 expression, the factors that affect initiation of translation at a given AUG codon, and how alternate in-frame AUG codons can be employed to produce N-terminally distinct protein isoforms.

3.3.1 The second in-frame AUG codon is required for Cdt1 expression

In this chapter, two in-frame AUG codons were identified in the *cdt1*$^+$ ORF and subsequent genetic analysis indicated that the second of these AUG codons was required to maintain wildtype Cdt1 protein levels and cell viability. Mutation of the first or second AUG codons produced Cdt1M1A or Cdt1M23A mutants respectively; analysis of each mutation as second copy in a wildtype *cdt1*$^+$ background indicated that the Cdt1M1A protein was an identical size to wildtype Cdt1 and accumulated to a similar level in exponentially growing cells. In comparison, the Cdt1M23A protein was not detected in exponentially growing or prometaphase-arrested cells, where wildtype Cdt1 and Cdt1M1A accumulated to a high level. Analysis of the viability of each mutation indicated that the Cdt1M23A but not the Cdt1M1A mutation was lethal in haploid cells without a wildtype copy of *cdt1*$^+$. This requirement for the second in-frame AUG codon to maintain Cdt1 levels and cell viability strongly suggests that it is employed as the initiator codon during translation of *cdt1*$^+$ mRNA. That translation of the Cdt1 coding sequence initiates at the second AUG codon is supported by the identical size of the wildtype and Cdt1M1A proteins and by an alignment of *Schizosaccharomyces* Cdt1 sequences, which demonstrated that the extreme N-terminus of *S. pombe* Cdt1, up to the second methionine at amino acid 23, was poorly conserved.

To extend the genetic analysis presented here, N-terminal protein sequencing could be employed to sequence endogenous *S. pombe* Cdt1. This would directly test the hypothesis presented here that the second in-frame AUG codon in *cdt1*$^{+}$ mRNA serves as the translation initiation site. N-terminal protein sequencing can be achieved using Edman sequencing or matrix-assisted laser desorption/ionisation in-source decay (MALDI-ISD), a mass spectrometry based method (Hardouin 2007).

Translation initiation in eukaryotes is proposed to occur by a linear scanning mechanism, whereby the 40S ribosomal subunit and associated initiation factors bind mRNA at the 5' capped end and scan 5' to 3' along the mRNA sequence until an AUG codon is encountered (Kozak 1978). In support of this model, early comparative analyses in yeast and higher eukaryotes indicated that the 5'-proximal AUG codon served as the translation initiation site in 95% of mRNAs (Kozak 1984; Cigan and Donahue 1987). However, subsequent work established that the nucleotide context of an AUG codon was important for its recognition as a translation initiation site (Kozak 1981). This resulted in a modified version of the original scanning hypothesis that included the concept of 'leaky scanning' whereby the 5'-proximal AUG codon is bypassed by the 40S ribosomal subunit if it resides in a suboptimal context, enabling initiation at a downstream AUG codon (Kozak 1986). Leaky scanning and the use of alternative translation initiation sites in eukaryotic mRNA are increasingly recognised phenomena, which serve to increase the complexity of the eukaryotic proteome (reviewed in Kochetov 2008). It is possible that in *S. pombe*, leaky scanning is responsible for recognition of the second in-frame AUG codon as the translation initiation site in the *cdt1*$^{+}$ mRNA.

3.3.2 A range of factors can affect translation initiation at an AUG codon

It is unclear why the second in-frame AUG codon should serve as the principal translation initiation site in *cdt1*$^{+}$ mRNA, in preference to the 5'-proximal AUG codon. However, one contributing factor could be the nucleotide context of each AUG codon. In mammals, the optimal context for efficient initiation of translation at an AUG codon is GCC**R**CCAUG**G** with the purine (R) at the -3 position and the guanine at the +4 position being particularly important for efficient initiation (Kozak 1986; Kozak 2005). In budding yeast, the sequence context of an AUG codon can also regulate initiation efficiency and there is a bias towards the presence of adenine in the -3 position (Cigan and Donahue 1987). A mutational study in this organism indicated that replacement of adenine in the -3 position with uracil reduced the level of translation by 50% (Yun et al. 1996). In support of a conserved requirement for adenine in the -3 position of eukaryotic initiator codons, a comparison of *S. pombe* mRNA sequences indicated a preference for this nucleotide in the -3 site (Zhang and Marr 1994). Interestingly, the first in-frame AUG codon in *cdt1*$^{+}$ has uracil in the -3 position, while the second in-frame AUG codon has adenine in the -3 position. Given the order of nucleotide preference in the -3 position of budding yeast initiation sites was A>G>C>U (Yun et al. 1996), the context of the first AUG codon in *cdt1*$^{+}$ appears suboptimal compared to the context of the second AUG codon. This could promote recognition of the second in-frame AUG codon as a translation initiation site.

It is unlikely that a uracil in the -3 position is wholly responsible for the inhibition of translation initiation at the first AUG codon as this nucleotide was replaced with adenine in the *mcm4pr/cdt1(control)-myc* and *mcm4pr/cdt1Δ100-myc* constructs and translation initiation at the first AUG codon was still not supported (Section 3.2.1).

Nonetheless, a number of features were altered in these constructs and it would be interesting to mutate the -3 position of endogenous *cdt1*$^{+}$ to adenine to determine if translation efficiency from the first AUG was improved. Improvement of the nucleotide context at the 5'-proximal AUG codon of the *S. cerevisiae MOD5* gene, which encodes a tRNA modification enzyme, resulted in a 5- to 10-fold increase in translation from the first AUG and a concomitant decrease in translation from a second in-frame AUG codon (Slusher et al. 1991).

Cdt1 expressed from the *nmt1* promoter on an extrachromosomal plasmid was detected as a double band by western blot. We hypothesised that this Cdt1 doublet represented initiation of translation at each in-frame AUG codon. In support of this hypothesis, both Cdt1M1A and Cdt1M23A proteins were detected when expressed from the *nmt1* promoter. As the Cdt1M1A and Cdt1M23A proteins were similar in size, it could not be conclusively shown by western blotting that they corresponded to the lower and upper band of the Cdt1 doublet respectively. N-terminal protein sequencing could be employed to directly demonstrate that the Cdt1 doublet represents initiation of translation at each in-frame AUG codon. Replacement of the native *cdt1* promoter with *nmt1* did not affect the immediate nucleotide context of the first AUG codon, suggesting that if the first AUG codon is recognised as a translation initiation site when Cdt1 is expressed from the *nmt1* promoter, it may be the result of alterations to the 5' UTR of the *cdt1*$^{+}$ mRNA.

A number of features of the 5' UTR can affect translational efficiency at an AUG codon. A comparison of eukaryotic mRNAs encoding abundant and scarce proteins indicated that low-expression mRNAs had longer 5'UTRs, a stronger ability to form

secondary structures in the 5'UTR and more frequently contained upstream AUG codons (uAUGs) (Kochetov et al. 1998). The inhibitory effects of secondary structure and uAUGs on translational efficiency has been demonstrated experimentally in *S. cerevisiae* with *HIS4* mRNA and in human cells with the small RNR subunit (M2) mRNA (Cigan et al. 1988; Dong et al. 2005). It is proposed that stable secondary structures in the 5' UTR inhibit scanning by the 40S ribosomal subunit and that uAUGs reduce initiation efficiency at the AUG codon of the main ORF (reviewed in Kozak 2005).

In addition, upstream ORFs (uORFs) in the 5' UTR can inhibit the initiation of translation at 3' AUG codons. The overlap of a uORF with a 3' AUG codon or the termination of a uORF in close proximity to a 3' AUG codon prevents reinitiation at the 3' AUG codon required for translation of the main ORF (reviewed in Kozak 2005). uORFs have been demonstrated to regulate expression of the *S. cerevisiae* amino acid biosynthesis gene *GCN4* in response to cell stress (reviewed in Meijer and Thomas 2002). The 5' UTR of the endogenous *cdt1*$^+$ mRNA contains one out-of-frame AUG triplet, 86 bp upstream of the first in-frame AUG codon. However, it is followed immediately by a UGA termination triplet and unlikely to represent a uORF that would affect initiation at either of the downstream in-frame AUG codons.

It is unclear why the features of 5' UTRs discussed above would specifically inhibit initiation of translation at the first AUG codon in *cdt1*$^+$ mRNA, as opposed to causing a general reduction in the translational efficiency from both in-frame AUG codons. It would be interesting to use primer extension to determine the 5' transcriptional start site and the sequence of the 5' UTR in the *cdt1*$^+$ mRNA produced when Cdt1 is

expressed from the *nmt1* promoter as opposed to the *cdt1* promoter, enabling a direct comparison of the two 5' UTRs. It is possible that features of the 5' UTR in combination with the nucleotide context of each AUG codon contribute to the recognition of the second in-frame AUG codon as the translation initiation site in the *cdt1*$^{+}$ mRNA.

3.3.3 Two in-frame AUG codons could enable the expression of N-terminally distinct Cdt1 isoforms

This study was unable to ascertain whether the first AUG codon was entirely unused as a translation initiation site or whether it supported an extremely low level of translation to produce an N-terminally extended Cdt1 isoform. The production of N-terminally distinct protein isoforms, from alternative AUG codons is recognised as a method to target proteins to distinct subcellular localisations, such as the nucleus and the mitochondria (reviewed in Kochetov 2008). A number of nuclear replication and repair factors are targeted to the mitochondria to support maintenance of the mitochondrial genome (reviewed in Holt 2009). In fission yeast, DNA ligase I (Cdc17), which is required for the ligation of Okazaki fragments during lagging strand synthesis, as well as for BER and NER is targeted both to the nucleus and mitochondria (Martin and MacNeill 2004). In addition, the UV-damage DNA endonuclease (UVDE) Uve1, which functions in the UVDE-dependent excision repair (UVER) pathway, is targeted both to the nucleus and mitochondria (Yasuhira and Yasui 2000). Both Cdc17 and Uve1 are exported to the mitochondria through translation of N-terminally extended isoforms from a 5' AUG codon (Yasuhira and Yasui 2000; Martin and MacNeill 2004).

A report describing the colocalisation of Cdt1 with the mitochondria (Matsuyama et al. 2006), in combination with the prediction that the extreme N-terminus of Cdt1 could support export to the mitochondria (Claros and Vincens 1996), resulted in speculation that Cdt1 might have a mitochondrial function in *S. pombe*. Translation initiation at the first AUG codon could produce an N-terminally extended Cdt1 isoform, capable of being targeted to the mitochondria. However, no evidence was found to support the colocalisation of Cdt1 with the mitochondria in exponentially growing fission yeast cells. The two protein isoforms produced when Cdt1 was expressed from the *nmt1* promoter both showed distinct nuclear localisation.

Therefore, it was not possible to verify the report from Matsuyama et al. (2006) that described a mitochondrial distribution for Cdt1. This suggests that if Cdt1 is exported to the mitochondria, it occurs at a low level or only under certain cellular conditions. It was noted in Matsuyama et al. (2006) that cells were grown on solid media, unlike in this study, where cells were grown in agitated liquid culture. A difference in culture methods will affect the level of nutrition and aeration that the cells are exposed to and could cause discrepancies between the data obtained. An argument against a mitochondrial role for Cdt1 is the lack of conservation in the extreme N-terminus of *S. pombe* Cdt1, which contains the predicted mitochondrial targeting sequence, suggesting that if Cdt1 does have a function in the mitochondria, it is not one that is phylogenetically conserved.

3.4 CONCLUSIONS

This chapter demonstrates that a second in-frame AUG codon in the *cdt1*$^{+}$ ORF is required to maintain wildtype Cdt1 protein levels and cell viability. Cdt1 expressed

from the second in-frame AUG codon in the Cdt1M1A mutant was an identical size and accumulated to a similar level as wildtype Cdt1, suggesting that this second AUG codon represents the principal translation initiation site in the *cdt1*$^{+}$ mRNA. The nucleotide context of each AUG codon, in combination with features of the 5' UTR of the *cdt1*$^{+}$ mRNA, is expected to regulate recognition of the second AUG codon as the translation initiation site. Finally, exponentially growing fission yeast cells that overexpress Cdt1 from the *nmt1* promoter produce two isoforms of Cdt1 that both appear to have a distinct nuclear localisation.

CHAPTER 4

A Role for Dual PIP Degrons in Cdt1 Proteolysis

4.1 INTRODUCTION

As discussed in Chapter 3, metazoan Cdt1 interacts with PCNA via a conserved N-terminal PIP box; an interaction which is required for the subsequent ubiquitylation of Cdt1 by $CRL4^{Cdt2}$ (Arias and Walter 2006; Nishitani et al. 2006; Senga et al. 2006). The N-terminus of *S. pombe* Cdt1 contains a partial match to the PIP box consensus sequence but the contribution of this motif to Cdt1 proteolysis has yet to be addressed. The first part of this chapter investigates the role of a PIP box-mediated Cdt1-PCNA interaction in *S. pombe* Cdt1 regulation.

Interestingly, numerous proteins that interact with PCNA via a PIP box are not subject to $CRL4^{Cdt2}$-dependent ubiquitylation and proteolysis (Havens and Walter 2009). While this work was in progress, a study using the *Xenopus* egg extracts system demonstrated that $CRL4^{Cdt2}$ targets, such as Cdt1, have a specialised 'PIP degron' sequence that contains two additional elements compared to the canonical PIP box sequence (Havens and Walter 2009). These include a TD motif at positions 5 and 6 of the PIP box that confers efficient binding to PCNA; and a positively-charged amino acid, four residues downstream of the PIP box that is required for recruitment of $CRL4^{Cdt2}$. The transfer of these sequence elements to Fen1, a stable PIP box-

containing protein, resulted in $CRL4^{Cdt2}$-dependent turnover of the modified protein (Havens and Walter 2009).

In response to the report by Havens et al. (2009), the *S. pombe* Cdt1 sequence was re-examined for potential matches to the PIP degron sequence. Interestingly, two variant PIP degron sequences were identified in *S. pombe* Cdt1. The second part of this chapter addresses the role of each of these PIP degrons in mediating the Cdt1-PCNA interaction and in regulating the proteolysis of Cdt1 via the $CRL4^{Cdt2}$ pathway. The results obtained demonstrate a critical role for the two PIP degrons in promoting Cdt1 proteolysis and the Cdt1-PCNA interaction. Some of the work from this chapter has been published (Guarino et al. 2011).

4.2 RESULTS

4.2.1 The N-terminal 26-100 amino acids of Cdt1 are required for correct nuclear localisation and contribute to the cell cycle- and DNA damage-dependent regulation of the protein

Given the involvement of an N-terminal PIP box in metazoan Cdt1 regulation (Arias and Walter 2006; Nishitani et al. 2006; Senga et al. 2006), the N-terminal 26-100 amino acids in fission yeast Cdt1, which contain a putative PIP box at amino acid 28, were deleted to examine if Cdt1 proteolysis was inhibited. The N-terminal 26 amino acids were unchanged to minimise disruption of Cdt1 expression; Chapter 3 demonstrated that a second AUG codon in the $cdt1^+$ ORF, corresponding to a methionine at residue 23 of the encoded protein, is required to maintain Cdt1 levels.

A *cdt1pr/cdt1(WT)-myc* plasmid was used to construct the *cdt1Δ26-100* deletion (Appendix II, 6; Figure 4.1A). As the effect of the 26-100 amino acid deletion on Cdt1 protein function was unclear, the *cdt1pr/cdt1(WT)-myc* and the *cdt1pr/cdt1Δ26-100-myc* plasmids were integrated as a second copy at the *ura4*$^{+}$ locus, in a wildtype *cdt1*$^{+}$ background. The *cdt1pr/cdt1(WT)-myc* plasmid was constructed for this study and before it was used to produce the *cdt1Δ26-100* deletion, it was transformed into a *cdt1Δ* strain containing an extra-chromosomal *nmt1-cdt1*$^{+}$ plasmid, to ensure the *cdt1pr/cdt1* sequence was functional. In the *cdt1Δ* strain, Cdt1 expression and therefore cell viability is regulated by the thiamine-repressible *nmt1* promoter. The *cdt1pr/cdt1(WT)-myc* plasmid was able to relieve the thiamine-sensitivity of the *cdt1Δ* strain, indicating that it was functional (Figure 4.1B).

To analyse whether deletion of the N-terminal 26-100 amino acids in Cdt1 inhibited turnover of the protein, Cdt1 levels in cells expressing Cdt1(WT)-Myc or Cdt1Δ26-100-Myc were compared by western blot analysis. In exponentially growing cells, the level of Cdt1(WT) was similar to the level of endogenous Myc-tagged Cdt1, suggesting that the wildtype construct was correctly regulated when integrated at the *ura4*$^{+}$ locus (Figure 4.1C, compare 'Wildtype' and 'Cdt1(WT)'). Interestingly, the level of Cdt1Δ26-100 was dramatically higher than the level of Cdt1(WT), and comparable to the level of Cdt1 in a *ddb1Δ* background, where CRL4^{Cdt2}-dependent ubiquitylation of Cdt1 was abolished (Figure 4.1C) (Ralph et al. 2006).

The elevated level of Cdt1Δ26-100 as compared to Cdt1(WT) could indicate a direct role for amino acids 26-100 in Cdt1 regulation. However, given Cdt1 ubiquitylation by CRL4^{Cdt2} requires an interaction with chromatin-bound PCNA (Arias and Walter

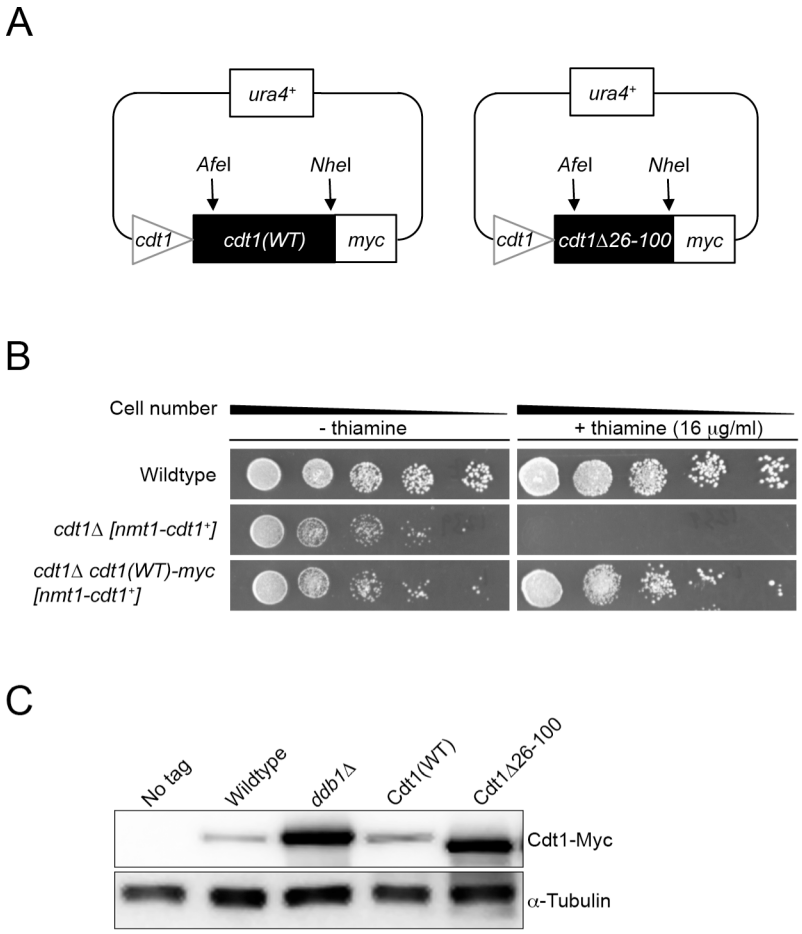


Figure 4.1 | N-terminal Cdt1 deletions that retain the second methionine are expressed. **(A)** A *cdt1pr/cdt1(WT)-myc* plasmid (p798) was used to construct the *cdt1Δ26-100* deletion. The *cdt1Δ26-100* sequence was amplified as an *Afe*I/*Nhe*I fragment and cloned into p798 to construct a *cdt1pr/cdt1Δ26-100-myc* plasmid (p804). **(B)** Functionality of the *cdt1pr/cdt1(WT)-myc* plasmid (p790) was confirmed by transformation into a *cdt1Δ* [*nmt1-cdt1+*] strain (1239). Its ability to relieve the thiamine-sensitivity of the resulting strain (2409) was analysed by spot tests on EMM plates plus or minus thiamine (16 μg/ml). **(C)** Western blot analysis of exponentially growing non-tagged (138) cells, cells expressing endogenous Cdt1-Myc in a wildtype (1489) or *ddb1Δ* (1615) background, and cells expressing Cdt1(WT)-Myc (2302) or Cdt1Δ26-100-Myc (2303) as a second copy.

2006), the 26-100 amino acid deletion could stabilise Cdt1 indirectly, through a loss of nuclear accumulation, which would preclude an interaction with PCNA. To examine the effect of the 26-100 amino acid deletion on the nuclear localisation of Cdt1, *cdt1(WT)* and *cdt1Δ26-100* sequences were fused to YFP and integrated as a second copy at the *ura4*$^{+}$ locus, enabling the cellular distribution of Cdt1(WT) and Cdt1Δ26-100 to be visualised by fluorescence microscopy (Appendix II, 7).

The nuclear accumulation of Cdt1Δ26-100 was compared with wildtype Cdt1 by fluorescence microscopy analysis of exponentially growing cells that expressed endogenous Cdt1-YFP, Cdt1(WT)-YFP or Cdt1Δ26-100-YFP. The endogenous Cdt1 signal and the Cdt1(WT) signal were detected in the nuclei of a subset of binucleate (late M/G1) cells (Figure 4.2A). Note that the Cdt1(WT) strain will hereafter be referred to simply as wildtype, as it behaves in an identical manner to endogenous Cdt1. In contrast, the Cdt1Δ26-100 signal was detected ubiquitously across the cell (Figure 4.2A), suggesting that although not excluded from the nucleus, the nuclear localisation of the Cdt1Δ26-100 protein was compromised.

It is unclear how fission yeast Cdt1 is targeted to the nucleus. In budding yeast cells, Cdt1 accumulation in the nucleus is dependent on an interaction with the Mcm2-7 complex (Tanaka and Diffley 2002). In contrast, human Cdt1 is targeted to the nucleus by a putative bipartite nuclear localisation sequence (NLS) in the N-terminus of the protein (Nishitani et al. 2004). Classic NLSs are monopartite or bipartite, consisting of one or two clusters of basic amino acids respectively (reviewed in Lange et al. 2007). The N-terminus of fission yeast Cdt1 does not contain a classic NLS. However, it may contain a variant NLS that is disrupted in the Cdt1Δ26-100 mutant.

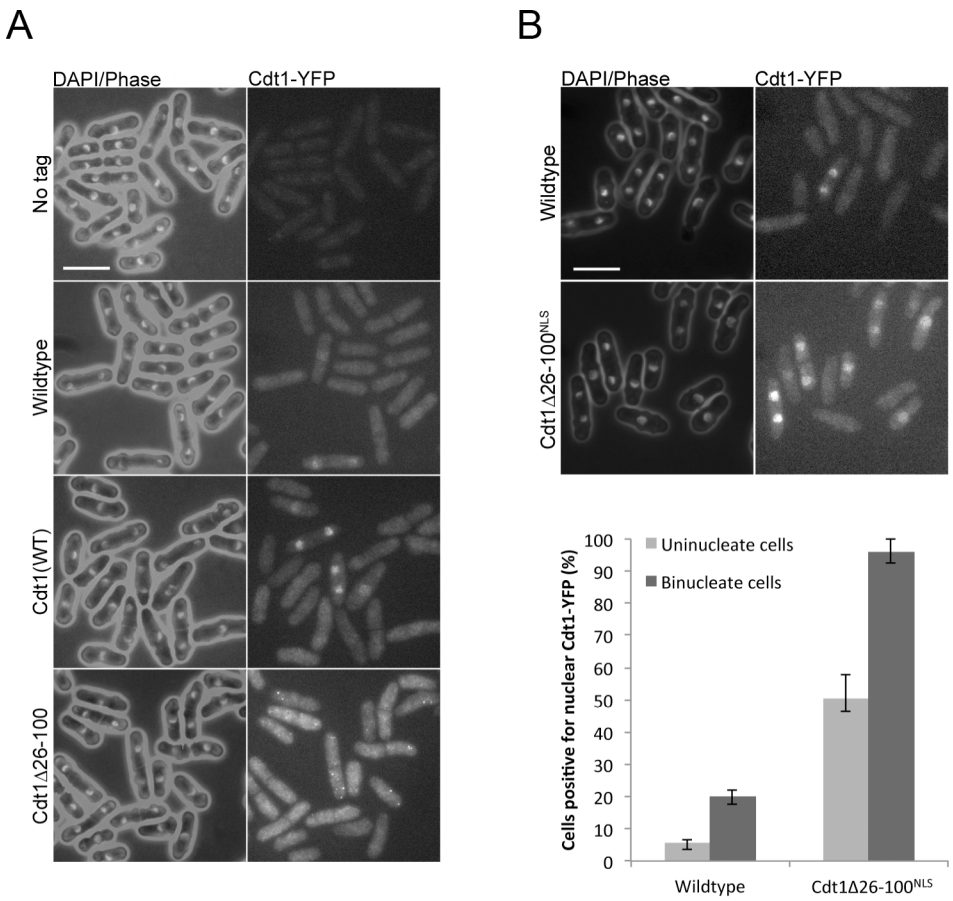


Figure 4.2 | The Cdt1Δ26-100 mutant requires an NLS for correct nuclear localisation.
(A) Fluorescence microscopy analysis of exponentially growing cells expressing non-tagged (138) or endogenous YFP-tagged (1262) Cdt1 and cells expressing Cdt1(WT)-YFP (2337) or Cdt1Δ26-100-YFP (2338) as a second copy. Scale bar: 10 μm. **(B)** *Upper panel:* Cdt1-YFP imaged in exponentially growing cells expressing wildtype Cdt1 (2337) or Cdt1Δ26-100^{NLS} (2339). Scale bar: 10 μm. *Lower panel:* the same strains were analysed to determine the percentage of uninucleate and binucleate cells positive for Cdt1-YFP. At least 100 cells, from two independent experiments, were counted for each data point. Error bars: 50% of range.

Alternatively, a sequence that regulates the interaction between Cdt1 and a protein required for its nuclear accumulation may be removed in the Cdt1Δ26-100 mutant.

The loss of Cdt1Δ26-100 nuclear localisation prevents direct investigation into the effect of the 26-100 amino acid deletion on Cdt1 proteolysis. Therefore, an attempt to restore the nuclear localisation of Cdt1Δ26-100 was made by cloning a tandem NLS into the *cdt1Δ26-100-YFP* sequence, at the C-terminus of YFP (Appendix II, 8). The tandem NLS had the sequence PKKKRKVEDPKKKRKVD and was derived from the Simian vacuolating virus 40 (SV40) large T antigen NLS (Kalderon et al. 1984). The resulting *cdt1pr/cdt1Δ26-100-YFP-2x NLS* plasmid was integrated as a second copy at the *ura4*$^{+}$ locus.

To analyse whether the tandem NLS restored the nuclear localisation Cdt1Δ26-100, exponentially growing cells expressing Cdt1-YFP or Cdt1Δ26-100^{NLS} were compared by fluorescence microscopy. Similar to wildtype Cdt1, the Cdt1Δ26-100^{NLS} signal had a distinct nuclear distribution (Figure 4.2B, upper panel), demonstrating that the addition of a tandem NLS restored the nuclear localisation of Cdt1Δ26-100. In addition, this comparison indicated that the Cdt1Δ26-100^{NLS} signal was detected in a higher percentage of uninucleate and binucleate cells, compared to wildtype (Figure 4.2B, lower panel). This suggests that deletion of the N-terminal 26-100 amino acids in Cdt1 perturbs the cell cycle-dependent regulation of the protein.

The effect of the N-terminal 26-100 amino acid deletion on the cell cycle-dependent regulation of Cdt1 was explored in more detail through comparison of the S phase-dependent proteolysis of Cdt1Δ26-100^{NLS} with wildtype Cdt1 in a synchronised cell

cycle. A synchronous cell cycle was achieved using the cold-sensitive *nda3-311* allele, which arrests cells in mitosis (prometaphase) at the restrictive temperature of 20°C. Mitotically-arrested *nda3-311* cells, expressing YFP-tagged wildtype Cdt1 or Cdt1Δ26-100^{NLS} were released in synchrony into the cell cycle by shifting to the permissive temperature of 32°C and samples were taken every 20 minutes for 1 hour (Figure 4.3A). Unexpectedly, Cdt1Δ26-100^{NLS} accumulated to a higher level than wildtype Cdt1 in the mitotically-arrested cells, for reasons that were unclear (Figure 4.3B, time [*t*] = 0 minutes). Flow cytometric analysis indicated that S phase occurred 40 minutes post release and a decline in both wildtype Cdt1 and Cdt1Δ26-100^{NLS} levels was observed at this time-point (Figure 4.3B and C). At 60 minutes following release, the level of Cdt1Δ26-100^{NLS} was higher than the level of wildtype Cdt1, which could reflect either a reduced efficiency in Cdt1Δ26-100^{NLS} proteolysis or the higher protein level in the mitotically-arrested Cdt1Δ26-100^{NLS} cells at the start of the experiment. Overall, this experiment suggests that the N-terminal 26-100 amino acids of Cdt1 are not essential for the S phase-dependent proteolysis of Cdt1 but may contribute to the efficiency of this process.

In addition to S phase, a range of forms of DNA damage, including UV irradiation, induce Cdt1 proteolysis in fission yeast cells (Ralph et al. 2006). To investigate the role of the N-terminal 26-100 amino acids in the DNA damage-dependent regulation of Cdt1, the proteolysis of YFP-tagged wildtype Cdt1 and Cdt1Δ26-100^{NLS} following UV irradiation was compared in mitotically-arrested cells (Figure 4.4A). The use of mitotically-arrested cells enabled the effect of UV irradiation on Cdt1 levels to be examined independently of changes that occur in the cell cycle. The percentage of uninucleate cells throughout the experiment was recorded to ensure the mitotic block

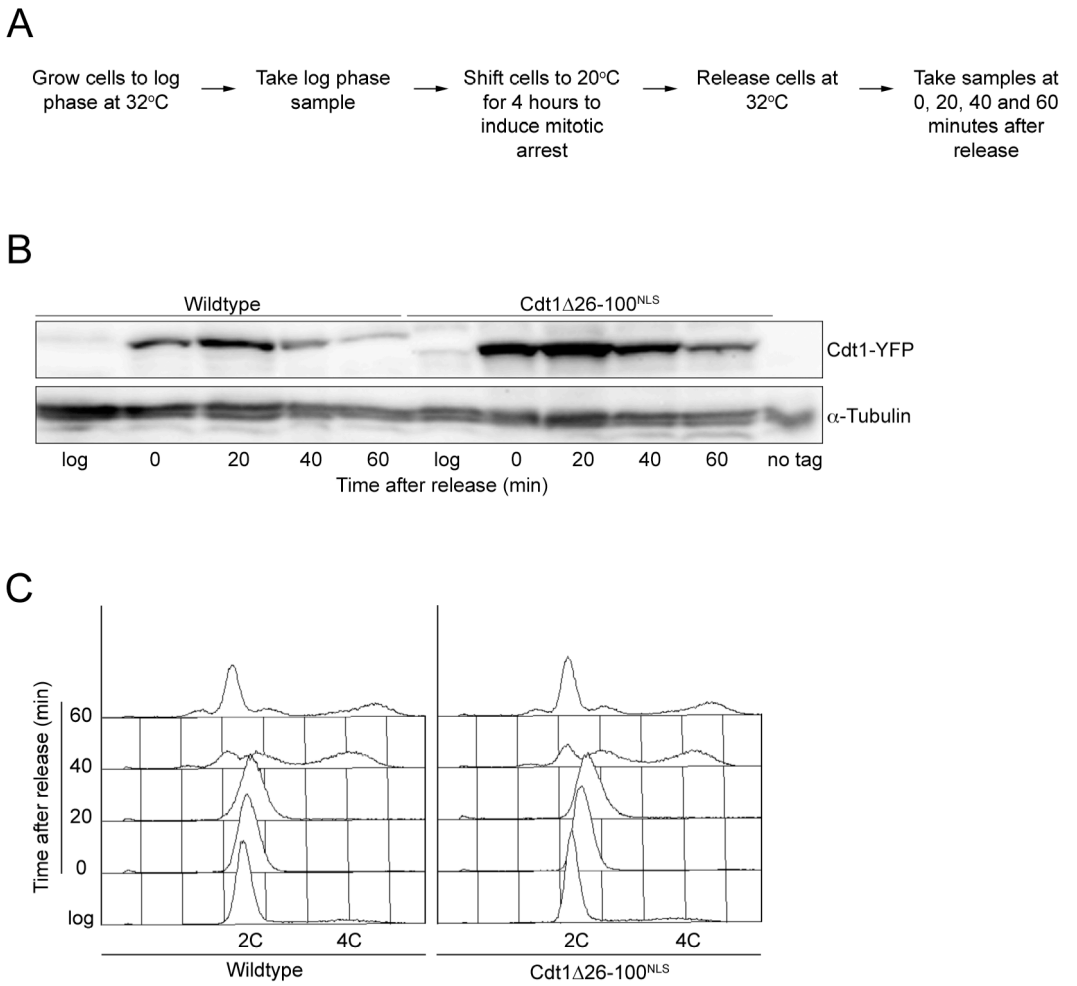


Figure 4.3 | Analysis of the cell cycle-dependent regulation of Cdt1Δ26-100^{NLS}.
(A) Scheme of experiment. **(B)** Western blot analysis of wildtype (2337) and Cdt1Δ26-100^{NLS} (2339) cells, following the experimental procedure outlined in (A). **(C)** Flow cytometry profiles of the cells analysed in (B).

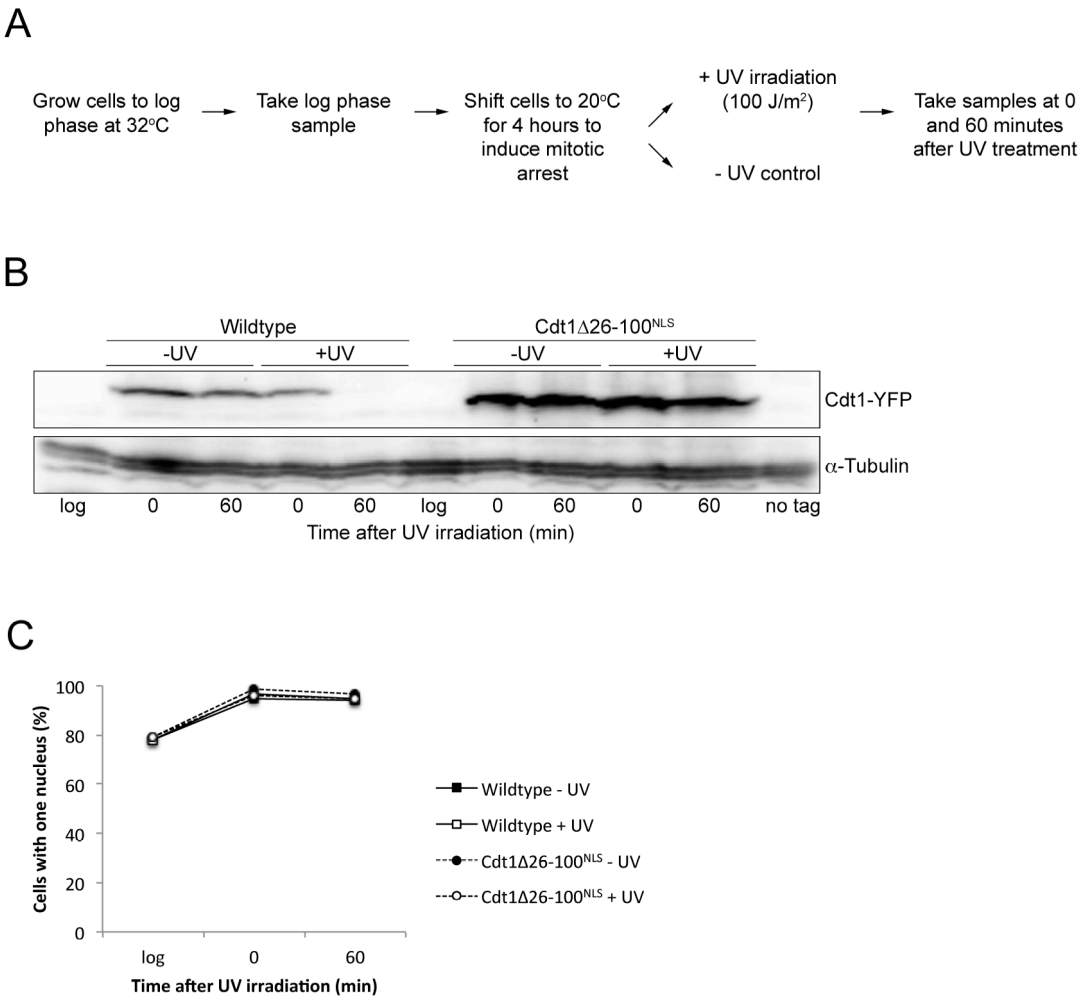


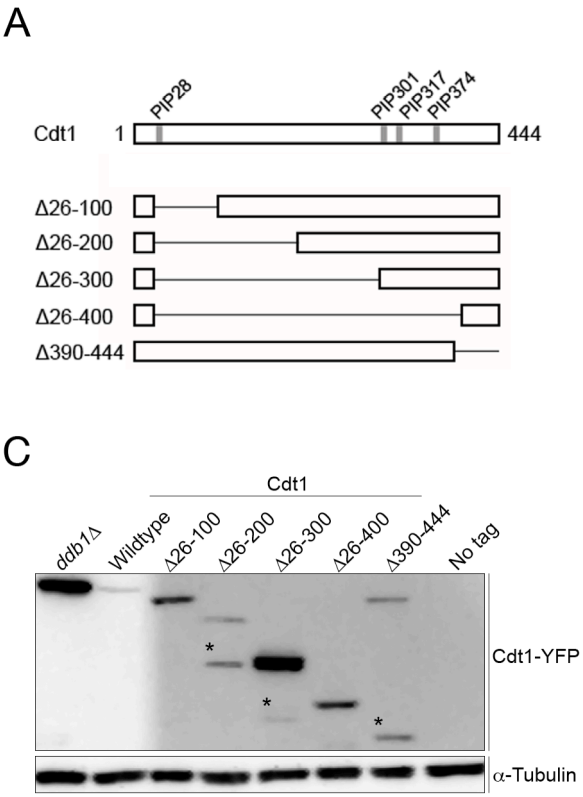
Figure 4.4 | Analysis of the DNA damage-dependent regulation of Cdt1Δ26-100^{NLS}.
(A) Scheme of experiment. **(B)** Western blot analysis of wildtype (2337) and Cdt1Δ26-100^{NLS} (2339) cells, following the experimental procedure outlined in (A). **(C)** Percentage of uninucleate cells during the experiment shown in (B).

was maintained (Figure 4.4C). Interestingly, whereas the level of wildtype Cdt1 decreased dramatically at 60 minutes after UV treatment, Cdt1Δ26-100^{NLS} levels were quite stable (Figure 4.4B). Although there was a small decrease in Cdt1Δ26-100^{NLS} levels between 0 and 60 minutes post UV treatment, this result suggests that amino acids 26-100 are required for a robust down-regulation of Cdt1 in response to DNA damage.

4.2.2 Truncation mutations in Cdt1 indicate a second putative PIP motif contributes to the cell cycle-dependent regulation of the protein

Deletion of a putative N-terminal PIP box in the Cdt1Δ26-100^{NLS} mutant does not abolish the cell cycle-dependent regulation of Cdt1, suggesting a second region is involved in the S phase proteolysis of the protein. There are a further three partial matches to the PIP box sequence at positions 301, 317 and 374 of the protein (Figure 4.5A) and five KA motifs between amino acids 318 and 436, which can also mediate interactions with PCNA (Xu et al. 2001). To identify the additional regions of Cdt1 that are required for its S phase-dependent proteolysis, four truncation mutants that spanned the protein sequence were constructed (Appendix II, 9): Cdt1Δ26-200, Cdt1Δ26-300, Cdt1Δ26-400 and Cdt1Δ390-444 (Figure 4.5A). Note that each truncation mutant was constructed with an NLS to ensure correct nuclear localisation but for simplicity this is not included in the text.

The effect of each large-scale deletion on the cell cycle-dependent regulation of Cdt1 was investigated by fluorescence microscopy analysis. Cells expressing each YFP-tagged Cdt1 truncation protein were compared with cells expressing Cdt1-YFP in a wildtype or *ddb1*Δ background (Figure 4.5B). In *ddb1*Δ cells, where CRL4^{Cdt2}



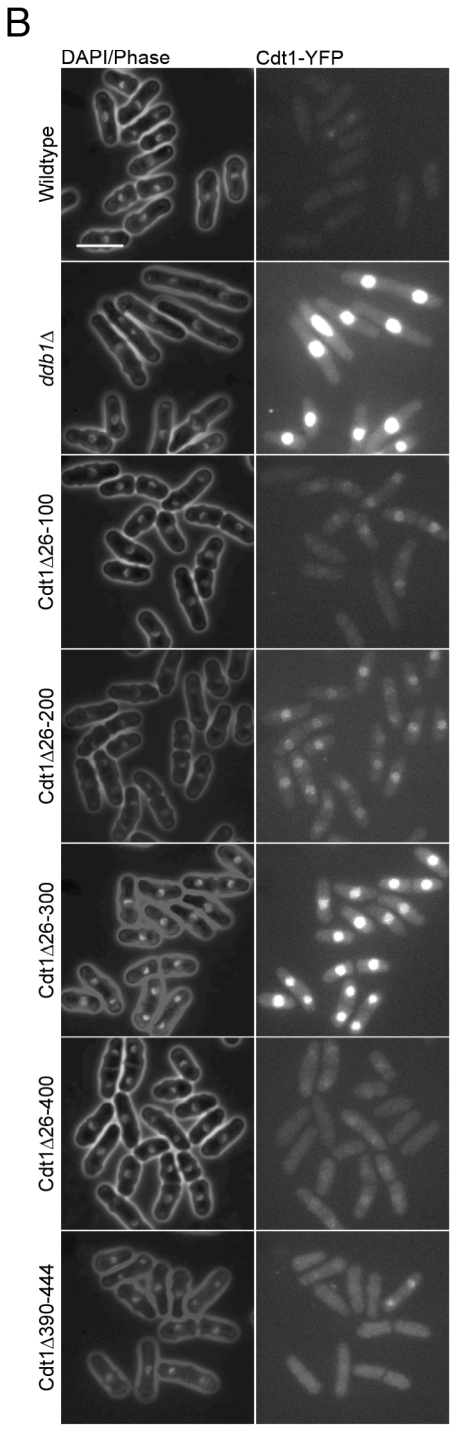


Figure 4.5 | A large-scale Cdt1 deletion study. **(A)** A summary of the large-scale Cdt1 deletion mutants constructed. **(B)** Cdt1-YFP imaged in exponentially growing cells in a wildtype (1262) or *ddb1*Δ (1769) background and in cells expressing Cdt1Δ26-100 (2339), Cdt1Δ26-200 (2421), Cdt1Δ26-300 (2422), Cdt1Δ26-400 (2423) or Cdt1Δ390-444 (2424). Scale bar: 10 μm. **(C)** Western blot analysis of the strains described in (B). Bands marked with an asterisk may be non-specific or represent degradation products.

ubiquitylation was abolished, an intense Cdt1 signal was detected in the nuclei of all cells, regardless of their cell cycle stage. Interestingly, as in the *ddb1*Δ background, most cells in the Cdt1Δ26-200 and Cdt1Δ26-300 strains were positive for YFP nuclear fluorescence, suggesting that the cell cycle regulation of these Cdt1 truncation proteins was compromised. The intensity of the nuclear Cdt1Δ26-300 signal was higher than the Cdt1Δ26-200 signal, indicating increased stabilisation of this protein. In the largest truncation mutant, the nuclear Cdt1Δ26-400 signal was weak, although a diffuse signal was visible in the nuclei of some cells. The Cdt1Δ390-444 strain was similar to the wildtype, with YFP fluorescence visible predominantly in binucleate cells. An analysis of protein levels in the truncation mutants by western blot suggested that the level of Cdt1Δ26-300 was particularly high and comparable to the level of Cdt1-YFP in a *ddb1*Δ background (Figure 4.5C).

To investigate whether $CRL4^{Cdt2}$-mediated turnover of the Cdt1 truncation proteins occurs, the level of each protein was compared in a wildtype and a *ddb1*Δ background, where $CRL4^{Cdt2}$-dependent ubiquitylation of Cdt1 was abolished. The intensity of nuclear YFP fluorescence and the overall protein level in cells expressing YFP-tagged Cdt1Δ26-100, Cdt1Δ26-200 or Cdt1Δ26-300 was elevated in a *ddb1*Δ background when compared to a wildtype background (Figure 4.6A and B). The intensity of nuclear Cdt1Δ390-444-YFP fluorescence and the overall protein level was also increased in a *ddb1*Δ background when compared to a wildtype background (Figure 4.6A and B). However, unlike the Cdt1Δ26-100, the Cdt1Δ26-200 and the Cdt1Δ26-300 mutant, the level of Cdt1Δ390-444 in *ddb1*Δ cells was not elevated to the extent of wildtype Cdt1 in a *ddb1*Δ background. Finally, there was only a moderate increase in the level of Cdt1Δ26-400 in *ddb1*Δ cells as compared to

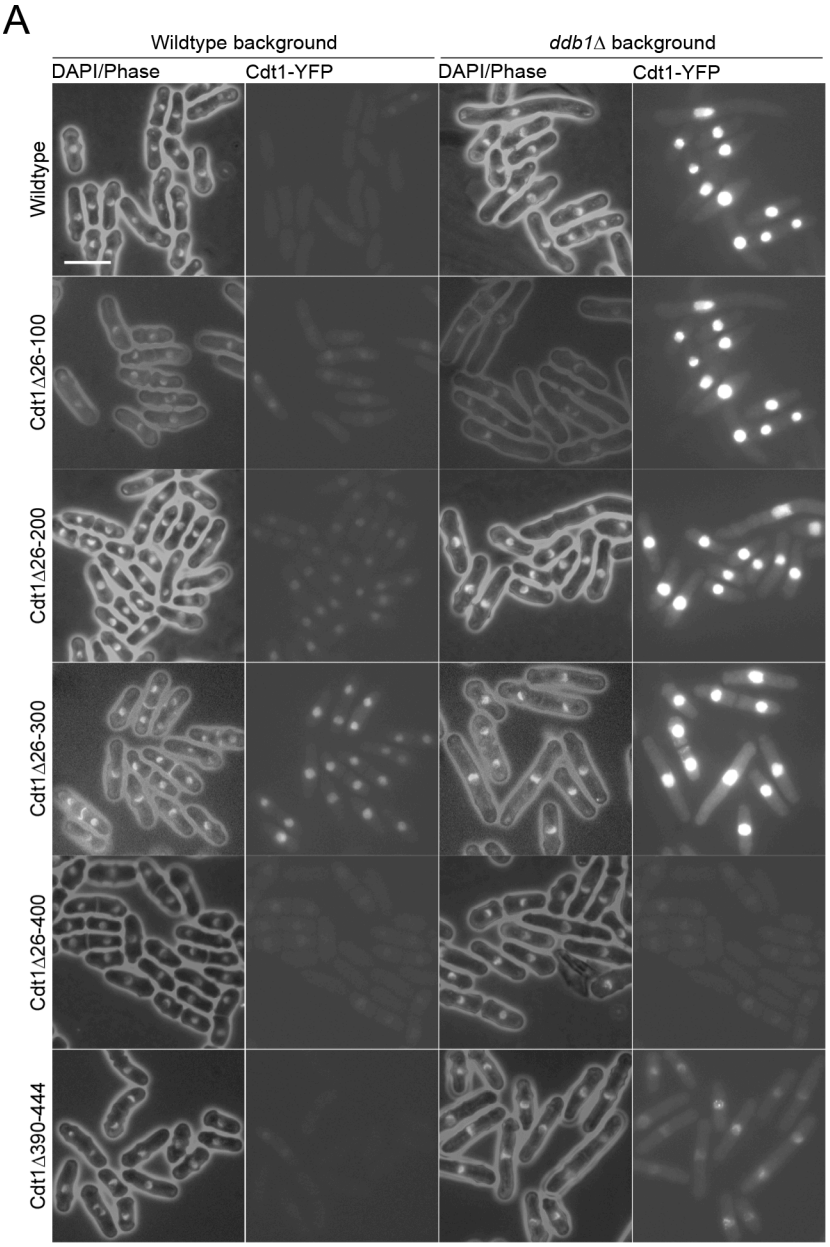
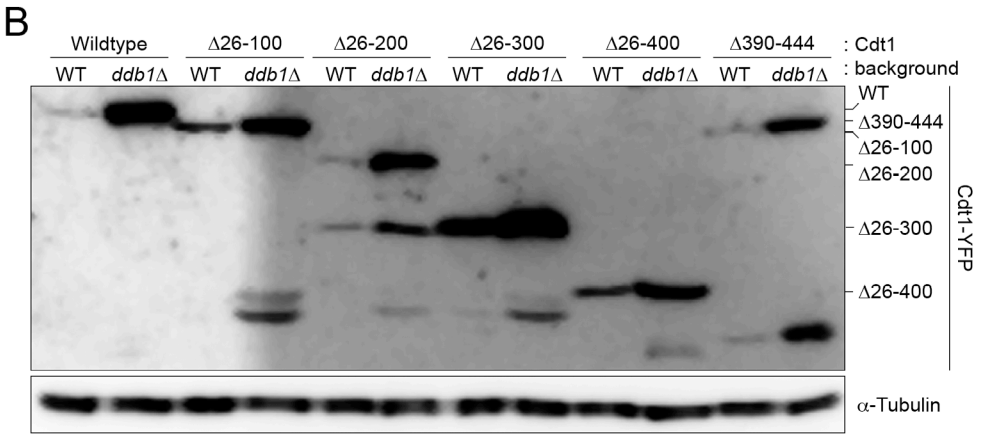


Figure 4.6 | Analysis of the Cdt1 deletion mutants in a *ddb1*Δ background.
(A) A comparison of Cdt1-YFP imaged in exponentially growing cells of wildtype or *ddb1*Δ background expressing:- wildtype Cdt1 (2337, 2425), Cdt1Δ26-100 (2339, 2426), Cdt1Δ26-200 (2421, 2427), Cdt1Δ 26-300 (2422, 2428), Cdt1Δ26-400 (2423, 2429) or Cdt1Δ390-444 (2424, 2430). Scale bar: 10 μm. **(B)** Western blot analysis of Cdt1-YFP levels in the strains described in (A).



wildtype cells (Figure 4.6B). The striking increase in the level of Cdt1Δ26-300 between wildtype and *ddb1*Δ cells indicates that a region outside of amino acids 26-300 contributes to the Ddb1-dependent turnover of Cdt1.

While this work was in progress, it was reported that *Xenopus* Cdt1 contains a specialised 'PIP degron' as opposed to a 'PIP box' that defines it as a $CRL4^{Cdt2}$ target (Havens and Walter 2009). In addition to the canonical PIP box sequence, the PIP degron consists of a TD motif within the PIP box and a positively-charged amino acid four residues downstream of the PIP box (B+4). In light of this finding, the fission yeast Cdt1 sequence was re-examined to determine if a PIP degron sequence could be identified. Interestingly, although none of the four partial matches to the PIP box sequence in fission yeast Cdt1 contain a TD motif, the N-terminal PIP motif at position 28 and a second motif at position 301 both contain a B+4 residue (Figure 4.7A). It was speculated that these two variant PIP degrons could regulate the cell cycle-dependent proteolysis of Cdt1. As the second putative PIP degron starts at amino acid 301, it might explain the Ddb1-dependent turnover of Cdt1Δ26-300.

The role of the two variant PIP degrons in Cdt1 regulation was examined by deleting both sequences in a Cdt1Δ26-316 mutant (Appendix II, 9). The effect of the Cdt1Δ26-316 deletion on the cell cycle-dependent regulation of Cdt1 was determined by fluorescence microscopy comparison of cells expressing YFP-tagged wildtype Cdt1, Cdt1Δ26-300 or Cdt1Δ26-316 (Figure 4.7B). Cdt1Δ26-316 was detected in the nuclei of all cells and interestingly, the intensity of this fluorescence was higher than Cdt1Δ26-300 fluorescence and comparable to that of wildtype Cdt1 in a *ddb1*Δ

A

```
            12345678+1+2+3+4
PIP box     QxxΨxxϑϑ
PIP degron  QxxΨTDϑϑxxxB
Cdt1_PIP28  QTKLNFSVRKTRSSSKRS
Cdt1_PIP301 QLTLRQSSLFDRVRKKQK
```

B

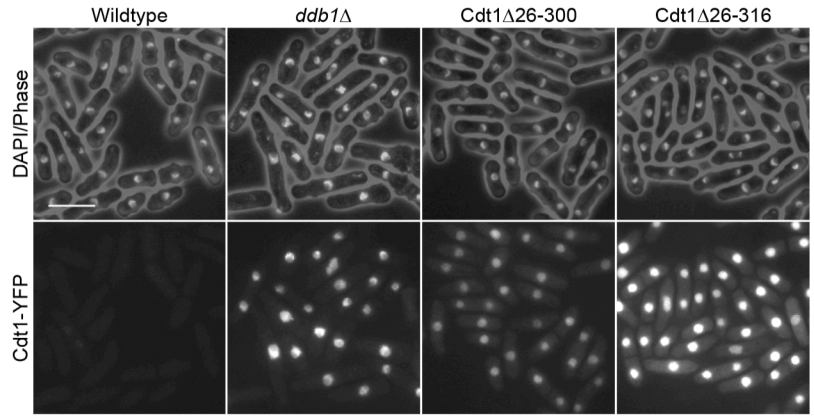


Figure 4.7 | Identification of two putative PIP degrons in Cdt1.
(A) An alignment of two putative PIP degrons in Cdt1 (Ψ: hydrophobic residue, ϑ: aromatic residue, B: basic residue, x: any residue). **(B)** Cdt1-YFP imaged in exponentially growing cells in a wildtype (2337) or a *ddb1*Δ (2425) background and in cells expressing Cdt1Δ26-300 (2422) or Cdt1Δ26-316 (2431). Scale bar: 10 μm.

background. This suggests that the putative PIP degron at position 301 contributes to the cell cycle-dependent regulation of Cdt1.

4.2.3 Dual PIP degrons at positions 28 and 301 are involved in the cell cycle- and DNA damage-dependent regulation of Cdt1

The involvement of the putative PIP degrons at positions 28 and 301 in Cdt1 regulation was analysed by mutating key residues in each motif either alone or in combination to generate PIP28^{A8}, PIP301^{A10} and PIP28^{A8} PIP301^{A10} mutants (Figure 4.8A). Residues affected by the PIP301^{A10} mutation are essential for *S. cerevisiae* viability (Jee et al. 2010) and therefore each PIP mutant was introduced as a second copy, in a wildtype *cdt1*$^{+}$ background (Appendix II, 10).

The role of the two PIP degrons in the cell cycle-dependent regulation of Cdt1 was analysed by a fluorescence microscopy comparison of Cdt1-YFP in wildtype cells and in each PIP mutant. The Cdt1 signal in wildtype, PIP28^{A8} and PIP301^{A10} strains was detected in the nuclei of between 20-30% of binucleate (late M/G1) cells (Figure 4.8B). The PIP28^{A8} mutant, but not the PIP301^{A10} mutant, showed an increase in the number of uninucleate (G2) cells with nuclear Cdt1-YFP compared to wildtype, perhaps suggesting a greater involvement of the PIP28 motif in the S phase proteolysis of Cdt1 (Figure 4.8B, lower panel). Strikingly, in the double PIP28^{A8} PIP301^{A10} mutant, YFP fluorescence was detected in the nuclei of all cells, regardless of their cell cycle stage, suggesting a complete loss of cell cycle regulation (Figure 4.8B). Western blot analysis confirmed these observations (Figure 4.8C); there was a dramatic increase in the level of the PIP28^{A8} PIP301^{A10} mutant protein compared to the level of the wildtype, PIP28^{A8} and PIP301^{A10} proteins.

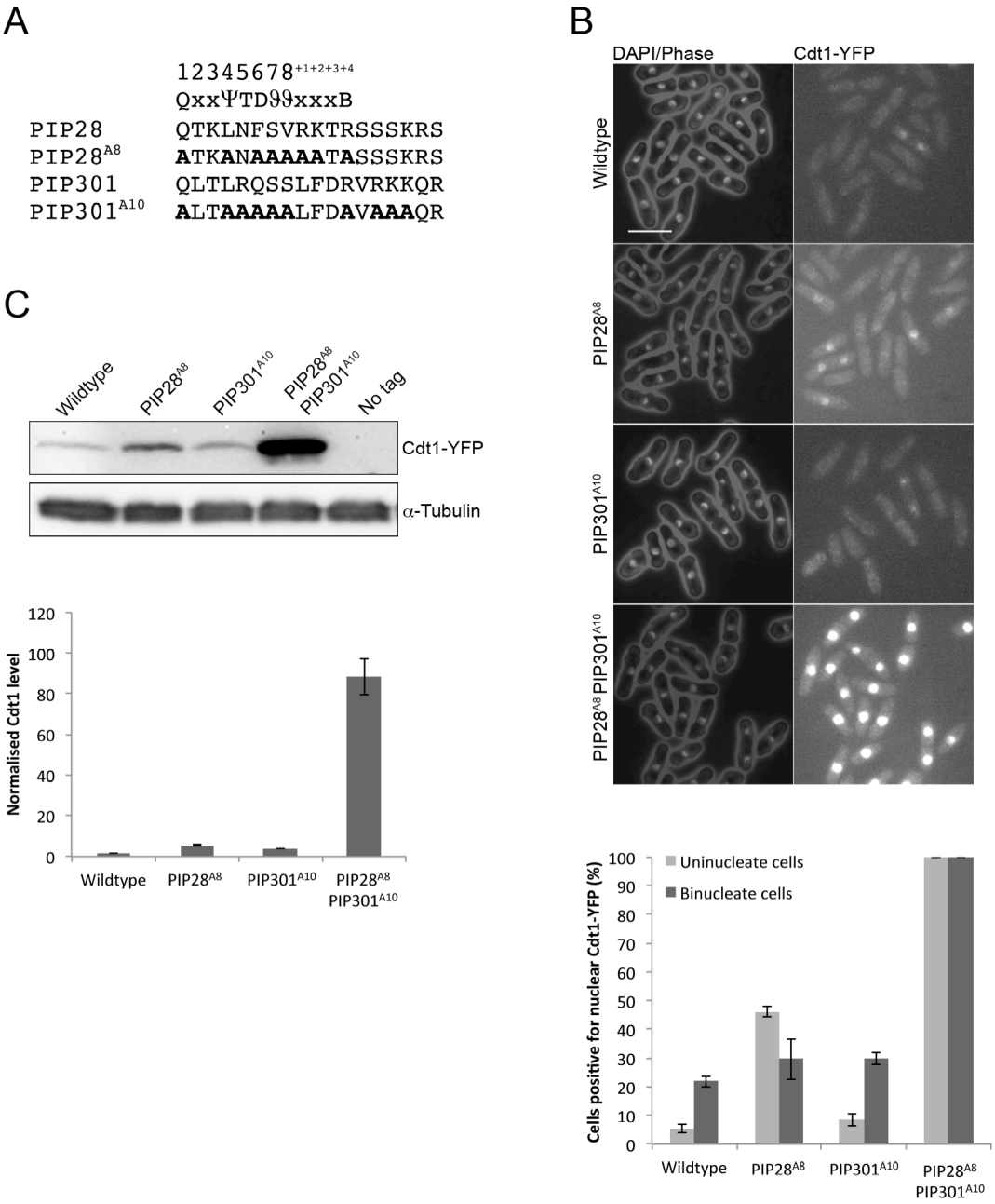


Figure 4.8 | Two putative PIP degrons are required for the cell cycle regulation of Cdt1. **(A)** An alignment of the two putative PIP degrons in Cdt1, together with the sequences of the PIP28^{A8} and PIP301^{A10} mutants (Ψ: hydrophobic residue, ϑ: aromatic residue, B: basic residue, x: any residue). **(B)** *Upper panel:* Cdt1-YFP imaged in exponentially growing cells in wildtype (2337) and PIP28^{A8} (2507), PIP301^{A10} (2513) and PIP28^{A8} PIP301^{A10} (2500) mutant strains. Scale bar: 10 μm. *Lower panel:* the same strains were analysed to determine the percentage of uninucleate and binucleate cells positive for Cdt1-YFP. At least 100 cells, from two independent experiments, were counted for each data point. Error bars: 50% of range. **(C)** *Upper panel:* Western blot analysis of Cdt1 levels in non-tagged (2270), wildtype (2337) and PIP28^{A8} (2507), PIP301^{A10} (2513) and PIP28^{A8} PIP301^{A10} (2500) mutant strains. *Lower panel:* Quantitation of Cdt1-YFP levels from the western blot analysis. Graph shows Cdt1 levels following normalisation to the α–tubulin loading control. The data are an average from two independent experiments. Error bars: 50% of range.

A comparison of Cdt1-YFP in the double PIP28^{A8} PIP301^{A10} mutant with wildtype Cdt1-YFP in a *ddb1*Δ mutant, indicated that the overall protein level and the nuclear Cdt1 signal in *ddb1*Δ cells was higher than in the PIP28^{A8} PIP301^{A10} mutant (Figure 4.9). This could imply that mutation of both PIP degrons in Cdt1 does not abolish CRL4^{Cdt2}-mediated proteolysis. Alternatively, deregulation of additional CRL4^{Cdt2} targets, such as the RNR inhibitor Spd1, in *ddb1*Δ cells may elevate Cdt1 levels (Liu et al. 2005a). For example, Spd1 deregulation has been reported to activate Rad3 and this could increase MBF-dependent transcription of Cdt1 (Liu et al. 2003; Watson et al. 2004; Liu et al. 2005a). Therefore, the level of Cdt1-YFP in the PIP28^{A8} PIP301^{A10} mutant was compared with the level of wildtype Cdt1-YFP in a *ddb1*Δ *spd1*Δ background and found to be similar (Figure 4.9). This suggests that CRL4^{Cdt2}-dependent turnover of Cdt1 in the PIP28^{A8} PIP301^{A10} mutant is largely inhibited.

To analyse whether the two PIP degrons have a role in Cdt1 proteolysis after DNA damage, the level of Cdt1-YFP in mitotically-arrested wildtype, PIP28^{A8}, PIP301^{A10} and PIP28^{A8} PIP301^{A10} cells following UV irradiated was monitored. The two single PIP28^{A8} and PIP301^{A10} mutants showed a slight stabilisation of Cdt1 at 60 minutes after UV irradiation compared to wildtype (Figure 4.10A and C). However, a dramatic stabilisation of Cdt1 was observed in the double PIP28^{A8} PIP301^{A10} mutant after UV irradiation, suggesting that both PIP degrons contribute to the DNA damage-dependent regulation of Cdt1 (Figure 4.10A and C). There was a slight increase in Cdt1 stabilisation in the PIP28^{A8} mutant compared to the PIP301^{A10} mutant after UV irradiation (Figure 4.10A), perhaps suggesting a greater role for the PIP28 motif in Cdt1 regulation after UV-induced DNA damage.

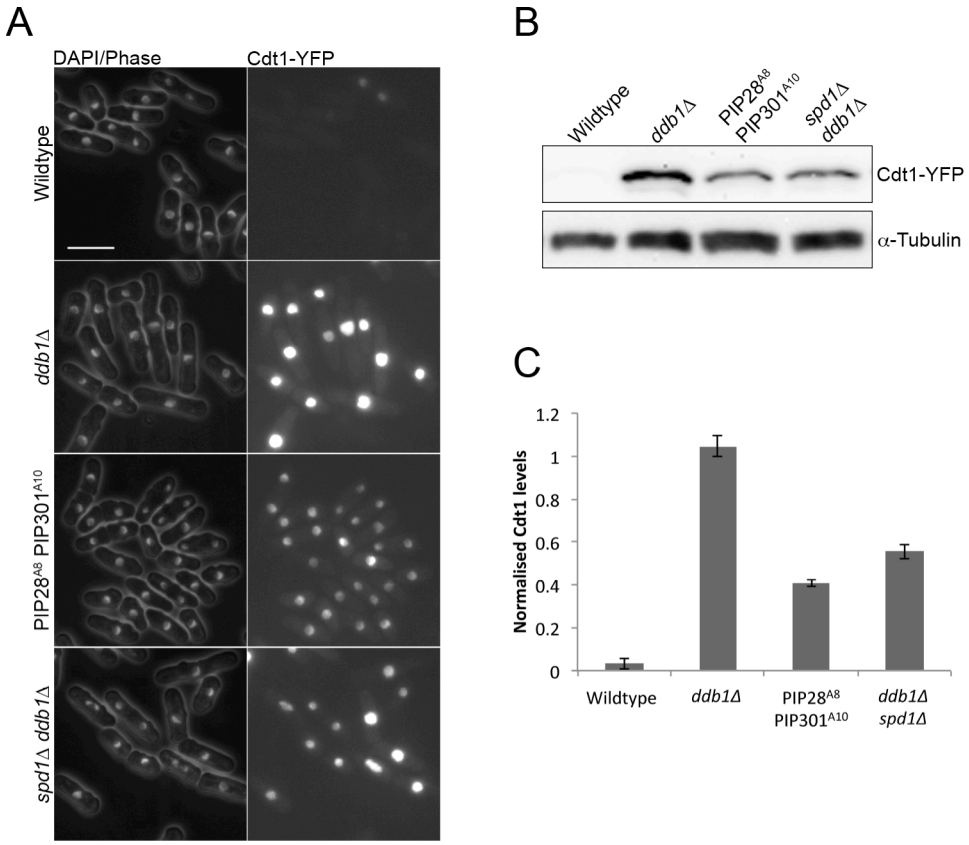


Figure 4.9 | Cdt1 levels in PIP28^{A8} PIP301^{A10} and *ddb1*Δ *spd1*Δ mutants are comparable. **(A)** Cdt1-YFP imaged in exponentially growing cells in wildtype (2337) and *ddb1*Δ (2425), PIP28^{A8} PIP301^{A10} (2500) and *ddb1*Δ *spd1*Δ (3135) mutant strains. Scale bar: 10 μm. **(B)** Western blot analysis of Cdt1 levels in the strains described in (A). **(C)** Quantitation of Cdt1-YFP levels from the western blot analysis. Graph shows Cdt1 levels following normalisation to the α-tubulin loading control. The data are an average from two independent experiments. Error bars: 50% of range.

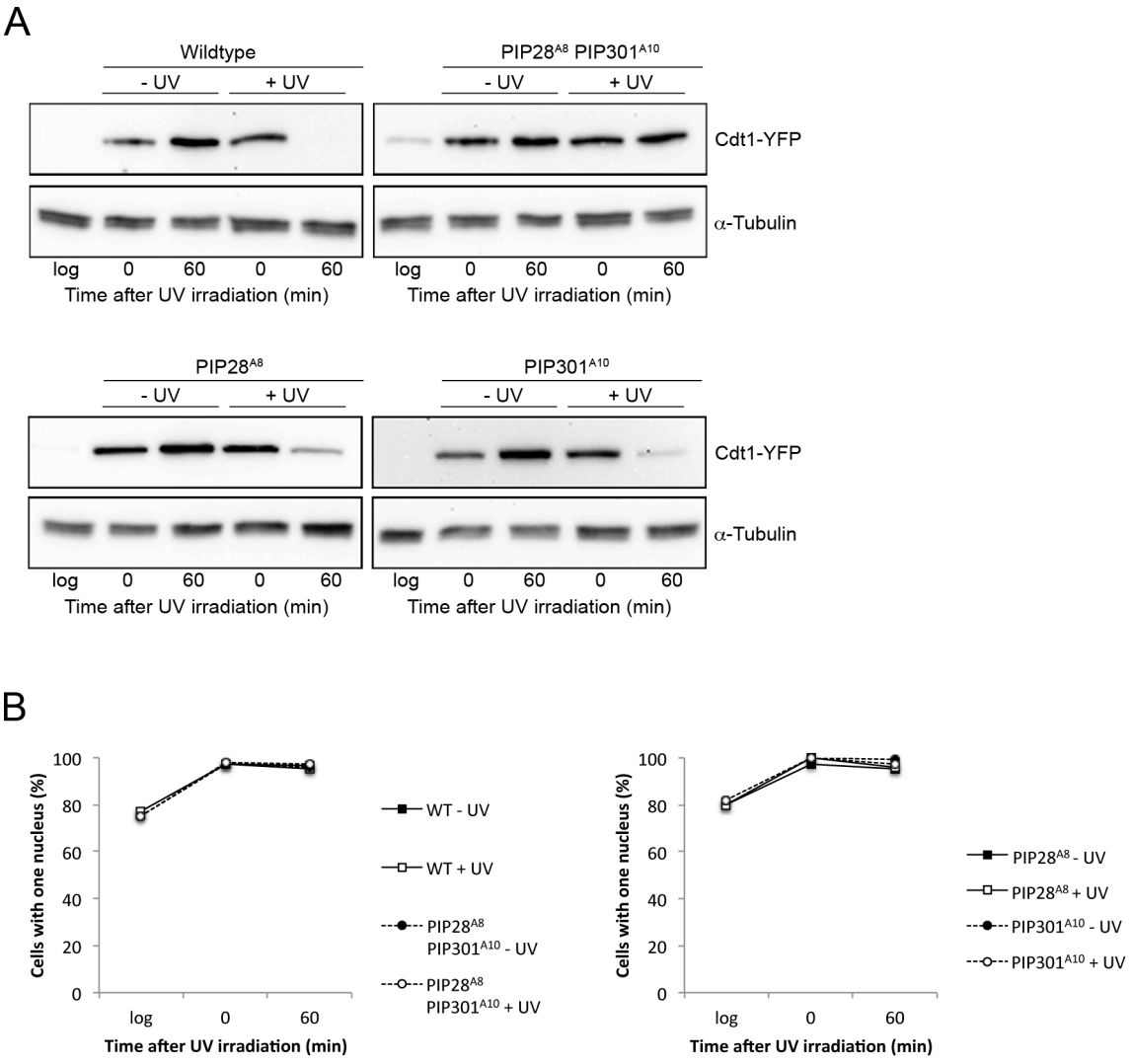


Figure 4.10 | Two putative PIP degrons are required for Cdt1 proteolysis after UV irradiation. **(A)** Western blot analysis of Cdt1 levels after mock or 100 J/m^2 UV treatment in prometaphase-arrested *nda3-311* cells (Wildtype, 2337; PIP28^{A8} PIP301^{A10}, 2500; PIP28^{A8}, 2507; PIP301^{A10}, 2513). Cells were arrested by incubation at 20°C for 4 hours and were returned to the restrictive temperature after UV treatment. **(B)** Percentage of uninucleate cells during the experiment shown in (A). **(C)** Quantitation of Cdt1 levels from western blot analysis in (A). Graph shows the ratio of Cdt1 levels (t = 1/t = 0), following normalisation to the α-tubulin loading control, 1 hour after UV irradiation. The data are an average from two independent experiments. Error bars: 50% of range.

The S phase-dependent proteolysis of Cdt1-YFP in each PIP mutant strain was analysed in detail in a synchronised cell cycle, following an *nda3-311* mitotic arrest. Flow cytometric analysis and the septation index were used to monitor progression through the cell cycle and indicated that S phase occurred 30 minutes after release (Figure 4.11B and C). Cdt1 levels in the wildtype and the single PIP28^{A8} and PIP301^{A10} mutant cells decreased as the cells traversed S phase, although Cdt1 proteolysis in the PIP28^{A8} mutant was less efficient compared to wildtype and the PIP301^{A10} mutant (Figure 4.11A). In contrast, no decline in Cdt1 levels in the double PIP28^{A8} PIP301^{A10} mutant was observed during S phase, despite a decrease in the level of Cdt1 at 105-120 minutes post release (Figure 4.11A). Therefore, it appears that both PIP degrons are required for the S phase-dependent proteolysis of Cdt1.

To verify the observation that the S phase-dependent proteolysis of Cdt1 requires both PIP degrons, wildtype and PIP28^{A8} PIP301^{A10} mutant cells were synchronised in G1 by nitrogen starvation (Figure 4.12). This method holds two advantages over the *nda3-311* mitotic arrest; the genetic background is wildtype and Cdt1 levels are maintained at more physiological levels. The wildtype and PIP28^{A8} PIP301^{A10} mutant nitrogen-starved cells were small and spherical with low Cdt1-YFP levels (Figure 4.12A and B, t = 0 hours). After refeeding and incubation at 32°C, wildtype Cdt1 levels increased 2 hours post release, then declined as the cells traversed S phase (Figure 4.12A-C). In contrast, once the level of Cdt1 in the PIP28^{A8} PIP301^{A10} mutant increased at 2 hours, it remained high and constant throughout S phase and the rest of the time-course, with all cells at 4 and 5 hours post release positive for nuclear Cdt1 (Figure 4.12A-C). This confirms the requirement for PIP28 and PIP301 in the S phase-dependent regulation of Cdt1.

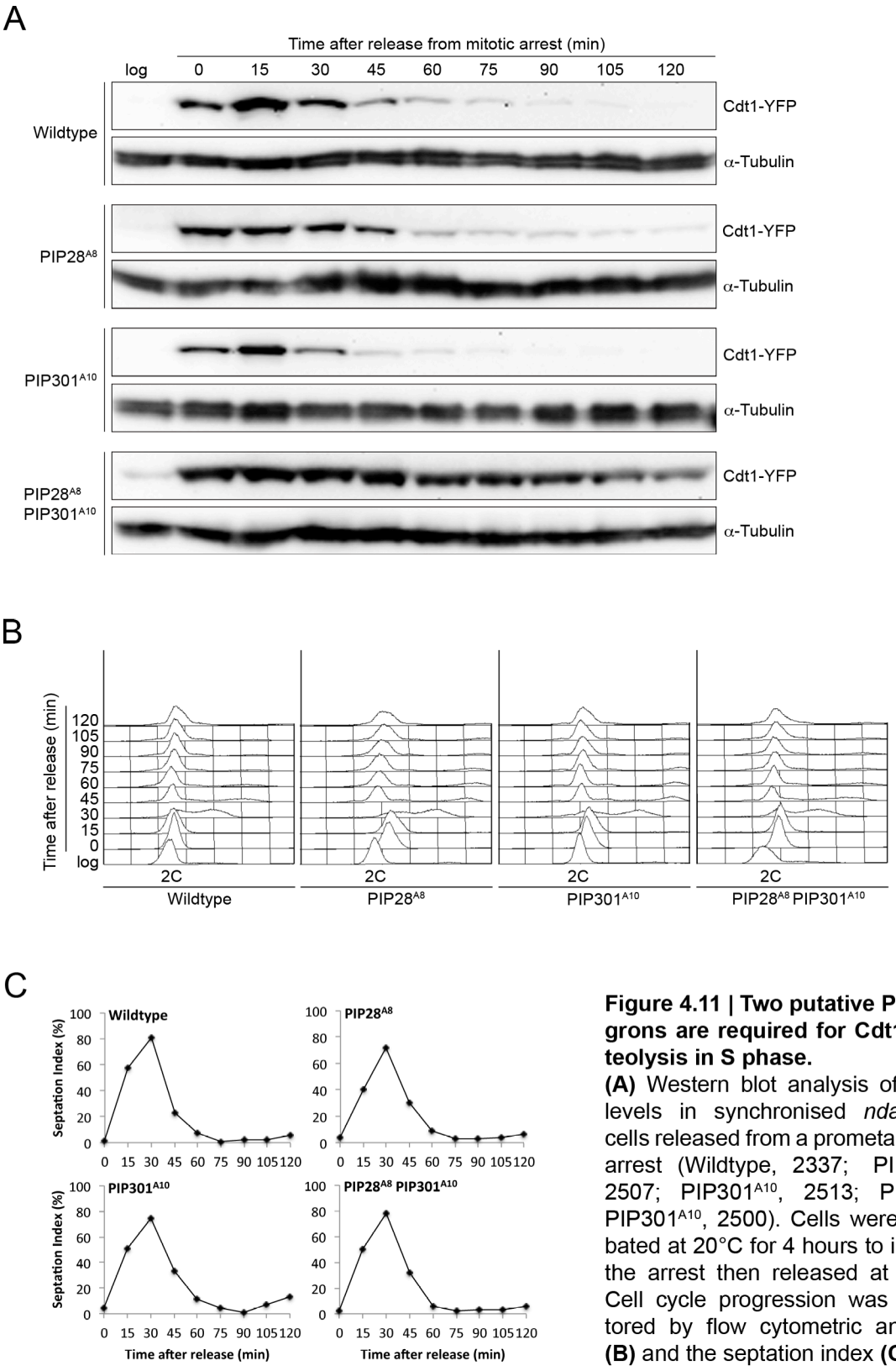


Figure 4.11 | Two putative PIP degrons are required for Cdt1 proteolysis in S phase.
(A) Western blot analysis of Cdt1 levels in synchronised *nda3-311* cells released from a prometaphase arrest (Wildtype, 2337; PIP28^{A8}, 2507; PIP301^{A10}, 2513; PIP28^{A8} PIP301^{A10}, 2500). Cells were incubated at 20°C for 4 hours to induce the arrest then released at 32°C. Cell cycle progression was monitored by flow cytometric analysis **(B)** and the septation index **(C)**.

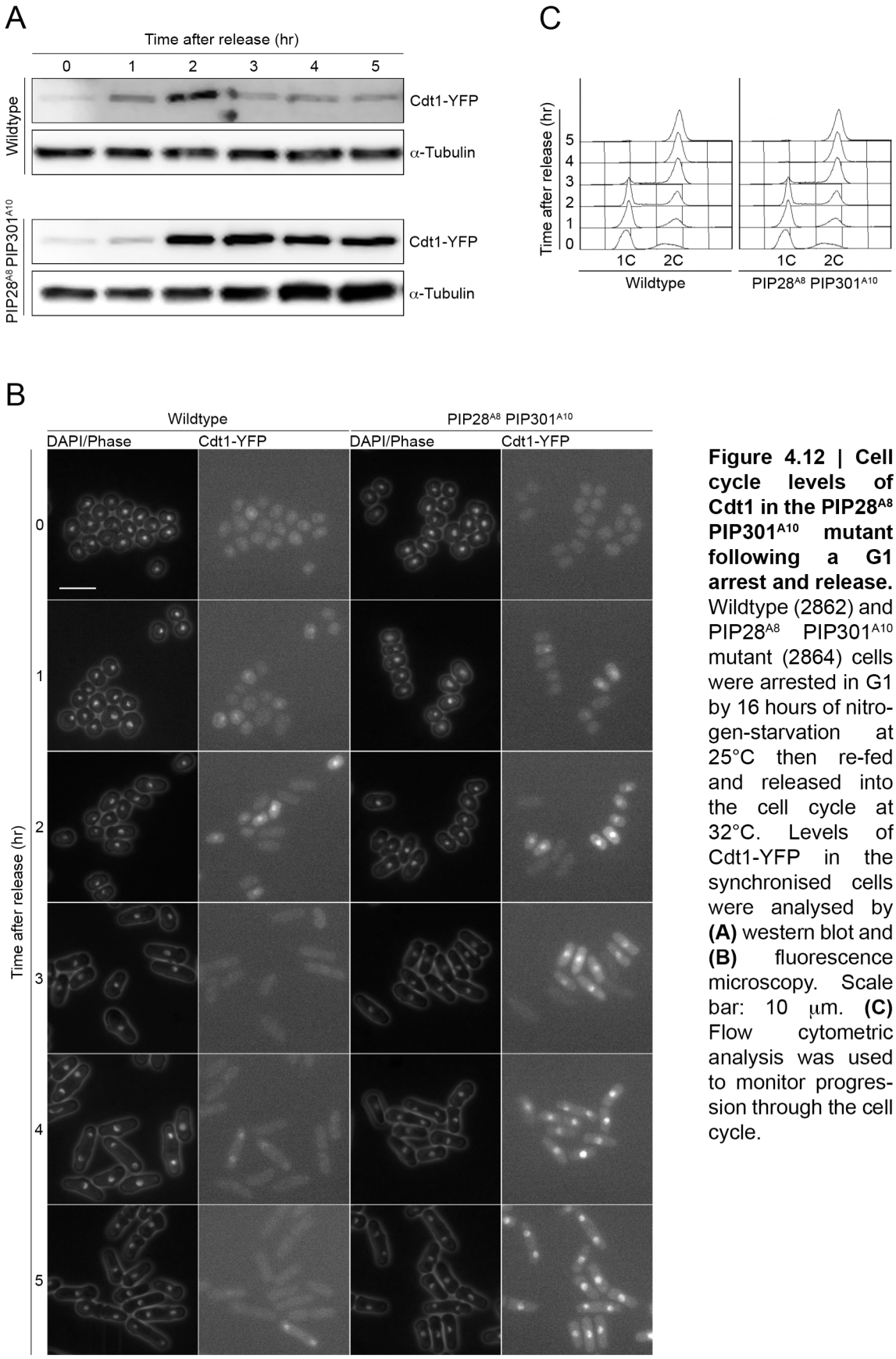


Figure 4.12 | Cell cycle levels of Cdt1 in the PIP28^{A8} PIP301^{A10} mutant following a G1 arrest and release. Wildtype (2862) and PIP28^{A8} PIP301^{A10} mutant (2864) cells were arrested in G1 by 16 hours of nitrogen-starvation at 25°C then re-fed and released into the cell cycle at 32°C. Levels of Cdt1-YFP in the synchronised cells were analysed by **(A)** western blot and **(B)** fluorescence microscopy. Scale bar: 10 μm. **(C)** Flow cytometric analysis was used to monitor progression through the cell cycle.

4.2.4 Residual Cdt2-independent turnover of Cdt1 occurs in the cell cycle

An S phase independent decline in PIP28^{A8} PIP301^{A10} Cdt1 levels at 105-120 minutes after release from a mitotic arrest was observed in Figure 4.11A. To examine whether this decline was CRL4^{Cdt2} dependent, a mitotic arrest and release experiment was performed with a *cdt2*Δ *spd1*Δ strain (Figure 4.13). Use of this strain ensured inhibition of CRL4^{Cdt2}-dependent proteolysis but avoided the cell cycle defects associated with Spd1 deregulation (Liu et al. 2003). The level of Cdt1-YFP in *cdt2*Δ *spd1*Δ cells released from the mitotic arrest increased between 0 and 75 minutes, before declining to a level similar to that observed during the mitotic arrest (Figure 4.13A and C). Cell cycle progression was monitored using the septation index (Figure 4.13B). The western blot analysis indicated that in comparison to the PIP28^{A8} PIP301^{A10} mutant, Cdt1 levels in the *cdt2*Δ *spd1*Δ mutant were more consistent over the course of the experiment (compare Figure 4.11A 'PIP28^{A8} PIP301^{A10}' with 4.13A). This indicates a Cdt2-dependent component contributes to the decline in Cdt1 levels observed in the PIP28^{A8} PIP301^{A10} mutant. Nevertheless, the decline in Cdt1 levels between 75-120 minutes after release in the *cdt2*Δ *spd1*Δ strain suggests Cdt2-independent turnover of Cdt1 can occur.

To compare the stability of the PIP28^{A8} PIP301^{A10} mutant protein and wildtype Cdt1 in a *cdt2*Δ *spd1*Δ background in more detail, the S phase-dependent turnover of each protein was examined in HU-treated cells in the presence of cycloheximide (CHX), an inhibitor of protein synthesis. Mitotically-arrested cells were released into media containing HU and treated with CHX at 45 minutes after release, to ensure entry into S phase occurred (Figure 4.14A). The wildtype, PIP28^{A8} PIP301^{A10} and *cdt2*Δ *spd1*Δ cells arrested in S phase at 60 minutes after release from the mitotic arrest (Figure

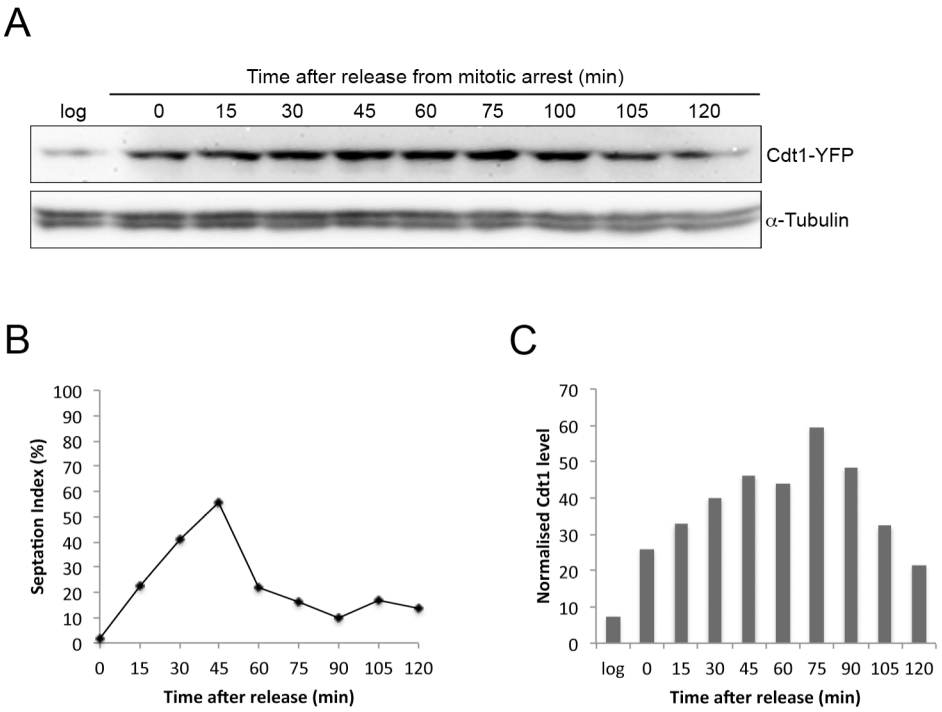


Figure 4.13 | Analysis of cell cycle Cdt1 levels in a *cdt2*Δ *spd1*Δ mutant.
(A) Western blot analysis of Cdt1 levels in synchronised *cdt2*Δ *spd1*Δ *nda3-311* (2582) cells released from a prometaphase arrest. Cells were incubated at 20°C for 4 hours to induce the arrest then released at 32°C. **(B)** Septation index to monitor the cell cycle progression of cells in (A). **(C)** Quantitation of western blot analysis in (A). Graph shows Cdt1 levels through the time-course, normalised to the α-tubulin loading control.

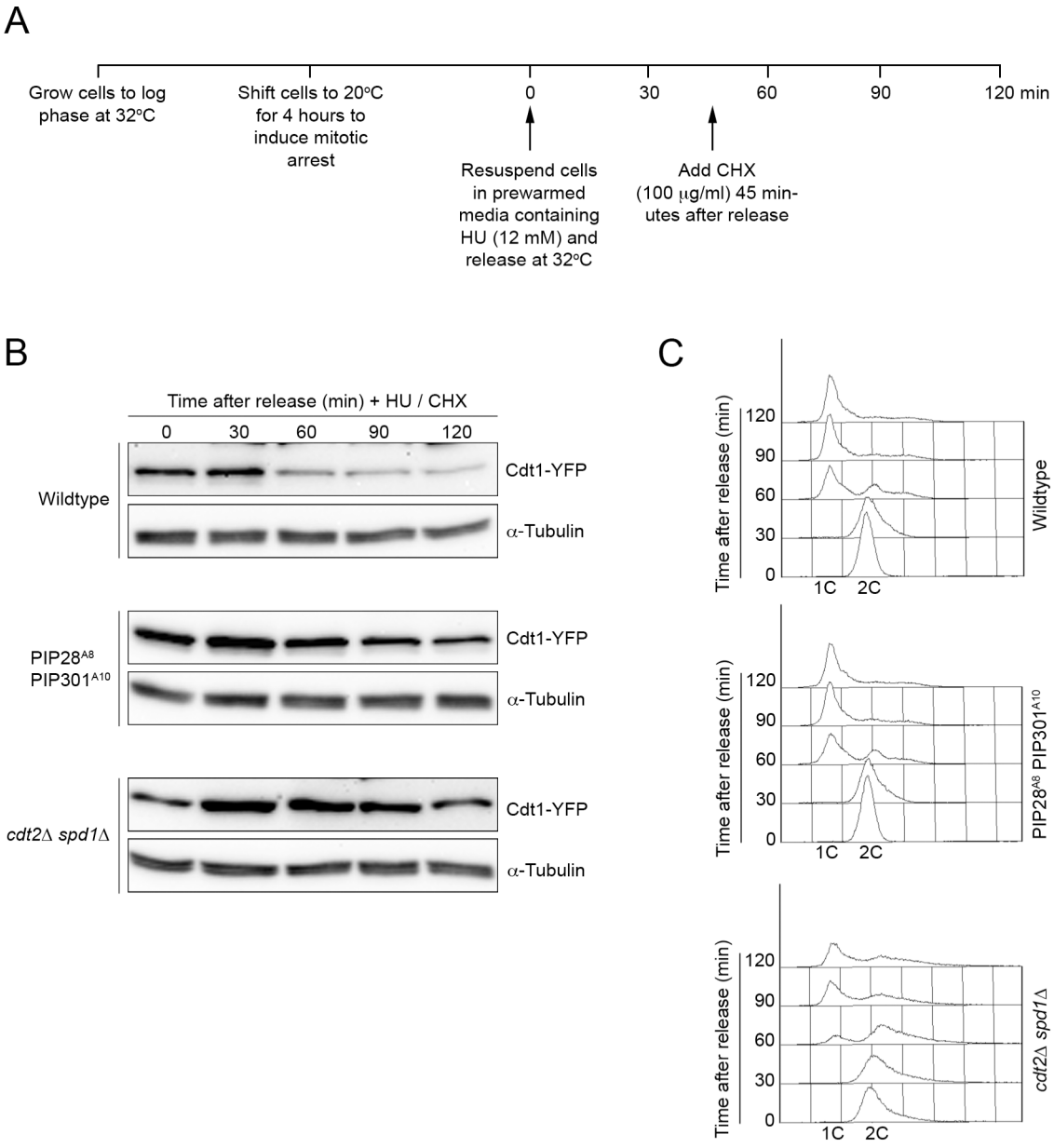


Figure 4.14 | Analysis of the stability of the PIP28^{A8} PIP301^{A10} protein.
(A) Scheme of experiment. **(B)** Western blot analysis of wildtype (1956), PIP28^{A8} PIP301^{A10} (2500) and *cdt2*Δ *spd1*Δ (2582) cells following the experimental procedure outlined in (A). **(C)** Flow cytometry profiles of the strains described in (B).

4.14C) and the level of Cdt1-YFP in the wildtype cells decreased at this time-point accordingly (Figure 4.14B). Interestingly, although the level Cdt1 in the PIP28^{A8} PIP301^{A10} and *cdt2*Δ *spd1*Δ mutant cells remained higher over the course of the experiment compared to the wildtype, there was a notable decrease in both protein levels between 60-120 minutes after release. In summary, this experiment indicates that although CRL4^{Cdt2}-dependent proteolysis is largely inhibited in the PIP28^{A8} PIP301^{A10} mutant, residual Cdt2-independent turnover of Cdt1 can occur.

4.2.5 Dual PIP degrons in Cdt1 are required for the protein to interact with PCNA

To address whether Cdt1 interacts with PCNA via the putative PIP degrons at positions 28 and 301 *in vivo* in fission yeast cells, the technique of bimolecular fluorescence complementation (BiFC) was employed (Hu et al. 2002). In this technique, two potentially interacting proteins are tagged with the N- and C-terminal fragments of a fluorescent protein. An association between the interacting proteins brings the N- and C-terminal fluorescent protein fragments into close proximity, which reconstitutes the fluorophore (Figure 4.15A). This technique permits *in vivo* visualisation of protein-protein interactions and can provide details of the subcellular localisation of these interactions (Hu et al. 2002).

PCNA and Cdt1 (wildtype, PIP28^{A8}, PIP310^{A10} and PIP28^{A8} PIP310A^{10} sequences) were tagged with the N- and C-terminal domains of Venus-YFP respectively and expressed from their endogenous promoters (Appendix II, 11) (Nagai et al. 2002; Shyu et al. 2006; Akman and MacNeill 2009). No signal was detected when cells expressed either the *VN173-pcn1* or the *cdt1-VC155* constructs separately

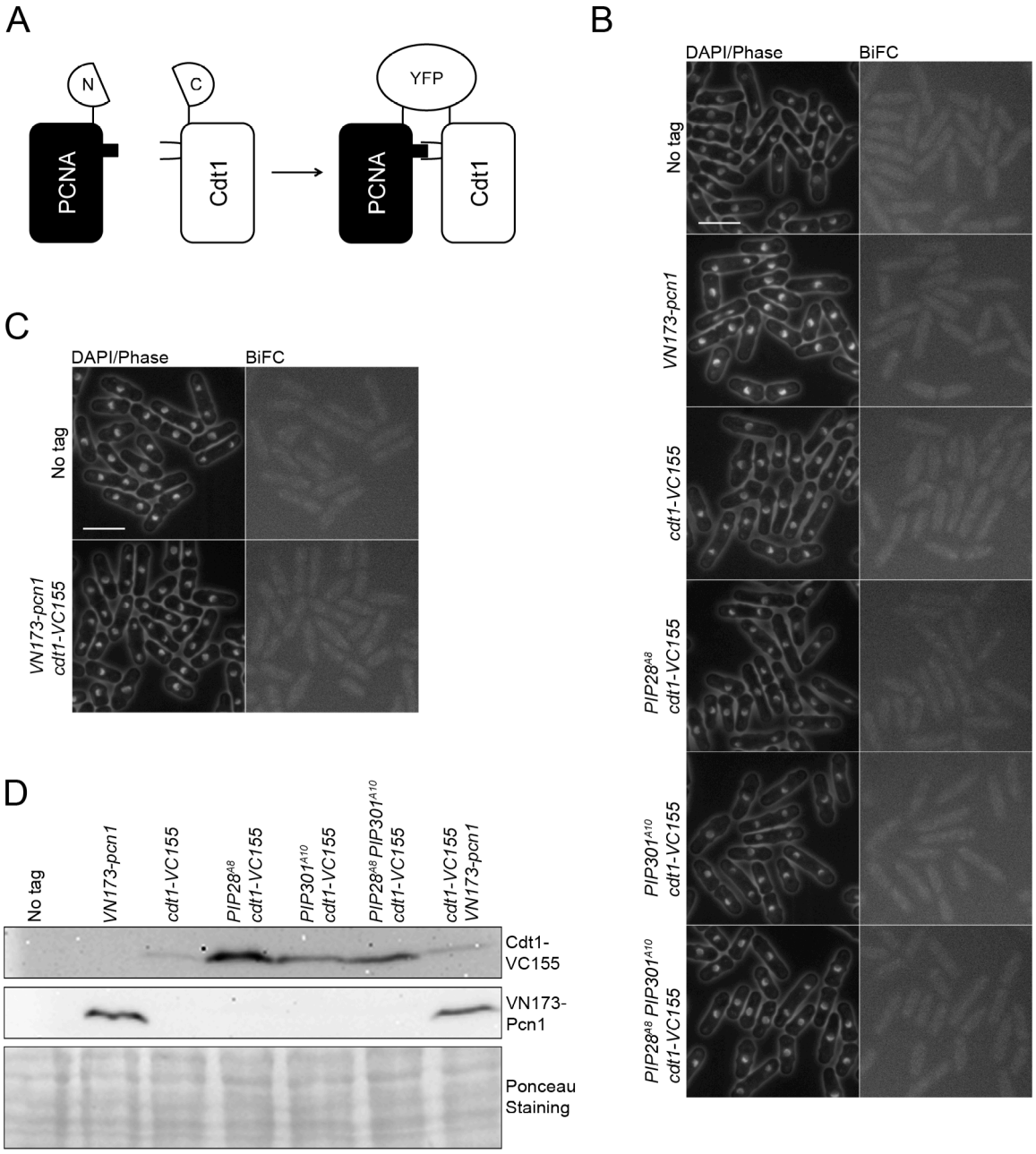


Figure 4.15 | Preliminary investigation of the BIFC technique.
(A) Diagram to illustrate the principle of the BiFC technique. **(B)** Fluorescence microscopy analysis of non-tagged cells (138) and of cells expressing *VN173-pcn1* (2535), *cdt1-VC155* (3136), *PIP28^{A8} cdt1-VC155* (3137), *PIP301^{A10} cdt1-VC155* (3138) and *PIP28^{A8} PIP301^{A10}cdt1-VC155* (3139). Scale bar: 10 μm. **(C)** Fluorescence microscopy analysis of non-tagged cells (138) and of cells expressing *VN173-pcn1 cdt1-VC155* (2600). Scale bar: 10 μm. **(D)** Western blot analysis of the strains described in (B) and (C).

(Figure 4.15B). Co-expression of *VN173-pcn1* and *cdt1-VC155* also did not produce a BiFC signal (Figure 4.15C). Western blot analysis confirmed that the *VN173-pcn1* and the *cdt1-VC155* constructs were expressed (Figure 4.15D).

The rapid turnover of Cdt1 following its interaction with PCNA could account for the lack of BiFC signal in *VN173-pcn1 cdt1-VC155* cells. In support of this hypothesis, co-expression of *VN173-pcn1* and *cdt1-VC155* in a *cdt2*Δ background, where Cdt1 was stabilised, produced a nuclear BiFC signal that was detected in all cells, irrespective of their cell cycle stage (Figure 4.16A). Quantitation of the nuclear BiFC signal showed that the signal was higher in binucleate cells than in uninucleate cells, which may indicate that the interaction is more predominant in S phase cells (Figure 4.16B 'Wildtype'). PCNA and Cdt1 can therefore interact *in vivo* and this interaction can occur in the absence of Cdt2, as previously reported in *Xenopus* egg extracts (Havens and Walter 2009).

Studies from *Xenopus* suggest that Cdt1 interacts only with chromatin-associated PCNA (Arias and Walter 2006; Havens and Walter 2009). PCNA predominantly associates with chromatin in S phase and the detection of a nuclear BiFC signal in all *VN173-pcn1 cdt1-VC155* cells may indicate that the fission yeast PCNA-Cdt1 interaction can occur off chromatin. Alternatively, the tight binding between the N- and C-terminal YFP fragments may prevent dissociation of PCNA and Cdt1 following an interaction in S phase, maintaining the BiFC signal through the cell cycle. This has been suggested as a limitation of BiFC as a technique for studying dynamic protein-protein interactions (Akman and MacNeill 2009).

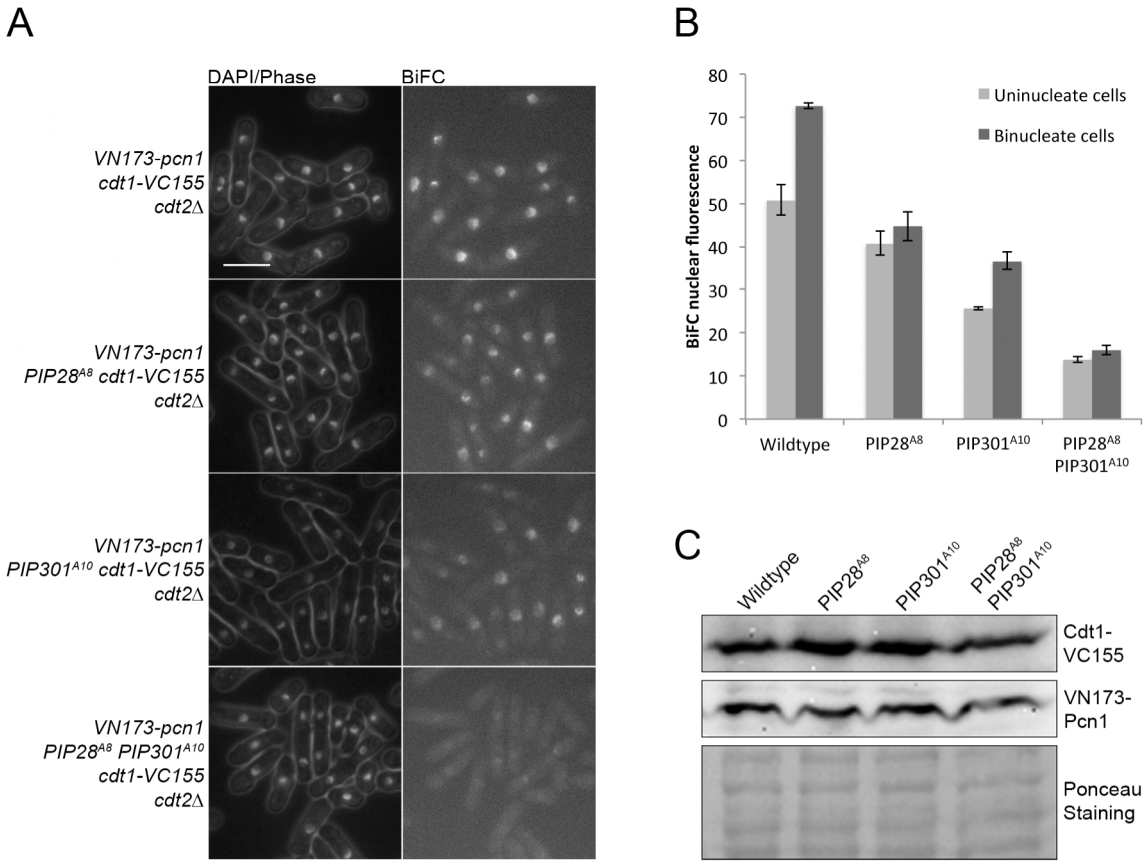


Figure 4.16 | Dual PIP degrons promote the fission yeast Cdt1-PCNA interaction.
(A) BiFC imaged in exponentially growing *cdt2*Δ cells expressing *VN173-pcn1 cdt1-VC155* (2601), *VN173-pcn1 PIP28^{A8} cdt1-VC155* (2602), *VN173-pcn1 PIP301^{A10} cdt1-VC155* (2603) or *VN173-pcn1 PIP28^{A8} PIP301^{A10} cdt1-VC155* (2604). Scale bar: 10 μm. **(B)** The intensity of nuclear BiFC fluorescence in uninucleate and binucleate cells of the strains described in (A) was quantitated using Micro-Manager 1.3. 100 uninucleate and 100 binucleate cells, from two independent experiments, were measured for each data point. Error bars: 50% of range. **(C)** Western blot analysis of Cdt1 levels in the cells described in (A).

BiFC was used to address whether mutation of the PIP28 and PIP301 degrons alone or in combination affected the interaction between Cdt1 and PCNA. Cells co-expressing *VN173-pcn1* with *PIP28^{A8} cdt1-VC155*, *PIP301^{A10} cdt1-VC155* or *PIP28^{A8} PIP301^{A10} cdt1-VC155* were grown to log phase and analysed by fluorescence microscopy. In the single PIP28^{A8} and PIP301^{A10} mutants, a nuclear BiFC signal was detected in all cells, although this signal was lower than in wildtype *VN173-pcn1 cdt1-VC155* cells (Figure 4.16A and B). Strikingly, the nuclear BiFC signal in the double PIP28^{A8} PIP301^{A10} mutant was dramatically reduced compared to both the wildtype and single PIP28^{A8} and PIP301^{A10} mutants (Figure 4.16A and B). Western blot analysis was used to confirm that the *VN173-pcn1* and the wildtype or the PIP box mutated *cdt1-VC155* constructs were expressed at similar levels in *cdt2*Δ cells (Figure 4.16C). In summary, this analysis indicates that PIP28 and PIP301 are *bona fide* PIP degrons that mediate the interaction between Cdt1 and PCNA. Cdt1 can interact with PCNA via either PIP degron but the interaction is strongest when both are intact.

4.3 DISCUSSION

Through a combination of large-scale and site-directed mutagenesis, two variant PIP degrons in *S. pombe* Cdt1 have been identified. The two PIP degrons promote the fission yeast Cdt1-PCNA interaction and are required for Cdt1 proteolysis in S phase and in response to DNA damage. In this section, three areas that relate to the work presented in this chapter are discussed: the limitations of a using a large-scale deletion approach to define the regulatory regions of a protein; the possible reasons behind the employment of dual PIP degrons in Cdt1 regulation; and the context of this work in our wider understanding of CRL4^{Cdt2}-mediated proteolysis.

4.3.1 The limitations of large-scale deletion mutants

Investigation into the regulatory motifs in *S. pombe* Cdt1 began before the distinction between PIP box and PIP degrons sequences in $CRL4^{Cdt2}$-mediated ubiquitylation was understood (Havens and Walter 2009). Therefore, it appeared that the fission yeast Cdt1 sequence contained numerous potential regions that could mediate an interaction with PCNA and stimulate $CRL4^{Cdt2}$ recruitment. In an attempt to exhaustively investigate the regions of Cdt1 required for proteolysis, a series of large-scale deletion mutants were constructed that spanned the protein sequence.

The large-scale deletion mutants produced some useful insights into Cdt1 regulation. Principally, interpretation of the phenotypes of the truncation mutants led to the concept that at least two motifs in fission yeast Cdt1 must contribute to its proteolysis. For example, analysis of the Cdt1Δ26-100 mutant indicated that although amino acids 26-100 were required for a robust down-regulation of Cdt1 after UV irradiation, a second region was involved in the S phase-dependent proteolysis of the protein. Furthermore, comparison of Cdt1Δ26-300 levels in a wildtype and a *ddb1*Δ background suggested that a region outside of amino acids 26-300 contributed to Ddb1-dependent turnover of Cdt1. Following recognition of the importance of a PIP degron in *Xenopus* Cdt1 regulation (Havens and Walter 2009), the identification and analysis of two variant PIP degrons in *S. pombe* Cdt1 regulation was straightforward.

Generating point mutants that disrupted the two variant PIP degrons in *S. pombe* Cdt1 was a more powerful technique than generating large-scale deletion mutants. It was often difficult to separate the direct effect of a large-scale deletion on Cdt1 proteolysis from secondary effects that indirectly influenced Cdt1 levels. For example, the

Cdt1Δ26-100 mutant compromised the nuclear localisation of Cdt1, which precluded an interpretation of the stabilised Cdt1 phenotype in terms of proteolysis. In addition, the level of Cdt1Δ26-400 was low in a wildtype and a *ddb1*Δ background, compared to the level of Cdt1Δ26-300. Given 85% of Cdt1 was deleted in the Cdt1Δ26-400 mutant, it is possible that the folding of the protein was affected. Misfolded proteins are ubiquitylated and targeted to the 26S proteasome for proteolysis by specific E3 ubiquitin ligases, either directly or indirectly, following recognition by molecular chaperones (Kriegenburg et al. 2012). Therefore, $CRL4^{Cdt2}$-independent proteolysis of Cdt1Δ26-400 may have been responsible for the unexpectedly low level of the protein in wildtype and *ddb1*Δ cells.

4.3.2 Dual PIP degrons promote Cdt1 proteolysis and Cdt1-PCNA interaction

Following the definition of a PIP degron in *Xenopus* Cdt1, two variant PIP degron sequences in *S. pombe* Cdt1 were identified, starting at amino acids positions 28 and 301. Point mutation of key residues in each PIP degron indicated that the two motifs function near-redundantly in Cdt1 regulation. Mutation of both PIP degrons prevented Cdt1 proteolysis in S phase and in response to DNA damage. Furthermore, BiFC analysis demonstrated that the *in vivo* Cdt1-PCNA interaction was inhibited by disruption of the two PIP degrons. These findings support recent work from *Xenopus* egg extract and human cells (Havens and Walter 2009; Michishita et al. 2011), and point to a conserved role for the PIP degron in promoting Cdt1-PCNA interaction and $CRL4^{Cdt2}$-dependent Cdt1 proteolysis.

Xenopus and human Cdt1 contain a single PIP degron, with the consensus sequence QxxΨTDϑϑxxxB; where Ψ represents a hydrophobic residue, ϑ represents an

aromatic residue, B represents a basic residue and x represents any residue (Havens and Walter 2009; Michishita et al. 2011). In contrast, the two variant PIP degrons in *S. pombe* Cdt1 contain only the glutamine, the hydrophobic residue and the basic residue at positions 1, 4 and +4 respectively. Although a complete PIP degron is conserved in some eukaryotic $CRL4^{Cdt2}$ substrates, such as human p21, variations in the sequence of the PIP degron and its critical elements have been noted (reviewed in Havens and Walter 2011). For example, the PIP degron of *Drosophila* Cdt1, which is required for regulation of the protein, does not contain a TD motif, similar to the *S. pombe* Cdt1 degron (Lee et al. 2010). Therefore, fission yeast Cdt1 is not unusual in containing a variant PIP degron sequence.

In situations where a variant PIP degron is present, it is possible that additional sequence elements in and around the motif compensate to promote efficient PCNA binding and $CRL4^{Cdt2}$ recruitment. For example, in addition to the B+4 residue, basic amino acids upstream of the Xic1 (a *Xenopus* CKI) PIP degron contribute to the $CRL4^{Cdt2}$-dependent regulation of the protein (Havens et al. 2012). It has been reported that two arginine residues at positions +4 and +5 of the human p21 PIP degron act to increase the affinity of the p21-PCNA interaction by mediated ion-pairing interactions with Asp122 and Glu124 in PCNA (Gulbis et al. 1996; Bruning and Shamoo 2004). Asp122 and Glu124 are conserved in *S. pombe* PCNA; both the PIP28 and the PIP301 degrons contain clusters of positively charged residues in the 10 amino acids C-terminal to the core PIP box and these might be available to mediate a similar interaction with PCNA to enhance binding affinity.

Determination of the crystal structure of human PCNA complexed to p21 has demonstrated that the hydrophobic and aromatic residues at positions 4, 7 and 8 of the PIP box interact with a hydrophobic pocket in PCNA, located under the interdomain connecting loop (IDCL) (Gulbis et al. 1996). Residues C-terminal to the PIP box can increase the affinity of the core PIP box-PCNA interaction by forming hydrogen-bonding and ion-pairing interactions with the IDCL and with N-terminal residues in PCNA (Gulbis et al. 1996; Bruning and Shamoo 2004). Fission yeast PCNA is 52% identical to human PCNA and the human gene can complement deletion of *pcn1*$^{+}$ in fission yeast cells (Waseem et al. 1992). The fission yeast flap endonuclease Rad2 can interact with human PCNA via its PIP box (Warbrick et al. 1997), demonstrating that the PIP box-PCNA interaction is conserved in eukaryotes and that crystal structure studies with human PCNA are relevant to *S. pombe*.

It is interesting that the *S. pombe* DNA replication proteins Rad2, Cdc17 and Cdc27 stably interact with PCNA via a consensus PIP box, which contains the glutamine, hydrophobic and two aromatic residues (Warbrick et al. 1997; Reynolds et al. 2000; Martin and MacNeill 2004). Neither of the variant PIP degrons in Cdt1 contain the aromatic residues at position 7 and 8 of the PIP box. Given these aromatic residues mediate important interactions with hydrophobic pocket of PCNA, it might be expected that these variant PIP degrons have a reduced affinity for PCNA, as compared to the consensus PIP box sequence. Mutation of either PIP degron in the PIP28^{A8} or PIP310^{A10} single mutants reduced the *in vivo* Cdt1-PCNA interaction, as judged by BiFC. Therefore, due to the partial sequence of each PIP degron, it is possible that two separate sequences are employed to promote a robust Cdt1-PCNA interaction. This may not be unique to Cdt1; it is notable that the two other confirmed

$CRL4^{Cdt2}$ substrates in *S. pombe*, Spd1 and Epe1, contain partial and possibly multiple PIP degrons (Braun et al. 2011; Havens and Walter 2011; Salguero et al. 2012).

A robust Cdt1-PCNA interaction and down-regulation of the protein via the $CRL4^{Cdt2}$ pathway may be particularly important in *S. pombe* as this organism does not contain the additional regulatory mechanisms for Cdt1, based on SCF^{Skp2} ubiquitylation or geminin inhibition, that are found in higher eukaryotes. Although fission yeast Cdt1 may be unusual in containing two PIP degrons, the concept of two regulatory motifs has been documented in detail in human Cdt1, which contains both a PIP degron and a cyclin binding (Cy) motif (Nishitani et al. 2006). The Cy motif mediates the interaction between Cdt1 and cyclin A-dependent kinases, which phosphorylate Cdt1 and target it for SCF^{Skp2}-dependent ubiquitylation in S and G2 phases (Li et al. 2003; Liu et al. 2004; Sugimoto et al. 2004; Takeda et al. 2005; Nishitani et al. 2006). The PIP degron in the extreme N-terminus is required for the interaction with PCNA and targets Cdt1 for $CRL4^{Cdt2}$-dependent ubiquitylation in S phase and after DNA damage (Nishitani et al. 2006; Senga et al. 2006; Michishita et al. 2011).

The two PIP degrons in *S. pombe* Cdt1 are not entirely redundant, as PIP28 appears to play a more dominant role in the S phase-dependent regulation of Cdt1. Mutation of key residues in the PIP28 degron resulted in detection of an increased number of uninucleate cells with a Cdt1 signal and a slight delay in the S phase proteolysis of the protein, as compared to wildtype; phenotypes not observed in the $PIP301^{A10}$ mutant. Given that mutation of either the PIP28 or the PIP301 degron reduced the Cdt1-PCNA interaction, as judged by quantitation of the BiFC signal, the dominant

contribution of PIP28 to Cdt1 regulation may reflect an increased proficiency in $CRL4^{Cdt2}$ recruitment.

It has been proposed that binding of a PIP degron to PCNA forms a composite surface, with a balance of positive and negative charges from the PIP degron and the PCNA residues respectively, to recruit $CRL4^{Cdt2}$ (Havens et al. 2012). The importance of positively charged residues downstream of the PIP box for $CRL4^{Cdt2}$-mediated proteolysis has been emphasised in human cells (Michishita et al. 2011). Basic residues at the +3 and the +4 position of the human Cdt1 PIP degron are necessary for Cdt1 proteolysis, while addition of an acidic residue at the +5 position is inhibitory to protein degradation (Michishita et al. 2011). Although both PIP28 and PIP301 contain clusters of basic amino acids C-terminal to the core PIP box, PIP301 contains aspartic acid at the +3 position, whereas PIP28 contains no acidic residues in this region. Michishita et al. (2011) speculated the basic +3 residue was important to create a positive surface to attract $CRL4^{Cdt2}$; therefore the position of aspartic acid in PIP301 could render the degron less effective in $CRL4^{Cdt2}$ recruitment, as compared to PIP28.

4.3.3 The mechanism and biological significance of $CRL4^{Cdt2}$-mediated Cdt1 proteolysis

In addition to addressing the importance of PIP28 and PIP301 degrons in the fission yeast Cdt1-PCNA interaction, the BiFC data also demonstrated that Cdt1 and PCNA interact *in vivo* in the absence of Cdt2, as previously reported *in vitro*, in *Xenopus* egg extract (Havens and Walter 2009). *In vivo* studies in human cells indicate that the accumulation of Cdt2 at cyclobutane pyrimidine dimer (CPD)-containing DNA damage sites is dependent on PCNA and the presence of a substrate (Ishii et al. 2010).

Together these data establish a hierarchy of events, whereby the PIP box-dependent binding of Cdt1 to chromatin-bound PCNA stimulates recruitment of $CRL4^{Cdt2}$. Recent work demonstrating that $CRL4^{Cdt2}$ recognises a composite surface composed of the PIP degron and PCNA further supports a direct role for the substrate-PCNA interaction in the recruitment of Cdt2 (Havens et al. 2012).

The proteolysis of Cdt1 in S phase is established as a mechanism to limit DNA replication to once per cell cycle (reviewed in Arias and Walter 2007). In contrast, the biological significance of Cdt1 degradation in response to DNA damage is unclear. It has been proposed that Cdt1 proteolysis after DNA damage could constitute a G1 checkpoint to delay S phase entry, or that it could prevent origin relicensing, which might inadvertently occur following CDK suppression in response to DNA damage checkpoint activation (Higa et al. 2003; Arias and Walter 2007). Alternatively, Cdt1 proteolysis after DNA damage may facilitate DNA repair. Microscopy observations of Cdt1 accumulation at damage sites following UV irradiation or laser-induced DNA damage indicate that Cdt1 recruitment to damage sites is rapid and that its degradation represents an early event in the overall repair process (Ishii et al. 2010; Roukos et al. 2011). Numerous repair factors interact with PCNA via a PIP box and at a common interface on PCNA (reviewed in Moldovan et al. 2007). The proteolysis of Cdt1 after DNA damage may be important to improve the accessibility of these repair factors to PCNA, enabling an efficient and coordinated DNA damage response to be conducted.

In order to address these questions, it would be necessary to examine the effect of a functional but stable form of Cdt1 on the timing of origin licensing and replication following the induction of DNA damage. In addition, it would interesting to construct

a mutant where the PCNA-binding and $CRL4^{Cdt2}$-recruitment regions of the *S. pombe* Cdt1 degron had been separated, as is possible in *Xenopus* Cdt1 (Havens and Walter 2009). This would permit investigation into whether a Cdt1 mutant proficient in PCNA binding but not $CRL4^{Cdt2}$-recruitment inhibits DNA repair.

4.4 CONCLUSIONS

This work describes two variant PIP degrons in *S. pombe* Cdt1 that start at positions 28 and 301 of the protein. Point mutation of key residues in each PIP degron has proved a powerful technique to investigate the role of each motif in Cdt1 regulation. The two PIP degrons function largely but not entirely redundantly in Cdt1 proteolysis; PIP28 appears to have a more dominant role in the S phase-dependent regulation of Cdt1, as compared to PIP301. Disruption of both PIP degrons inhibits Cdt1 proteolysis and the Cdt1-PCNA interaction. It is possible that the variant nature of each PIP degron reduces its affinity of PCNA; therefore *S. pombe* Cdt1 might employ dual PIP degrons to achieve a robust Cdt1-PCNA interaction and ensure down-regulation of the protein by $CRL4^{Cdt2}$-dependent proteolysis. Further work that builds on the PIP mutants developed in this study will help to elucidate the biological significance of Cdt1 proteolysis after DNA damage.

CHAPTER 5

A Genome-wide Screen for Novel Genes Involved in Cdt1 Regulation

---

5.1 INTRODUCTION

Cdt1 levels are exquisitely regulated in eukaryotic cells through a combination of transcriptional control, subcellular localisation, functional inhibition and proteolysis (reviewed in Kearsey and Cotterill 2003; Arias and Walter 2007). In metazoan and fission yeast cells, Cdt1 is degraded in S phase and after DNA damage in response to ubiquitylation by $CRL4^{Cdt2}$ (reviewed in Havens and Walter 2011). An interesting feature of Cdt1 ubiquitylation by $CRL4^{Cdt2}$ is that it is stimulated by chromatin-bound PCNA (Arias and Walter 2006; Havens and Walter 2009; Guarino et al. 2011). Given PCNA is loaded onto DNA in S phase and after DNA damage to perform essential replication and repair functions (reviewed in Moldovan et al. 2007), this provides an elegant mechanism to coordinate Cdt1 proteolysis with the onset of S phase and the occurrence of DNA damage. However, how the $CRL4^{Cdt2}$-dependent ubiquitylation of Cdt1 is triggered by chromatin-bound PCNA is unknown.

Studies using *Xenopus* egg extracts suggest Cdt1 has a greater affinity for chromatin-bound PCNA than for soluble PCNA (Havens and Walter 2009). As the recruitment of $CRL4^{Cdt2}$ depends on its recognition of a composite surface containing both PCNA and substrate residues (Havens et al. 2012), the selective binding of Cdt1 to PCNA on

DNA would coordinate recruitment of $CRL4^{Cdt2}$ and Cdt1 ubiquitylation with the occurrence of chromatin-bound PCNA. This model, however, raises the question of why only chromatin-bound PCNA supports an interaction with Cdt1. It is conceivable that chromatin binding might cause a conformational change in PCNA, which increases its affinity for Cdt1. Alternatively, the chromatin environment might promote modification of PCNA or facilitate the binding of additional proteins, which promote the Cdt1-PCNA interaction. Posttranslational modification of PCNA has previously been reported to modulate the binding affinity between PCNA and its interaction partners. For example, fission yeast PCNA is modified in response to DNA damage by ubiquitylation on lysine 164 and this modification determines its binding affinity for proteins that regulate repair pathway choice (Frampton et al. 2006; Moldovan et al. 2007).

However, microscopy observations of the kinetics of PCNA and Cdt1 accumulation at laser-induced DNA damage sites demonstrate that the presence of chromatin-bound PCNA alone is not sufficient to recruit Cdt1 (Roukos et al. 2011). This implies that other factors, in addition to the loading of PCNA onto DNA, can modulate the Cdt1-PCNA interaction. Furthermore, evidence using the *Xenopus* system suggests that $CRL4^{Cdt2}$ recruitment is not simply regulated at the level of substrate binding to PCNA, as $CRL4^{Cdt2}$ discriminated between substrates bound to PCNA on DNA and those bound to soluble PCNA (Havens and Walter 2009). These observations collectively imply that the regulation of $CRL4^{Cdt2}$-mediated Cdt1 ubiquitylation by chromatin-bound PCNA is complex. It is possible that the chromatin environment is able to promote $CRL4^{Cdt2}$ recruitment to the DNA-bound PCNA-substrate complex via modification of PCNA or through the activity of auxiliary proteins.

In an attempt to address some of these outstanding questions, an *S. pombe* deletion library was screened to identify novel genes involved in Cdt1 regulation. The focus of the screen was to identify deletion backgrounds that exhibited up-regulation of Cdt1, the expectation being that candidate genes involved in the proteolysis of Cdt1 could be isolated in this way. The $CRL4^{Cdt2}$ E3 ubiquitin ligase is emerging as a major regulator of eukaryotic proteins in S phase and in response to DNA damage (reviewed in Havens and Walter 2011). It was hoped that findings from the *S. pombe* deletion library screen would be relevant to the regulation of $CRL4^{Cdt2}$ targets in higher eukaryotes. The screen was conducted in collaboration with Dr Timothy Humphrey and utilised Version I of the Bioneer *S. pombe* Genome-wide Deletion Mutant Library, a collection of 2662 deletion strains, covering approximately 74% of the non-essential genes of fission yeast (Kim et al. 2010b). This chapter describes the development of a medium-throughput fluorescence-based screening method, its application to screening the *S. pombe* deletion library and the results of the screen.

5.2 RESULTS

5.2.1 The development of a medium-throughput fluorescence-based screening method

In order to screen for novel genes involved in Cdt1 regulation, the level of Cdt1 in each deletion library strain would need to be quantified. YFP fluorescence, as measured by microscopy or flow cytometry, is directly proportional to protein concentration in fission yeast cells (Wu and Pollard 2005). Therefore, a screening approach based on the quantitation of Cdt1-YFP fluorescence in each deletion library strain was proposed. To this end, the application of fluorescence microscopy and flow

cytometry to the measurement of Cdt1-YFP fluorescence in *S. pombe* deletion mutants was investigated.

5.2.1.1 The use of flow cytometry as a screening method

Flow cytometry was investigated as a method to measure Cdt1-YFP fluorescence in fission yeast cells. The flow cytometry profiles of exponentially growing non-tagged wildtype cells and Cdt1-YFP-expressing wildtype, *csn1*Δ or *ddb1*Δ cells were compared. In both *csn1*Δ and *ddb1*Δ cells, Cdt1 levels are elevated due to inhibition of $CRL4^{Cdt2}$-dependent proteolysis. Ddb1 is a component of $CRL4^{Cdt2}$ and Cdt1 levels are increased in a *ddb1*Δ mutant because Cdt1 ubiquitylation is abolished (Ralph et al. 2006). Csn1 is a subunit of the CSN complex, which is involved in the regulation of CRLs (reviewed in Cope and Deshaies 2003). Deletion of $csn1^{+}$ down-regulates the activity of $CRL4^{Cdt2}$, although the precise mechanism by which this occurs is unclear (Higa et al. 2003; Liu et al. 2003; Liu et al. 2005a). In addition to comparing the level of Cdt1-YFP fluorescence in *S. pombe* cells of different genetic backgrounds, the effect on the flow cytometry profile of growing cells in rich (YE3S) or minimal (EMM) media; and of processing cells live or fixed for cytometry was examined (Figure 5.1).

It was only possible to distinguish between the histograms of the wildtype non-tagged strain and the wildtype Cdt1-YFP strain when cells were grown in YE3S media and processed live for flow cytometry (Figure 5.1A). Interestingly, in each condition used there was a rightwards shift in the histogram of the *ddb1*Δ strain, which was most prominent in the profile from cells processed live for flow cytometry, suggesting the level of Cdt1-YFP fluorescence in this strain was higher than wildtype (Figure 5.1A

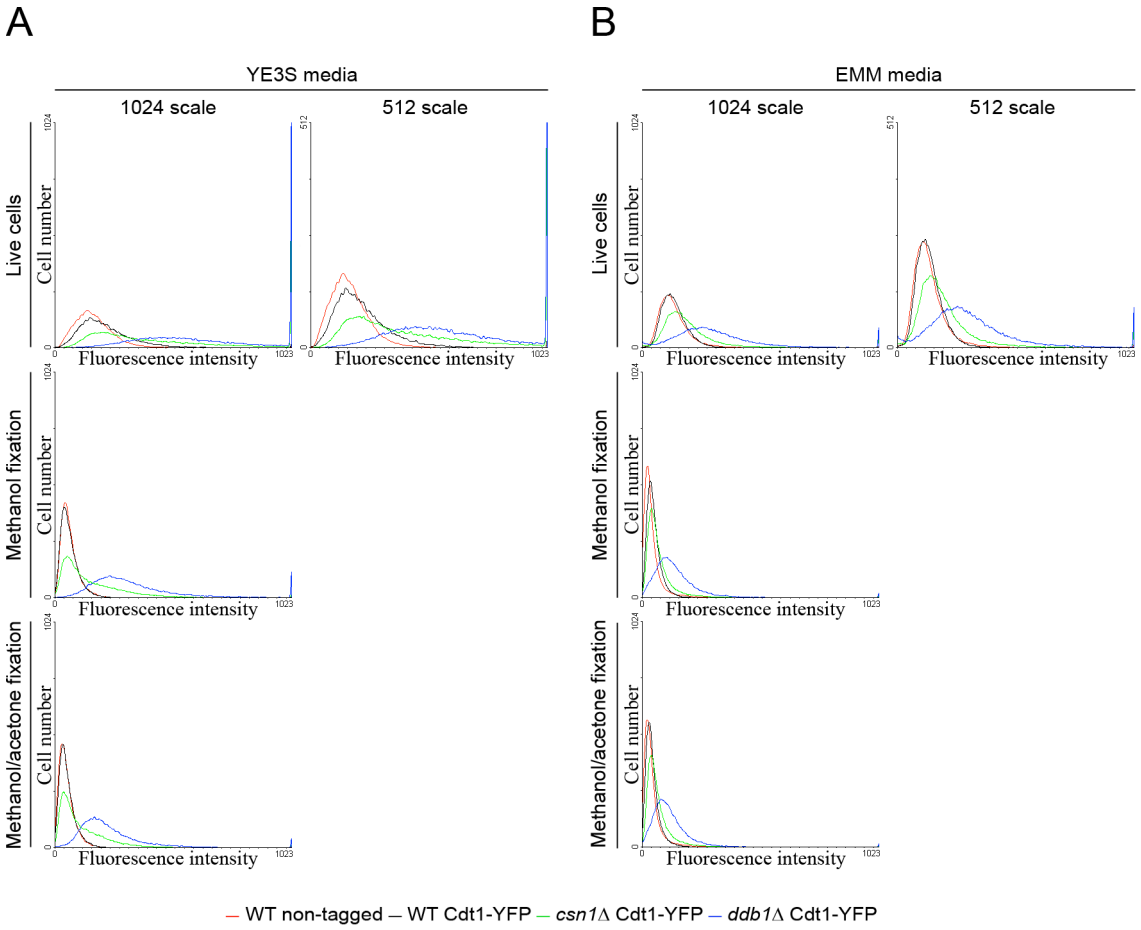


Figure 5.1 | Assessment of flow cytometry as a method to measure Cdt1-YFP fluorescence. Flow cytometric analysis of non-tagged (138) cells and of Cdt1-YFP-expressing wildtype (1262), *csn1*Δ (1594) and *ddb1*Δ (1769) cells. Samples were collected from YE3S **(A)** or EMM **(B)** cultures then processed either live for flow cytometry or following methanol or methanol and acetone fixation (Materials and Methods 2.10.1.1). The *y*-axis represents cell number while the *x*-axis represents fluorescence intensity (arbitrary units).

and B). The histogram of the *csn1*Δ strain also showed a rightwards shift, although less pronounced than that of the *ddb1*Δ strain, in live cells grown in both media types and in fixed cells grown in YE3S (Figure 5.1A and B). This analysis indicates that flow cytometry can be used to detect differences in the level of Cdt1-YFP fluorescence in wildtype, *csn1*Δ and *ddb1*Δ cells, particularly when cells are grown in rich media and processed live for flow cytometry.

Flow cytometry can provide a quantitative assessment of Cdt1-YFP fluorescence in fission yeast cells and a high sample throughput can be achieved through use of an automated multi-carousel loader. However, two key disadvantages with this method were noted: first, the positioning of the histogram peak for each of the control strains was not always reproducible and was sensitive to the growth conditions used and to the degree of saturation of the cell culture. Second, in contrast to the fluorescence microscopy analysis, information relating to the subcellular localisation of Cdt1-YFP fluorescence and the cell cycle stage of individual cells positive for nuclear Cdt1-YFP cannot be obtained using flow cytometry. It was a concern that cells with subtle deregulation of Cdt1-YFP would not be detected using this technique and so fluorescence microscopy was investigated as an alternative screening method.

5.2.1.2 The use of fluorescence microscopy as a screening method

Fluorescence microscopy can be used to detect and measure the level of Cdt1-YFP fluorescence in wildtype, *csn1*Δ or *ddb1*Δ cells (Figure 5.2). In wildtype cells, a Cdt1 signal was detected in the nuclei of some binucleate (late M/G1) cells. However, in *csn1*Δ or *ddb1*Δ cells, where Cdt1 levels are increased owing to inhibition of $CRL4^{Cdt2}$-dependent proteolysis, the intensity of nuclear Cdt1-YFP fluorescence was

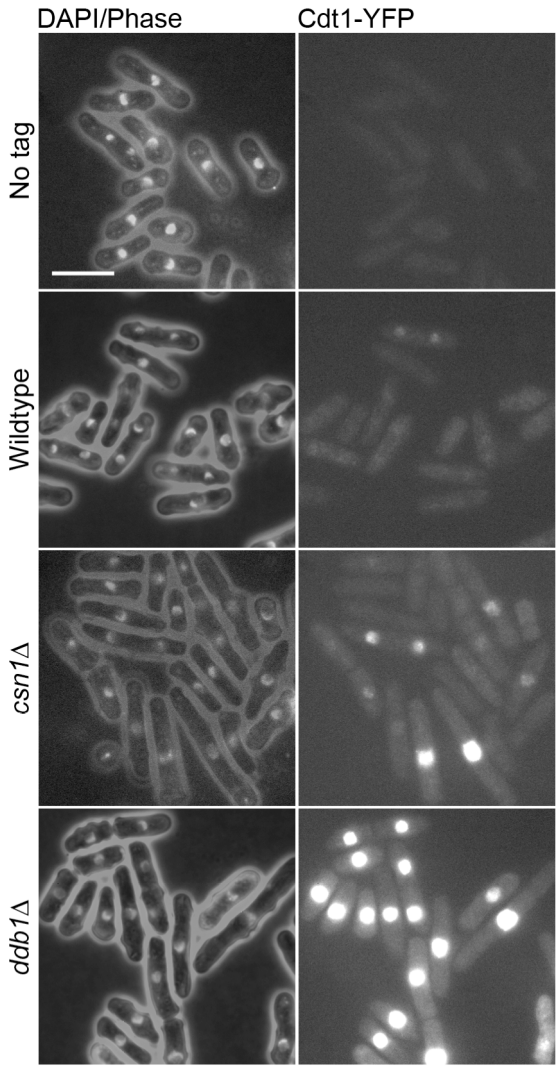


Figure 5.2 | Deregulation of Cdt1 levels can be detected by fluorescence microscopy. Cdt1-YFP imaged in exponentially growing cells in a non-tagged (138) strain or in wildtype (1262), *csn1*Δ (1594) and *ddb1*Δ (1769) strains that express endogenous YFP-tagged Cdt1. Scale bar: 10 μm.

elevated and an increased number of uninucleate and binucleate cells with a nuclear Cdt1 signal were detected (Figure 5.2). However, this technique would require scaling up before it could be used with the *S. pombe* deletion library, as cells were typically grown in liquid culture and a sample from each strain collected, fixed and mounted individually onto a slide. Therefore, a method where cells were grown to log phase on agar plates and then transferring directly to a multiwell slide was investigated. Based on this principle, a medium-throughput protocol was developed for use with the fluorescence microscope that enabled approximately 100 samples to be processed in a day (Figure 5.3A). Non-tagged wildtype cells and Cdt1-YFP-expressing wildtype, *csn1*Δ or *ddb1*Δ cells could be accurately distinguished using this method (Figure 5.3B) and information relating to the subcellular localisation of Cdt1-YFP fluorescence and to the cell cycle stage of cells positive for Cdt1-YFP could be gathered.

5.2.1.3 MATLAB can be used to automatically quantitate nuclear fluorescence in fission yeast

Conducting a screen of the *S. pombe* deletion library by fluorescence microscopy would generate a large image dataset. In order for objective comparisons to be made between gene deletion backgrounds, the intensity of Cdt1-YFP fluorescence per strain would need to be quantitated. To this end, a collaboration was formed with Simon Li, who developed MATLAB code to automatically detect and quantitate the nuclear fluorescence intensity of individual *S. pombe* cells. MATLAB is a programing environment that is developed and licensed by MathWorks and can be used for a wide range of applications including image processing.

A

Wake up 96 strains onto two YE3S plates and incubate at 30°C for 2 days.

↓

Dilute the strains in sterile distilled water (SDW) and pin out to new YE3S plates. Incubate at 30°C for 14 hours, after which cells should be in log phase.

↓

Mix a small amount of each strain with 5 μl of SDW, containing 0.01% Triton-X-100, in each well of a 12 well slide.

↓

Dry the slides, immerse in 100% ice-cold ethanol for 10 seconds and dry again at room temperature.

↓

Immerse the slides in 100% ice-cold acetone for 1 minute, dry at room temperature and then store at -20°C.

↓

To view a slide, mount by adding 3 μl of 0.6% agarose, containing 0.5 ng/ml DAPI, to each well and press a 22 x 50 mm coverslide over the slide.

B

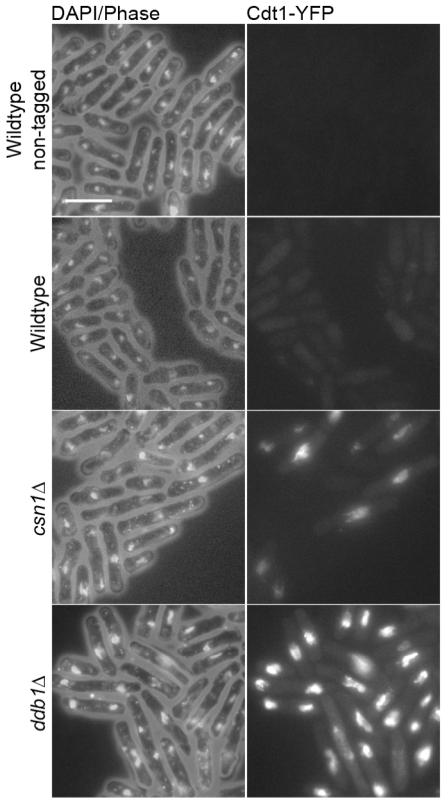


Figure 5.3 | Development of a medium-throughput fluorescence microscopy-based screening method.
(A) Overview of the medium-throughput fluorescence microscopy-based screening protocol. **(B)** Cdt1-YFP imaged in non-tagged (138) cells and in Cdt1-YFP expressing wildtype (1262), *csn1*Δ (1594) or *ddb1*Δ cells, processed as per the protocol in (A). Scale bar: 10 μm.

To validate the MATLAB code developed by Simon Li, the value of mean nuclear fluorescence intensity generated through MATLAB analysis of an image of *S. pombe* cells would need to be compared with that generated by manual quantitation of the data. To this end, Micro-Manager 1.3 (Edelstein et al. 2010) was used to manually quantitate the mean nuclear fluorescence intensity of two images of exponentially growing wildtype non-tagged cells and Cdt1-YFP-expressing wildtype, *csn1*Δ or *ddb1*Δ cells (Materials and Methods 2.7.3). The values of mean nuclear fluorescence intensity generated through manual quantitation of the data were comparable to those generated through MATLAB analysis of the same images (Figure 5.4A and B). This suggests that the MATLAB code is suitable for the quantitation of nuclear Cdt1-YFP fluorescence intensity levels in *S. pombe* cells.

5.2.2 A screen of the *S. pombe* deletion library for genes that regulate cell cycle Cdt1 levels

A Cdt1-YFP strain containing the PEM-2 anti-diploid and mating-type selection system was crossed to 97% of the *S. pombe* deletion library to enable the fluorescence-based detection of gene deletion backgrounds with deregulated Cdt1 levels (Materials and Methods 2.10.2). The PEM-2 system employs a recessive cycloheximide-resistance allele to select for h^+ haploid meiotic products (Roguev et al. 2007). In combination with selection for Cdt1-YFP and the relevant gene deletion using the antibiotics hygromycin B and geneticin respectively, the PEM-2 system enables the high-throughput introduction of distinct genetic backgrounds, marked with unique selectable markers, into haploid cells via a genetic cross.

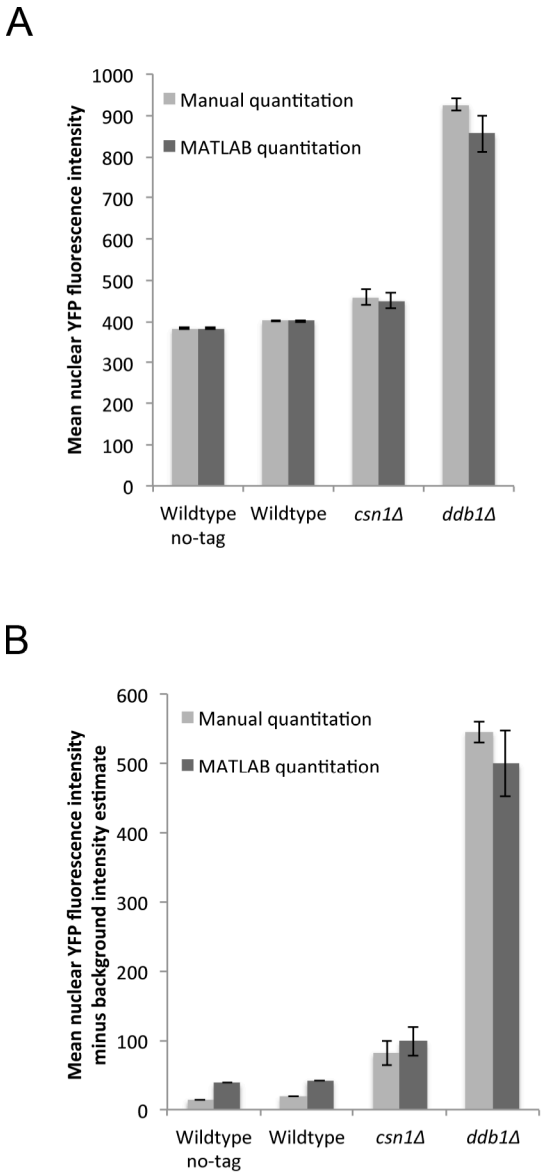


Figure 5.4 | Validation of MATLAB code to quantitate *S. pombe* nuclear fluorescence.
(A) Comparison of mean nuclear YFP fluorescence intensity values of wildtype non-tagged (138) cells and of Cdt1-YFP-expressing wildtype (1262), *csn1*Δ (1594) or *ddb1*Δ (1769) cells, generated through manual quantitation of images using MicroManager 1.3 or automatic quantitation of the images in MATLAB. **(B)** Comparison of the same mean nuclear YFP fluorescence intensity values in (A) but with an estimate of the background intensity subtracted. Mean nuclear YFP fluorescence intensity on the *y*-axis is measured in arbitrary units. Two images were quantitated per strain. Error bars: 50% of range.

5.2.2.1 Data collection for the *S. pombe* deletion library screen

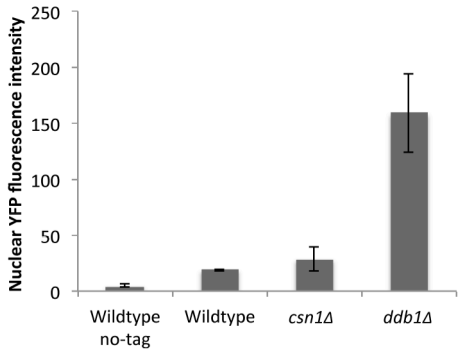
The level of Cdt1-YFP fluorescence in each *S. pombe* deletion library strain was screened using the medium-throughput fluorescence microscopy-based protocol developed in section 5.2.1.2 (Materials and Methods 2.10.1.2). Approximately 100 deletion library strains, in addition to non-tagged wildtype and Cdt1-YFP-expressing wildtype, *csn1*Δ and *ddb1*Δ control strains, were imaged per day. On average, two images per strain were taken, with at least 50 cells per field.

5.2.2.2 Analysis of data from the *S. pombe* deletion library screen

The image dataset generated from the screen was analysed in MATLAB to quantitate the nuclear Cdt1-YFP fluorescence intensity levels in each gene deletion background (Appendix IV). The output from the MATLAB analysis included different methods by which to define the nuclear fluorescence intensity of cells in an image. These included the mean nuclear fluorescence intensity of an image and a range of percentile values of nuclear fluorescence intensity for an image. To determine which measurement of nuclear fluorescence intensity would be most useful for analysis of the image dataset, the different outputs that had been generated from control wildtype non-tagged and Cdt1-YFP-expressing wildtype, *csn1*Δ and *ddb1*Δ strains examined during the screen were compared.

First, an average of the mean nuclear fluorescence intensity values from three independent images of each control strain was calculated and compared (Figure 5.5A). Using this value, wildtype and *ddb1*Δ cells can be clearly distinguished but the *csn1*Δ mutant appeared similar to the wildtype. Second, an average of the 25th, 50th, 75th and 90-100th percentile value of nuclear fluorescence intensity from the same

A



B

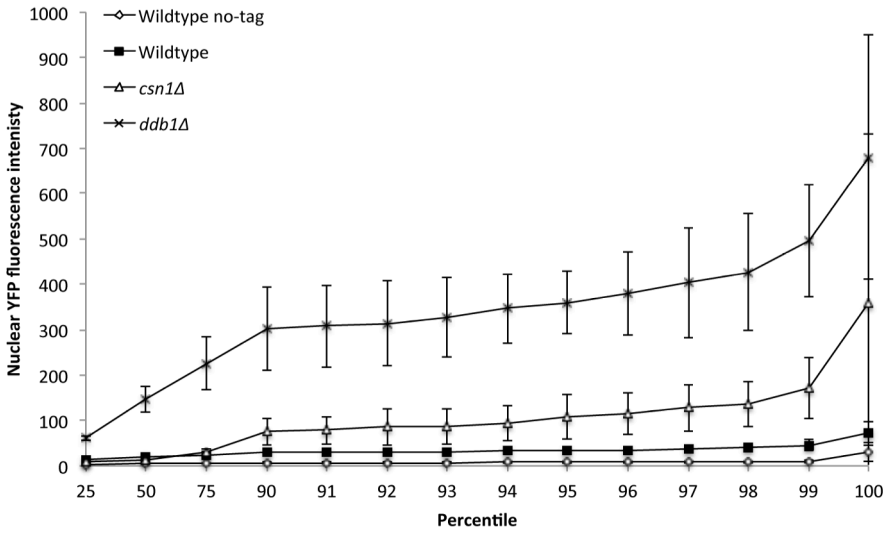
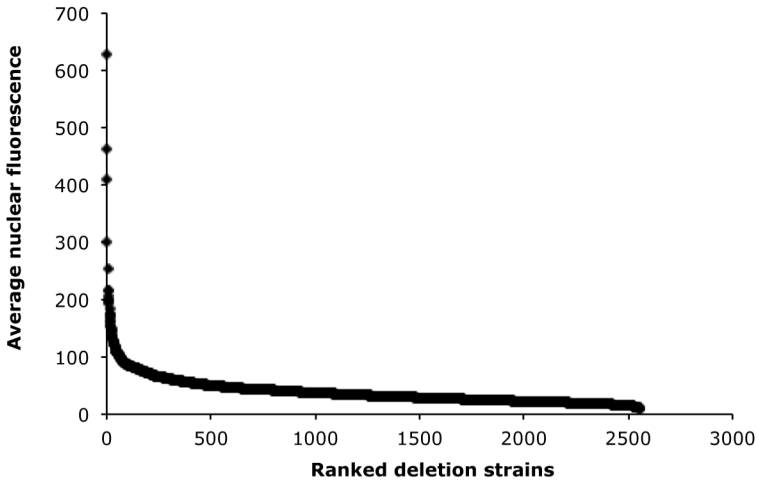


Figure 5.5 | A comparison of nuclear fluorescence intensity values generated by MATLAB analysis of control strain images.
(A) Graph displays an average of the mean nuclear fluorescence intensity values (arbitrary units) from three independent images of wildtype non-tagged (138) and Cdt1-YFP-expressing wildtype (1262), *csn1*Δ (1594) and *ddb1*Δ (1769) control cells. Error bars: ± SD. **(B)** Graph displays an average of the 25th, 50th, 75th and 90-100th percentile values of nuclear fluorescence intensity (arbitrary units) from three independent images of wildtype non-tagged (138) and Cdt1-YFP-expressing wildtype (1262), *csn1*Δ (1594) and *ddb1*Δ (1769) control cells. Error bars: ± SD.

three independent images of each control strain was calculated and compared (Figure 5.5B). With an increased percentile value, there was increased separation between the nuclear fluorescence intensity of the control strains. However, the highest percentile values were associated with increased variation. This may be due to spurious fluorescence associated with unhealthy and dead cells, which exhibit high, uniform autofluorescence. Based on this comparison, it was decided that the 95th percentile value of the nuclear fluorescence intensity should be used to analyse the image dataset. It provided a clear separation between the control strains and so should enable detection of gene deletion backgrounds with deregulated Cdt1 levels. In addition, it excluded the highest values of nuclear fluorescence that are often associated with the spurious autofluorescence of dead cells and in doing so, it should reduce the number of false positives generated from the analysis.

Approximately two images were taken per deletion library strain during the screen and the 95th percentile value of nuclear fluorescence intensity from each image was averaged, enabling each strain to be represented by a single 'average nuclear fluorescence' value. Each deletion library strain was ranked by its average nuclear fluorescence value, from highest to lowest, as represented in Figure 5.6A. Genes previously described as involved in Cdt1 regulation were represented in the top 10% of the ranked deletion strains (Figure 5.6B). These included *ddb1*$^{+}$, *cdt2*$^{+}$ and *csn1*$^{+}$, which regulate the ubiquitylation of Cdt1 as well as *res2*$^{+}$ and *yox1*$^{+}$, which regulate *cdt1*$^{+}$ transcription (Baum et al. 1997; Lyapina et al. 2001; Zhou et al. 2001; Ralph et al. 2006; Aligianni et al. 2009). Identification of gene deletion backgrounds where Cdt1 deregulation is expected indicates that MATLAB can be used to provide a biologically relevant analysis of the image dataset.

A



B

Rank in top 10%	Average nuclear fluorescence	Systematic name	Gene	Gene product
3	409	*SPAC17H9.10c*	*ddb1*	Damaged DNA binding protein Ddb1
8	205	*SPAC17H9.19c*	*cdt2*	WD repeat protein Cdt2
28	130	*SPBC21B10.13c*	*yox1*	MBF complex negative regulatory component Yox1
96	87	*SPAC22F3.09c*	*res2*	MBF transcription factor complex subunit Res2
239	67	*SPBC215.03c*	*csn1*	COP9/signalosome complex subunit Csn1

Figure 5.6 | MATLAB analysis of nuclear Cdt1-YFP fluoresence intensity levels in the *S. pombe* deletion library image dataset.
(A) Graph displays each gene deletion background ranked in order of its average 95th percentile value of nuclear fluorescence intensity (average nuclear fluorescence, arbitrary units). **(B)** MATLAB can provide a biologically relevant analysis of the image dataset as genes with recognised roles in Cdt1 regulation are represented in the top 10% of strains ranked by their average nuclear fluorescence. Gene and gene product data was obtained from GeneDB (http://old.genedb.org/genedb/pombe/).

5.2.3 Identification of candidate gene deletion backgrounds with elevated Cdt1 levels

Section 5.2.2.2 focused on the detection of gene deletion backgrounds with elevated Cdt1-YFP levels. Technically, it should be possible to screen for gene deletion backgrounds with lower-than-wildtype Cdt1-YFP levels but it is unlikely that the screening and analysis methods employed here would have been sensitive enough to achieve this, owing the small differences recorded between wildtype non-tagged and wildtype Cdt1-YFP levels in the control cells (Figure 5.4 and Figure 5.5). The images in the top 10% of the deletion strains, ranked by average nuclear fluorescence, were carefully re-examined manually to exclude false positives generated by spurious autofluorescence from unhealthy and dead cells. This analysis identified 60 candidate gene deletion backgrounds that showed a genuine elevation of Cdt1-YFP fluorescence (Table 5.1).

Each of the 60 candidate strains was grown to log phase in liquid culture and re-analysed by fluorescence microscopy. On re-examination, 63% of these strains showed wildtype levels and distributions of Cdt1-YFP (Appendix V). The 22 gene deletion backgrounds that showed a reproducible deregulation of Cdt1 by fluorescence microscopy (Table 5.2) were further analysed by western blot to objectively compare Cdt1-YFP levels between populations of cells from each strain (Figure 5.7). Western blot analysis suggested that *SPBC887.17*Δ, *SPAC16C4.20c*Δ, *iec1*Δ, *SPAC821.05*Δ and *SPAC26H5.05*Δ mutants did not show a significant elevation of Cdt1-YFP levels compared to wildtype, despite the appearance of an increased cytoplasmic Cdt1-YFP signal by fluorescence microscopy (compare Table 5.2 and Figure 5.7).

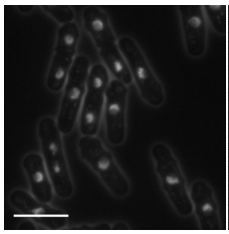
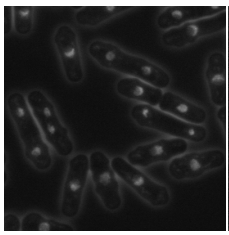
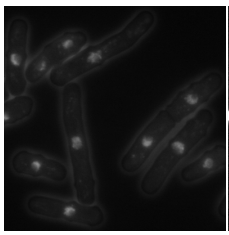
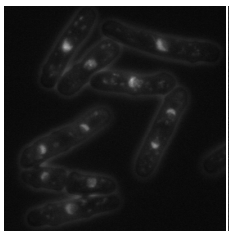
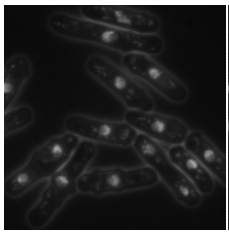
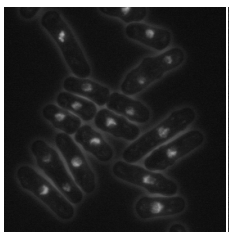
Table 5.1 | Candidate deletion library strains that exhibit an elevated level of Cdt1-YFP fluorescence

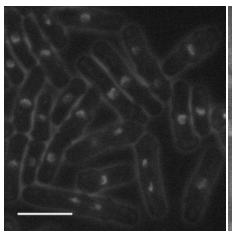
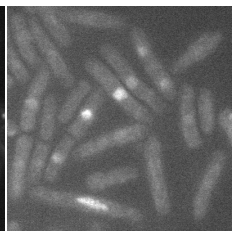
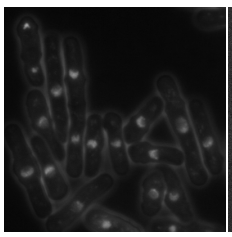
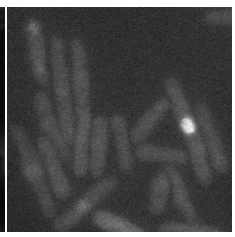
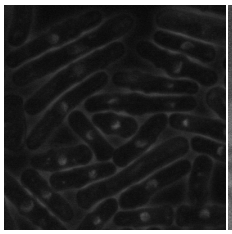
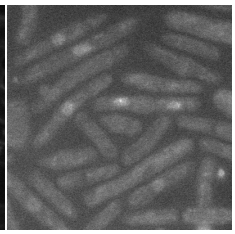
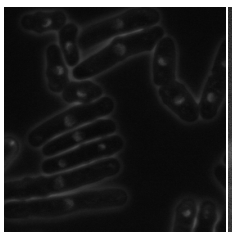
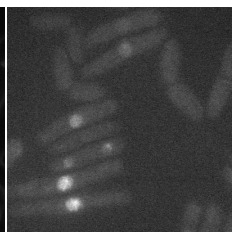
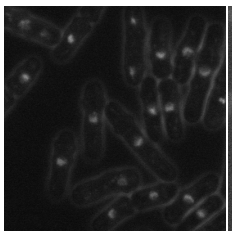
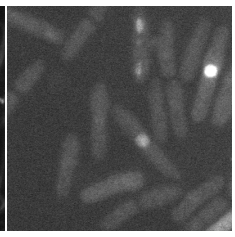
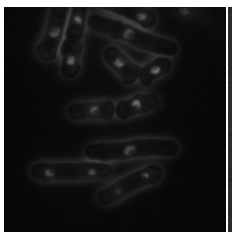
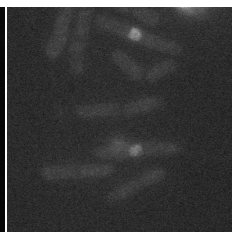
Rank in top 10%	Average nuclear fluorescence	Systematic name	Gene*	Gene product*
1	628	*SPBC27.02c*	*ask1*	DASH complex subunit Ask1
2	461	*SPCC895.05*	*for3*	Formin For3
3	409	*SPAC17H9.10c*	*ddb1*	Damaged DNA binding protein Ddb1
4	300	*SPAC1805.07c*	*dad2*	DASH complex subunit Dad2
7	214	*SPAC3F10.15c*	*spo12*	Spo12 family protein
8	205	*SPAC17H9.19c*	*cdt2*	WD repeat protein Cdt2
9	202	*SPAC644.14c*	*rhp51*	RecA family recombinase Rhp51
13	184	*SPAC637.11*	*rpm2*	Mitochondrial ATP-dependent RNA helicase Rpm2
14	176	*SPAC110.02*	*pds5*	Cohesin-associated protein Pds5
17	168	*SPAC589.02c*	*med13*	Mediator complex subunit Srb9
18	162	*SPBC887.17*		Transmembrane transporter (predicted)
19	162	*SPAC167.01*	*ire1*	Serine/threonine protein kinase Ppk4/ sensor for unfolded proteins in the ER (predicted)
20	156	*SPAC664.13*		Sequence orphan
25	139	*SPBC31F10.09c*	*nut2*	Mediator complex subunit Med10
26	138	*SPCC338.16*	*pof3*	F-box protein Pof3
28	130	*SPBC21B10.13c*	*yox1*	MBF complex negative regulatory component Yox1
30	129	*SPBC13G1.08c*	*ash2*	Ash2-trithorax family protein
35	124	*SPCC417.02*	*dad5*	DASH complex subunit Dad5
36	123	*SPAC328.03*	*tps1*	Alpha,alpha-trehalose-phosphate synthase [UDP-forming]
39	120	*SPAC18G6.02c*	*chp1*	Chromodomain protein Chp1
40	118	*SPCC16C4.20c*		Ino80 complex subunit (predicted)
42	115	*SPAC4F10.11*	*spn1*	Septin Spn1
46	110	*SPCC306.04c*	*set1*	Histone lysine methyltransferase Set1
47	109	*SPAC24B11.08c*		COPII-coated vesicle component Erv46 (predicted)
55	105	*SPAC30D11.02c*		Sequence orphan
67	98	*SPAC11E3.08c*	*nse6*	Smc5-6 complex non-SMC subunit Nse6
70	97	*SPAC1952.07*	*rad1*	Checkpoint clamp complex protein Rad1
71	97	*SPBC23G7.04c*	*nif1*	SEL1 repeat protein Nif1
76	93	*SPAPB1A10.13*		Sequence orphan
77	93	*SPAC824.04*		WD repeat protein (predicted)
96	87	*SPAC22F3.09c*	*res2*	MBF transcription factor complex subunit Res2
103	86	*SPCC895.07*	*alp14*	TOG ortholog Alp14

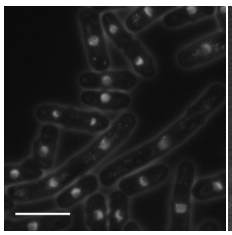
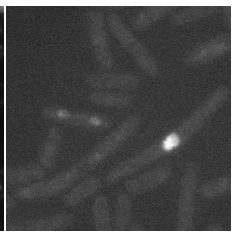
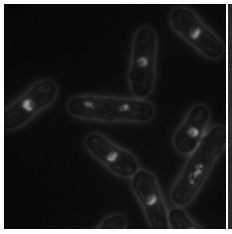
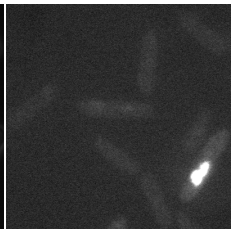
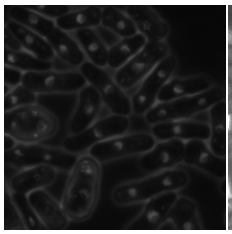
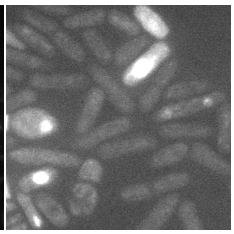
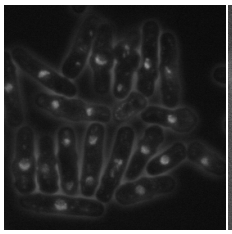
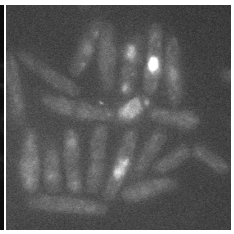
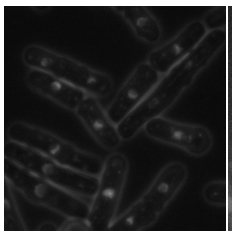
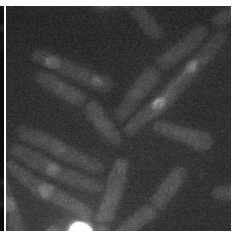
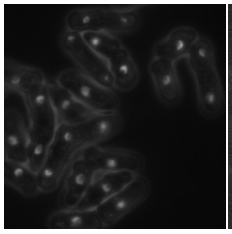
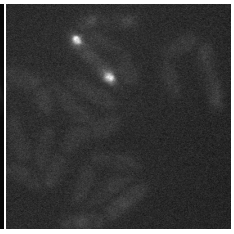
Rank in top 10%	Average nuclear fluorescence	Systematic name	Gene*	Gene product*
104	86	*SPAC9G1.11c*	*spn4*	Septin Spn4
107	86	*SPBC1271.05c*		Zf-AN1 type zinc finger protein
110	85	*SPCC338.08*	*ctp1*	CtIP-related endonuclease
111	85	*SPAC1687.05*	*pli1*	SUMO E3 ligase Pli1
114	84	*SPAC821.05*		Translation initiation factor eIF3h (p40)
119	84	*SPBC3E7.08c*	*rad13*	DNA repair nuclease Rad13
124	83	*SPAC1805.14*		Sequence orphan
135	82	*SPCC645.11c*	*mug117*	Meiotically upregulated gene Mug117
148	80	*SPCP31B10.07*	*eft202*	Translation elongation factor 2 (EF-2) Eft2,B
163	77	*SPBC651.10*	*nse5*	Smc5-6 complex non-SMC subunit Nse5
165	77	*SPCC594.04c*		Steroid oxidoreductase superfamily protein (predicted)
176	75	*SPAC3A11.06*	*mvp1*	Sorting nexin Mvp1 (predicted)
179	75	*SPAC13C5.07*	*rad32*	Rad32 nuclease
183	74	*SPBC365.14c*	*uge1*	UDP-glucose 4-epimerase Uge1
184	74	*SPCC24B10.22*	*pog1*	Mitochondrial DNA polymerase
195	72	*SPAC144.02*	*iec1*	Ino80 complex subunit Iec1
196	72	*SPCC737.09c*	*hmt1*	ATP-binding cassette-type vacuolar membrane transporter Hmt1
203	71	*SPBC365.02c*	*cox10*	Protoheme IX farnesyltransferase (predicted)
208	71	*SPAC1B9.02c*	*sck1*	Serine/threonine protein kinase Sck1
211	70	*SPAC664.02c*	*arp8*	Actin-like protein Arp8
216	70	*SPAC3H1.10*		Phytochelatin synthetase
225	68	*SPBC14F5.07*	*doa10*	ER-localized ubiquitin ligase Doa10 (predicted)
232	67	*SPAC26H5.05*		IPT/TIG ankyrin repeat containing transcription regulator of fatty acid biosynthesis (predicted)
235	67	*SPCC895.09c*	*ucp12*	ATP-dependent RNA helicase Ucp12 (predicted)
239	67	*SPBC215.03c*	*csn1*	COP9/signalosome complex subunit Csn1
241	66	*SPBC6B1.02*	*ppk30*	Ark1/Prk1 family protein kinase Ppk30
242	66	*SPBC428.03c*	*pho4*	Thiamine-repressible acid phosphatase Pho4
249	66	*SPCC569.07*		Aromatic aminotransferase (predicted)

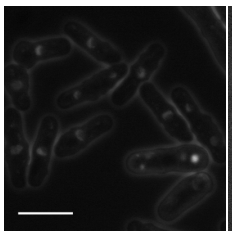
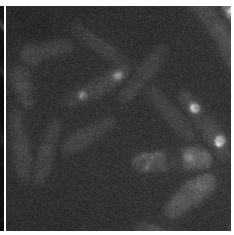
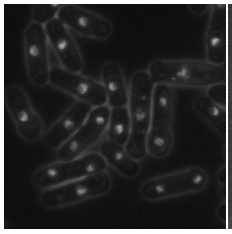
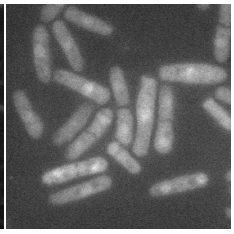
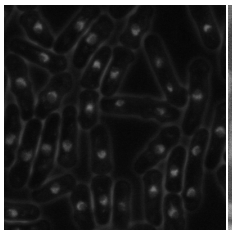
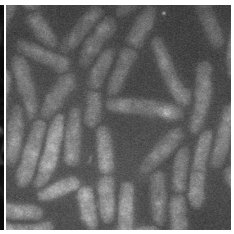
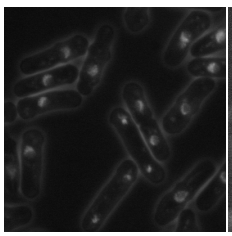
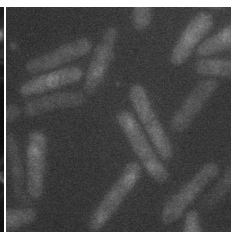
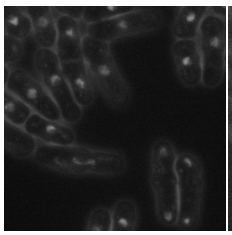
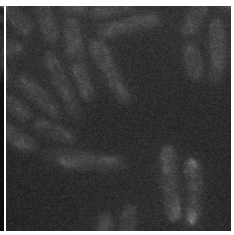
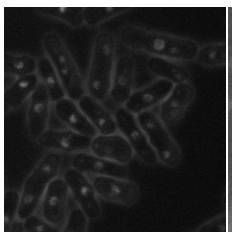
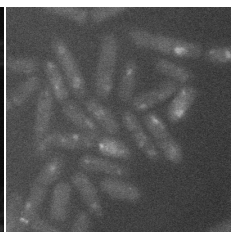
* Data from GeneDB (http://old.genedb.org/genedb/pombe/)

Table 5.2 | Fluorescence microscopy analysis of candidate deletion library strains that exhibit a reproducible deregulation of Cdt1-YFP

DAPI/Phase	Cdt1-YFP	Gene deletion	Gene product	Microscopy comments
		Wildtype no-tag		
		Wildtype Cdt1-YFP		
		*ddb1*Δ	Damaged DNA binding protein Ddb1	Strong nuclear Cdt1-YFP signal in all cells, regardless of cell cycle stage
		*cdt2*Δ	WD repeat protein Cdt2	Strong nuclear Cdt1-YFP signal in all cells, regardless of cell cycle stage
		*yox1*Δ	MBF complex negative regulator component Yox1	Strong nuclear Cdt1-YFP in the majority of cells except septating binucleate cells
		*res2*Δ	MBF transcription factor complex subunit Res2	Strong nuclear Cdt1-YFP in the majority of cells except septating binucleate cells

DAPI/Phase	Cdt1-YFP	Gene deletion	Gene product	Microscopy comments
		*csn1*Δ	COP9/ signalosome complex subunit Csn1	Strong nuclear Cdt1-YFP signal in subpopulation of binucleate and uninucleate cells
		*rad32*Δ	Rad32 nuclease	Bright nuclear Cdt1-YFP signal in subpopulation of binucleate and uninucleate cells
		*ctp1*Δ	CtIP-related endonuclease	Bright nuclear Cdt1-YFP signal in subpopulation of binucleate and uninucleate cells
		*rhp51*Δ	RecA family recombinase Rhp51	Bright nuclear Cdt1-YFP signal in subpopulation of binucleate and uninucleate cells
		*nse5*Δ	Smc5-6 complex non-SMC subunit Nse5	Bright nuclear Cdt1-YFP signal in subpopulation of binucleate and uninucleate cells
		*nse6*Δ	Smc5-6 complex non-SMC subunit Nse6	Bright nuclear Cdt1-YFP signal in subpopulation of binucleate and uninucleate cells

DAPI/Phase	Cdt1-YFP	Gene deletion	Gene product	Microscopy comments
		*SPAC824.04*Δ	WD repeat protein (predicted)	Bright nuclear Cdt1-YFP signal in subpopulation of binucleate and uninucleate cells
		*dad5*Δ	DASH complex subunit Dad5	Intense nuclear Cdt1-YFP signal in subpopulation of cells
		*dad2*Δ	DASH complex subunit Dad2	Intense nuclear Cdt1-YFP signal in subpopulation of cells
		*ask1*Δ	DASH complex subunit Ask1	Intense nuclear Cdt1-YFP signal in subpopulation of cells
		*pof3*Δ	F-box protein Pof3	Increased number of uninucleate cells positive for nuclear Cdt1-YFP
		*nut2*Δ	Mediator complex subunit Med10	Increased intensity of nuclear Cdt1-YFP in binucleate cells

DAPI/Phase	Cdt1-YFP	Gene deletion	Gene product	Microscopy comments
		*SPAC1805.14*Δ	Sequence orphan	Increased intensity of nuclear Cdt1-YFP in binucleate cells
		*SPBC887.17*Δ	transmembrane transporter (predicted)	Increase in cytoplasmic Cdt1-YFP signal
		*SPCC16C4.20c*Δ	Ino80 complex subunit (predicted)	Increase in cytoplasmic Cdt1-YFP signal
		*iec1*Δ	Ino80 complex subunit Iec1	Increase in cytoplasmic Cdt1-YFP signal
		*SPAC821.05*Δ	translation initiation factor eIF3h (p40)	Increase in cytoplasmic Cdt1-YFP signal
		*SPAC26H5.05*Δ	IPT/TIG ankyrin repeat containing transcription regulator of fatty acid biosynthesis (predicted)	Increase in cytoplasmic Cdt1-YFP signal

Scale bar: 10 µm

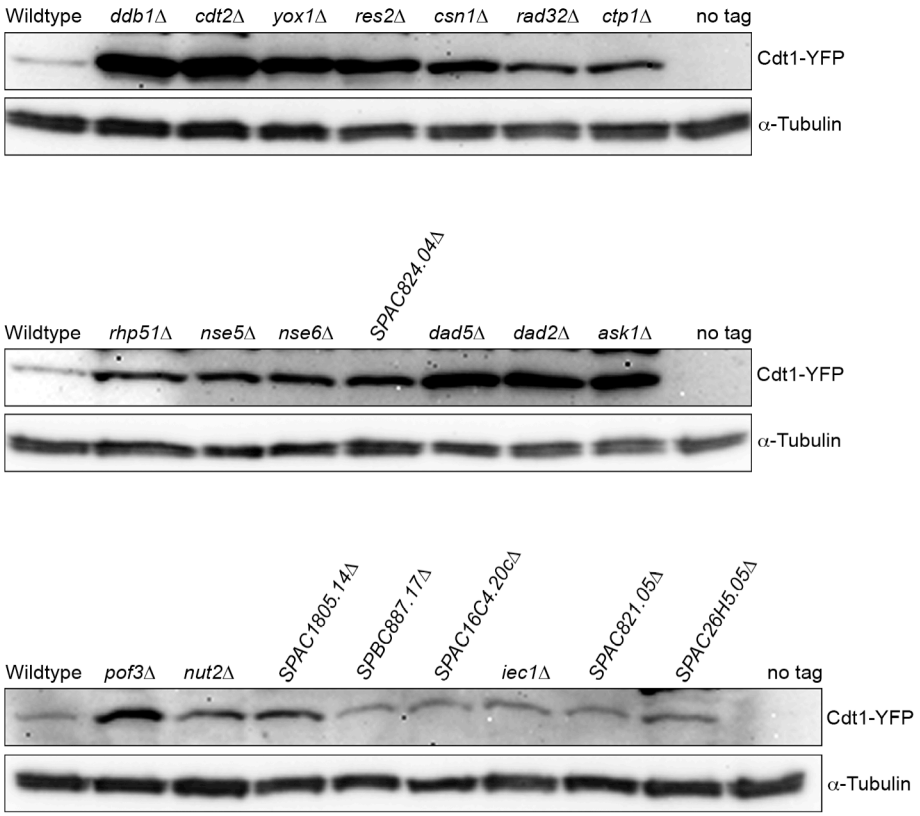


Figure 5.7 | Identification of deletion library strains that exhibit an elevated level of Cdt1-YFP by western blot analysis.
Western blot analysis of Cdt1-YFP levels in 22 candidate *S. pombe* deletion library strains that exhibited a reproducible deregulation of Cdt1-YFP by fluorescence microscopy (Table 5.2).

The analysis up to this point has identified 17 candidate genes with a potential role in Cdt1 regulation (Figure 5.8). Gene ontology (GO) analysis was employed as a preliminary investigation into the function of these candidate genes. GO analysis involves the assignment of a GO term, describing the biological process associated with each gene product, to each candidate gene (Table 5.3). GO terms were assigned using the Gene Ontology database (http://amigo.geneontology.org), a project that seeks to provide consistent and controlled gene product descriptions for various organisms. Gene products are described in terms of their cellular localisation, the biological process they are involved in and their associated molecular function. It is a powerful tool to investigate gene function as 98% of *S. pombe* genes have at least one GO annotation assigned (Aslett and Wood 2006). The GO analysis suggested that a range of biological processes were represented by the candidate genes, including ubiquitin-dependent processes (*ddb1*$^+$, *cdt2*$^+$, *pof3*$^+$), DNA repair pathways (*rad32*$^+$, *ctp1*$^+$, *rhp51*$^+$, *nse5*$^+$, *nse6*$^+$), the regulation of transcription (*res2*$^+$, *yox1*$^+$, *nut2*$^+$) and chromosome partition (*dad5*$^+$, *dad2*$^+$, *ask1*$^+$).

5.3 DISCUSSION

The *S. pombe* deletion library screen to identify novel genes involved in Cdt1 regulation led to the identification of 17 strains with elevated Cdt1 levels. Five of the candidate genes (*ddb1*$^+$, *cdt1*$^+$, *csn1*$^+$, *res2*$^+$ and *yox1*$^+$) have a previously described role in Cdt1 regulation. The remaining 12 candidate genes have diverse functions, including roles in DNA repair, chromosome partition, mRNA processing and transcriptional regulation. The possible involvement of these genes in Cdt1 regulation is discussed in this section.

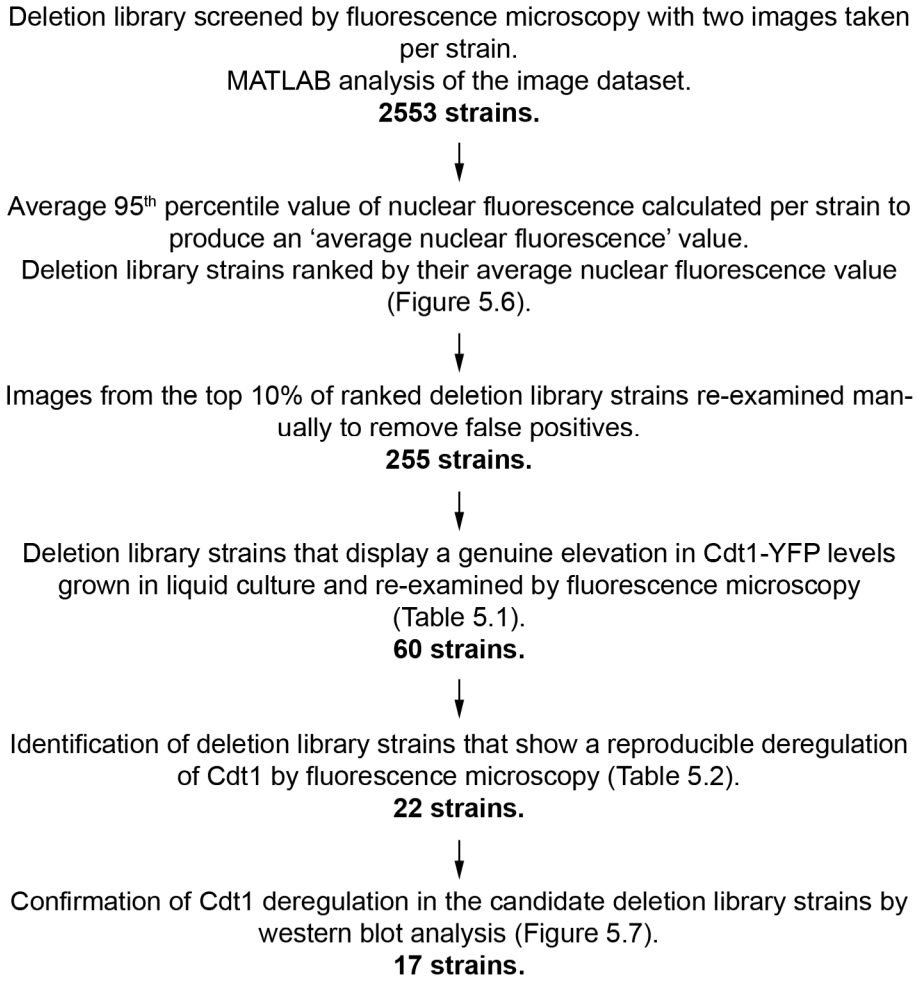


Figure 5.8 | A summary of the steps in the *S. pombe* deletion library screen.
A scheme detailing the steps in the screening process that led to the identification of 17 candidate genes with a potential role in Cdt1 regulation. The number of strains at each screening stage are shown in bold.

Table 5.3 | Gene ontology analysis of candidate genes with a potential involvement in Cdt1 regulation

Systematic name	Gene name	GO term associations
SPAC17H9.10c	*ddb1*	Ubiquitin-dependent protein catabolic process
SPAC17H9.19c	*cdt2*	Ubiquitin-dependent protein catabolic process
SPBC21B10.13c	*yox1*	Regulation of transcription
SPAC22F3.09c	*res2*	Regulation of transcription
SPBC215.03c	*csn1*	Protein catabolic process
SPAC13C5.07	*rad32*	DNA damage checkpoint/double-strand break repair
SPCC338.08	*ctp1*	Double-strand break repair via homologous recombination
SPAC644.14c	*rhp51*	Double-strand break repair via homologous recombination
SPBC651.10	*nse5*	Replication fork protection/response to DNA damage stimulus
SPAC11E3.08c	*nse6*	Replication fork protection/response to DNA damage stimulus
SPAC824.04		mRNA cleavage and polyadenylation
SPCC417.02	*dad5*	Mitotic spindle organization/sister chromatid biorientation
SPAC1805.07c	*dad2*	Mitotic spindle organization/sister chromatid biorientation
SPBC27.02c	*ask1*	Mitotic spindle organization/sister chromatid biorientation
SPCC338.16	*pof3*	Ubiquitin-dependent protein catabolic process/telomere maintenance
SPBC31F10.09c	*nut2*	Regulation of transcription
SPAC1805.14		No annotation

A GO term to describe the biological process in which each gene product functions was subjectively assigned from the Gene Ontology database (http://amigo.geneontology.org)

Unfortunately, no candidate genes that might hold an obvious explanation for the dependence of Cdt1 proteolysis on chromatin-bound PCNA were identified. This may reflect a limitation of screening Version I of the Bioneer *S. pombe* Genome-wide Deletion Mutant Library, which did not contain a complete coverage of the non-essential *S. pombe* genes. Alternatively, it may reflect a more general limitation of screening a haploid deletion library, which contains only non-essential genes. Based on the prediction that the *S. pombe* genome contains at least 5050 protein coding genes (Wood et al. 2012), Version I of the *S. pombe* deletion library used in this screen covers only 53% of the total *S. pombe* genes. It is therefore possible that a gene linking the dependence of Cdt1 proteolysis to chromatin-bound PCNA, which is either essential for cell viability or was not included in Version I of the *S. pombe* deletion library, remains to be discovered.

5.3.1 *res2*$^+$, *yox1*$^+$, *ddb1*$^+$, *cdt2*$^+$ and *csn1*$^+$ have well recognised roles in Cdt1 regulation

Five of the genes identified in the *S. pombe* deletion library screen with elevated Cdt1 levels have previously described roles in Cdt1 regulation. As discussed below, *res2*$^+$ and *yox1*$^+$ regulate the transcription of *cdt1*$^+$ while *ddb1*$^+$, *cdt2*$^+$ and *csn1*$^+$ regulate ubiquitylation of the gene product.

Transcription of *cdt1*$^+$ is regulated by the MBF transcription factor complex and occurs periodically in the cell cycle, with a peak in late M/G1 phase (Hofmann and Beach 1994). In fission yeast, MBF activates a wave of transcription at the G1-S phase transition and consists of Cdc10, Res1 and Res2 proteins (reviewed in Bähler 2005). Correct cell cycle regulation of MBF-dependent transcription requires the co-

regulators Rep2, Nrm1 and Yox1 (Nakashima et al. 1995; Baum et al. 1997; de Bruin et al. 2006; Aligianni et al. 2009). Both Res2 and Yox1 are implicated in confining MBF transcription to the G1-S phase transition and deletion of either *res2*$^+$ or *yox1*$^+$ results in high and constitutive expression of MBF target genes throughout the cell cycle (Baum et al. 1997; Aligianni et al. 2009). Therefore, the elevated level of Cdt1 in *res2*Δ and *yox1*Δ mutants can be explained through up-regulation of Cdt1 expression.

Res2 negatively regulates MBF activity by interacting with the B-type cyclin Cig2. The cell cycle expression of *cig2*$^+$ is dependent on MBF and the protein accumulates in G1/S phase, where it binds Res2 and mediates Cdc2-Cig2 dependent phosphorylation of Res1 (Ayte et al. 2001). Cig2-dependent phosphorylation of Res1 at residue S130 appears to reduce MBF-dependent transcription in late S/G2 phase (Ayte et al. 2001). Yox1 is also a negative regulator of MBF (Aligianni et al. 2009). Transcription of *yox1*$^+$ is MBF-dependent and the Yox1 protein accumulates in S phase, where it binds the MBF complex through interactions with Res2 and Nrm1 and represses MBF activity (Aligianni et al. 2009). Therefore, similar to Cig2, Yox1 is involved in a negative feedback loop that confines MBF-dependent transcription to the G1-S phase transition. Constitutive transcription of *cdt1*$^+$ in *res2*Δ and *yox1*Δ mutants would explain the pattern of Cdt1 deregulation observed in these strains by fluorescence microscopy. A Cdt1 signal was detected in the nuclei of almost all cells, except septating binucleate (S phase) cells, suggesting that although inappropriate transcription of *cdt1*$^+$ in G2 phase occurs in *res2*Δ and *yox1*Δ mutants, the S phase-dependent proteolysis of Cdt1 is unaffected in these strains.

Ddb1 and Cdt2 are components of $CRL4^{Cdt2}$, which ubiquitylates Cdt1 and targets it for proteolysis in S phase and after DNA damage (Hu et al. 2004; Arias and Walter 2006; Higa et al. 2006; Jin et al. 2006; Ralph et al. 2006; Sansam et al. 2006). In contrast to mammalian cells, where Cdt1 is redundantly regulated in S phase by both the $CRL4^{Cdt2}$ and SCF^{Skp2} pathways, the S-phase-dependent proteolysis of Cdt1 in fission yeast cells is entirely dependent on $CRL4^{Cdt2}$ (Nishitani et al. 2006; Ralph et al. 2006; Senga et al. 2006). Therefore, deletion of *ddb1*$^+$ or *cdt2*$^+$ in fission yeast cells results in a dramatic elevation of Cdt1 levels and detection of a Cdt1 signal in the nuclei of all cells, regardless of their cell cycle stage, as noted in the deletion library screen and as previously reported (Ralph et al. 2006). Although the role of Cdt2 as the $CRL4^{Cdt2}$ substrate receptor is well characterised, there are outstanding questions with regards to Cdt2 regulation, a point that is addressed in Chapter 6.

Csn1 is a subunit of the CSN complex, which has been shown to inhibit CRL activity through both enzymatic and non-enzymatic methods. First, CSN enzymatically inhibits CRL activity *in vitro* through deneddylation and deubiquitylation (Lyapina et al. 2001; Zhou et al. 2001; Zhou et al. 2003). CSN removes the stimulatory Nedd8 modification from the cullin subunit of CRLs and also recruits the deubiquitylating enzyme Ubp12 to CSN-bound CRL complexes, which acts to further neutralise their ubiquitin ligase activity (Lyapina et al. 2001; Zhou et al. 2001; Zhou et al. 2003). Second, CSN has recently been reported to non-enzymatically inhibit $CRL4^{DDB2}$, a ubiquitin ligase that functions in the global genome repair branch of NER. Binding of $CRL4^{DDB2}$ to its substrate, which is UV-damaged DNA, triggered release of CSN and timely activation of $CRL4^{DDB2}$ (Fischer et al. 2011).

Although the intrinsic and Ubp12-associated activities of CSN inhibit CRL function *in vitro*, CSN has been shown to promote CRL activity *in vivo* (Higa et al. 2003; Liu et al. 2003; Liu et al. 2005a). As discussed in Chapter 1, the adaptor instability model has been proposed to resolve this paradox (Wee et al. 2005). The inhibitory activity of CSN is proposed to counterbalance the autocatalytic ubiquitylation of SRSs by the CRL. This creates an appropriate environment for *de novo* assembly and maintenance of CRLs, which is required to promote their overall activity (Wee et al. 2005). CSN is implicated in promoting $CRL4^{Cdt2}$ function as deletion of *csn1*$^+$ stabilises the $CRL4^{Cdt2}$ target Spd1 in *S. pombe* (Liu et al. 2003). In addition, down-regulation of CSN subunits in human and *Drosophila* cells suppresses Cdt1 proteolysis in response to DNA damage (Higa et al. 2003; Raman et al. 2011). Therefore, the elevated Cdt1 level in the *csn1*Δ mutant is likely to result from the down-regulation of $CRL4^{Cdt2}$ activity, in the absence of a functional CSN complex. It is interesting that the steady state level of Cdt1 is lower in the *csn1*Δ mutant as compared to *ddb1*Δ and *cdt2*Δ mutants, and that a Cdt1 signal is detected in the nuclei of only a subset of *csn1*Δ cells. This suggests that $CRL4^{Cdt2}$ function may not be entirely abrogated by deletion of *csn1*$^+$. The mechanism and extent to which $CRL4^{Cdt2}$ activity is compromised by deletion of *csn1*$^+$ is investigated in Chapter 6.

5.3.2 *rad32*$^+$, *ctp1*$^+$, *rhp51*$^+$, *nse5*$^+$ and *nse6*$^+$ function in DNA repair

Rad32, Ctp1 and Rhp51 play key roles in the pathway of HR (Figure 5.9). HR promotes the accurate repair of DSBs and is involved in processing replication-associated DNA damage (reviewed in Lambert et al. 2007; San Filippo et al. 2008). Nse5 and Nse6 are subunits of the Smc5-Smc6 complex, which is also implicated in HR and DNA repair (reviewed in De Piccoli et al. 2009). In this section, the roles of

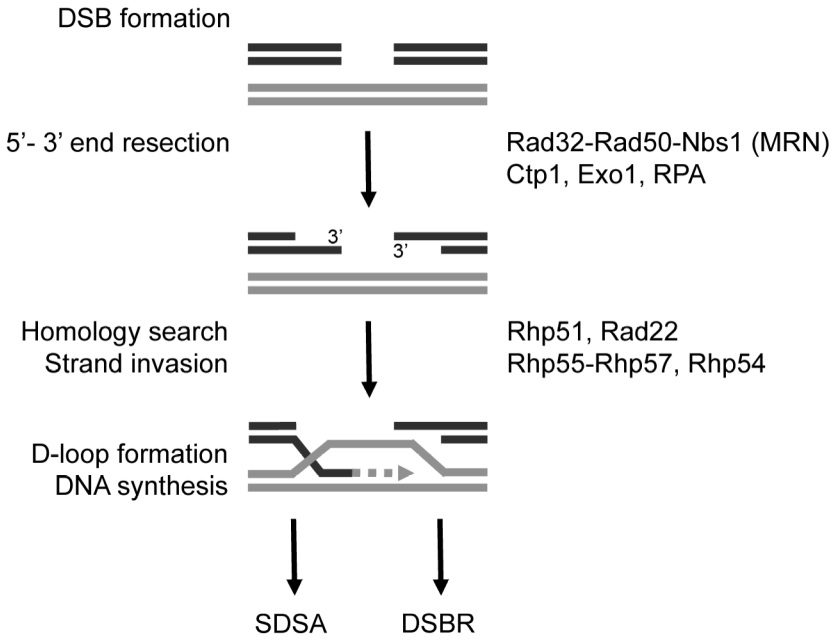


Figure 5.9 | A schematic of homologous recombination repair.
Following induction of a DSB, the DNA ends are resected in a 5' - 3' direction to produce 3' ssDNA overhangs. Resection is initiated by the MRN complex (Rad32-Rad50-Nbs1), in association with Ctp1. Extended resection at the DSB site requires Exo1. The ssDNA overhangs are initially bound by RPA but are subsequently replaced by Rhp51, with assistance from the mediator proteins Rad22 and the Rhp55-Rhp57 heterodimer. Rhp51 binding to the ssDNA overhangs produces a nucleoprotein filament (also termed presynaptic filament) that is able to initiate a search for homology. Following a successful search for homology, strand invasion by the presynaptic filament into a homologous duplex DNA molecule generates a displacement loop (D-loop) structure. DNA synthesis is primed from the 3' end of the invading strand and HR can proceed through either synthesis-dependent strand annealing (SDSA) or double-strand break repair (DSBR) pathways. During SDSA, the invading strand is displaced following DNA synthesis and anneals to the second resected DSB end, producing only non-crossover products. In the DSBR pathway, capture of the second DSB end occurs resulting in formation of a double-Holliday junction (HJ). The DSBR pathway can produce crossover or non-crossover products depending on the manner of HJ resolution/dissolution. The proteins involved in each step of HR repair are shown using *S. pombe* nomenclature. Adapted from San Filippo et al. (2008); Heyer et al. (2010).

rad32^{+}, *ctp1*$^{+}$, *rhp51*$^{+}$, *nse5*$^{+}$ and *nse6*$^{+}$ in DNA repair are briefly reviewed and the connection between a genetic background deficient in DNA repair and the up-regulation of Cdt1 is considered.

Rad32 (also referred to as Mre11) is a component of the MRN complex, which in fission yeast and vertebrate cells consists of Rad32, Rad50 and Nbs1 (Chahwan et al. 2003). The MRN complex is involved in pathways that are critical for checkpoint signalling, DNA repair and DNA replication, telomere maintenance and meiosis (reviewed in Borde and Cobb 2009). During DSB repair by HR, the MRN complex binds to DSB ends and, in association with Ctp1, initiates 5'-3' resection at the break site (reviewed in Heyer et al. 2010). End resection produces ssDNA overhangs that are bound by RPA, activate checkpoint signalling and initiate the process of HR (Figure 5.9). In *S. pombe*, Rad32 and Ctp1 are essential for end resection at a DSB (Langerak et al. 2011). In addition, Rad32 and Ctp1 have recently been shown to promote efficient RPA recruitment and checkpoint activation at DSBs by ensuring correct release of the MRN complex and the Ku70-Ku80 non-homologous end-joining (NHEJ) complex from DSB ends (Langerak et al. 2011).

Fission yeast cells with *rad32*$^{+}$, *rad50*$^{+}$ or *nbs1*$^{+}$ genes deleted display identical DNA damage sensitivities and slow growth phenotypes (Chahwan et al. 2003). In addition, triple mutant combinations of *rad32*Δ, *rad50*Δ and *nbs1*Δ are similar to the single mutants with respect to these phenotypes, suggesting that Rad32, Rad50 and Nbs1 predominantly function within the MRN complex (Chahwan et al. 2003). On this basis, one might expect *rad50*Δ and *nbs1*Δ mutants to be detected in the deletion library screen with elevated Cdt1 levels. However, examination of the Bioneer *S.*

pombe Genome-wide Deletion Mutant Library documentation indicated that *rad50*Δ and *nbs1*Δ strains were not present in Version I of the library. Independent *rad50*Δ and *nbs1*Δ strains could be examined to determine if Cdt1 is also up-regulated in these mutants.

Rhp51 is a RecA-family recombinase that is homologous to *S. cerevisiae* and vertebrate *RAD51* (Muris et al. 1993; Jang et al. 1994). Rhp51 performs a central role in HR through its ability to form helical nucleoprotein filaments on ssDNA and catalyse DNA strand annealing and DNA strand exchange reactions (Sauvageau et al. 2005). Rhp51 assembles on the ssDNA overhangs produced by 5'- 3' resection at a DSB site and forms a nucleoprotein filament (reviewed in San Filippo et al. 2008). The Rhp51 nucleoprotein filament initiates a search for homology and mediates strand invasion once a homologous duplex DNA molecule is found, generating a displacement loop (D-loop) structure (Figure 5.9). Although disruption of *RAD51* is lethal in vertebrate cells, fission yeast *rhp51*Δ mutants are viable (Muris et al. 1993; Sonoda et al. 1998). However, the *rhp51*Δ mutants display a slow growth phenotype, impaired HR and hypersensitivity to X-ray, UV and methyl methanesulphonate (MMS) treatment (Muris et al. 1993; Muris et al. 1997; Park et al. 1998).

Nse5 and Nse6 interact as heterodimers and are subunits of the Smc5-Smc6 complex (Pebernard et al. 2006). In yeast, this complex is composed of two structural maintenance of chromosome (SMC) proteins (Smc5 and Smc6) plus six additional *n*on-*S*mc *e*lements (Nse1-6). A role for the Smc5-Smc6 complex in numerous cellular processes is implicated, including in Rad51-dependent homologous recombination, DNA repair, the processing of stalled replication forks and telomere maintenance

(reviewed in De Piccoli et al. 2009). In contrast to the other Smc5-Smc6 complex subunits, *nse5*$^{+}$ and *nse6*$^{+}$ are non-essential genes; fission yeast cells deleted for *nse5*$^{+}$ and *nse6*$^{+}$ display heterogeneity in cell length and hypersensitivity to UV, MMS and HU treatment (Pebernard et al. 2006). The Nse5/6 dimer is proposed to facilitate DNA repair in the context of the Smc5-Smc6 complex and in particular, may function to mitigate damage that is associated with replication fork stalling (Pebernard et al. 2006).

S. pombe cells in which *rad32*$^{+}$, *ctp1*$^{+}$, *rhp51*$^{+}$, *nse5*$^{+}$ or *nse6*$^{+}$ has been deleted all show a slow growth phenotype and heterogeneity in cell length (Kim et al. 2001; Chahwan et al. 2003; Pebernard et al. 2006; Limbo et al. 2007). This phenotype is indicative of genetic backgrounds that undergo spontaneous DNA damage, leading to checkpoint activation and a cell cycle arrest (Chahwan et al. 2003; Pebernard et al. 2006). Evidence that the checkpoint is activated in these mutants is provided by the observation that the master checkpoint regulator Rad3 contributes to the maintenance of genome integrity and cell viability of *rad32*Δ, *rhp51*Δ and *nse6*Δ strains (Tavassoli et al. 1995; Smeets et al. 2003; Pebernard et al. 2006).

In support of the hypothesis that *rad32*Δ, *ctp1*Δ, *rhp51*Δ, *nse5*Δ and *nse6*Δ mutants might undergo elevated levels of spontaneous DNA damage, nuclear Rad22 foci were detected in an increased percentage of asynchronous *rad32*$^{+}$, *rhp51*$^{+}$ and *nse6*$^{+}$ cells, in the absence of exogenous DNA damage, as compared to wildtype (Meister et al. 2003; Pebernard et al. 2006). Rad22 is recruited to DSBs and abnormal structures produced during DNA replication; hence Rad22 foci formation can be used to monitor the occurrence of spontaneous and induced DNA damage (Meister et al.

2003). The increased level of spontaneous DNA damage in the *rad32*Δ, *ctp1*Δ, *rhp51*Δ, *nse5*Δ and *nse6*Δ mutants may reflect a requirement for these proteins in the repair of replication-associated DNA damage (Chahwan et al. 2003; Pebernard et al. 2006). In vertebrate cells, *RAD51* disruption is lethal and this is thought to reflect the essential role played by HR in replication fork repair (Sonoda et al. 1998; San Filippo et al. 2008). Depletion of Rad51 in chicken DT40 cells resulted in cells arresting at the G2/M boundary with an accumulation of chromosome aberrations and subsequent cell death (Sonoda et al. 1998).

Although *rad32*Δ, *ctp1*Δ, *rhp51*Δ, *nse5*Δ and *nse6*Δ mutants exhibited a general increase in Cdt1 levels by western blot analysis, fluorescence microscopy analysis indicated that there was a striking disparity between the nuclear Cdt1 signals detected in individual cells. Those cells where an intense nuclear Cdt1 signal was detected were predominantly elongated uninucleate cells. Spindle pole body and α-tubulin staining of *rhp51*Δ cells indicate that these elongated uninucleate cells are predominantly in G2 phase (Kim et al. 2001). Interestingly, G2-synchronised cells subject to ionising radiation up-regulate the transcription of MBF target genes, such as *cdt1*$^{+}$, in a proposed checkpoint-dependent manner (Watson et al. 2004). Therefore, one hypothesis is that in *rad32*Δ, *ctp1*Δ, *rhp51*Δ, *nse5*Δ and *nse6*Δ mutants, replication-associated DNA damage occurs in a subset of cells and cannot be repaired, leading to activation of the DNA integrity checkpoint. Checkpoint activation causes a G2 arrest and MBF-dependent up-regulation of *cdt1*$^{+}$ transcription, resulting in the appearance of elongated uninucleate cells with an intense nuclear Cdt1 signal. The relationship between DNA repair, cell cycle progression, checkpoint activation and Cdt1 regulation is addressed in Chapter 6.

5.3.3 Defects in cell cycle progression and large-scale effects on gene expression may underlie the up-regulation of Cdt1 that is observed in *pof3*Δ, *ask1*Δ, *dad2*Δ, *dad5*Δ, *nut2*Δ, *SPAC1805.14*Δ and *SPAC824.04*Δ mutants

Pof3 is an F-box protein and a substrate recognition subunit for the SCF ubiquitin ligase (Katayama et al. 2002). Deletion of *pof3*$^{+}$ affects the genome integrity of *S. pombe* cells; *pof3*Δ mutants exhibit increased minichromosome loss, impaired chromosome segregation, spontaneous DNA damage and hypersensitivity to UV irradiation (Katayama et al. 2002). These phenotypes lead to constitutive activation of the DNA damage checkpoint, which is required for the viability of *pof3*Δ cells, and a G2 cell cycle delay (Katayama et al. 2002). The genome integrity defects of *pof3*Δ cells are proposed to result from the stabilisation of SCF^{Pof3} substrates, such as the GATA-type transcription factor Ams2, the correct regulation of which is required to limit core histone gene expression to S phase (Takayama et al. 2010). The pattern of Cdt1 misregulation in *pof3*Δ cells was similar to that observed in the strains defective in HR; an increased percentage of elongated uninucleate cells were detected with a nuclear Cdt1 signal. Given deletion of *pof3*$^{+}$ has been demonstrated to cause checkpoint activation and a G2 cell cycle delay, the upregulation of Cdt1 in this mutant may also reflect a checkpoint-mediated and MBF-dependent induction of *cdt1*$^{+}$ transcription in G2-arrested cells.

Ask1, Dad2 and Dad5 are components of the heterodecameric DASH complex (Liu et al. 2005b; Sanchez-Perez et al. 2005). The DASH complex is a kinetochore component that maintains correct attachment between kinetochores and the mitotic spindle to ensure precise chromosome segregation (reviewed in Buttrick and Millar 2011). Although the DASH complex is conserved in *S. cerevisiae*, direct homologues

of the complex have not been identified in higher eukaryotes (Buttrick and Millar 2011). *S. pombe* DASH mutants exhibit activation of the spindle assembly checkpoint (SAC) and consequently spend a prolonged period in prometaphase/metaphase (Sanchez-Perez et al. 2005). In addition, these mutants display lagging kinetochores in anaphase A and an increased rate of chromosome mis-segregation (Liu et al. 2005b).

In *ask1*Δ, *dad2*Δ and *dad5*Δ mutants, an intense nuclear Cdt1 signal is detected in a subpopulation of cells. Interestingly, this strong Cdt1 signal is localised in a number of nuclei that display aberrant nuclear morphology. The cold-sensitive *nda3-311* mutation in β-tubulin arrests cells in prometaphase owing to activation of the SAC, and Cdt1 accumulates to a high level in these cells owing to continued transcription (He et al. 1997; Ralph et al. 2006). Given DASH mutants have been reported to activate the SAC, it is possible that the *ask1*Δ, *dad2*Δ or *dad5*Δ cells with an intense nuclear Cdt1 signal represent those arrested in prometaphase or metaphase. This observation could be extended by examining whether Cdt1 levels are reduced in a double DASH and SAC component mutant, which has been reported to exhibit a reduced delay to anaphase onset (Sanchez-Perez et al. 2005).

Nut2 is a component of the Mediator complex (Spahr et al. 2000; Spahr et al. 2001). Mediator is a multisubunit regulator of RNA polymerase II (pol II) that functions both in the activation and repression of pol II transcription in eukaryotic cells (reviewed in Conaway and Conaway 2011). Deletion of *nut2*$^{+}$ in fission yeast cells resulted in an increase in the intensity of the nuclear Cdt1 signal in binucleate cells. Given Nut2 is a Mediator component, it is expected that the increase in Cdt1 levels in the *nut2*Δ

mutant is the result of alterations to the rate of *cdt1*$^{+}$ transcription. A Cdt1 signal is still detected predominantly in binucleate cells in the *nut2*Δ mutant, suggesting the timing of *cdt1*$^{+}$ transcription in the cell cycle is unaffected. Interestingly, conditional mutant analysis of *NUT2/MED10*, the budding yeast *nut2*$^{+}$ homologue, implicated Nut2/Med10 as a negative regulator of the *HO* promoter (Gustafsson et al. 1998; Tabtiang and Herskowitz 1998). It is therefore possible that in fission yeast cells, Nut2 exerts a similarly repressive activity at the *cdt1* promoter.

Deletion of *SPAC1805.14*$^{+}$ also resulted in an increase in the intensity of the nuclear Cdt1 signal in binucleate fission yeast cells. However, *SPAC1805.14*$^{+}$ is a sequence orphan with no apparent eukaryotic orthologues (Wood et al. 2012) so it is unclear how deletion of this gene might affect Cdt1 levels. Interestingly, the increase in Cdt1 levels in the *SPAC1805.14*Δ mutant, as measured by western blot analysis, was similar to that observed in the *nut2*Δ mutant. Given the similarity in the up-regulation phenotypes between the *nut2*Δ and the *SPAC1805.14*Δ mutants, SPAC1805.14 may also affect Cdt1 levels through the regulation of *cdt1*$^{+}$ transcription. The involvement of Nut2 and SPAC1805.14 in *cdt1*$^{+}$ transcription could be examined further through real-time reverse transcription PCR (RT-qPCR) analysis of *cdt1*$^{+}$ mRNA levels in wildtype, *nut2*Δ and *SPAC1805.14*Δ mutant cells.

In eukaryotic cells, 3’ end processing of pre-mRNA is important for efficient protein synthesis; it promotes transport of the mRNA from the nucleus to the cytoplasm and enhances mRNA stability and the rate of translation in the cytoplasm (reviewed in Mandel et al. 2008). The eukaryotic pre-mRNA 3’ end processing machinery consists of a several protein sub-complexes, one of which in yeast is termed cleavage and

polyadenylation factor (CPF) (Mandel et al. 2008). SPAC824.04 is a component of the fission yeast CPF (Roguev et al. 2004). It is unclear precisely why Cdt1 levels are elevated in the *SPAC824.04*Δ mutant, as a defect in pre-mRNA processing machinery is expected to impact on multiple cellular processes. The *SPAC824.04*Δ mutant has been reported to exhibit a reduced growth rate, therefore it is possible that a defect in cell cycle progression underlies the observed up-regulation of Cdt1 in this strain (Roguev et al. 2004).

5.4 CONCLUSIONS

To conclude, this chapter describes the development of a medium-throughput fluorescence microscopy-based screening method, suitable for use with the Bioneer *S. pombe* Genome-wide Deletion Mutant Library. Subsequent analysis of the *S. pombe* deletion library image dataset using MATLAB led to the identification of 17 candidate genes with a possible involvement in Cdt1 regulation. Five of these candidate genes (*ddb1*$^+$, *cdt1*$^+$, *csn1*$^+$, *res2*$^+$ and *yox1*$^+$) have a previously described role in Cdt1 regulation. A further five of the candidate genes are involved in DNA repair pathways (*rad32*$^+$, *ctp1*$^+$, *rhp51*$^+$, *nse5*$^+$ and *nse6*$^+$) and their involvement in Cdt1 up-regulation merits further investigation. At least some of the remaining seven candidate genes (*pof3*$^+$, *ask1*$^+$, *dad2*$^+$, *dad5*$^+$, *nut2*$^+$, *SPAC1805.14*$^+$ and *SPAC824.04*$^+$) may elevate Cdt1 levels through defects in cell cycle progression and large-scale effects on gene expression.

CHAPTER 6

Analysis of Candidate Genes Involved in Cdt1 Regulation

6.1 INTRODUCTION

In Chapter 5, a genome-wide screen for novel genes involved in Cdt1 regulation was conducted, which led to the identification of 17 deletion mutants that exhibited an up-regulation of Cdt1. Following a literature review of each candidate gene, three areas of research pertaining to the involvement of a subset of these candidate genes in Cdt1 regulation were identified that merited further investigation. These three areas of research address the relationship between HR, cell cycle progression, checkpoint activation and Cdt1 regulation; the role of the CSN complex in promoting $CRL4^{Cdt2}$ activity and finally, the regulation of Cdt2 levels and their effect on $CRL4^{Cdt2}$ activity. Further investigation into these three topics was undertaken and the findings from each topic are presented and discussed in turn.

6.2 RESULTS

6.2.1 Analysis of Cdt1 regulation in genetic backgrounds defective in DNA repair

The genome-wide screen for novel genes involved in Cdt1 regulation identified five candidate genes (*rad32*$^+$, *ctp1*$^+$, *rhp51*$^+$, *nse5*$^+$ and *nse6*$^+$) with previously established roles in DNA repair. Rad32, Ctp1 and Rhp51 have well-characterised roles in DSB

repair by HR but have not previously been implicated in Cdt1 regulation. This section addresses the connection between a genetic background defective in DNA repair and the up-regulation of Cdt1.

6.2.1.1 Investigation into Cdt1 levels in genetic backgrounds defective in DNA repair

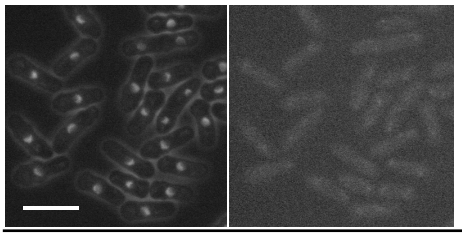
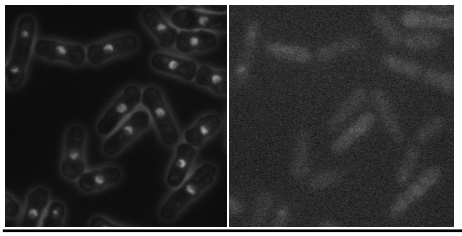
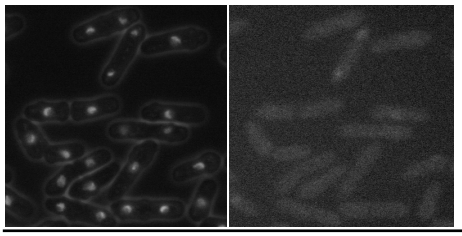
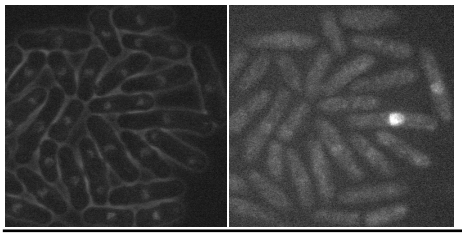
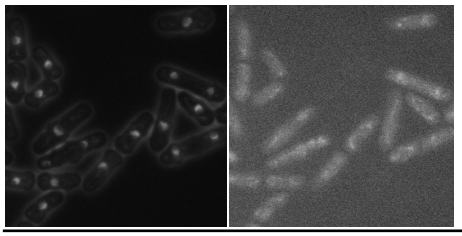
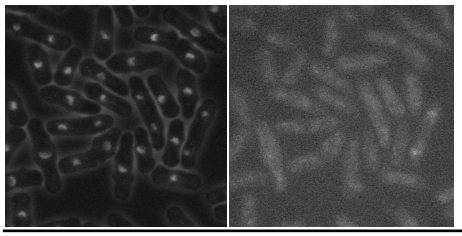
To extend the observation that *rad32*Δ*, ctp1*Δ and *rhp51*Δ cells exhibit elevated levels of Cdt1, investigations were undertaken to establish whether this was a common feature of genetic backgrounds that are defective in DNA repair. A screen of *S. pombe* deletion library strains, where the deleted gene product was involved in the repair pathway of either BER, NER or DSB repair by NHEJ or HR was performed (Table 6.1). Strains that displayed non-wildtype levels and distributions of Cdt1-YFP by fluorescence microscopy were subject to western blot analysis (Figure 6.1).

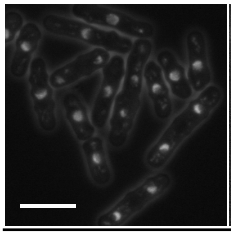
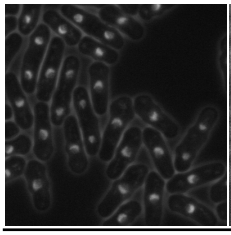
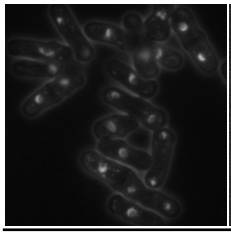
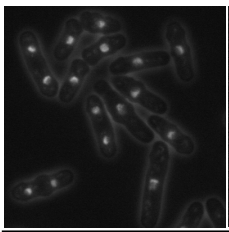
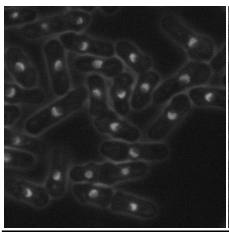
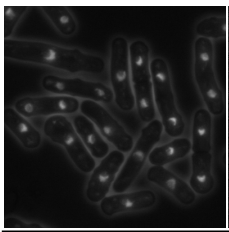
A moderate increase in Cdt1 levels was observed in *nth1*Δ, *apn2*Δ and *rhp41*Δ mutants (Figure 6.1A and B). Nth1 and Apn2 function in BER, which is the main pathway for the removal of damaged bases arising from oxidatation, methylation, hydroxylation and deanimation activity. Briefly, in BER the damaged base is removed by a specialised DNA glycosylase to generate an apurinic or an apyrimidinic (AP) site. The AP site is then removed by AP lyase or AP endonuclease activity, which cleaves the phosphodiester DNA backbone 3' or 5' respectively of the AP site and initiates repair by short- or long-patch BER (reviewed in Seeberg et al. 1995; Hoeijmakers 2001). Nth1 has DNA glycosylase and AP lyase activity (Osman et al. 2003) and Apn2 is the major AP endonuclease in *S. pombe* (Ribar et al. 2004). Rhp41 is the homologue of human XPC and is involved in damage recognition during global

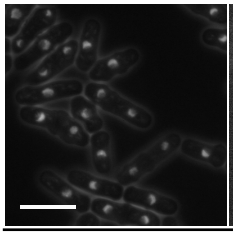
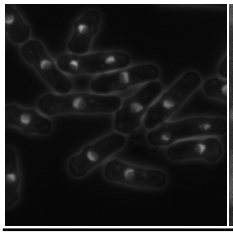
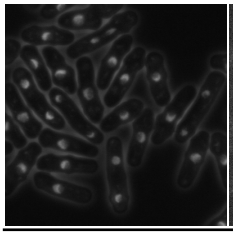
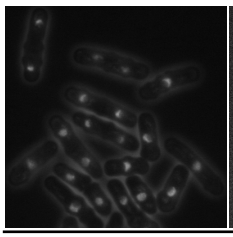
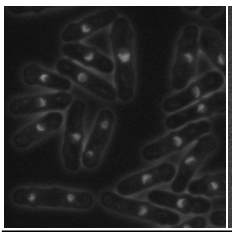
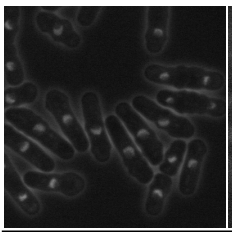
genome repair, an NER sub-pathway (Marti et al. 2003). The NER pathway recognises and repairs damage produced by exposure to UV irradiation (pyrimidine dimers) or chemicals (intrastrand cross-links) that distort the DNA helix. A small oligonucleotide containing the damage site is excised and the resulting gap is repaired through DNA synthesis and ligation (reviewed in Hoeijmakers 2001; Sancar et al. 2004).

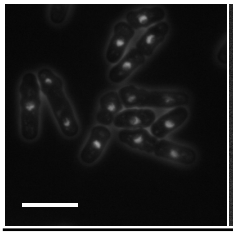
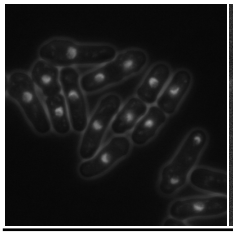
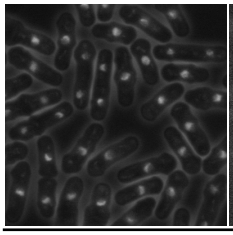
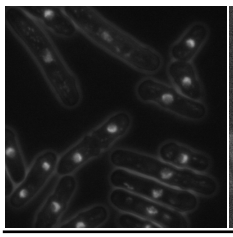
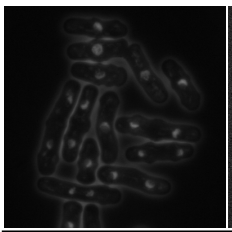
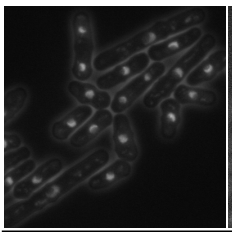
The most significant increase in Cdt1 levels was observed in *exo1*Δ, *rhp55*Δ, *rhp57*Δ and *rhp54*Δ mutants (Figure 6.1A and B). The *exo1*$^{+}$, *rhp55*$^{+}$, *rhp57*$^{+}$ and *rhp54*$^{+}$ gene products are all involved in DSB repair by HR. Exo1 functions with the MRN complex and Ctp1 to initiate the process of HR through 5' to 3' resection at the DSB site (reviewed in Mimitou and Symington 2011). *rhp55*$^{+}$, *rhp57*$^{+}$ and *rhp54*$^{+}$ are members of the *RAD52* epistasis group. This group of genes, initially identified in *S. cerevisiae* based on sensitivity of the mutants to ionising radiation, is highly conserved in eukaryotes and constitutes the core genes required for HR (reviewed in Krogh and Symington 2004; San Filippo et al. 2008). Rhp55 and Rhp57 act as recombination mediators to promote formation of a Rhp51 nucleoprotein filament on RPA-coated ssDNA, which initiates a search for homology (Krogh and Symington 2004). Rhp54 belongs to the Snf2-family of DNA stimulated/dependent ATPases. It interacts with Rhp51 and performs multiple, central functions during HR. These functions include stabilising Rhp51 on ssDNA to promote nucleoprotein filament formation, stimulating D-loop formation and branch migration, and promoting disassembly of the Rhp51-dsDNA complex (reviewed in Heyer et al. 2006).

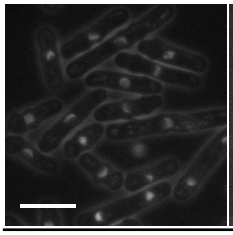
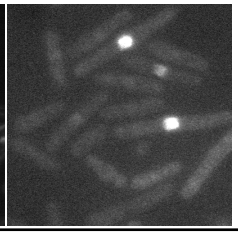
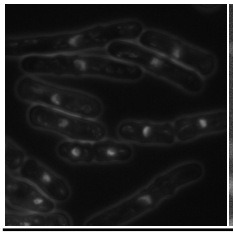
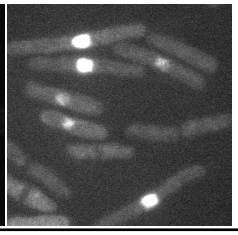
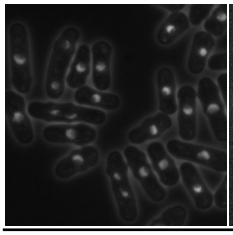
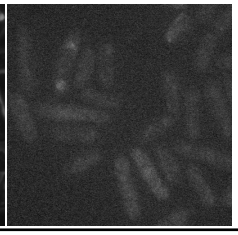
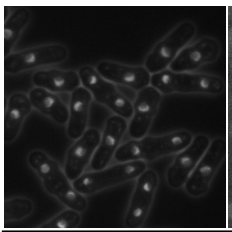
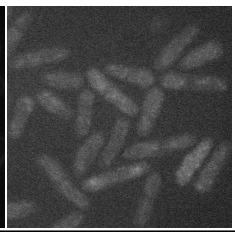
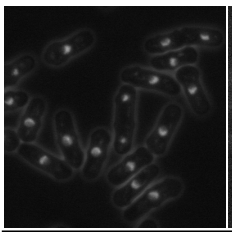
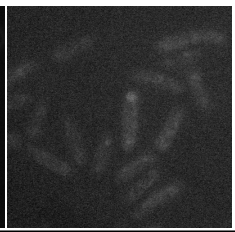
Table 6.1 | Fluorescence microscopy analysis of Cdt1-YFP in various DNA repair mutants

DAPI/Phase	Cdt1-YFP	Gene deletion	Gene product*	Repair pathway involvement*
		Wildtype no-tag		
		Wildtype Cdt1-YFP		
		*myh1*Δ	Adenine DNA glycosylase Myh1	Base excision repair
		*nth1*Δ	DNA endonuclease III	Base excision repair
		*mag1*Δ	DNA-3-methyladenine glycosylase Mag1	Base excision repair
		*mag2*Δ	DNA-3-methyladenine glycosylase Mag2	Base excision repair

DAPI/Phase	Cdt1-YFP	Gene deletion	Gene product*	Repair pathway involvement*
		*apn2*Δ	AP-endonuclease Apn2	Base excision repair
		*ung1*Δ	uracil DNA N-glycosylase Ung1	Base excision repair
		*mms19*Δ	TFIIH regulator Mms19	Nucleotide excision repair
		*rhp41*Δ	DNA repair protein Rhp41	Nucleotide excision repair
		*rad8*Δ	ubiquitin-protein ligase E3 Rad8	Nucleotide excision repair
		*pnk1*Δ	DNA kinase/ phosphatase Pnk1	Nucleotide excision repair

DAPI/Phase	Cdt1-YFP	Gene deletion	Gene product*	Repair pathway involvement*
		*tfb2*Δ	transcription factor TFIIH complex subunit Tfb2	Nucleotide excision repair
		*def1*Δ	RNAPII degradation factor Def1 (predicted)	Nucleotide excision repair
		*rad13*Δ	DNA repair nuclease Rad13	Nucleotide excision repair
		*rhp16b*Δ	ATP-dependent DNA helicase Rhp16b (predicted)	Nucleotide excision repair
		*rhp14*Δ	XP-A family homolog Rhp14	Nucleotide excision repair
		*rhp7*Δ	Rad7 homolog Rhp7	Nucleotide excision repair

DAPI/Phase	Cdt1-YFP	Gene deletion	Gene product*	Repair pathway involvement*
		*rhp26*Δ	SNF2 family helicase Rhp26	Nucleotide excision repair
		*pku70*Δ	Ku domain protein Pku70	Double-strand break repair by non-homologous end-joining
		*pku80*Δ	Ku domain protein Pku80	Double-strand break repair by non-homologous end-joining
		*exo1*Δ	exonuclease I Exo1	Double-strand break repair by homologous recombination
		*ssb3*Δ	DNA replication factor A subunit Ssb3	Double-strand break repair by homologous recombination
		*rhp55*Δ	RecA family ATPase Rhp55	Double-strand break repair by homologous recombination

DAPI/Phase	Cdt1-YFP	Gene deletion	Gene product*	Repair pathway involvement*
		*rhp57*Δ	RecA family ATPase Rhp57	Double-strand break repair by homologous recombination
		*rhp54*Δ	Rad54 homolog Rhp54	Double-strand break repair by homologous recombination
		*rdh54*Δ	ATP-dependent DNA helicase Rdh54	Double-strand break repair by homologous recombination
		*slx1*Δ	structure-specific endonuclease catalytic subunit	Double-strand break repair by homologous recombination
		*rti1*Δ	Rad22 homolog Rti1	Double-strand break repair by homologous recombination

* Data from GeneDB (http://old.genedb.org/genedb/pombe/)
Cdt1-YFP imaged in exponentially growing DNA repair mutants
Scale bar: 10 μm

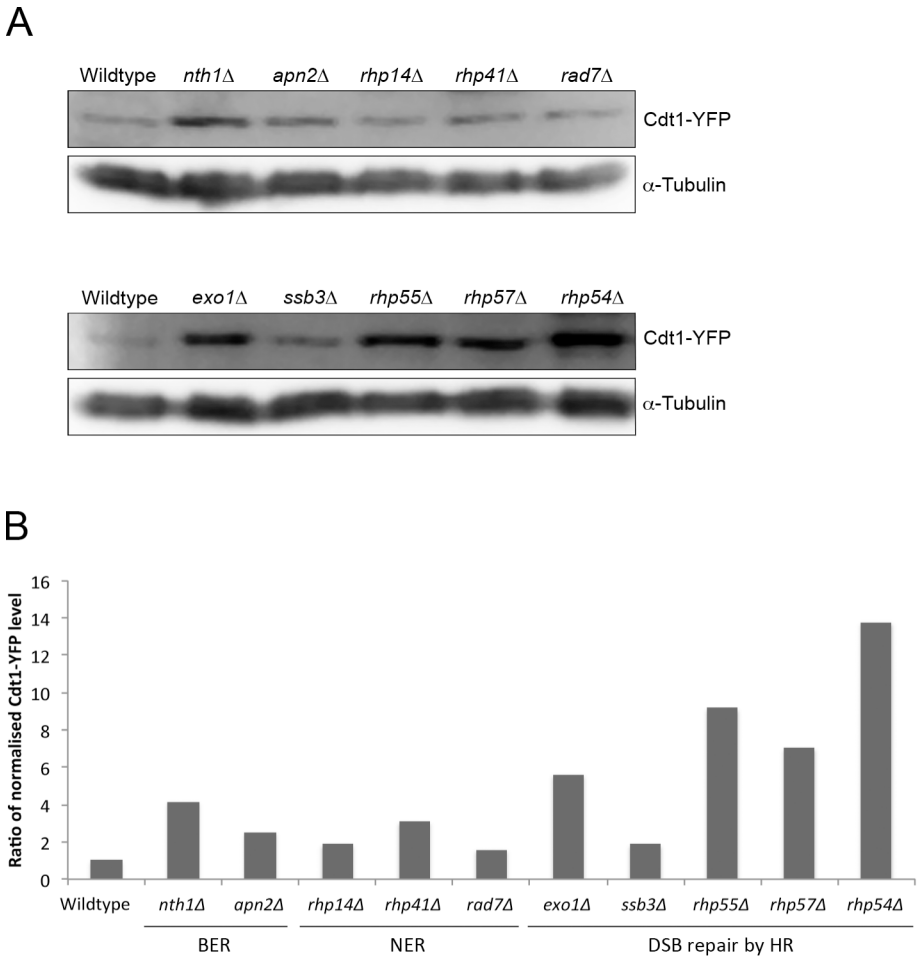


Figure 6.1 | Analysis of Cdt1-YFP levels in different DNA repair mutants.
(A) Western blot analysis of Cdt1-YFP levels in exponentially growing wildtype cells (2009) and in ten DNA repair mutants from the *S. pombe* deletion library, which exhibit Cdt1 up-regulation by fluorescence microscopy analysis (Table 6.1) **(B)** Quantitation of western blot analysis in (A). Graph shows ratio of Cdt1-YFP levels (deletion background / wildtype) in the wildtype (2009) and DNA repair mutants, normalised to the α-tubulin loading control. The DNA repair pathway that each gene is involved in is indicated below the *x*-axis.

In summary, deletion of *rad32*$^+$, *ctp1*$^+$, *exo1*$^+$, *rhp51*$^+$, *rhp55*$^+$, *rhp57*$^+$ or *rhp54*$^+$ in *S. pombe* cells resulted in a striking up-regulation of Cdt1. The gene products from these seven genes perform central roles in HR. Interestingly, deletion of genes that function in other DNA repair pathways, such as BER, NER or NHEJ did not produce such a dramatic elevation in Cdt1 levels. Given the up-regulation of Cdt1 is predominantly associated with genetic backgrounds defective in HR, subsequent work in this section specifically addressed why Cdt1 levels are elevated in these HR mutants.

6.2.1.2 Comparison of Cdt1 levels throughout the cell cycle in wildtype, *rhp55*Δ and *rhp51*Δ cells

Fluorescence microscopy analysis of the HR mutants indicated a striking disparity between the intensity of the nuclear Cdt1 signals detected in individual cells (Table 5.2 and Table 6.1). A subset of the cell population, predominantly represented by elongated uninucleate cells, exhibited an intense nuclear Cdt1 signal. Analysis of the *rhp51*Δ mutant has indicated that these elongated uninucleate cells are predominantly in G2 phase (Kim et al. 2001). A number of HR mutants are proposed to undergo a G2 delay and it is possible that this defect in cell cycle progression underlies the Cdt1 up-regulation phenotype (Kim et al. 2001; Chahwan et al. 2003). In vertebrate and yeast cells, HR is implicated in the repair of replication-associated DNA damage, in addition to the repair of DSBs arising from exogenous agents (Sonoda et al. 1998; Meister et al. 2003). To investigate the relationship between a requirement for the HR machinery, cell cycle progression and Cdt1 regulation, wildtype, *rhp55*Δ and *rhp51*Δ cells that expressed Cdt1-YFP were arrested in G1 by nitrogen starvation and released in synchrony. This permits comparison of Cdt1 levels throughout the cell cycle, in the

wildtype and HR mutant strains, to determine whether variations in the nuclear Cdt1 signal observed in the HR mutants correlates with a particular cell cycle stage.

In the wildtype strain, Cdt1 levels were low in the G1-arrested cells but increased as the cells were released, reaching a maximum level at 2 hours after release (Figure 6.2A and B). Flow cytometry was used to monitor cell cycle progression and indicated that S phase occurred between 2 and 3 hours after release, which coincided with a decrease in Cdt1 levels (Figure 6.2A-C). After the completion of S phase, Cdt1 levels remained low and the majority of Cdt1-YFP fluorescence was detected in the nuclei of binucleate cells. Cdt1 levels in the G1-arrested *rhp55*Δ and *rhp51*Δ cells were low and increased between 1 and 2 hours after release, in accordance with the wildtype (Figure 6.3A-B and Figure 6.4A-B). The *rhp55*Δ and *rhp51*Δ cells entered and completed S phase between 2 and 3 hours after release (Figure 6.3C and Figure 6.4C), suggesting that deletion of these genes did not inhibit bulk DNA replication, as previously reported for *rhp51*Δ cells released from an HU arrest (Meister et al. 2005). Cdt1 levels decreased during S phase in the *rhp55*Δ and *rhp51*Δ mutants, indicating that the S phase-dependent regulation of Cdt1 was not affected by deletion of $rhp55^{+}$ or $rhp51^{+}$. However, in contrast to the wildtype cells, the *rhp55*Δ and *rhp51*Δ cells became progressively elongated throughout the remainder of the time-course and accumulated increasing levels of Cdt1 (Figure 6.3A-B and Figure 6.4A-B). There was a striking increase in the number of uninucleate cells positive for an intense nuclear Cdt1 signal at the later time-points of the experiment (Figure 6.3B and Figure 6.4B).

The appearance of elongated *rhp55*Δ and *rhp51*Δ cells post-S phase is consistent with these strains undergoing a G2 delay. As discussed in Chapter 5, G2-synchronised

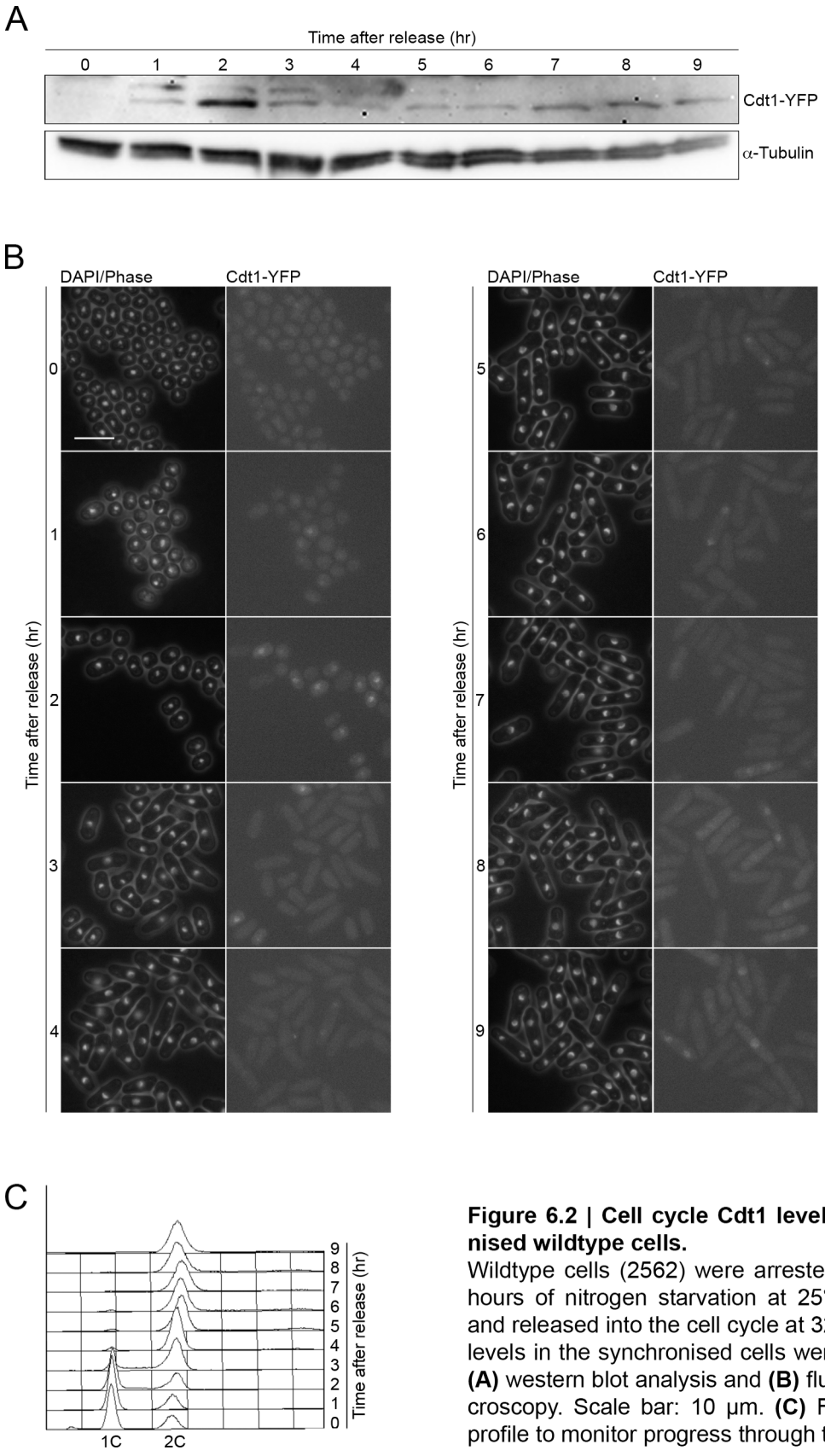


Figure 6.2 | Cell cycle Cdt1 levels in synchronised wildtype cells.
Wildtype cells (2562) were arrested in G1 by 16 hours of nitrogen starvation at 25°C then re-fed and released into the cell cycle at 32°C. Cdt1-YFP levels in the synchronised cells were analysed by **(A)** western blot analysis and **(B)** fluorescence microscopy. Scale bar: 10 µm. **(C)** Flow cytometry profile to monitor progress through the cell cycle.

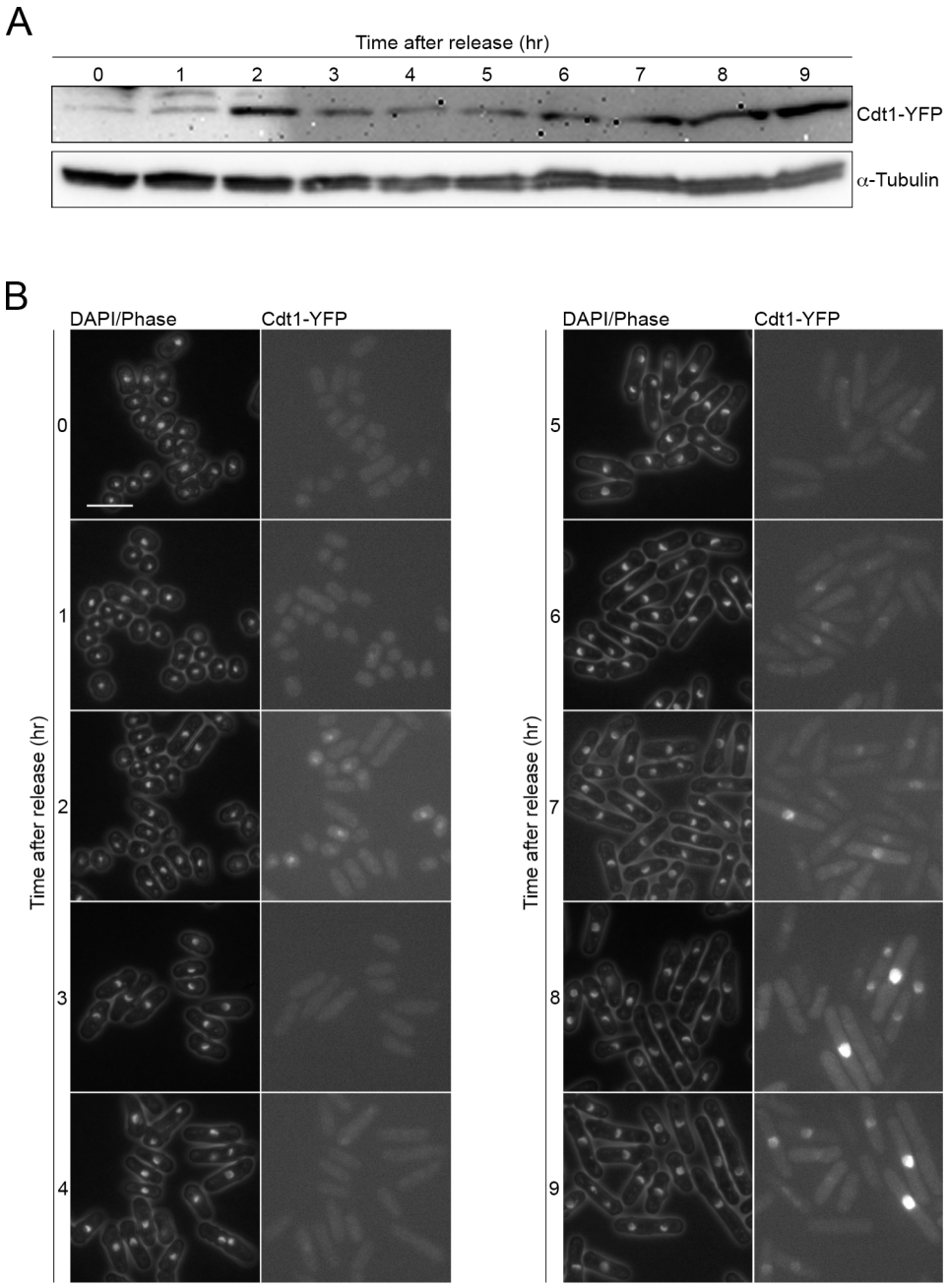


Figure 6.3 | Cell cycle Cdt1 levels in synchronised *rhp55*Δ cells.
*rhp55*Δ cells (2774) were arrested in G1 by 16 hours of nitrogen starvation at 25°C then re-fed and released into the cell cycle at 32°C. Cdt1-YFP levels in the synchronised cells were analysed by **(A)** western blot analysis and **(B)** fluorescence microscopy. Scale bar: 10 μm. **(C)** Flow cytometry profile to monitor progress through the cell cycle.

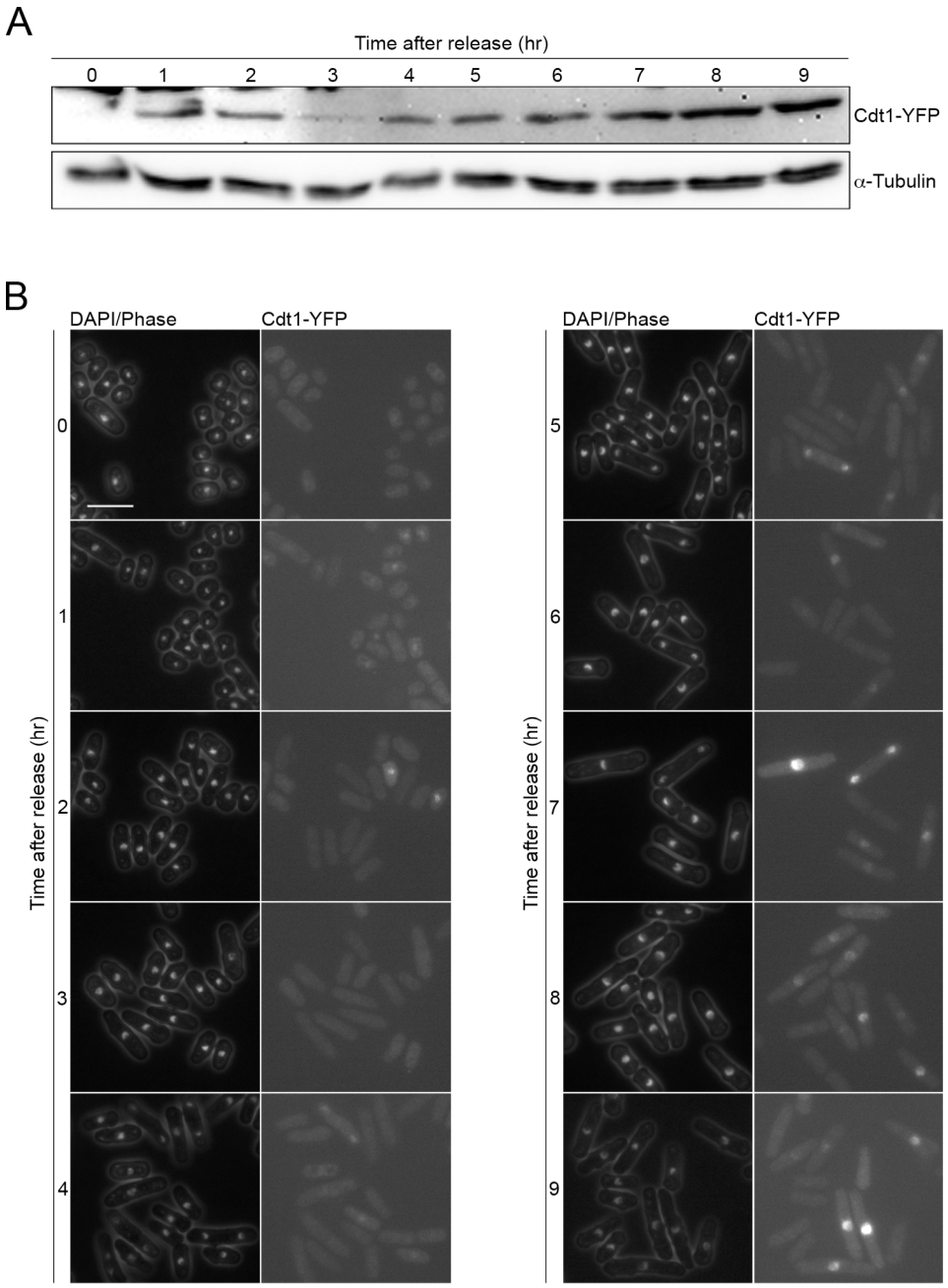


Figure 6.4 | Cell cycle Cdt1 levels in synchronised *rhp51*Δ cells.
*rhp51*Δ cells (2804) were arrested in G1 by 16 hours of nitrogen starvation at 25°C then re-fed and released into the cell cycle at 32°C. Cdt1-YFP levels in the synchronised cells were analysed by **(A)** western blot analysis and **(B)** fluorescence microscopy. Scale bar: 10 μm. **(C)** Flow cytometry profile to monitor progress through the cell cycle.

cells subject to ionising radiation are thought to up-regulate the transcription of MBF target genes in a checkpoint-dependent manner (Watson et al. 2004). Various DNA repair mutants are reported to undergo high levels of spontaneous DNA damage, which may be linked to the role of the HR machinery in the repair of replication-associated DNA damage (Chahwan et al. 2003; Meister et al. 2003; Pebernard et al. 2006). It is possible that an inability to repair this damage in a subset of cells results in activation of the DNA integrity checkpoint, an inhibition of cell cycle progression and an MBF-dependent up-regulation of *cdt1*$^{+}$ transcription. To explore this hypothesis, the involvement of the DNA integrity checkpoint in Cdt1 regulation in the HR mutants was examined.

6.2.1.3 The deregulation of Cdt1 in *rhp55*Δ and *rhp51*Δ mutants is dependent on Rad3 activity

Rad3 mediates the *S. pombe* DNA integrity checkpoint, which comprises the DNA replication and DNA damage checkpoint, through activation of the serine/threonine effector kinases Cds1 and Chk1 respectively. Activated Cds1 and Chk1 arrest cells at the G2/M transition through inhibition of the CDK, Cdc2 (reviewed in Rhind and Russell 2000; Melo and Toczyski 2002). To investigate whether Rad3 activation is responsible for the up-regulation of Cdt1 observed in the HR mutants, Cdt1-YFP levels were compared in *rhp55*Δ *rad3*^{ts} and *rhp51*Δ *rad3*^{ts} double mutants at the permissive (26°C) and the restrictive (35°C) temperature of the *rad3* temperature-sensitive allele (*rad3*^{ts}) (Martinho et al. 1998).

Immediately after the shift of the *rad3*^{ts}, *rhp55*Δ *rad3*^{ts} and *rhp51*Δ *rad3*^{ts} cells to the restrictive temperature, the three strains showed a similar distribution of Cdt1-YFP to

cells of a *rad3*$^{+}$ wildtype background; a Cdt1 signal was predominantly detected in the nuclei of binucleate *rad3*^{ts} cells but in an increased number of uninucleate cells in the *rhp55*Δ *rad3*^{ts} and *rhp51*Δ *rad3*^{ts} backgrounds (Figure 6.5A and B, *t* = 0 hours). At 2 and 4 hours after the shift to the restrictive temperature, *rad3*^{ts} cells retained a Cdt1 signal predominantly in the nuclei of binucleate cells. However, in the *rhp55*Δ *rad3*^{ts} and *rhp51*Δ *rad3*^{ts} cells there was a striking reduction in the number of uninucleate cells with a nuclear Cdt1 signal (Figure 6.5A). After 4 hours at the restrictive temperature, the percentage of uninucleate and binucleate cells with a nuclear Cdt1 signal was not significantly different between the *rad3*^{ts} cells and the *rhp55*Δ *rad3*^{ts} and *rhp51*Δ *rad3*^{ts} cells (Figure 6.5B, *t* = 4 hours). The *rhp55*Δ *rad3*^{ts} and *rhp51*Δ *rad3*^{ts} cells decreased in length following incubation at the restrictive temperature and cells with aberrant nuclei could be observed (Figure 6.5A, *t* = 4 hours, white arrows). This suggests that Rad3 activity is responsible for the elongated cell phenotype of *rhp55*Δ and *rhp51*Δ cells and that checkpoint activation contributes to the genome stability of these mutants. This is consistent with a report that a *rhp51*Δ *rad3*Δ double mutant was almost synthetically lethal (Smeets et al. 2003).

The transcription of *cdt2*$^{+}$and *cdc18*$^{+}$ at the G1/S phase transition is dependent on MBF and the expression of these genes is also induced following ionising radiation of G2-synchronised cells (Kelly et al. 1993; Hofmann and Beach 1994; Watson et al. 2004). To determine whether the up-regulation of Cdt1 observed in HR-deficient strains was a common feature of proteins expressed from MBF target promoters, endogenous Cdt2-YFP and Cdc18-YFP levels were examined in *rhp51*Δ and *rhp55*Δ mutants respectively. In wildtype cells, Cdt2-YFP was predominantly detected in the nuclei of binucleate cells, while Cdc18-YFP was detected exclusively in the nuclei of

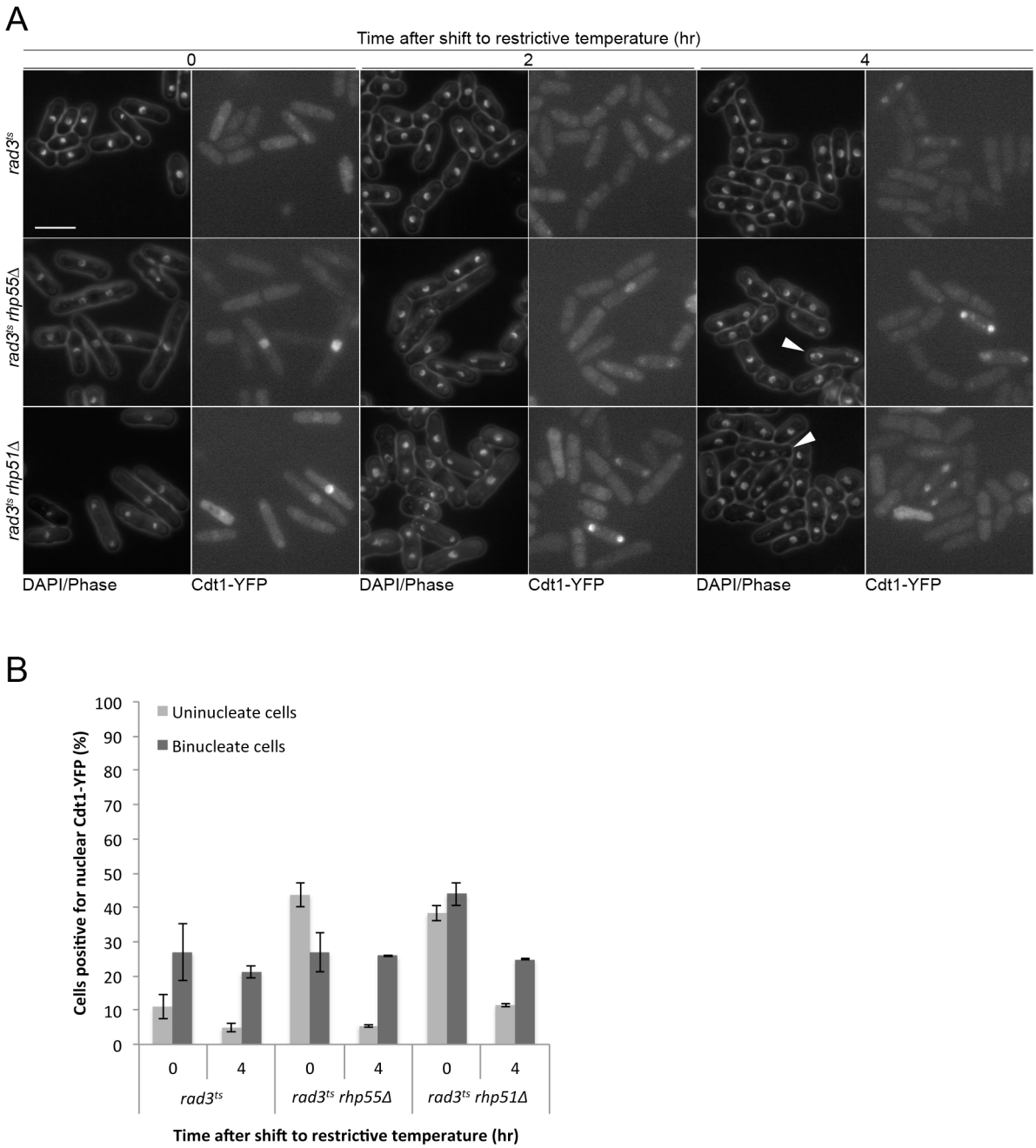


Figure 6.5 | The deregulation of Cdt1 in *rhp55*Δ and *rhp51*Δ cells is dependent on Rad3 activity. **(A)** Cdt1-YFP imaged in exponentially growing *rad3*^{ts} (2923), *rhp55*Δ *rad3*^{ts} (2925) and *rhp51*Δ *rad3*^{ts} (2928) mutant cells at 0, 2 and 4 hours after shifting from 26°C to the restrictive temperature of 35°C. Cells with aberrant nuclei are indicated (white arrowheads). Scale bar: 10 μm. **(B)** Analysis of the strains in (A) to determine the percentage of uninucleate and binucleate cells positive for nuclear Cdt1-YFP. At least 100 cells, from two independent experiments, were counted for each data point. Error bars: 50% of the range.

binucleate cells (Figure 6.6A and B). In *rhp51*Δ cells, nuclear Cdt2-YFP was detected in an increased number of uninucleate cells, and these cells were often elongated in appearance (Figure 6.6A). Similarly, in an *rhp55*Δ background, nuclear Cdc18-YFP was detected in an increased number of elongated uninucleate cells as compared to wildtype (Figure 6.6B). The increased number of uninucleate cells with nuclear Cdt2 and Cdc18 signals in the *rhp51*Δ and *rhp55*Δ cells respectively suggests some disruption to the regulation of these proteins occurs in HR-deficient cells.

Interestingly, the intensities of the nuclear Cdt2 and Cdc18 signals in the *rhp51*Δ and *rhp55*Δ cells were not strikingly higher than the nuclear signals of wildtype cells, in contrast to the situation observed for Cdt1 (compare Figure 6.6A-B with Table 5.2 and 6.1). In keeping with this observation, western blot analysis indicated that there was not a significant increase in the overall level of Cdc18-YFP in the *rhp55*Δ mutant as compared to wildtype, again in contrast to the situation observed for Cdt1 (compare Figure 6.6C with Figure 6.1A). The initial interpretation of Cdt2 levels was complicated by the reproducible appearance of an upper band in the Cdt2-YFP *rhp51*Δ sample (Figure 6.6C). However, unexpected bands were frequently observed with the α-GFP antibody used for this western blot, which were subsequently not observed with different tag and antibody combinations, suggesting this upper band might be non-specific (for example, compare *csn1*Δ sample in Figure 6.13A and D on page 199). The overall level of Cdt2 in the *rhp51*Δ mutant is therefore likely to be similar to wildtype. The difference between Cdt1, Cdt2 and Cdc18 accumulation in the HR mutants may reflect a difference in the rate of transcription of each gene and/or the rate of protein turnover.

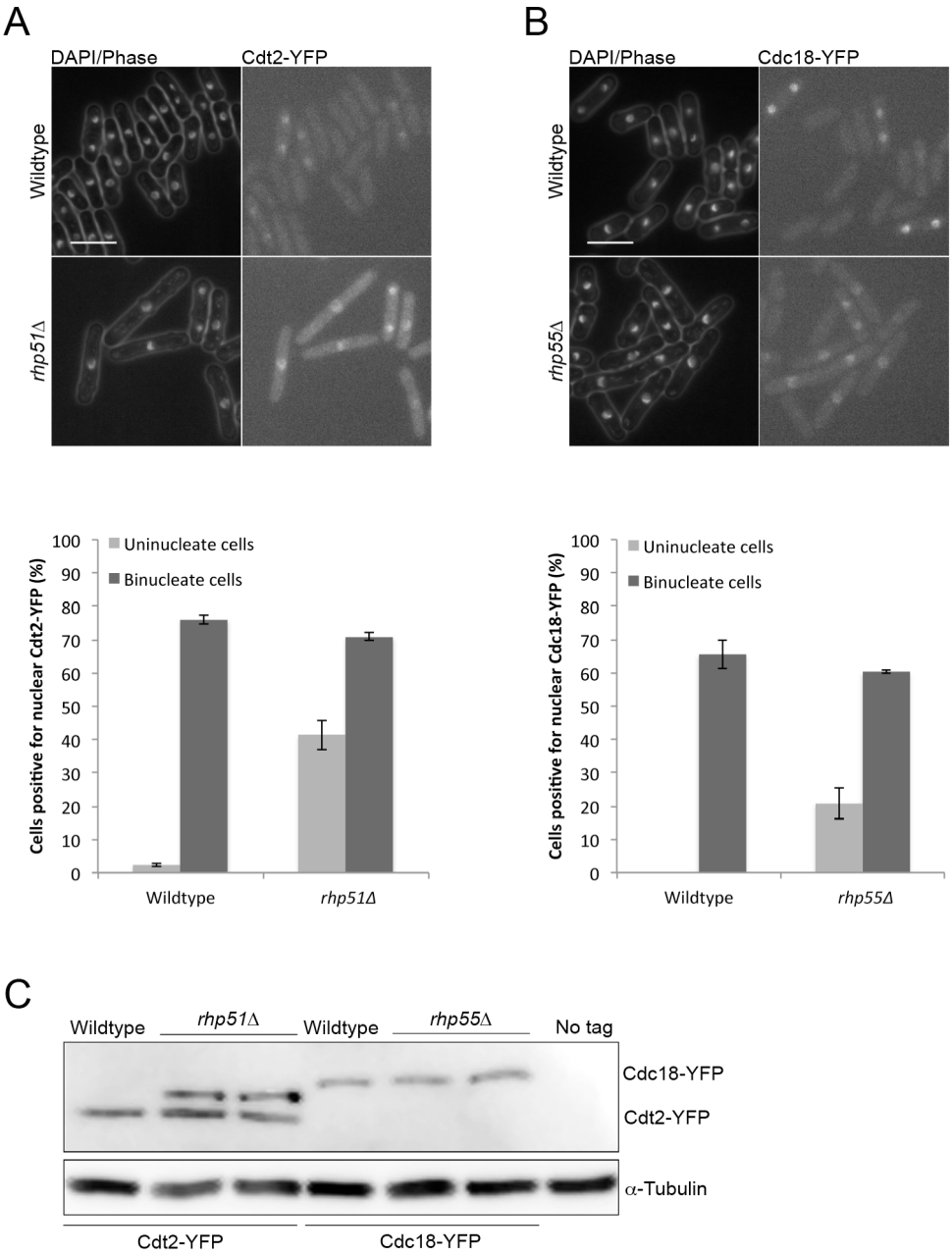


Figure 6.6 | Analysis of Cdt2 and Cdc18 levels in HR mutants.
(A) *Upper panel*: Cdt2-YFP imaged in exponentially growing wildtype (1698) and *rhp51*Δ mutant (2849) cells. Scale bar: 10 μm. *Lower panel*: the same strains were analysed to determine the percentage of uninucleate and binucleate cells positive for nuclear Cdt2-YFP. At least 100 cells, from two independent experiments, were counted for each data point. Error bars: 50% of range. **(B)** *Upper panel*: Cdc18-YFP imaged in exponentially growing wildtype (2227) and *rhp55*Δ mutant (2829) cells. Scale bar: 10 μm. *Lower panel*: the same strains were analysed to determine the percentage of uninucleate and binucleate cells positive for nuclear Cdc18-YFP. At least 100 cells, from two independent experiments, were counted for each strain. Error bars: 50% of range. **(C)** Western blot analysis of Cdt2-YFP levels in exponentially growing wildtype (1698) and *rhp51*Δ mutant (2849 and 2850) cells and of Cdc18 -YFP levels in exponentially growing wildtype (2227) and *rhp55*Δ mutant (2829 and 2830) cells.

6.2.1.4 Abolishing mating-type switching does not affect Cdt1 levels in *rhp55*Δ and *rhp51*Δ mutants

The precise cause of the Rad3-dependent checkpoint activation in *rhp55*Δ and *rhp51*Δ cells that leads to Cdt1 up-regulation is unclear. One hypothesis is that mating-type switching might contribute to checkpoint activation; in fission yeast the process involves formation of a single-ended DSB that may remain unresolved in *rhp55*Δ and *rhp51*Δ cells. The entire process of mating-type switching occurs over two replication cycles. In the first round of replication, pausing of the replication fork at the MPS1 site in the *mat1* locus delivers an imprint to the lagging strand, which is thought to be a protected single-strand break (SSB). In the second round of DNA replication, the leading strand stalls at the SSB, producing a single-ended DSB. Regression of the fork leads to extrusion of the leading strand, the 3' end of which is able to initiate gene conversion using either the silent *mat2P* or *mat3M* cassettes on the sister chromatid as a template (reviewed in Egel 2005). This process requires the HR machinery, as evidenced by the observation that *rhp51*Δ cells are defective in mating-type switching (Grishchuk et al. 2004). Interestingly, the introduction of a *mat1* locus unable to support DSB formation improved the viability of *rhp51*Δ cells, suggesting that the process of mating-type switching is detrimental to recombination-deficient strains (Grishchuk et al. 2004).

To ascertain whether mating-type switching contributed to the Rad3-dependent up-regulation of Cdt1, Cdt1-YFP levels were examined in double *rhp55*Δ *smt-0* and *rhp51*Δ *smt-0* mutants (Figure 6.7). The *smt-0* mutation is a 263 bp deletion that abolishes DSB formation at the *mat1* locus and consequently mating-type switching (Styrkarsdottir et al. 1992). Introduction of the *smt-0* deletion did not reduce Cdt1

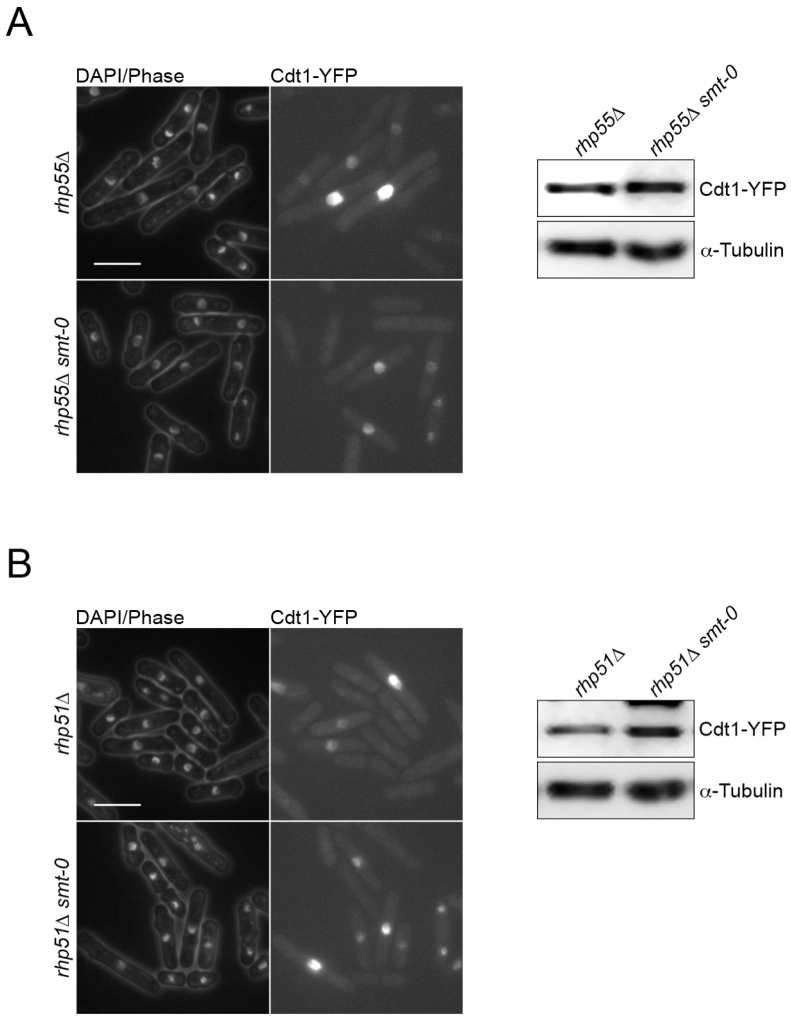


Figure 6.7 | The *smt-0* mutation that abolishes mating-type switching does not reduce Cdt1 levels in *rhp55*Δ and *rhp51*Δ mutants.
(A) Fluorescence microscopy and western blot analysis of Cdt1-YFP in exponentially growing *rhp55*Δ (2635) and *rhp55*Δ *smt-0* (2717) cells. Scale bar: 10 μm. **(B)** Fluorescence microscopy and western blot analysis of Cdt1-YFP in exponentially growing *rhp51*Δ (2804) and *rhp51*Δ *smt-0* (3140) cells. Scale bar: 10 μm.

levels in *rhp55*Δ and *rhp51*Δ cells (Figure 6.7A and B). An intense nuclear Cdt1 signal was still detected in the elongated uninucleate cells of the double *rhp55*Δ *smt-0* and *rhp51*Δ *smt-0* mutants (Figure 6.7A and B, left panels). Therefore, the process of mating-type switching is not responsible for the Rad3-dependent up-regulation of Cdt1 in *rhp55*Δ and *rhp51*Δ mutants. It is possible that the role of these HR proteins in the repair of more general replication-associated DNA damage underlies the Rad3-dependent checkpoint activation observed in *rhp55*Δ and *rhp51*Δ mutants.

6.2.2 The role of the CSN subunit Csn1 in Cdt1 regulation

The genome-wide screen for novel genes involved in Cdt1 regulation identified *csn1*$^{+}$ as a candidate gene. As discussed in Chapter 5, Csn1 is a component of the CSN complex (Mundt et al. 1999). In *S. pombe*, CSN function is implicated in promoting CRL4^{Cdt2} activity, as *csn1*Δ cells exhibit stabilisation of the RNR inhibitor and CRL4^{Cdt2} target Spd1 (Liu et al. 2003). Although it was unsurprising that *csn1*$^{+}$ was identified in the screen for novel genes involved in Cdt1 regulation, it was of interest that the deregulation of Cdt1 observed in *csn1*Δ cells was distinct from that observed in *cdt2*Δ or *ddb1*Δ cells, where CRL4^{Cdt2} function is completely abolished. The steady state level of Cdt1 was lower in the *csn1*Δ mutant, as compared to *cdt2*Δ or *ddb1*Δ mutants, and a nuclear Cdt1 signal was detected in only a subset of *csn1*Δ cells. This suggests CRL4^{Cdt2} activity is not entirely abolished in the absence of CSN function. Therefore, investigations were undertaken to establish the mechanism and extent to which deletion of *csn1*$^{+}$ compromises CRL4^{Cdt2} activity towards Cdt1 in *S. pombe*.

6.2.2.1 *csn1*Δ cells in S and G2 phase exhibit high Cdt1 levels

Fluorescence microscopy analysis indicates Cdt1 is not entirely stabilised in *csn1*Δ cells. Imaging of Cdt1-YFP in *csn1*Δ cells demonstrated that although a nuclear Cdt1 signal was detected in an increased number of uninucleate cells and the intensity of the signal in both uninucleate and binucleate cells was generally higher compared to wildtype, not all *csn1*Δ cells were positive for a nuclear Cdt1 signal and there was variation in the intensity of the signal between cells (Figure 6.8A). To investigate whether variation in the nuclear Cdt1 signal of *csn1*Δ cells was linked to cell cycle stage, Cdt1-TAP levels were analysed in detail throughout the cell cycle of wildtype and *csn1*Δ cells. A synchronised cell cycle was achieved using a temperature-sensitive *cdc25-22* mutant, which at the restrictive temperature arrests cells at the G2/M transition. Progress through the cell cycle was monitored using the septation index; S phase occurred in wildtype and *csn1*Δ cells at approximately 100 minutes after release (Figure 6.8B). Cdt1 levels were low in the G2-arrested wildtype and *csn1*Δ mutant cells but increased between 0 and 50 minutes after release (Figure 6.8C). In contrast to the wildtype cells where Cdt1 levels declined in S phase, Cdt1 levels in the *csn1*Δ mutant remained consistently high throughout S phase and the remainder of the time-course (Figure 6.8C). This suggests that the S phase-dependent regulation of Cdt1 is inhibited by deletion of $csn1^{+}$.

6.2.2.2 The high Cdt1 levels in *csn1*Δ cells are a consequence of inefficient proteolysis and increased protein synthesis

The high Cdt1 levels observed in S phase *csn1*Δ cells could result from an inhibition of protein proteolysis or an induction of protein synthesis. To distinguish between these possibilities, Cdt1-TAP levels were examined in wildtype and *csn1*Δ HU-

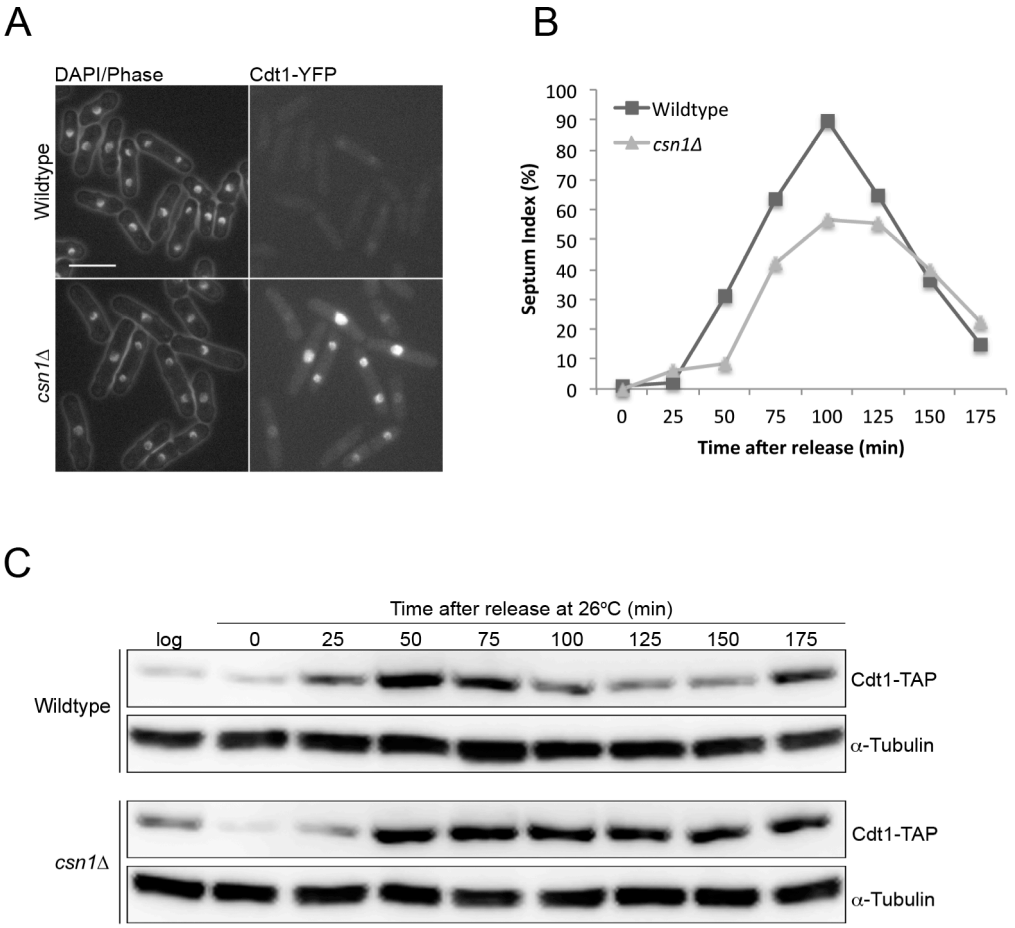


Figure 6.8 | Cdt1 levels are deregulated in a *csn1*Δ mutant.
(A) Cdt1-YFP imaged in exponentially growing cells in wildtype (1590) and *csn1*Δ mutant (3084) strains. Scale bar: 10 μm. **(B)** Septation index to monitor the cell cycle progression of wildtype (2147) and *csn1*Δ mutant (2146) cells synchronised by *cdc25-22* block and release. **(C)** Western blot analysis of wildtype (2147) and *csn1*Δ mutant (2146) cells synchronised by *cdc25-22* block and release.

arrested S phase cells in the presence or absence of CHX to inhibit *de novo* protein synthesis (Figure 6.9A). Maintenance of the HU arrest was monitored using flow cytometry (Figure 6.9B and C, right panels). Cdt1 levels declined rapidly in the HU-arrested wildtype cells regardless of CHX treatment (Figure 6.9B, left panel), indicating a robust S phase-dependent down-regulation of Cdt1. Interestingly, Cdt1 levels in the CHX-treated cells were slightly reduced relative to the untreated cells, suggesting a low level of Cdt1 protein synthesis occurred in response to HU treatment in a wildtype background. In the absence of CHX, Cdt1 levels remained high in the HU-arrested *csn1*Δ cells but levels declined following CHX treatment (Figure 6.9C, left panel). However, Cdt1 levels in the HU- and CHX-treated *csn1*Δ cells remained higher than those in wildtype cells under the same conditions. This experiment indicates that an increased rate of protein synthesis contributes to the high Cdt1 levels observed in S phase *csn1*Δ cells. Inhibition of protein synthesis by CHX treatment resulted in a moderate decline in Cdt1 levels suggesting that turnover of the protein can occur in the absence of $csn1^{+}$.

Loss of CSN function through down-regulation of CSN subunits in human and *Drosophila* cells results in a robust stabilisation of Cdt1 in response to DNA damage (Higa et al. 2003; Raman et al. 2011). Investigations were undertaken to establish if deletion of $csn1^{+}$ in fission yeast cells also abolished Cdt1 degradation in response to DNA damage or if residual turnover of the protein occurred, as observed in S phase-arrested cells. Cdt1-TAP levels were examined in mitotically-arrested *nda3-311 csn1*Δ cells following mock or UV irradiation (Figure 6.10A, -UV or +UV) and minus or plus CHX treatment (Figure 6.10A, -CHX or +CHX) to determine if protein synthesis contributed to any observed stabilisation of Cdt1. The percentage of

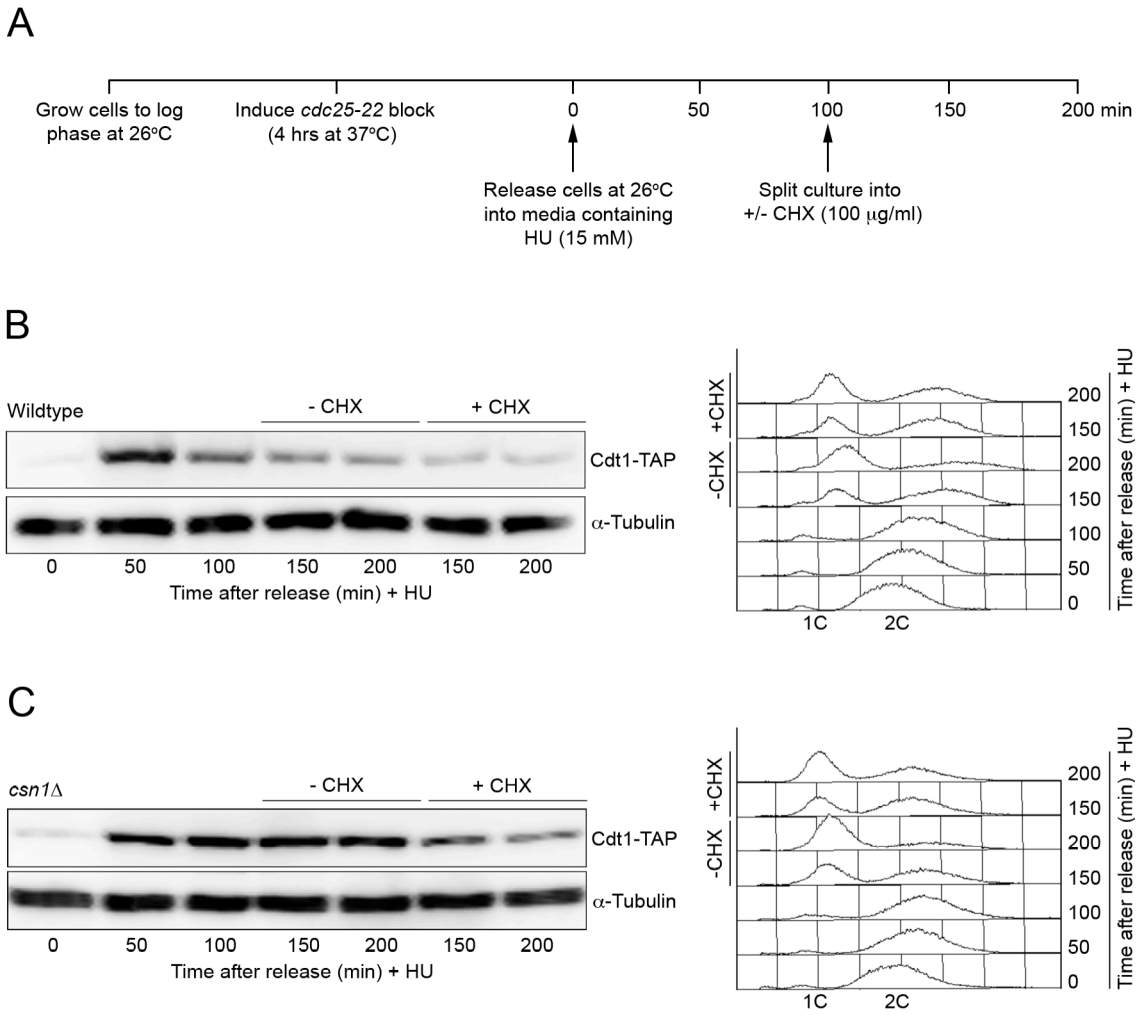


Figure 6.9 | Cell cycle-dependent Cdt1 turnover can occur in a *csn1*Δ mutant.
(A) Scheme of experiment. **(B)** Western blot analysis and flow cytometry profile of wildtype (2147) cells following the experimental procedure outlined in (A). **(C)** Western blot analysis and flow cytometry profile of *csn1*Δ mutant (2146) cells following the experimental procedure outlined in (A). HU: hydroxyurea; CHX: cycloheximide.

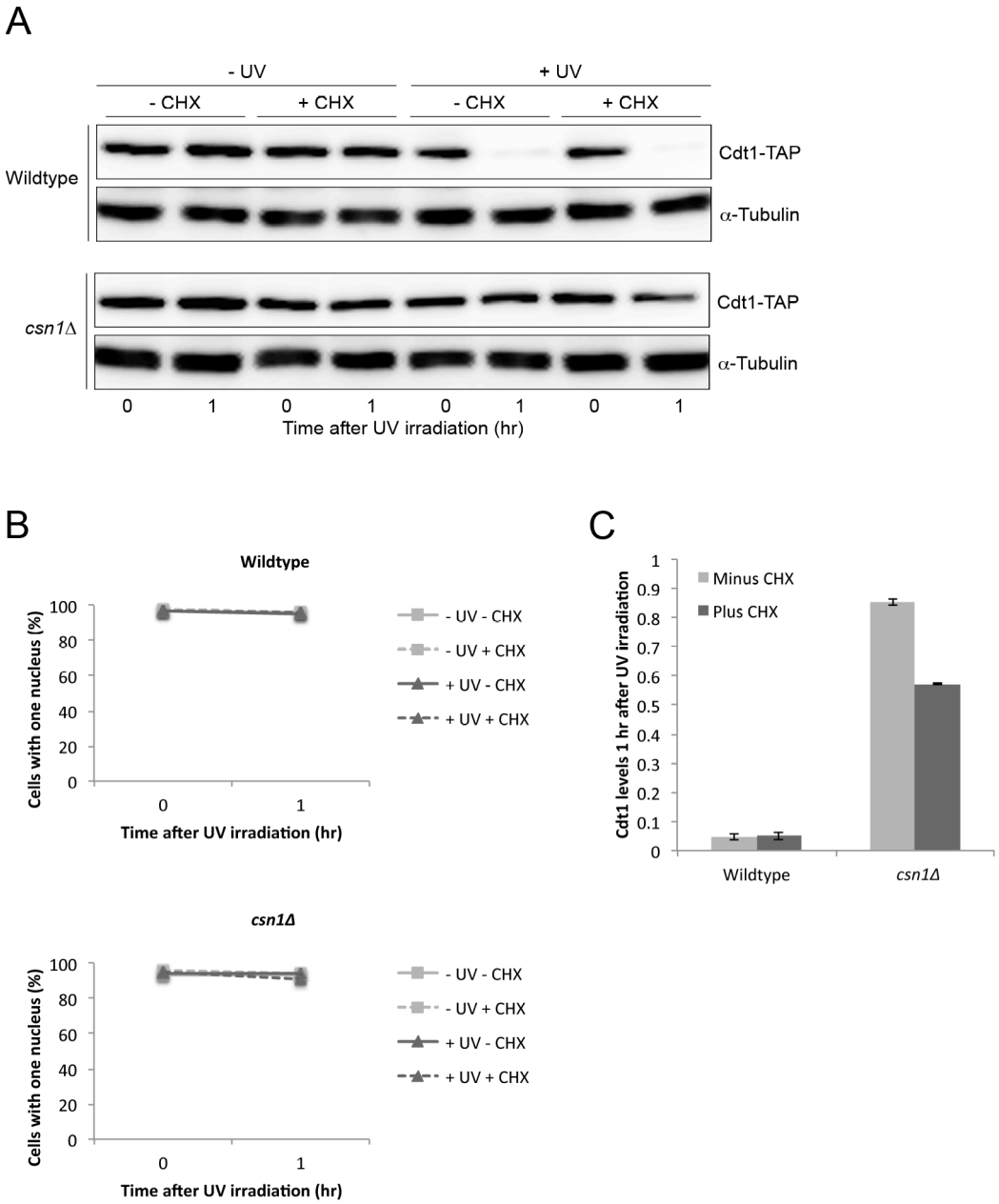


Figure 6.10 | UV irradiation can induce Cdt1 proteolysis in a *csn1*Δ mutant.
(A) Western blot analysis of prometaphase-arrested wildtype (2070) and *csn1*Δ mutant (3050) *nda3-311* cells at 0 and 1 hour after mock or 100 J/m^2 UV irradiation, plus or minus cycloheximide ('CHX' 100 µg/ml) treatment. *nda3-311* cells were arrested in prometaphase by incubation at 20°C for 4 hours and following UV treatment, cells were resuspended in media plus or minus cycloheximide then returned to the restrictive temperature. **(B)** Percentage of uninucleate cells during the experiment. **(C)** Quantitation of UV irradiation data from western blot analysis. Graph shows the ratio of Cdt1 levels (t = 1/t = 0), following normalisation to the α-tubulin loading control, 1 hour after UV irradiation, plus or minus cycloheximide treatment. The data are averaged from two independent experiments. Error bars: 50% of range.

uninucleate cells throughout the experiment was monitored to ensure maintenance of the mitotic arrest (Figure 6.10B).

In wildtype cells, Cdt1 levels were stable in the mock-irradiated cells and declined dramatically in response to UV irradiation regardless of CHX treatment (Figure 6.10A and C), as previously reported (Ralph et al. 2006). Cdt1 levels in the UV-irradiated *csn1*Δ cells were more stable compared to wildtype, both in the presence and absence of CHX treatment (Figure 6.10A). However, quantitation of the western blot data in Figure 6.10A revealed that Cdt1 levels in the UV- and CHX-treated cells declined by 40% between 0 and 1 hour after UV irradiation (Figure 6.10C, *csn1*Δ 'Plus CHX'). Therefore, although Cdt1 proteolysis in response to UV irradiation can occur in a *csn1*Δ mutant, it appears that CSN function is required for a robust down-regulation of Cdt1 in response to DNA damage.

6.2.2.3 Rad3 activity contributes to Cdt1 stabilisation in *csn1*Δ cells

The *csn1*Δ mutant is synthetically lethal in combination with *rad3*Δ, *cds1*Δ or *chk1*Δ and exhibits endogenous activation of Cds1 and Chk1 (Mundt et al. 1999). Deletion of $csn1^+$ therefore results in checkpoint activation, which is essential for cell viability. Rad3-dependent checkpoint activation causes the transcriptional up-regulation of MBF target genes (de Bruin et al. 2008). Therefore, it is possible that checkpoint- and MBF-dependent $cdt1^+$ transcription underlies the increased Cdt1 synthesis observed in the *csn1*Δ mutant. To explore the contribution of Rad3-dependent checkpoint activation to the elevation of Cdt1 levels in the *csn1*Δ mutant, Cdt1-TAP levels were examined in a *csn1*Δ $rad3^{ts}$ background, where Rad3 can be inactivated at the restrictive temperature of 35°C (Martinho et al. 1998).

Exponentially growing wildtype and *csn1*Δ cells expressing Cdt1-TAP were treated with HU at 32°C and time-points taken at 0, 2 and 4 hours after HU addition (Figure 6.11A). The level of Cdt1 in the *csn1*Δ mutant was dramatically higher compared to wildtype and remained high in response to HU treatment, increasing slightly over the time-course (Figure 6.11B and D). The *csn1*Δ *rad3*^{ts} cells were grown to log phase at the permissive temperature of 26°C and following HU addition were shifted to the restrictive temperature of 35°C to inactivate Rad3 (Figure 6.11A). In comparison to the *csn1*Δ cells, Cdt1 levels at the restrictive temperature in the double *csn1*Δ *rad3*^{ts} mutant declined in response to HU addition (Figure 6.11B and D). Flow cytometry was used to ensure that the HU arrest was maintained throughout the time-course (Figure 6.11C).

The decline in Cdt1 levels in the *csn1*Δ *rad3*^{ts} mutant at the restrictive temperature suggests Rad3 activity contributes to the increased rate of Cdt1 synthesis observed in the *csn1*Δ mutant. Checkpoint activation in the *csn1*Δ mutant is proposed to result from misregulation of the RNR inhibitor Spd1, rendering cells unable to correctly regulate dNTP levels for replication and repair purposes (Liu et al. 2003; Liu et al. 2005a). To examine if deregulation of Spd1 contributes to Cdt1 up-regulation in the *csn1*Δ mutant, the level and distribution of Cdt1-YFP was analysed in wildtype, *csn1*Δ and *csn1*Δ *spd1*Δ cells by fluorescence microscopy. However, the *csn1*Δ *spd1*Δ double mutant exhibited up-regulation of Cdt1 and an elongated cell phenotype that was quite similar to the single *csn1*Δ mutant (Figure 6.11E). The elongated cell phenotype of the *csn1*Δ *spd1*Δ double mutant suggests that factors in addition to Spd1 can cause checkpoint activation in cells where *csn1*$^{+}$ has been deleted. This continued checkpoint activation and the inefficient CRL4^{Cdt2}-dependent proteolysis of Cdt1 that

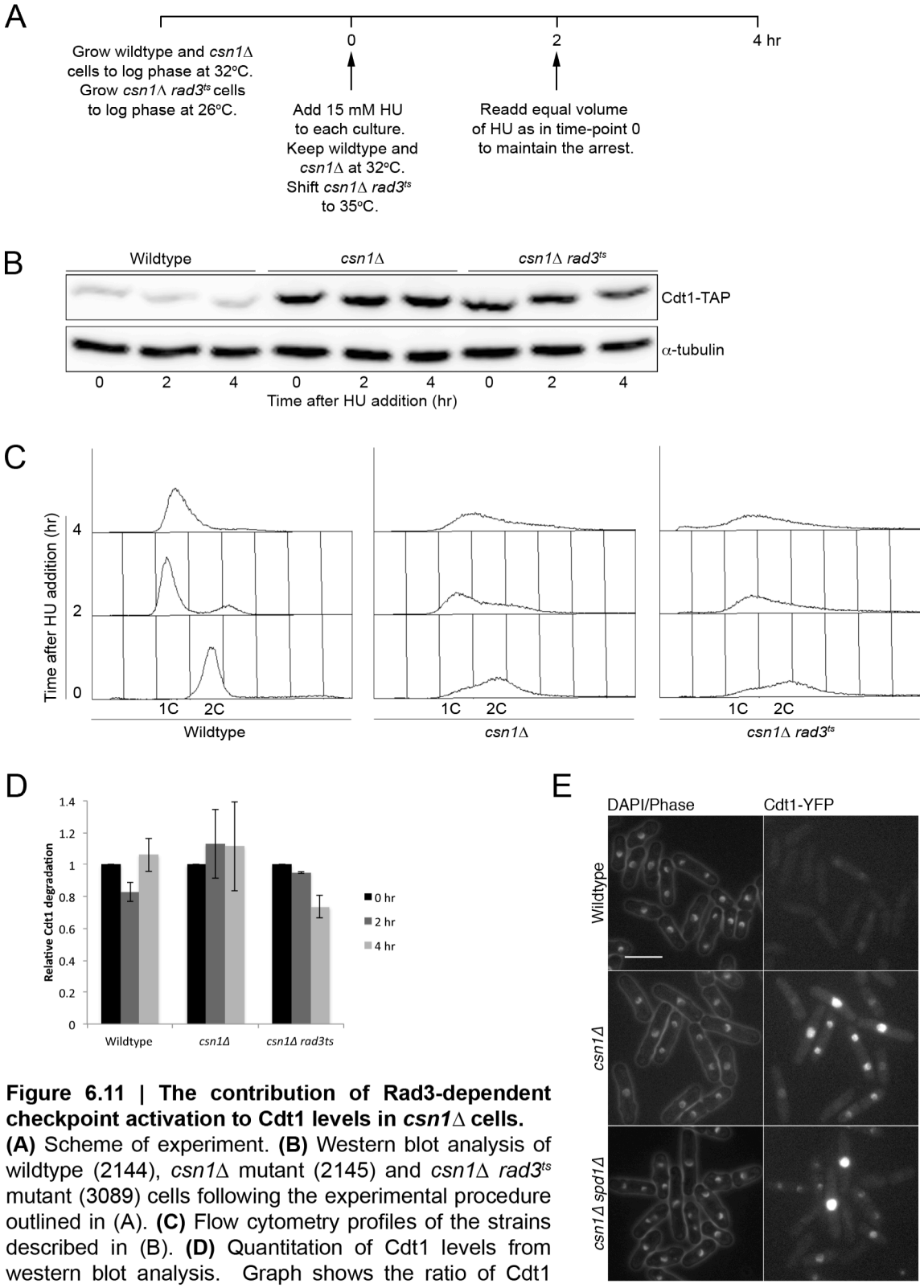


Figure 6.11 | The contribution of Rad3-dependent checkpoint activation to Cdt1 levels in *csn1*Δ cells.
(A) Scheme of experiment. **(B)** Western blot analysis of wildtype (2144), *csn1*Δ mutant (2145) and *csn1*Δ *rad3*^{ts} mutant (3089) cells following the experimental procedure outlined in (A). **(C)** Flow cytometry profiles of the strains described in (B). **(D)** Quantitation of Cdt1 levels from western blot analysis. Graph shows the ratio of Cdt1 levels (t = 0, 2, 4/t = 0), following normalisation to the α-tubulin loading control, at 0, 2 and 4 hours after HU addition. The data are an average from two independent experiments. Error bars: 50% of range. **(E)** Cdt1-YFP imaged in exponentially growing wildtype (1590), *csn1*Δ (3084) and *csn1*Δ *spd1*Δ (3086) cells. Scale bar 10 μm. HU: hydroxyurea.

occurs in CSN-deficient cells may explain the observed up-regulation of Cdt1 in the double *csn1*Δ *spd1*Δ mutant.

In summary, inefficient $CRL4^{Cdt2}$-dependent Cdt1 proteolysis and an increased rate of Cdt1 synthesis contribute to the elevated Cdt1 levels observed in the *csn1*Δ mutant. The demonstration that Cdt1 proteolysis can occur in the *csn1*Δ mutant explains the original observation that the misregulation of Cdt1 in *csn1*Δ cells is not as severe as that observed in *ddb1*Δ or *cdt2*Δ cells.

6.2.2.4 S phase and G2 phase *csn1*Δ cells exhibit high Cdt2 levels

Although CSN inhibits CRL activity *in vitro*, loss-of-function mutations in CSN subunits stabilise CRL substrates *in vivo*, suggesting a positive role for CSN in CRL regulation (Lyapina et al. 2001; Zhou et al. 2001; Cope and Deshaies 2003). To resolve this paradox, the adaptor instability model has been proposed, whereby the inhibitory activity of CSN towards CRLs prevents CRL-dependent autoubiquitylation of substrate recognition subunits (Wee et al. 2005). The autocatalytic destruction of SRSs inhibits CRL function and therefore by promoting their stabilisation, CSN increases CRL activity towards *in vivo* substrates (Wee et al. 2005). For example, Cdt1 stabilisation in response to UV irradiation in CSN-depleted human cells is proposed to result from destabilisation of Cdt2 (Raman et al. 2011).

The destabilisation of Cdt2 is unlikely to explain the inefficient $CRL4^{Cdt2}$-mediated proteolysis of Cdt1 in fission yeast as Liu et al. (2005a) reported that Cdt2 levels in asynchronous *csn1*Δ cells were elevated compared to wildtype and that the half-life of Cdt2 in wildtype and *csn1*Δ cells was similar. It is unclear why $CRL4^{Cdt2}$-dependent

proteolysis of Cdt1 is compromised in *csn1*Δ cells, if not through destabilisation of Cdt2. It was hypothesised that alterations in Cdt2 localisation or cell cycle kinetics could affect its ability to function in the $CRL4^{Cdt2}$ complex. To this end, Cdt2-YFP localisation was examined in wildtype and *csn1*Δ cells by fluorescence microscopy, and Cdt2-TAP levels were examined throughout a synchronised cell cycle in wildtype and *csn1*Δ backgrounds.

Cdt2-YFP was imaged in wildtype and *csn1*Δ cells that co-expressed Cdt1-CFP to provide information about the level and distribution of Cdt2 individually and in relation to Cdt1 (Figure 6.12A). In wildtype cells, Cdt1 and Cdt2 were predominantly detected in the nuclei of binucleate cells but often in distinct populations: Cdt2 was detected predominantly in septating (S phase) binucleate cells whereas Cdt1 was present in binucleate cells without septa (late M/G1 cells). Cdt2 remained nuclear in *csn1*Δ cells but compared to the wildtype cells, a higher signal was detected in an increased number of uninucleate cells. Cdt1 and Cdt2 colocalised in binucleate *csn1*Δ cells, presumably reflecting the delayed S phase degradation and increased expression of Cdt1 in these cells. The presence of both Cdt1 and Cdt2 in the nuclei of binucleate *csn1*Δ cells suggests that Cdt2 localisation is unlikely to be a limiting factor in $CRL4^{Cdt2}$-dependent Cdt1 proteolysis.

This observation was confirmed by analysis of Cdt2-TAP levels through the cell cycle in wildtype and *csn1*Δ cells following a *cdc25-22* arrest and release experiment (Figure 6.12C). Progress through the cell cycle was monitored using the septation index, which indicated that S phase occurred in the wildtype and *csn1*Δ cells at 100 minutes and 125 minutes respectively after release from the G2 arrest (Figure 6.12B).

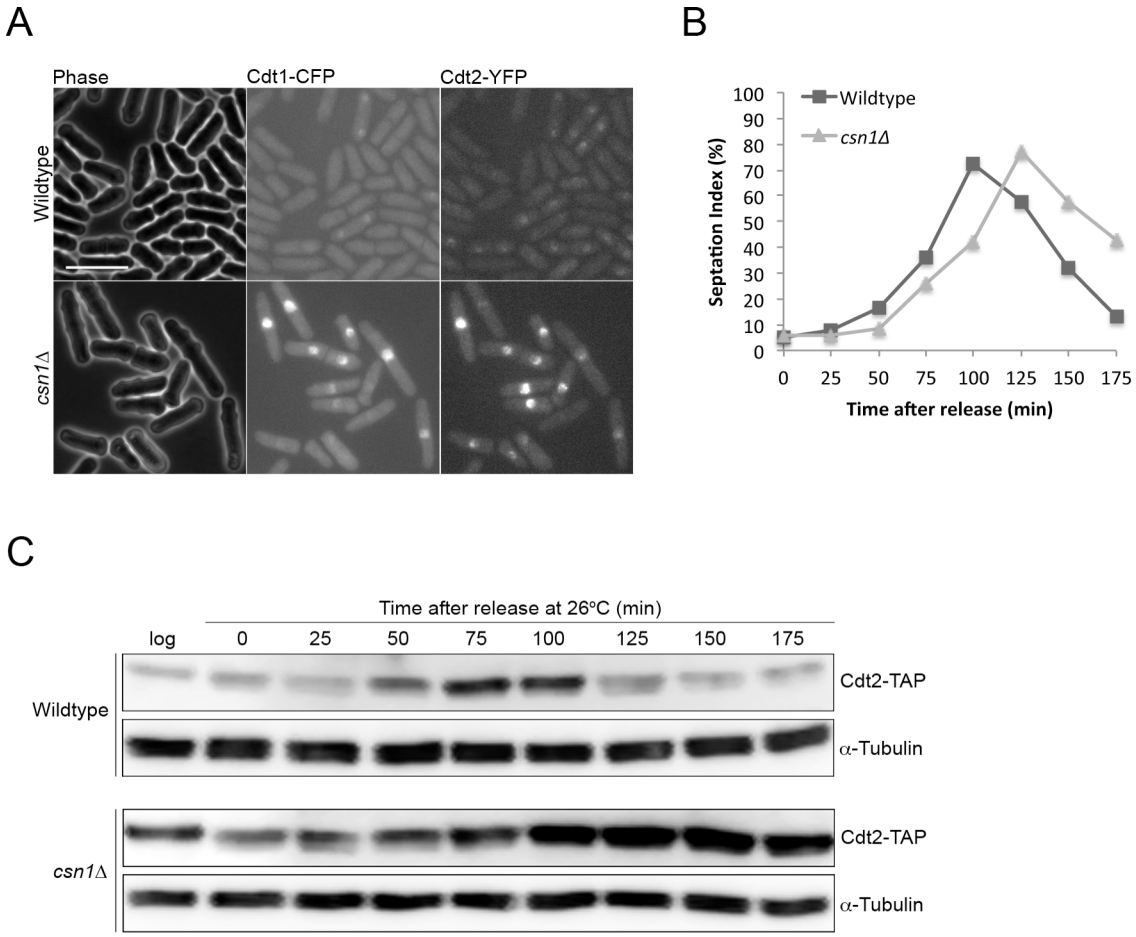


Figure 6.12 | A comparison of Cdt1 and Cdt2 levels in the *csn1*Δ mutant.
(A) Cdt1-CFP and Cdt2-YFP imaged in exponentially growing cells in wildtype (1710) and *csn1*Δ mutant (2831) strains. Scale bar: 10 μm. **(B)** Septation index to monitor the cell cycle progression of wildtype (2878) and *csn1*Δ mutant (2881) cells synchronised by *cdc25-22* block and release. **(C)** Western blot analysis of wildtype (2878) and *csn1*Δ mutant (2881) cells synchronised by *cdc25-22* block and release.

In the wildtype cells, Cdt2 levels peaked in S phase and then declined in G2 phase (Figure 6.12C), as previously reported (Yoshida et al. 2003). However, Cdt2 levels in *csn1*Δ mutant increased as the cells approached S phase and remained high throughout the rest of the time-course (Figure 6.12C), which strongly suggests that Cdt2 levels are not limiting in S phase and therefore unlikely to contribute to the inefficient degradation of Cdt1 observed in *csn1*Δ cells.

6.2.2.5 Spd1 deregulation in *csn1*Δ cells promotes an increase in Cdt2 levels

Cdt2 levels decline in HU- and CHX-treated *csn1*Δ cells, suggesting that the high Cdt2 levels in the *csn1*Δ mutant are the product of increased protein synthesis (Liu et al. 2005a). The transcription of $cdt2^{+}$ is regulated by MBF (Hofmann and Beach 1994) so it possible that Rad3-dependent activation of MBF transcription contributes to the elevated Cdt2 levels observed in the *csn1*Δ mutant. To examine this possibility, Cdt2-TAP levels were analysed in a *csn1*Δ $rad3^{ts}$ double mutant, where Rad3 could be inactivated at the restrictive temperature of 35°C (Martinho et al. 1998). After 2 hours at the restrictive temperature, Cdt2 levels in the *csn1*Δ $rad3^{ts}$ strain had declined dramatically and were comparable to wildtype levels of Cdt2, suggesting that Rad3 activity is entirely responsible for the high Cdt2 levels of *csn1*Δ cells (Figure 6.13A).

As mentioned in Section 6.2.2.3, misregulation of Spd1 contributes to checkpoint activation in the *csn1*Δ mutant. To investigate the extent to which Spd1 misregulation contributes to the Rad3-dependent increase in Cdt2 levels in the *csn1*Δ mutant, Cdt2-YFP levels in wildtype, *csn1*Δ and *csn1*Δ *spd1*Δ cells were compared (Figure 6.13B-D). Interestingly, deletion of $spd1^{+}$ largely suppressed the increased number of uninucleate cells with a nuclear Cdt2 signal observed in the single *csn1*Δ mutant

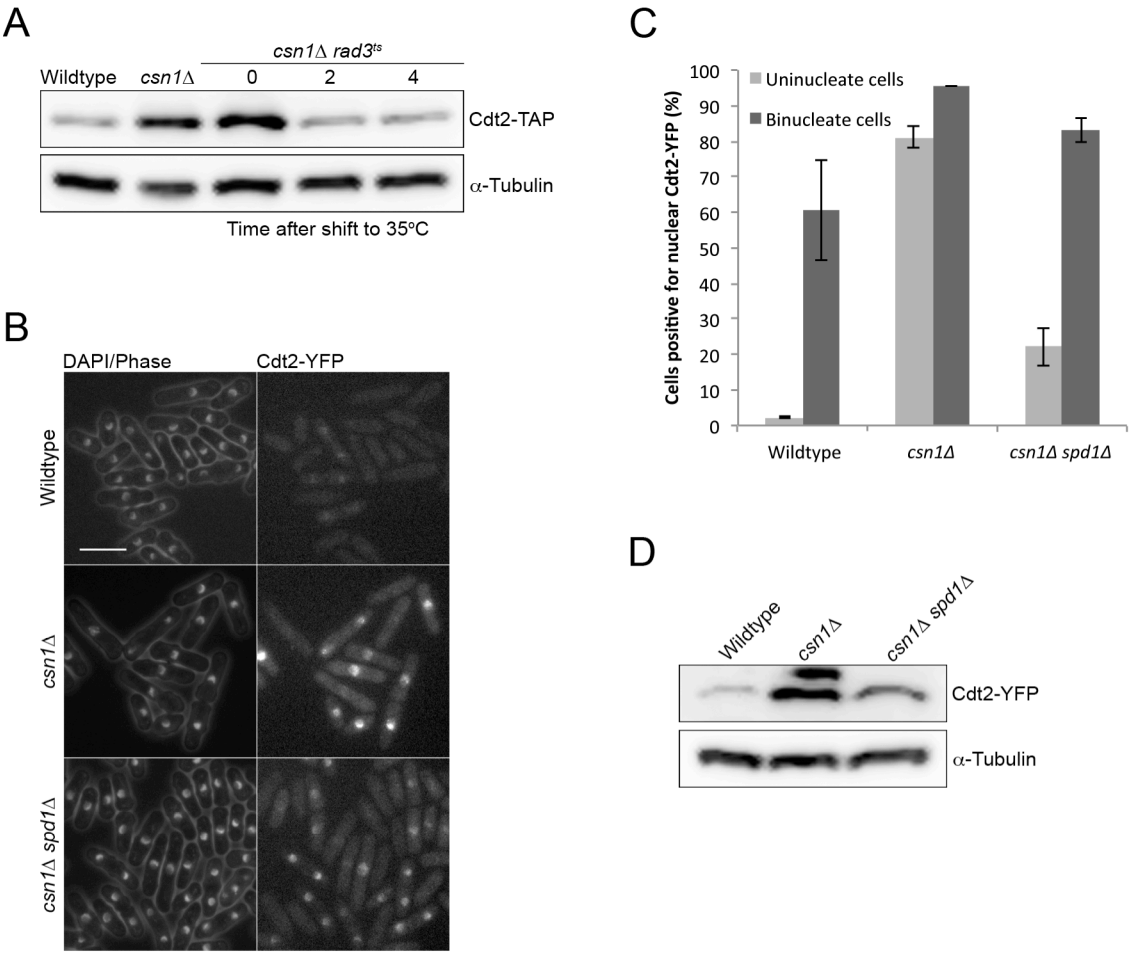


Figure 6.13 | Rad3 activity and Spd1 deregulation elevate Cdt2 levels in the *csn1*Δ mutant. **(A)** Western blot analysis of Cdt2-TAP levels in a *csn1*Δ *rad3*^{ts} (3075) mutant at 0, 2 and 4 hours after shifting cells from 26°C to the restrictive temperature of 35°C. Exponentially growing wild-type (2595) and *csn1*Δ mutant (2844) cells are shown for comparison. **(B)** Cdt2-YFP imaged in exponentially growing cells in wildtype (1698), *csn1*Δ (3071) and *csn1*Δ *spd1*Δ (3069) mutant cells. Scale bar: 10 μm. **(C)** Strains shown in (B) were analysed to determine the percentage of uninucleate and binucleate cells positive for nuclear Cdt2-YFP. At least 100 cells, from two independent experiments, were counted for each data point. Error bars: 50% of range. **(D)** Western blot analysis of Cdt2-YFP levels in wildtype (1698), *csn1*Δ (3071) and *csn1*Δ *spd1*Δ (3069) mutant cells.

(Figure 6.13B and C). Furthermore, western blot analysis indicated that Cdt2 levels were reduced in the double *csn1*Δ *spd1*Δ mutant compared to the single *csn1*Δ mutant (Figure 6.13D). This analysis suggests that Spd1 deregulation is an important contributor to the Rad3-dependent up-regulation of Cdt2 protein levels in the *csn1*Δ mutant. It is possible that deletion of *spd1*$^{+}$ in the *csn1*Δ mutant had a more pronounced impact on Cdt2 as opposed to Cdt1 levels because Cdt1 levels in the *csn1*Δ mutant were also affected by an inefficient rate of protein turnover.

6.2.3 Investigation into the regulation of Cdt2 and the effect of Cdt2 levels on CRL4^{Cdt2} activity

As the substrate recognition subunit of the CRL4^{Cdt2} complex, Cdt2 is required for the ubiquitylation and proteolysis of Cdt1 (Higa et al. 2006; Jin et al. 2006; Ralph et al. 2006). Therefore, *cdt2*$^{+}$ was identified in the screen for novel genes involved in Cdt1 regulation. The role of Cdt2 as a component of CRL4^{Cdt2} is well characterised but the mechanism of Cdt2 regulation is poorly understood. It has been established that the cell cycle transcription of *cdt2*$^{+}$ is periodical and regulated by MBF, with a peak in G1-S phase, which corresponds to an accumulation of the protein in S phase (Hofmann and Beach 1994; Yoshida et al. 2003). Cdt2 is degraded through the ubiquitin proteasome system in a manner independent of the three *S. pombe* cullin genes (*pcu1*$^{+}$, *pcu3*$^{+}$ and *pcu4*$^{+}$) (Liu et al. 2005a). The mechanism of Cdt2 proteolysis and how Cdt2 regulation affects the activity of CRL4^{Cdt2} is unclear and these questions are addressed in this section.

6.2.3.1 Cdt2 protein levels peak as Cdt1 is degraded in the mitotic cell cycle

To gain insight into the regulation of Cdt2, the kinetics of Cdt2 protein accumulation through the mitotic cell cycle were observed. It was noted that although transcription of both *cdt1*$^{+}$ and *cdt2*$^{+}$ is regulated by MBF, the two proteins accumulated in the cell cycle with similar but distinct timings. In a *cdc25-22* synchronised cell cycle, Cdt2-TAP levels accumulated later than Cdt1-TAP levels and persisted into S phase after Cdt1 levels had declined (compare wildtype panels of Figure 6.8C and Figure 6.12C).

To confirm this observation, Cdt1 and Cdt2 levels were examined in prometaphase-arrested *nda3-311* cells that were released at the permissive temperature of 32°C. The *nda3-311* cells co-expressed Cdt1-CFP and Cdt2-YFP, enabling a detailed examination of the two proteins as the cells progressed through G1 and S phase (Figure 6.14A). The septation index was used to monitor cell cycle progression and indicated that the cells entered S phase approximately 30 minutes after release (Figure 6.14B). Cdt1 levels were highest in the first 20 minutes after release and then declined as the cells entered S phase. In contrast, Cdt2 levels peaked at 40 minutes after release, when the cells had already entered S phase (Figure 6.14A and B). Therefore, the peak in Cdt2 protein levels is delayed with respect to the peak in Cdt1 levels in the mitotic cell cycle.

6.2.3.2 Cdt2 regulation is independent of CRL4^{Cdt2} substrate ubiquitylation

The S phase decline in Cdt2 levels occurred subsequent to a decline in Cdt1 levels. To address whether the relationship between substrate and Cdt2 levels was causative or simply a correlation, the turnover of Cdt2 in response to the deregulation of CRL4^{Cdt2} target proteins was analysed. Cdt2 levels were examined following overexpression of

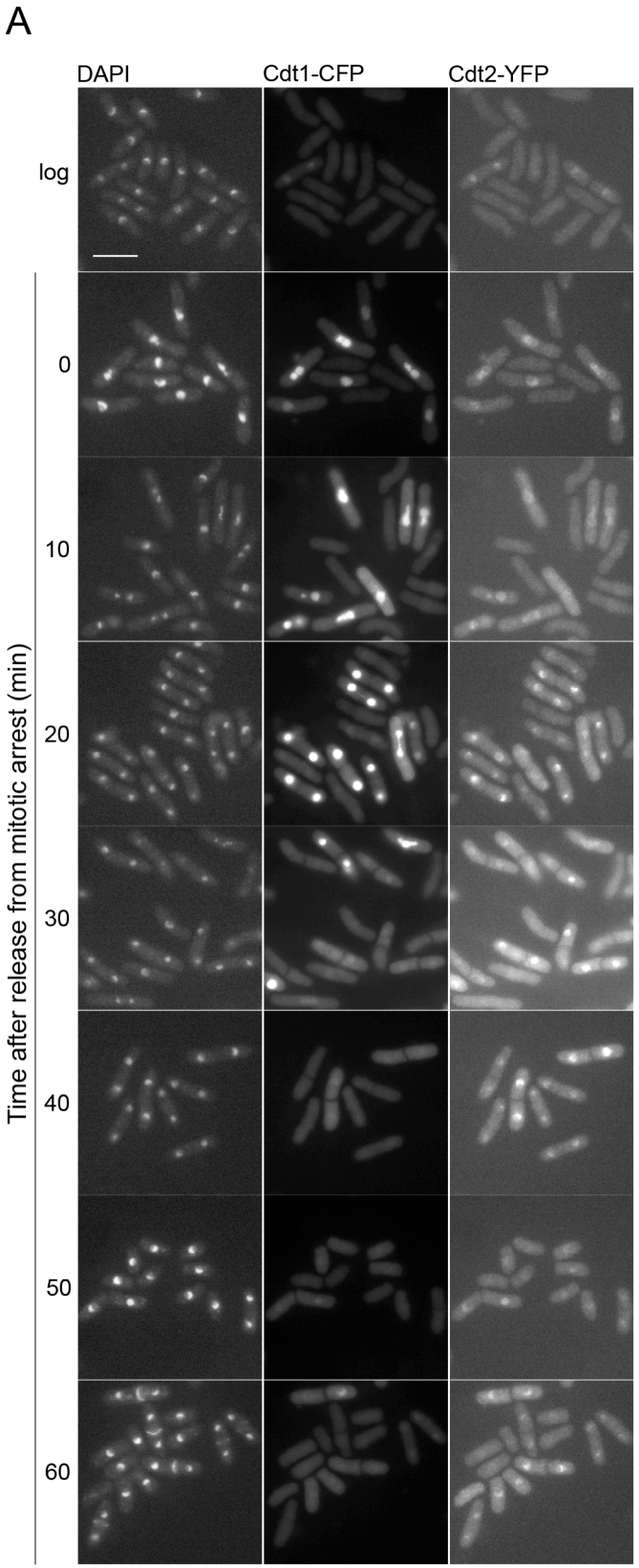


Figure 6.14 | A comparison of Cdt1 and Cdt2 levels in synchronised cells released from a mitotic arrest.
(A) Cdt1-CFP and Cdt2-YFP imaged in synchronised *nda3-311* cells (1734) released from a prometaphase arrest. Cells were incubated at 20°C for 4 hours to induce the arrest then released at 32°C. Scale bar: 10 μm **(B)** Strains shown in (A) were analysed to determine the septation index and the percentage of cells positive for nuclear Cdt1-CFP and Cdt2-YFP. At least 100 cells were counted per time-point.

Cdt1 and the half-life of Cdt2 was examined in a $PCNA^{D122A}$ mutant, where $CRL4^{Cdt2}$ substrates are stabilised due to a failure to recruit Cdt2 to the PCNA-substrate complex (Havens et al. 2012).

Cdt1-GFP was overexpressed from the *nmt1* promoter on an extra-chromosomal pREP3x plasmid in the absence of thiamine (Figure 6.15A). Cdt2 levels in the absence of thiamine were unchanged in wildtype cells, in cells overexpressing Cdt1 and in cells containing an empty pREP3x control plasmid (Figure 6.15A, -T compare lanes 2, 4 and 6). This suggests that the level of Cdt1 has no effect on Cdt2 regulation. Unexpectedly, Cdt2 levels were higher in media containing thiamine as compared to media without thiamine and the reason behind this difference is unclear (Figure 6.15A, +T vs. –T). The half-life of Cdt2 in wildtype and $PCNA^{D122A}$ cells was examined by treated asynchronous cultures with CHX and monitoring the decline in Cdt2-TAP levels. The half-life of Cdt2 in wildtype and $PCNA^{D122A}$ cells was similar, indicating that inhibition of the interaction between Cdt2 and the PCNA-substrate complex does not affect Cdt2 turnover (Figure 6.15B). Therefore, Cdt2 regulation is independent of $CRL4^{Cdt2}$ substrate levels and the recruitment of Cdt2 to PCNA.

6.2.3.3 High Cdt2 levels are necessary but not sufficient for Spd1 proteolysis

In addition to the G1-S phase transcription of $cdt2^+$ that occurs in an unperturbed cell cycle, $cdt2^+$ transcription is up-regulated in response to DNA damage in a Rad3- and Chk1-dependent manner (Liu et al. 2005a; Moss et al. 2010). In *S. pombe* cells, it has been reported that modulations in the Cdt2 protein level are directly linked to the $CRL4^{Cdt2}$-dependent proteolysis of Spd1 (Liu et al. 2005a). This is in contrast to Cdt1, where chromatin loading of PCNA represents the determining factor that stimulates

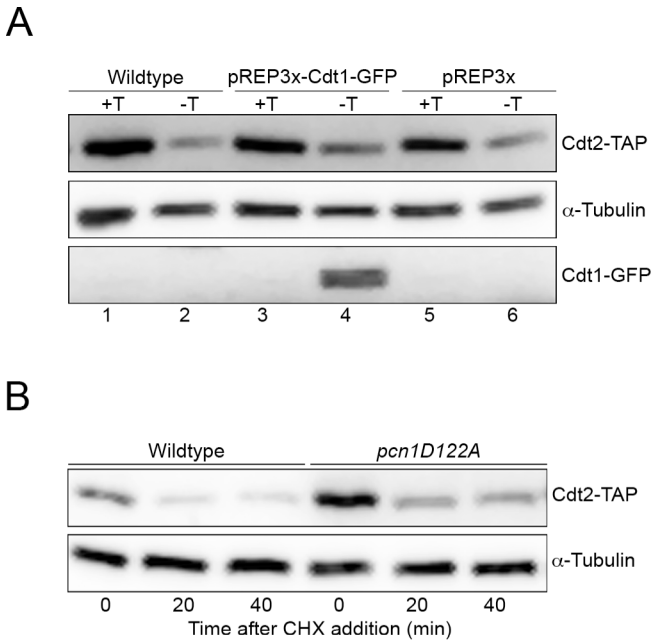


Figure 6.15 | Cdt2 regulation is independent of CRL4^{Cdt2} substrate levels.
(A) Western blot analysis of Cdt2-TAP levels in exponentially growing wildtype (2595), Cdt1-GFP overexpression (pREP3x-Cdt1-GFP; 3111) or control (pREP3x; 3113) strains, grown in either plus or minus thiamine media (+T or -T; 10 μg/ml) for 16 hours. **(B)** Western blot analysis of wildtype (2595) and PCNA^{D122A} (3101) strains following cycloheximide (CHX; 100 μg/ml) treatment.

$CRL4^{Cdt2}$-dependent proteolysis (Guarino et al. 2011). The profile of Spd1 proteolysis correlates with the peaks in Cdt2 protein levels; Spd1 is degraded in S phase and after DNA damage, enabling the cell to stimulate dNTP production for replication and repair purposes (Liu et al. 2003; Moss et al. 2010). Although Spd1 proteolysis in S phase is checkpoint independent, in response to DNA damage in G2-synchronised cells, it becomes Rad3- and Chk1-dependent (Liu et al. 2003). Given Rad3-dependent checkpoint activation in DNA-damaged G2 phase cells is required both to increase Cdt2 protein levels and for Spd1 proteolysis, it is unclear whether the checkpoint plays an additional role in Spd1 proteolysis beyond simply elevating Cdt2 levels. This question was addressed by examining Spd1 proteolysis in response to DNA damage in a *yox1*Δ mutant. Yox1 is a negative regulator of MBF and confines MBF-dependent transcription to the G1-S phase of the cell cycle (Aligianni et al. 2009). Deletion of $yox1^{+}$ results in constitutive expression of MBF target genes, as noted in the *S. pombe* deletion library screen in relation to Cdt1 levels (Table 5.2 and Figure 5.7). In a *yox1*Δ background, $cdt2^{+}$ was constitutively expressed and the protein accumulated to a high level, independent of checkpoint activation (Figure 6.16A).

Asynchronous exponentially growing cells were treated with the alkylating agent MMS to induce DNA damage and the proteolysis of Spd1-TAP was monitored by western blot analysis. In a $yox1^{+}$ background, Spd1 proteolysis in response to DNA damage was Rad3 dependent (Figure 6.16B). In *yox1*Δ cells, Spd1 was efficiently degraded after DNA damage but this degradation was no longer Rad3 dependent; the rate of Spd1 degradation in *yox1*Δ *rad3*Δ cells was indistinguishable from wildtype (Figure 6.16C). This suggests that the sole function of the Rad3-dependent checkpoint

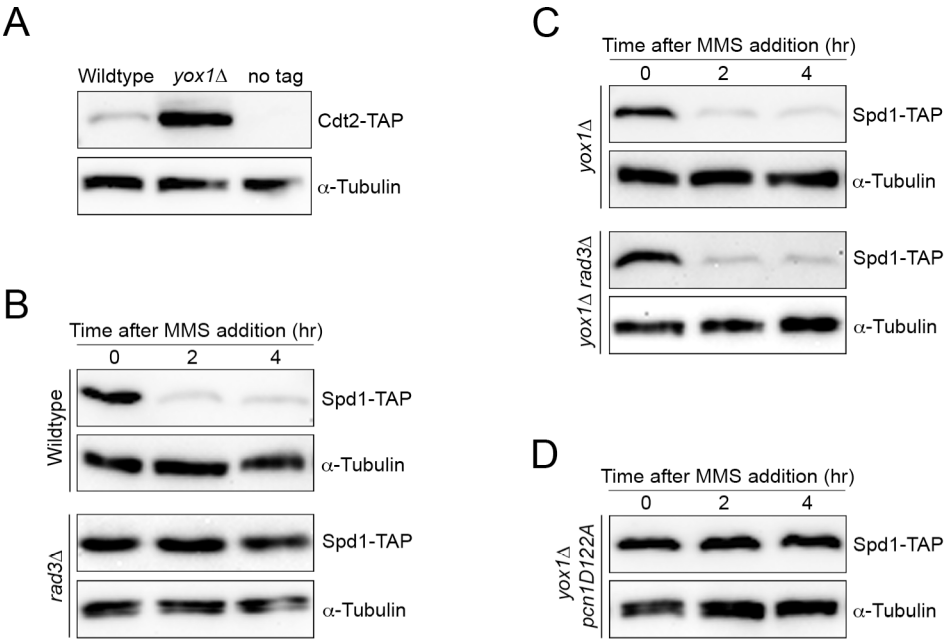


Figure 6.16 | High Cdt2 levels are necessary but not sufficient for Spd1 proteolysis.
(A) Western blot analysis to compare Cdt2-TAP levels in exponentially growing wildtype (2704) and *yox1*Δ mutant (2698) cells. **(B)** Western blot analysis of Spd1-TAP levels in wildtype (1766) and *rad3*Δ mutant (2658) strains after 0.2% MMS treatment. **(C)** Western blot analysis of Spd1-TAP levels in *yox1*Δ (2711) and *yox1*Δ *rad3*Δ (2713) mutant strains after 0.2% MMS treatment. **(D)** Western blot analysis of Spd1-TAP levels in *yox1*Δ *pcn1D122A* mutant (2755) cells after 0.2% MMS treatment. MMS: methyl methanesulfonate.

in the DNA damage-dependent proteolysis of Spd1 is to maintain adequate Cdt2 levels.

Cdt2 protein abundance has been cited as a key step in activating $CRL4^{Cdt2}$-dependent Spd1 proteolysis (Liu et al. 2005a). This is in contrast to other $CRL4^{Cdt2}$ substrates (such as Cdt1, p21 and Set8) where an interaction between the substrate and chromatin-bound PCNA is required for recruitment of $CRL4^{Cdt2}$ and proteolysis of the substrate (reviewed in Havens and Walter 2011). To investigate whether high Cdt2 levels were sufficient to induce Spd1 proteolysis, or whether PCNA played a role in the process, Spd1 degradation was examined in a *yox1*Δ *pcn1D122A* background, where recruitment of $CRL4^{Cdt2}$ to PCNA is impaired (Havens et al. 2012). In response to DNA damage, Spd1-TAP was not degraded in *yox1*Δ *pcn1D122A* cells (Figure 6.16D), suggesting that high Cdt2 levels alone are not sufficient for Spd1 degradation and that PCNA has an important role in the process. A requirement for PCNA in Spd1 regulation is interesting as provides a direct link between DNA synthesis and RNR regulation (Salguero et al. 2012).

6.3 DISCUSSION

In this chapter, three areas of research were addressed; the up-regulation of Cdt1 in HR-deficient strains, the role of CSN in promoting $CRL4^{Cdt2}$ activity and finally, the regulation of Cdt2 levels and their effect on $CRL4^{Cdt2}$ activity. The findings from each area of research, together with the outstanding questions that require further work, are discussed below.

6.3.1 The relationship between HR, cell cycle progression, checkpoint activation and Cdt1 regulation in fission yeast cells

Section 6.2.1 addressed the relationship between DNA repair, cell cycle progression, checkpoint activation and Cdt1 regulation in *S. pombe*. Deletion of genes involved in the process of HR, including *rad32*$^+$, *ctp1*$^+$, *exo1*$^+$, *rhp51*$^+$, *rhp55*$^+$, *rhp57*$^+$ and *rhp54*$^+$ resulted in an elevation of Cdt1 levels. Strikingly, the HR-deficient mutants exhibited elongated uninucleate cells with an intense nuclear Cdt1 signal. The accumulation of elongated cells with a strong Cdt1 signal was dependent on the master checkpoint regulator protein Rad3. It is likely that the up-regulation of Cdt1 in HR-deficient mutants results from checkpoint activation of MBF-dependent *cdt1*$^+$ transcription. Outstanding questions, including the specific checkpoint pathway activated in the HR mutants, how MBF-dependent gene transcription is regulated in response to an impaired HR pathway, and whether Cdt1 up-regulation in the HR mutants is biologically significant, are considered in this section.

Checkpoint activation in the HR-deficient mutants is proposed to result from the role of HR in the repair of replication-associated DNA damage. There is strong evidence from vertebrate cells that HR is required for normal cell cycle progression (Sonoda et al. 1998). In addition, agents that stall or result in the collapse of replication forks have been shown to induce HR in mammalian cells and impairment of the HR process increases the sensitivity of cells to replication inhibitors (Arnaudeau et al. 2001; Lundin et al. 2003). Obstacles on the DNA template that impede replication fork progression can cause replication forks to stall or collapse. These obstacles include: DNA lesions (caused by exogenous or endogenous DNA damage), chemical alteration of the DNA, secondary structure, DNA-bound proteins or transcriptional

machinery (Jones and Petermann 2012). A stalled replication fork is defined as one that can resume replication once the replication fork barrier has been removed, while a collapsed replication fork is defined as one that has been inactivated and experiences dissociation of replisome components (Lambert et al. 2007; Jones and Petermann 2012).

In mammalian cells, Rad51 is implicated both in the restart of stalled replication forks and in the repair of collapsed replication forks, caused by either a short or a prolonged exposure to HU respectively (Petermann et al. 2010). Long tract HR repair was shown to be associated specifically with the repair of collapsed replication forks (Petermann et al. 2010). HR is also implicated in the repair of replication-associated DNA damage in yeast (reviewed in Lambert et al. 2007). In fission yeast, spontaneous Rad22 foci formation in late S/G2 phase cells is proposed to represent sites of post-replicative repair (Meister et al. 2003). Furthermore, analysis of a site-specific replication fork barrier provides evidence that Rad22 is recruited to, and recombination is initiated at, a site of replication fork stalling at a euchromatic locus in *S. pombe* (Lambert et al. 2005). Cell viability was decreased in response to fork stalling at this site-specific replication fork barrier in the absence of the HR proteins Rhp51 and Rad50 (Lambert et al. 2005). This suggests that HR provides a mechanism by which fission yeast cells can overcome replication fork stalling.

The accumulation of elongated uninucleate cells with an intense nuclear Cdt1 signal occurred post-S phase in synchronised *rhp51*Δ and *rhp55*Δ cells and was dependent on Rad3 activity. Combined with a previous report indicating that elongated uninucleate *rhp51*Δ cells are predominantly in G2 phase (Kim et al. 2001), this is

consistent with the elongated uninucleate cell population of *rhp51*Δ and *rhp55*Δ strains representing G2-arrested cells. In *S. pombe*, Rad3 mediates both the DNA damage and the DNA replication checkpoint through phosphorylation and activation of Chk1 and Cds1 respectively (reviewed in Humphrey 2000; Melo and Toczyski 2002). Chk1 is activated in response to DNA damage in late S/G2 phase and activates the DNA damage checkpoint (Walworth et al. 1993; Walworth and Bernards 1996; Martinho et al. 1998). Cds1 is specifically activated in S phase in response to replication stress or DNA damage and is in involved in activation of the DNA replication and the intra-S phase checkpoint (Lindsay et al. 1998; Rhind and Russell 1998). Chk1 and Cds1 can both prevent cell cycle progression by arresting cells at the G2/M phase transition through inhibition of Cdc2, the fission yeast CDK required for entry into mitosis (reviewed in Rhind and Russell 2000). Therefore, either Chk1 or Cds1 activity could be responsible for the G2 delay observed in the HR mutants. It would be interesting to examine the phosphorylation status of Chk1 and Cds1 in a synchronised cell cycle of an HR mutant to gain insight into the activation kinetics of each effector kinase and how these correlate with the up-regulation of Cdt1.

In addition to the up-regulation of Cdt1, *rhp51*Δ and *rhp55*Δ mutants also exhibited an increased percentage of uninucleate cells with a nuclear Cdt2 or Cdc18 signal. Given *cdt1*$^{+}$, *cdt2*$^{+}$ and *cdc18*$^{+}$ are all targets of the MBF transcription factor complex it seems likely that alterations to the regulation of MBF-dependent transcription contribute to the up-regulation of Cdt1 observed in the HR mutants. Consistent with the accumulation of uninucleate cells with an intense Cdt1 signal in the *rhp51*Δ and *rhp55*Δ mutants being Rad3 dependent, Rad3-mediated checkpoint activation is proposed to up-regulate MBF-dependent transcription outside of the G1/S phase

transition (Watson et al. 2004; de Bruin et al. 2008). In response to replication stress in S phase, Cds1 is activated and phosphorylates multiple proteins, including Cdc10, Nrm1, Yox1 and Ste9 to maintain MBF-dependent transcription (de Bruin et al. 2008; Dutta et al. 2008; Chu et al. 2009; Caetano et al. 2011). The timely de-repression of the MBF-dependent transcription programme in S phase is an important component of the cellular response to replication stress (de Bruin et al. 2008; Caetano et al. 2011). In response to ionising radiation in G2-synchronised cells, MBF-dependent transcription is also up-regulated and this is proposed to be checkpoint dependent (Watson et al. 2004). To investigate further the contribution of MBF-dependent transcription to Cdt1 up-regulation in the HR mutants and how this is regulated by the DNA integrity checkpoints, it would be of interest to measure *cdt1*$^{+}$ mRNA transcript levels by RT-qPCR in wildtype and *rhp51*Δ cells and in *rhp51*Δ *chk1*Δ and *rhp51*Δ *cds1*Δ double mutants.

Interestingly, although *rhp51*Δ and *rhp55*Δ cells exhibited an increased percentage of uninucleate cells with a nuclear Cdt2 or Cdc18 signal, the overall level of each protein as measured by western blot was not significantly elevated in the HR mutants as compared to wildtype. In contrast, Cdt1 levels were notably higher in the HR mutants as compared to wildtype. This discrepancy between Cdt1 and Cdt2/Cdc18 levels in the HR mutants could reflect a difference in the rate of transcription of each gene and/or a difference in the rate of protein turnover.

There are reported differences in the induction and rate of transcription of MBF target genes (Watson et al. 2004). Therefore, although the same transcription factor complex regulates *cdt1*$^{+}$, *cdt2*$^{+}$ and *cdc18*$^{+}$, it does not necessarily follow that the rate of

transcription of each gene is identical. MBF binds to MCB motifs that are present in the promoters of its target genes (Lowndes et al. 1992; Maqbool et al. 2003). Analysis of the *cdc22* promoter (*cdc22*$^{+}$ is also an MBF target gene) indicates that it contains a complex pattern of MCB motifs, which are organised into two clusters each containing four motifs (Maqbool et al. 2003). The two MCB clusters have distinct roles in promoting *cdc22*$^{+}$ transcription at the G1/S phase transition (Maqbool et al. 2003). Interestingly, *cdt1*$^{+}$, *cdt2*$^{+}$ and *cdc18*$^{+}$ are also reported to have complex arrays of MCB motifs in their promoters (Maqbool et al. 2003). It is possible that these MCB motifs permit the fine-tuning of *cdt1*$^{+}$, *cdt2*$^{+}$ and *cdc18*$^{+}$ transcription by MBF during the cell cycle and in response to genotoxic stress.

The degree to which Cdt1, Cdt2 and Cdc18 accumulate in the HR mutants will also depend on the rate of proteolysis of each protein. It has been demonstrated that Cdt2 is degraded through the ubiquitin proteasome system at all stages of the cell cycle (Liu et al. 2005a) and this may preclude the protein accumulating to a high level in the G2-arrested HR-deficient cells. In an unperturbed cell cycle, Cdc18 is phosphorylated at the onset of S phase by the CDK Cdc2, which stimulates its ubiquitylation by $SCF^{Pop1/Pop2}$ and subsequent proteolysis by the 26S proteasome (Jallepalli et al. 1997; Kominami and Toda 1997; Jallepalli et al. 1998). In HU-treated cells, however, Rad3-dependent checkpoint activation results in inhibitory phosphorylation of Cdc2 and an accumulation of Cdc18 (Hermand and Nurse 2007). Given that the activity of Cdc2 is inhibited by the DNA integrity checkpoint to delay the onset of mitosis, it seems unlikely that Cdc18 will be subject to a high rate of proteolysis in the G2-arrested HR-deficient cells. Therefore, level of Cdc18 that

accumulated in the *rhp55*Δ mutant may directly reflect the rate of *cdc18*$^{+}$ transcription.

Cdt1 proteolysis is dependent on chromatin-bound PCNA and is not active in G2 cells during an unperturbed cell cycle (Guarino et al. 2011). It is unclear if the DNA damage that activates Rad3 in the HR mutants would result in PCNA loading onto DNA and Cdt1 proteolysis. To address this point, the chromatin-loading of PCNA in the elongated uninucleate cells of an *rhp51*Δ mutant could be assessed using a chromatin binding assay (Kearsey et al. 2005). The occurrence of Cdt1 proteolysis in the G2-arrested HR-deficient cells could be addressed using quantitative fluorescence microscopy. Treatment of *rhp51*Δ cells with CHX would inhibit *de novo* protein synthesis and changes in Cdt1 protein levels in the G2-arrested *rhp51*Δ cells, which would be attributable to proteolysis, could be measured by quantitating the nuclear Cdt1-YFP fluorescence signal in the elongated uninucleate *rhp51*Δ cells (Wu and Pollard 2005).

The specific up-regulation of Cdt1 in the HR mutants is intriguing. Perhaps the most important question that arises from this work is whether this up-regulation of Cdt1 is biologically significant or simply the coincident by-product of a defect in cell cycle progression. Interestingly, a role for Cdt1 in DNA repair pathways of human and *S. cerevisiae* cells has been proposed. Microscopy observations of the kinetics of Cdt1 recruitment to sites of laser-induced DNA damage in human cells indicated that there is a delay between Cdt1 recruitment and proteolysis, leading to speculation that Cdt1 may serve a specific role at the DNA damage site (Roukos et al. 2011). Analysis of the factors required for the HR pathway of BIR in *S. cerevisiae* demonstrated that

Cdt1 but not Cdc6 or ORC were essential for this repair pathway (Lydeard et al. 2010). It was suggested that Cdt1 might function to load the Mcm2-7 complex onto the BIR template DNA (Lydeard et al. 2010). If Cdt1 served a role in DNA repair in *S. pombe*, its up-regulation in the HR mutants might reflect an active role played by the protein in the repair of replication-associated DNA damage. It would be extremely interesting to analyse the kinetics of DNA repair in G2-synchronised cells by pulsed field gel electrophoresis (PFGE), following DNA damage induction in wildtype cells and in cells where Cdt1 had been inactivated, for example using a temperature-sensitive mutation.

6.3.2 CSN function promotes efficient CRL4^{Cdt2}-dependent Cdt1 proteolysis

Section 6.2.2 addressed the extent and mechanism by which the CRL4^{Cdt2}-dependent proteolysis of Cdt1 was affected by deletion of the CSN component *csn1*$^{+}$. It was established that Cdt1 proteolysis was not abolished in *csn1*Δ cells but occurred at an inefficient rate as compared to wildtype. CHX treatment indicated that *de novo* Cdt1 synthesis contributed to the elevated level of Cdt1 observed in the *csn1*Δ mutant. Rad3 activity may promote Cdt1 synthesis in the *csn1*Δ mutant via stimulation of MBF-dependent transcription. In contrast to human cells, adaptor instability of Cdt2 is unlikely to explain the inhibition of CRL4^{Cdt2} function observed in fission yeast *csn1*Δ cells (Raman et al. 2011). Fission yeast *csn1*Δ cells exhibited high Cdt2 levels, which were largely the result of the Spd1 deregulation and Rad3 activation that occur following inhibition of CSN function (Mundt et al. 1999; Liu et al. 2003).

Given CSN function is not required to maintain the stability of Cdt2, it is unclear why the loss of CSN function inhibits CRL4^{Cdt2} activity in *S. pombe* (this study and Liu et

al. 2003). Deletion of *csn1*$^{+}$ has been shown to alter the neddylation status of Pcu4, the cullin subunit of CRL4^{Cdt2}, in fission yeast cells. In wildtype cells, Pcu4 is present in both neddylated and unneddylated states but in a *csn1*Δ mutant, Pcu4 accumulates exclusively in the neddylated form (Osaka et al. 2000; Liu et al. 2003). It is therefore possible that the deneddylation function of CSN is important to promote CRL4^{Cdt2} activity. CRLs cycle between unneddylated (inactive) and neddylated (active) states, through the activity of the Nedd8-conjugating enzyme Ubc12 and the CSN complex (Figure 6.17). CRL activation cycles are thought to be important for optimum CRL function in eukaryotic cells (reviewed in Bosu and Kipreos 2008). Dynamic cycling is proposed to promote CRL stability and SRS interchange and may mediate direct effects on CRL activity (Bosu and Kipreos 2008). It is possible that the global effect that loss of CSN function has on the dynamic activation cycles of CRLs underlies the inhibition of CRL4^{Cdt2} function in fission yeast *csn1*Δ cells.

CRLs constitute a large subfamily of E3 ubiquitin ligases; bioinformatics analysis of genes encoding potential CRL SRSs predict that over 200 distinct CRL complexes may assemble in human cells (reviewed in Sarikas et al. 2011). Through targeting an extensive range of protein substrates, CRLs impact on numerous biological processes. These include the control of DNA replication, DNA repair and cell cycle progression; processes that when misregulated can contribute to carcinogenesis (Sarikas et al. 2011). The regulation of CRL activity is emerging as a target for rational drug design with the development of MLN4924, a small molecule inhibitor of Nedd8-activating enzyme (NAE) (Soucy et al. 2009). MLN4924 selectively inhibits CRL-dependent protein turnover and stimulates human tumour cell apoptosis through the deregulation of DNA replication in S phase (Soucy et al. 2009). The NAE inhibitor has entered

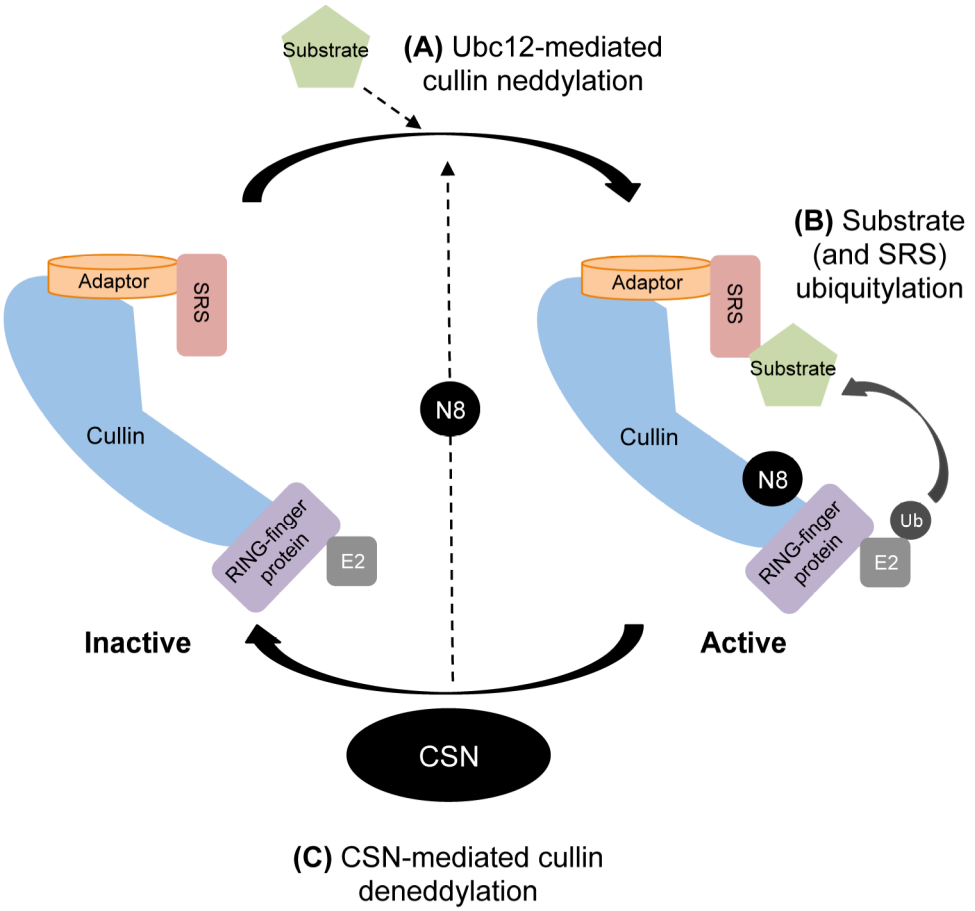


Figure 6.17 | A schematic of the CRL activation cycle.
(A) Cullin-RING E3 ubiquitin ligases are activated following substrate-induced neddylation of the cullin subunit. **(B)** The active (neddylated) CRL ubiquitylates its substrate and in some instances may autoubiquitylate the substrate recognition subunit (SRS), resulting in SRS proteolysis and a reduction in CRL activity. **(C)** CSN-mediated cullin deneddylation, in conjunction with the CSN-associated deubiquitylation activity of Ubp12, results in CRL inactivation. Inhibition of CRL function may be important for the maintenance and *de novo* assembly of CRL complexes. Note that unneddylated CRL core complexes can be bound by CAND1, which may promote continuous and rapid SRS exchange. Ub: ubiquitin; N8: Nedd8. Adapted from Zhou et al. (2003); Schmidt et al. (2009).

clinical trials following its ability to suppress tumour xenograph growth in animal models (Soucy et al. 2009). Therefore, a detailed understanding of the regulation of CRL activation cycles and their impact on overall CRL function represents an important topic of research, which may present new targets for the development of cancer therapies.

6.3.3 The regulation of Cdt2 levels and their effect on CRL4^{Cdt2} activity

The regulation of Cdt2 levels in the mitotic cell cycle was briefly addressed in Section 6.2.3. As previously reported, Cdt2 accumulated in S phase (Yoshida et al. 2003) and a comparison of the kinetics of Cdt2 and Cdt1 accumulation indicated that the peak in Cdt2 levels occurred subsequent to the peak in Cdt1 levels. This observation is consistent with a requirement for Cdt2 in the CRL4^{Cdt2}-dependent proteolysis of Cdt1 (Ralph et al. 2006). Despite the close correlation between changes in Cdt1 and Cdt2 protein levels in the mitotic cell cycle, no evidence was found to support the notion that CRL4^{Cdt2} substrate levels affect Cdt2 regulation.

Turnover of Cdt2 has been demonstrated to occur in S phase and G2 phase cells (Liu et al. 2005a). If the turnover of Cdt2 is constant through the cell cycle then the accumulation of Cdt2 in S phase may directly reflect the rate of MBF-dependent *cdt2*$^+$ transcription (Yoshida et al. 2003; Liu et al. 2005a). It is interesting that although *cdt1*$^+$ and *cdt2*$^+$ are both MBF targets (Hofmann and Beach 1994), the Cdt1 and Cdt2 proteins accumulate with distinct kinetics in the mitotic cell cycle. This may reflect differences in the induction and rate of MBF-dependent *cdt1*$^+$ and *cdt2*$^+$ transcription at the G1/S phase transition, possibly mediated through the complex

arrays of MCB motifs in the promoter of each gene, as discussed in Section 6.3.1 (Maqbool et al. 2003).

Cdt2 is an unstable protein that is degraded through the ubiquitin proteasome system (Liu et al. 2005a). However, the identity of the E3 ubiquitin ligase that mediates Cdt2 ubiquitylation in *S. pombe* is unknown. E3 ubiquitin ligases are classified into three families based on whether they contain a HECT (*h*omologous to *E*6-AP *C*-*t*erminus), RING-finger or U-box domain (reviewed in Robinson and Ardley 2004; Deshaies and Joazeiro 2009). In *S. pombe*, Cdt2 turnover is independent of the CRLs, which form a subfamily of the RING-finger E3 ubiquitin ligases (Liu et al. 2005a; Sarikas et al. 2011). Interestingly, 83 *S. pombe* genes have the GO annotation of ubiquitin-protein ligase activity (GO:0004842) as the associated molecular function of their gene product (Aslett and Wood 2006; Wood et al. 2012). Given analysis of Cdt2-interacting proteins has not shed light on the mechanism of Cdt2 ubiquitylation (Liu et al. 2005a), an alternative method to investigate Cdt2 turnover might be to screen genetic backgrounds, where genes with ubiquitin-protein ligase activity had been deleted or inactivated, for increased stability of the Cdt2 protein.

The extent to which Cdt2 levels regulate the $CRL4^{Cdt2}$-dependent proteolysis of Spd1 was considered in Section 6.2.3.3. Cdt2 protein abundance has been cited as a key step in activating $CRL4^{Cdt2}$-dependent Spd1 proteolysis (Liu et al. 2005a). However, it was demonstrated in Section 6.2.3.3 that although high Cdt2 levels are necessary for Spd1 proteolysis, they are not sufficient. A key role for PCNA in activating $CRL4^{Cdt2}$-dependent Spd1 proteolysis was identified. The high Cdt2 levels required for Spd1 proteolysis are achieved in S phase through the MBF-dependent G1/S phase

transition transcription programme; and through the Rad3-dependent checkpoint in response to DNA damage outside of S phase. This explains the observation that the Rad3-dependent checkpoint is essential for Spd1 proteolysis following DNA damage in G2 phase cells, but not in S phase cells (Liu et al. 2003). This work has contributed to a publication (Salguero et al. 2012) that describes a key role for chromatin-bound PCNA in $CRL4^{Cdt2}$-dependent Spd1 proteolysis. This finding is consistent with the PCNA-substrate interaction representing a common and central feature of $CRL4^{Cdt2}$-dependent ubiquitylation, both in fission yeast and in higher eukaryotes (reviewed in Havens and Walter 2011).

6.4 CONCLUSIONS

The conclusions drawn from each of the three areas of research are considered in turn. First, Cdt1 up-regulation in the HR mutants is Rad3 dependent and is expected to reflect checkpoint-mediated activation of MBF-dependent transcription in G2-arrested cells. Cdt1 levels are specifically elevated in HR-deficient cells with respect to Cdt2 and Cdc18 levels, and it remains to be determined whether this up-regulation is biologically significant. Second, the elevated level of Cdt1 in the *csn1*Δ mutant is the result of an increased rate of Cdt1 synthesis and inefficient $CRL4^{Cdt2}$-dependent Cdt1 proteolysis. It is possible that CSN function is required for efficient $CRL4^{Cdt2}$ activity because of its role in promoting dynamic CRL activation cycles. Third, although the mechanism of Cdt2 proteolysis remains elusive, Cdt2 turnover is not dependent on $CRL4^{Cdt2}$ substrate levels. Investigation into the role of Cdt2 levels in the activation of $CRL4^{Cdt2}$-dependent Spd1 proteolysis identifies a key role for PCNA in this process.

CHAPTER 7

Conclusions and Further Work

7.1 PRINCIPAL CONCLUSIONS

This study investigated the mechanism of the Cdt1-PCNA interaction in *S. pombe* and the extent to which it regulates the $CRL4^{Cdt2}$-dependent proteolysis of Cdt1 in S phase and after DNA damage. In addition, the study employed a genomics approach to identify novel genes involved in Cdt1 regulation in *S. pombe*. Two variant PIP degrons have been identified in *S. pombe* Cdt1, which function near-redundantly to promote the Cdt1-PCNA interaction and the $CRL4^{Cdt2}$-dependent proteolysis of Cdt1 in S phase and after DNA damage. The mutational analysis of the $cdt1^+$ sequence, which resulted in the identification of these dual PIP degrons, also led to the characterisation of two in-frame AUG codons in the $cdt1^+$ ORF. The second of these AUG codons was shown to be required to maintain wildtype Cdt1 protein levels and cell viability. A screen of an *S. pombe* haploid deletion library resulted in the identification of 17 candidate genes that exhibited an up-regulation of Cdt1. Further characterisation of a subset of these genes demonstrated that a Rad3-dependent up-regulation of Cdt1 could be observed in a range of HR-deficient strains. This study has also identified opportunities for further work, which are discussed below and concern the role of PCNA in the $CRL4^{Cdt2}$ ubiquitylation pathway and the biological significance of Cdt1 regulation in response to DNA damage.

7.2 PCNA IS A CENTRAL COMPONENT OF THE CRL4^{CDT2} UBIQUITYLATION PATHWAY

The mutational analysis presented in Chapter 4 demonstrates that *S. pombe* Cdt1 contains two variant PIP degrons, which mediate a robust Cdt1-PCNA interaction and are required for the CRL4^{Cdt2}-dependent down-regulation of Cdt1 in S phase and after DNA damage. Although the dual PIP degrons in *S. pombe* Cdt1 contain fewer conserved sequence elements than the single PIP degrons identified in *Xenopus* and human Cdt1 (Havens and Walter 2009; Michishita et al. 2011), the analysis presented here emphasises the conserved involvement of a PIP degron sequence in CRL4^{Cdt2}-dependent Cdt1 regulation. It is possible that dual PIP degrons are employed in *S. pombe* Cdt1 to compensate for their variant nature and ensure a robust Cdt1-PCNA interaction. A robust Cdt1-PCNA interaction that promotes CRL4^{Cdt2}-dependent Cdt1 proteolysis might be particularly important in *S. pombe*, as additional Cdt1 regulatory mechanisms based on SCF^{Skp2} ubiquitylation or geminin inhibition are not present in this organism.

PCNA is emerging as a universal component of the CRL4^{Cdt2}-mediated ubiquitylation pathway in fission yeast and higher eukaryotes (reviewed in Abbas and Dutta 2011; Havens and Walter 2011). Work presented in Chapter 6 confirms the involvement of PCNA in the CRL4^{Cdt2}-mediated regulation of Spd1 in fission yeast. Additional studies from our group point to a conserved requirement for chromatin-bound PCNA in *S. pombe* CRL4^{Cdt2}-dependent substrate proteolysis (Guarino et al. 2011; Salguero et al. 2012). A major outstanding question in the field is why only chromatin-bound PCNA stimulates CRL4^{Cdt2} ubiquitylation? This question was addressed in Chapter 5 and it was hoped that the *S. pombe* deletion library screen might provide data relevant

to the subject. However, no candidate genes that held an obvious explanation for the dependence of Cdt1 proteolysis on chromatin-bound PCNA were identified in the screen. Subsequent versions of the *S. pombe* deletion library contain a more complete coverage of the non-essential *S. pombe* genes and it would be useful, as part of a further study, to examine these additional strains for up-regulation of Cdt1. Alternatively, a different screen could be devised to investigate the role of chromatin-bound PCNA in $CRL4^{Cdt2}$ ubiquitylation. For example, PCNA mutants could be generated and screened for Cdt1 up-regulation, using the fluorescence-based screening protocol developed in Chapter 5. This screen may identify PCNA mutants that provide insight into the dependence of $CRL4^{Cdt2}$ activity on chromatin-bound PCNA.

The regulation of $CRL4^{Cdt2}$ activity, whether through chromatin-bound PCNA or by the CSN complex, is poorly understood. It is well established that CSN interacts with $CRL4^{Cdt2}$ and promotes its activity, but precisely how CSN achieves this in *S. pombe* is unclear (Liu et al. 2003; Liu et al. 2005a). For example, it is uncertain whether CSN regulates $CRL4^{Cdt2}$ activity through its effect on CRL activation cycles or whether it has a more direct role in stimulating $CRL4^{Cdt2}$ function. To obtain a more complete understanding of the mechanism of $CRL4^{Cdt2}$ and the role of DNA and additional proteins in the process, one could attempt to reconstitute $CRL4^{Cdt2}$-dependent ubiquitylation of a substrate *in vitro*, using purified proteins. This would enable a number of questions to be addressed directly, such as are additional proteins required for chromatin-bound PCNA to stimulate $CRL4^{Cdt2}$ activity? It would also be of interest to compile a more complete catalogue of $CRL4^{Cdt2}$ substrates. This could be achieved systematically in *S. pombe* by using bioinformatics to identify proteins that

contain a match to the variant PIP degron sequence. Candidate proteins could then be verified as $CRL4^{Cdt2}$ targets experimentally, for example by investigating whether they are stabilised in a *cdt2*Δ mutant. Given that Cul4a and Cdt2 misregulation in humans has been linked with oncogenesis (reviewed in Abbas and Dutta 2011; Lee and Zhou 2012), it is hoped that expanding our understanding of $CRL4^{Cdt2}$ activity will provide insight into the mechanism of $CRL4^{Cdt2}$ in human disease and perhaps help to identify novel therapeutic targets.

7.3 THE BIOLOGICAL SIGNIFICANCE OF CDT1 REGULATION IN RESPONSE TO DNA DAMAGE

Chapter 4 highlights an additional outstanding question in the field, which pertains to the biological significance of Cdt1 proteolysis after DNA damage. As discussed in Section 4.3.3, one possibility is that Cdt1 proteolysis is important to improve the accessibility of repair factors to PCNA at the DNA damage site, as Cdt1 recruitment may interfere in the interaction of other PIP-box containing proteins with PCNA. Constructing a mutant where the PCNA-binding and $CRL4^{Cdt2}$-recruitment regions of the *S. pombe* PIP degron are separated, as is possible in *Xenopus* Cdt1 (Havens and Walter 2009), would permit investigation into whether a non-degradable Cdt1 mutant proficient in PCNA binding inhibits DNA repair.

Chapter 5 describes the development and implementation of a medium-throughput fluorescence-based screening method for the genome-wide identification of novel genes involved in Cdt1 regulation. Five candidate genes involved in DNA repair were identified from the screen (*rad32*$^+$, *ctp1*$^+$, *rhp51*$^+$, *nse5*$^+$ and *nse6*$^+$), all of which exhibited a reproducible up-regulation of Cdt1. Work presented in Chapter 6 indicates

that the most pronounced up-regulation of Cdt1 is observed in HR-deficient strains. Further characterisation of *rhp51*Δ and *rhp55*Δ mutants demonstrates that Cdt1 up-regulation in these strains is Rad3-dependent and may reflect checkpoint-mediated activation of MBF-dependent transcription in G2-arrested cells. Interestingly, Cdt1 levels are specifically up-regulated in the HR-deficient strains with respect to other MBF targets such as Cdc18 and Cdt2. This raises the question of whether Cdt1 up-regulation in the HR mutants is biologically significant. HR-deficient cells are reported to undergo high levels of spontaneous DNA damage, owing to the role of HR in the repair of replication-associated DNA damage. Is Cdt1 up-regulation relevant to the repair of this damage in HR-deficient cells? A study using *S. cerevisiae* has suggested that Cdt1 has an essential role in BIR (Lydeard et al. 2010). That Cdt1 should have a function outside of its role in replication licensing is not without precedence: human Cdt1 has been shown to have an independent and essential mitotic function (Varma et al. 2012). It would be of interest to compare the kinetics of DNA repair by PFGE in wildtype cells and in cells where Cdt1 had been inactivated, to determine if Cdt1 activity influenced the efficiency of DNA repair. Furthermore, one could speculate that if Cdt1 were to function in DNA repair in yeast, then its specific up-regulation with respect to Cdc18 would be advantageous to the cell. The simultaneous up-regulation of both proteins might lead to inadvertent relicensing and re-replication of the genome (Gopalakrishnan et al. 2001; Yanow et al. 2001).

A recent study postulated that Cdt1 might function at the DNA damage site in human cells (Roukos et al. 2011). In laser-damaged human cells, the kinetics of Cdt1 degradation are much slower than the kinetics of Cdt1 recruitment to the damage site, providing a window of opportunity for Cdt1 to execute a function at the DNA damage

site (Roukos et al. 2011). It would be interesting to compare the kinetics of Cdt1 recruitment and degradation at DNA damage sites in *S. pombe* and determine whether there is a conserved delay between the two processes. The interaction between Cdt1 and chromatin-bound PCNA enables Cdt1 to be efficiently targeted to the DNA damage site. Whether this targeting mechanism is relevant to DNA repair could be examined by constructing a Cdt1 mutant that is functional for licensing but unable to interact with PCNA. It would be useful to investigate whether this mutant had any effect on the efficiency of DNA repair in *S. pombe* cells.

It is curious that *S. pombe* Cdt1 is subject to two opposing forms of regulation in response to DNA damage. The *cdt1*$^{+}$ gene is transcriptionally up-regulated after DNA damage, yet the protein is subject to CRL4^{Cdt2}-mediated proteolysis (Watson et al. 2004; Ralph et al. 2006). Investigating the biological significance of these opposing forms of Cdt1 regulation in response to DNA damage presents an interesting topic for future research. Further work on this subject would improve our understanding of the role of licensing factors in DNA repair and the role of CRL4^{Cdt2} in fine-tuning the associations between PCNA and its interacting partners at the site of DNA damage.

Bibliography

Abbas, T., U. Sivaprasad, K. Terai, V. Amador, M. Pagano and A. Dutta (2008). "PCNA-dependent regulation of p21 ubiquitylation and degradation via the $CRL4^{Cdt2}$ ubiquitin ligase complex." Genes Dev **22**(18): 2496-2506.

Abbas, T. and A. Dutta (2011). "$CRL4^{Cdt2}$: master coordinator of cell cycle progression and genome stability." Cell Cycle **10**(2): 241-249.

Akman, G. and S. A. MacNeill (2009). "MCM-GINS and MCM-MCM interactions *in vivo* visualised by bimolecular fluorescence complementation in fission yeast." BMC Cell Biol **10**: 12.

Aligianni, S., D. H. Lackner, S. Klier, G. Rustici, B. T. Wilhelm, S. Marguerat, S. Codlin, A. Brazma, R. A. de Bruin and J. Bähler (2009). "The fission yeast homeodomain protein Yox1p binds to MBF and confines MBF-dependent cell-cycle transcription to G1-S via negative feedback." PLoS Genet **5**(8): e1000626.

Angers, S., T. Li, X. Yi, M. J. MacCoss, R. T. Moon and N. Zheng (2006). "Molecular architecture and assembly of the DDB1-CUL4A ubiquitin ligase machinery." Nature **443**(7111): 590-593.

Aparicio, O. M., D. M. Weinstein and S. P. Bell (1997). "Components and dynamics of DNA replication complexes in *S. cerevisiae*: redistribution of MCM proteins and Cdc45p during S phase." Cell **91**(1): 59-69.

Arias, E. E. and J. C. Walter (2005). "Replication-dependent destruction of Cdt1 limits DNA replication to a single round per cell cycle in *Xenopus* egg extracts." Genes Dev **19**(1): 114-126.

Arias, E. E. and J. C. Walter (2006). "PCNA functions as a molecular platform to trigger Cdt1 destruction and prevent re-replication." Nat Cell Biol **8**(1): 84-90.

Arias, E. E. and J. C. Walter (2007). "Strength in numbers: preventing rereplication via multiple mechanisms in eukaryotic cells." Genes Dev **21**(5): 497-518.

Arnaudeau, C., C. Lundin and T. Helleday (2001). "DNA double-strand breaks associated with replication forks are predominantly repaired by homologous recombination involving an exchange mechanism in mammalian cells." J Mol Biol **307**(5): 1235-1245.

Aslett, M. and V. Wood (2006). "Gene Ontology annotation status of the fission yeast genome: preliminary coverage approaches 100%." Yeast **23**(13): 913-919.

Ayte, J., C. Schweitzer, P. Zarzov, P. Nurse and J. A. DeCaprio (2001). "Feedback regulation of the MBF transcription factor by cyclin Cig2." Nat Cell Biol **3**(12): 1043-1050.

Bähler, J., J. Q. Wu, M. S. Longtine, N. G. Shah, A. McKenzie, 3rd, A. B. Steever, A. Wach, P. Philippsen and J. R. Pringle (1998). "Heterologous modules for efficient and versatile PCR-based gene targeting in *Schizosaccharomyces pombe*." Yeast **14**(10): 943-951.

Bähler, J. (2005). "Cell-cycle control of gene expression in budding and fission yeast." Annu Rev Genet **39**: 69-94.

Balestrini, A., C. Cosentino, A. Errico, E. Garner and V. Costanzo (2010). "GEMC1 is a TopBP1-interacting protein required for chromosomal DNA replication." Nat Cell Biol **12**(5): 484-491.

Ballabeni, A., M. Melixetian, R. Zamponi, L. Masiero, F. Marinoni and K. Helin (2004). "Human geminin promotes pre-RC formation and DNA replication by stabilizing CDT1 in mitosis." EMBO J **23**(15): 3122-3132.

Baum, B., J. Wuarin and P. Nurse (1997). "Control of S-phase periodic transcription in the fission yeast mitotic cycle." EMBO J **16**(15): 4676-4688.

Bell, S. P. and B. Stillman (1992). "ATP-dependent recognition of eukaryotic origins of DNA replication by a multiprotein complex." Nature **357**(6374): 128-134.

Bernal, J. A. and A. R. Venkitaraman (2011). "A vertebrate N-end rule degron reveals that Orc6 is required in mitosis for daughter cell abscission." J Cell Biol **192**(6): 969-978.

Bicknell, L. S., E. M. Bongers, A. Leitch, S. Brown, J. Schoots, M. E. Harley, S. Aftimos, J. Y. Al-Aama, M. Bober, P. A. Brown, et al. (2011). "Mutations in the pre-replication complex cause Meier-Gorlin syndrome." Nat Genet **43**(4): 356-359.

Bochman, M. L. and A. Schwacha (2009). "The Mcm complex: unwinding the mechanism of a replicative helicase." Microbiol Mol Biol Rev **73**(4): 652-683.

Borde, V. and J. Cobb (2009). "Double functions for the Mre11 complex during DNA double-strand break repair and replication." Int J Biochem Cell Biol **41**(6): 1249-1253.

Bosu, D. R. and E. T. Kipreos (2008). "Cullin-RING ubiquitin ligases: global regulation and activation cycles." Cell Div **3**: 7.

Botchan, M. and J. Berger (2010). "DNA replication: making two forks from one prereplication complex." Mol Cell **40**(6): 860-861.

Bousset, K. and J. F. Diffley (1998). "The Cdc7 protein kinase is required for origin firing during S phase." Genes Dev **12**(4): 480-490.

Bowers, J. L., J. C. Randell, S. Chen and S. P. Bell (2004). "ATP hydrolysis by ORC catalyzes reiterative Mcm2-7 assembly at a defined origin of replication." Mol Cell **16**(6): 967-978.

Braun, S., J. F. Garcia, M. Rowley, M. Rougemaille, S. Shankar and H. D. Madhani (2011). "The Cul4-Ddb1^{Cdt2} ubiquitin ligase inhibits invasion of a boundary-associated antisilencing factor into heterochromatin." Cell **144**(1): 41-54.

Brown, G. W. and T. J. Kelly (1998). "Purification of Hsk1, a minichromosome maintenance protein kinase from fission yeast." J Biol Chem **273**(34): 22083-22090.

Bruning, J. B. and Y. Shamoo (2004). "Structural and thermodynamic analysis of human PCNA with peptides derived from DNA polymerase-delta p66 subunit and flap endonuclease-1." Structure **12**(12): 2209-2219.

Buttrick, G. J. and J. B. Millar (2011). "Ringing the changes: emerging roles for DASH at the kinetochore-microtubule Interface." Chromosome Res **19**(3): 393-407.

Caetano, C., S. Klier and R. A. de Bruin (2011). "Phosphorylation of the MBF repressor Yox1p by the DNA replication checkpoint keeps the G1/S cell-cycle transcriptional program active." PLoS One **6**(2): e17211.

Caspari, T., M. Dahlen, G. Kanter-Smoler, H. D. Lindsay, K. Hofmann, K. Papadimitriou, P. Sunnerhagen and A. M. Carr (2000). "Characterization of *Schizosaccharomyces pombe* Hus1: a PCNA-related protein that associates with Rad1 and Rad9." Mol Cell Biol **20**(4): 1254-1262.

Chahwan, C., T. M. Nakamura, S. Sivakumar, P. Russell and N. Rhind (2003). "The fission yeast Rad32 (Mre11)-Rad50-Nbs1 complex is required for the S-phase DNA damage checkpoint." Mol Cell Biol **23**(18): 6564-6573.

Chandrasekaran, S., T. X. Tan, J. R. Hall and J. G. Cook (2011). "Stress-stimulated mitogen-activated protein kinases control the stability and activity of the Cdt1 DNA replication licensing factor." Mol Cell Biol **31**(22): 4405-4416.

Chen, S., M. A. de Vries and S. P. Bell (2007). "Orc6 is required for dynamic recruitment of Cdt1 during repeated Mcm2-7 loading." Genes Dev **21**(22): 2897-2907.

Chen, S. and S. P. Bell (2011). "CDK prevents Mcm2-7 helicase loading by inhibiting Cdt1 interaction with Orc6." Genes Dev **25**(4): 363-372.

Chilkova, O., P. Stenlund, I. Isoz, C. M. Stith, P. Grabowski, E. B. Lundstrom, P. M. Burgers and E. Johansson (2007). "The eukaryotic leading and lagging strand DNA polymerases are loaded onto primer-ends via separate mechanisms but have comparable processivity in the presence of PCNA." Nucleic Acids Res **35**(19): 6588-6597.

Chu, Z., M. Eshaghi, S. Y. Poon and J. Liu (2009). "A Cds1-mediated checkpoint protects the MBF activator Rep2 from ubiquitination by anaphase-promoting complex/cyclosome-Ste9 at S-phase arrest in fission yeast." Mol Cell Biol **29**(18): 4959-4970.

Chuang, R. Y., L. Chretien, J. Dai and T. J. Kelly (2002). "Purification and characterization of the *Schizosaccharomyces pombe* origin recognition complex: interaction with origin DNA and Cdc18 protein." J Biol Chem **277**(19): 16920-16927.

Cigan, A. M. and T. F. Donahue (1987). "Sequence and structural features associated with translational initiator regions in yeast-a review." Gene **59**(1): 1-18.

Cigan, A. M., E. K. Pabich and T. F. Donahue (1988). "Mutational analysis of the HIS4 translational initiator region in *Saccharomyces cerevisiae*." Mol Cell Biol **8**(7): 2964-2975.

Claros, M. G. and P. Vincens (1996). "Computational method to predict mitochondrially imported proteins and their targeting sequences." Eur J Biochem **241**(3): 779-786.

Coleman, T. R., P. B. Carpenter and W. G. Dunphy (1996). "The *Xenopus* Cdc6 protein is essential for the initiation of a single round of DNA replication in cell-free extracts." Cell **87**(1): 53-63.

Conaway, R. C. and J. W. Conaway (2011). "Function and regulation of the Mediator complex." Curr Opin Genet Dev **21**(2): 225-230.

Cook, J. G., D. A. Chasse and J. R. Nevins (2004). "The regulated association of Cdt1 with minichromosome maintenance proteins and Cdc6 in mammalian cells." J Biol Chem **279**(10): 9625-9633.

Cope, G. A., G. S. Suh, L. Aravind, S. E. Schwarz, S. L. Zipursky, E. V. Koonin and R. J. Deshaies (2002). "Role of predicted metalloprotease motif of Jab1/Csn5 in cleavage of Nedd8 from Cul1." Science **298**(5593): 608-611.

Cope, G. A. and R. J. Deshaies (2003). "COP9 signalosome: a multifunctional regulator of SCF and other cullin-based ubiquitin ligases." Cell **114**(6): 663-671.

Costa, A., I. Ilves, N. Tamberg, T. Petojevic, E. Nogales, M. R. Botchan and J. M. Berger (2011). "The structural basis for MCM2-7 helicase activation by GINS and Cdc45." Nat Struct Mol Biol **18**(4): 471-477.

Coxon, A., K. Maundrell and S. E. Kearsey (1992). "Fission yeast *cdc21*$^{+}$ belongs to a family of proteins involved in an early step of chromosome replication." Nucleic Acids Res **20**(21): 5571-5577.

de Bruin, R. A., T. I. Kalashnikova, C. Chahwan, W. H. McDonald, J. Wohlschlegel, J. Yates, 3rd, P. Russell and C. Wittenberg (2006). "Constraining G1-specific transcription to late G1 phase: the MBF-associated corepressor Nrm1 acts via negative feedback." Mol Cell **23**(4): 483-496.

de Bruin, R. A., T. I. Kalashnikova, A. Aslanian, J. Wohlschlegel, C. Chahwan, J. R. Yates, 3rd, P. Russell and C. Wittenberg (2008). "DNA replication checkpoint promotes G1-S transcription by inactivating the MBF repressor Nrm1." Proc Natl Acad Sci U S A **105**(32): 11230-11235.

De Marco, V., P. J. Gillespie, A. Li, N. Karantzelis, E. Christodoulou, R. Klompmaker, S. van Gerwen, A. Fish, M. V. Petoukhov, M. S. Iliou, et al. (2009). "Quaternary structure of the human Cdt1-Geminin complex regulates DNA replication licensing." Proc Natl Acad Sci U S A **106**(47): 19807-19812.

De Piccoli, G., J. Torres-Rosell and L. Aragon (2009). "The unnamed complex: what do we know about Smc5-Smc6?" Chromosome Res **17**(2): 251-263.

DePamphilis, M. L. (2005). "Cell cycle dependent regulation of the origin recognition complex." Cell Cycle **4**(1): 70-79.

Deshaies, R. J. and C. A. Joazeiro (2009). "RING domain E3 ubiquitin ligases." Annu Rev Biochem **78**: 399-434.

Di Paola, D. and M. Zannis-Hadjopoulos (2012). "Comparative analysis of pre-replication complex proteins in transformed and normal cells." J Cell Biochem **113**(4): 1333-1347.

Ding, L. and S. L. Forsburg (2011). "*Schizosaccharomyces pombe* minichromosome maintenance-binding protein (MCM-BP) antagonizes MCM helicase." J Biol Chem **286**(38): 32918-32930.

Donaldson, A. D., W. L. Fangman and B. J. Brewer (1998). "Cdc7 is required throughout the yeast S phase to activate replication origins." Genes Dev **12**(4): 491-501.

Dong, Z., Y. Liu and J. T. Zhang (2005). "Regulation of ribonucleotide reductase M2 expression by the upstream AUGs." Nucleic Acids Res **33**(8): 2715-2725.

Donovan, S., J. Harwood, L. S. Drury and J. F. Diffley (1997). "Cdc6p-dependent loading of Mcm proteins onto pre-replicative chromatin in budding yeast." Proc Natl Acad Sci U S A **94**(11): 5611-5616.

Dowell, S. J., P. Romanowski and J. F. Diffley (1994). "Interaction of Dbf4, the Cdc7 protein kinase regulatory subunit, with yeast replication origins *in vivo*." Science **265**(5176): 1243-1246.

Drury, L. S., G. Perkins and J. F. Diffley (1997). "The Cdc4/34/53 pathway targets Cdc6p for proteolysis in budding yeast." EMBO J **16**(19): 5966-5976.

Drury, L. S., G. Perkins and J. F. Diffley (2000). "The cyclin-dependent kinase Cdc28p regulates distinct modes of Cdc6p proteolysis during the budding yeast cell cycle." Curr Biol **10**(5): 231-240.

Duda, D. M., L. A. Borg, D. C. Scott, H. W. Hunt, M. Hammel and B. A. Schulman (2008). "Structural insights into NEDD8 activation of cullin-RING ligases: conformational control of conjugation." Cell **134**(6): 995-1006.

Duncker, B. P., I. N. Chesnokov and B. J. McConkey (2009). "The origin recognition complex protein family." Genome Biol **10**(3): 214.

Dutta, C., P. K. Patel, A. Rosebrock, A. Oliva, J. Leatherwood and N. Rhind (2008). "The DNA replication checkpoint directly regulates MBF-dependent G1/S transcription." Mol Cell Biol **28**(19): 5977-5985.

Eaton, M. L., K. Galani, S. Kang, S. P. Bell and D. M. MacAlpine (2010). "Conserved nucleosome positioning defines replication origins." Genes Dev **24**(8): 748-753.

Edelstein, A., N. Amodaj, K. Hoover, R. Vale and N. Stuurman (2010). "Computer control of microscopes using microManager." Curr Protoc Mol Biol **Chapter 14**: Unit14 20.

Edwards, M. C., A. V. Tutter, C. Cvetic, C. H. Gilbert, T. A. Prokhorova and J. C. Walter (2002). "MCM2-7 complexes bind chromatin in a distributed pattern surrounding the origin recognition complex in *Xenopus* egg extracts." J Biol Chem **277**(36): 33049-33057.

Egel, R. (2005). "Fission yeast mating-type switching: programmed damage and repair." DNA Repair (Amst) **4**(5): 525-536.

Evrin, C., P. Clarke, J. Zech, R. Lurz, J. Sun, S. Uhle, H. Li, B. Stillman and C. Speck (2009). "A double-hexameric MCM2-7 complex is loaded onto origin DNA during licensing of eukaryotic DNA replication." Proc Natl Acad Sci U S A **106**(48): 20240-20245.

Fachinetti, D., R. Bermejo, A. Cocito, S. Minardi, Y. Katou, Y. Kanoh, K. Shirahige, A. Azvolinsky, V. A. Zakian and M. Foiani (2010). "Replication termination at eukaryotic chromosomes is mediated by Top2 and occurs at genomic loci containing pausing elements." Mol Cell **39**(4): 595-605.

Ferenbach, A., A. Li, M. Brito-Martins and J. J. Blow (2005). "Functional domains of the *Xenopus* replication licensing factor Cdt1." Nucleic Acids Res **33**(1): 316-324.

Fischer, E. S., A. Scrima, K. Bohm, S. Matsumoto, G. M. Lingaraju, M. Faty, T. Yasuda, S. Cavadini, M. Wakasugi, F. Hanaoka, et al. (2011). "The molecular basis of $CRL4^{DDB2/CSA}$ ubiquitin ligase architecture, targeting, and activation." Cell **147**(5): 1024-1039.

Fisher, D. L. and P. Nurse (1996). "A single fission yeast mitotic cyclin B p34cdc2 kinase promotes both S-phase and mitosis in the absence of G1 cyclins." EMBO J **15**(4): 850-860.

Frampton, J., A. Irmisch, C. M. Green, A. Neiss, M. Trickey, H. D. Ulrich, K. Furuya, F. Z. Watts, A. M. Carr and A. R. Lehmann (2006). "Postreplication repair and PCNA modification in *Schizosaccharomyces pombe*." Mol Biol Cell **17**(7): 2976-2985.

Gambus, A., G. A. Khoudoli, R. C. Jones and J. J. Blow (2011). "MCM2-7 form double hexamers at licensed origins in *Xenopus* egg extract." J Biol Chem **286**(13): 11855-11864.

Garcia, V., K. Furuya and A. M. Carr (2005). "Identification and functional analysis of TopBP1 and its homologs." DNA Repair (Amst) **4**(11): 1227-1239.

Garg, P. and P. M. Burgers (2005). "DNA polymerases that propagate the eukaryotic DNA replication fork." Crit Rev Biochem Mol Biol **40**(2): 115-128.

Gillespie, P. J., A. Li and J. J. Blow (2001). "Reconstitution of licensed replication origins on *Xenopus* sperm nuclei using purified proteins." BMC Biochem **2**: 15.

Gilljam, K. M., E. Feyzi, P. A. Aas, M. M. Sousa, R. Muller, C. B. Vagbo, T. C. Catterall, N. B. Liabakk, G. Slupphaug, F. Drablos, et al. (2009). "Identification of a novel, widespread, and functionally important PCNA-binding motif." J Cell Biol **186**(5): 645-654.

Gopalakrishnan, V., P. Simancek, C. Houchens, H. A. Snaith, M. G. Frattini, S. Sazer and T. J. Kelly (2001). "Redundant control of rereplication in fission yeast." Proc Natl Acad Sci U S A **98**(23): 13114-13119.

Green, B. M., K. J. Finn and J. J. Li (2010). "Loss of DNA replication control is a potent inducer of gene amplification." Science **329**(5994): 943-946.

Grishchuk, A. L., R. Kraehenbuehl, M. Molnar, O. Fleck and J. Kohli (2004). "Genetic and cytological characterization of the RecA-homologous proteins Rad51 and Dmc1 of *Schizosaccharomyces pombe*." Curr Genet **44**(6): 317-328.

Guarino, E., M. E. Shepherd, I. Salguero, H. Hua, R. S. Deegan and S. E. Kearsey (2011). "Cdt1 proteolysis is promoted by dual PIP degrons and is modulated by PCNA ubiquitylation." Nucleic Acids Res **39**(14): 5978-5990.

Gulbis, J. M., Z. Kelman, J. Hurwitz, M. O'Donnell and J. Kuriyan (1996). "Structure of the C-terminal region of $p21^{WAF1/CIP1}$ complexed with human PCNA." Cell **87**(2): 297-306.

Gustafsson, C. M., L. C. Myers, J. Beve, H. Spahr, M. Lui, H. Erdjument-Bromage, P. Tempst and R. D. Kornberg (1998). "Identification of new mediator subunits in the RNA polymerase II holoenzyme from *Saccharomyces cerevisiae*." J Biol Chem **273**(47): 30851-30854.

Hardouin, J. (2007). "Protein sequence information by matrix-assisted laser desorption/ionization in-source decay mass spectrometry." Mass Spectrom Rev **26**(5): 672-682.

Hardy, C. F., O. Dryga, S. Seematter, P. M. Pahl and R. A. Sclafani (1997). "*mcm5/cdc46-bob1* bypasses the requirement for the S phase activator Cdc7p." Proc Natl Acad Sci U S A **94**(7): 3151-3155.

Hartwell, L. H. (1973). "Three additional genes required for deoxyribonucleic acid synthesis in *Saccharomyces cerevisiae*." J Bacteriol **115**(3): 966-974.

Havens, C. G. and J. C. Walter (2009). "Docking of a specialized PIP Box onto chromatin-bound PCNA creates a degron for the ubiquitin ligase $CRL4^{Cdt2}$." Mol Cell **35**(1): 93-104.

Havens, C. G. and J. C. Walter (2011). "Mechanism of $CRL4^{Cdt2}$, a PCNA-dependent E3 ubiquitin ligase." Genes Dev **25**(15): 1568-1582.

Havens, C. G., N. Shobnam, E. Guarino, R. C. Centore, L. Zou, S. E. Kearsey and J. C. Walter (2012). "Direct Role for proliferating cell nuclear antigen (PCNA) in substrate recognition by the E3 ubiquitin ligase $CRL4^{Cdt2}$." J Biol Chem.

Hayashi, T., M. Hatanaka, K. Nagao, Y. Nakaseko, J. Kanoh, A. Kokubu, M. Ebe and M. Yanagida (2007). "Rapamycin sensitivity of the *Schizosaccharomyces pombe* tor2 mutant and organization of two highly phosphorylated TOR complexes by specific and common subunits." Genes Cells **12**(12): 1357-1370.

He, X., T. E. Patterson and S. Sazer (1997). "The *Schizosaccharomyces pombe* spindle checkpoint protein mad2p blocks anaphase and genetically interacts with the anaphase-promoting complex." Proc Natl Acad Sci U S A **94**(15): 7965-7970.

Henley, S. A. and F. A. Dick (2012). "The retinoblastoma family of proteins and their regulatory functions in the mammalian cell division cycle." Cell Div **7**(1): 10.

Heringa, J. (1999). "Two strategies for sequence comparison: profile-preprocessed and secondary structure-induced multiple alignment." Comput Chem **23**(3-4): 341-364.

Hermand, D. and P. Nurse (2007). "Cdc18 enforces long-term maintenance of the S phase checkpoint by anchoring the Rad3-Rad26 complex to chromatin." Mol Cell **26**(4): 553-563.

Heyer, W. D., M. R. Rao, L. F. Erdile, T. J. Kelly and R. D. Kolodner (1990). "An essential *Saccharomyces cerevisiae* single-stranded DNA binding protein is homologous to the large subunit of human RP-A." EMBO J **9**(7): 2321-2329.

Heyer, W. D., X. Li, M. Rolfsmeier and X. P. Zhang (2006). "Rad54: the Swiss Army knife of homologous recombination?" Nucleic Acids Res **34**(15): 4115-4125.

Heyer, W. D., K. T. Ehmsen and J. Liu (2010). "Regulation of homologous recombination in eukaryotes." Annu Rev Genet **44**: 113-139.

Higa, L. A., I. S. Mihaylov, D. P. Banks, J. Zheng and H. Zhang (2003). "Radiation-mediated proteolysis of CDT1 by CUL4-ROC1 and CSN complexes constitutes a new checkpoint." Nat Cell Biol **5**(11): 1008-1015.

Higa, L. A., D. Banks, M. Wu, R. Kobayashi, H. Sun and H. Zhang (2006). "L2DTL/CDT2 interacts with the CUL4/DDB1 complex and PCNA and regulates CDT1 proteolysis in response to DNA damage." Cell Cycle **5**(15): 1675-1680.

Hiraoka, Y., T. Toda and M. Yanagida (1984). "The *NDA3* gene of fission yeast encodes beta-tubulin: a cold-sensitive *nda3* mutation reversibly blocks spindle formation and chromosome movement in mitosis." Cell **39**(2 Pt 1): 349-358.

Hodgson, B., A. Li, S. Tada and J. J. Blow (2002). "Geminin becomes activated as an inhibitor of Cdt1/RLF-B following nuclear import." Curr Biol **12**(8): 678-683.

Hoege, C., B. Pfander, G. L. Moldovan, G. Pyrowolakis and S. Jentsch (2002). "RAD6-dependent DNA repair is linked to modification of PCNA by ubiquitin and SUMO." Nature **419**(6903): 135-141.

Hoeijmakers, J. H. (2001). "Genome maintenance mechanisms for preventing cancer." Nature **411**(6835): 366-374.

Hofmann, J. F. and D. Beach (1994). "*cdt1* is an essential target of the Cdc10/Sct1 transcription factor: requirement for DNA replication and inhibition of mitosis." EMBO J **13**(2): 425-434.

Holt, I. J. (2009). "Mitochondrial DNA replication and repair: all a flap." Trends Biochem Sci **34**(7): 358-365.

Hsu, K. S. and T. Toda (2011). "Ndc80 internal loop interacts with Dis1/TOG to ensure proper kinetochore-spindle attachment in fission yeast." Curr Biol **21**(3): 214-220.

Hu, C. D., Y. Chinenov and T. K. Kerppola (2002). "Visualization of interactions among bZIP and Rel family proteins in living cells using bimolecular fluorescence complementation." Mol Cell **9**(4): 789-798.

Hu, J., C. M. McCall, T. Ohta and Y. Xiong (2004). "Targeted ubiquitination of CDT1 by the DDB1-CUL4A-ROC1 ligase in response to DNA damage." Nat Cell Biol **6**(10): 1003-1009.

Hua, X. H. and J. Newport (1998). "Identification of a preinitiation step in DNA replication that is independent of origin recognition complex and cdc6, but dependent on cdk2." J Cell Biol **140**(2): 271-281.

Humphrey, T. (2000). "DNA damage and cell cycle control in *Schizosaccharomyces pombe*." Mutat Res **451**(1-2): 211-226.

Ilves, I., T. Petojevic, J. J. Pesavento and M. R. Botchan (2010). "Activation of the MCM2-7 helicase by association with Cdc45 and GINS proteins." Mol Cell **37**(2): 247-258.

Ishii, T., Y. Shiomi, T. Takami, Y. Murakami, N. Ohnishi and H. Nishitani (2010). "Proliferating cell nuclear antigen-dependent rapid recruitment of Cdt1 and $CRL4^{Cdt2}$ at DNA-damaged sites after UV irradiation in HeLa cells." J Biol Chem **285**(53): 41993-42000.

Iyer, V. R., C. E. Horak, C. S. Scafe, D. Botstein, M. Snyder and P. O. Brown (2001). "Genomic binding sites of the yeast cell-cycle transcription factors SBF and MBF." Nature **409**(6819): 533-538.

Jackson, A. L., P. M. Pahl, K. Harrison, J. Rosamond and R. A. Sclafani (1993). "Cell cycle regulation of the yeast Cdc7 protein kinase by association with the Dbf4 protein." Mol Cell Biol **13**(5): 2899-2908.

Jagannathan, M., A. M. Sakwe, T. Nguyen and L. Frappier (2012). "The MCM-associated protein MCM-BP is important for human nuclear morphology." J Cell Sci **125**(Pt 1): 133-143.

Jallepalli, P. V., G. W. Brown, M. Muzi-Falconi, D. Tien and T. J. Kelly (1997). "Regulation of the replication initiator protein p65^{cdc18} by CDK phosphorylation." Genes Dev **11**(21): 2767-2779.

Jallepalli, P. V., D. Tien and T. J. Kelly (1998). "*sud1*$^{+}$ targets cyclin-dependent kinase-phosphorylated Cdc18 and Rum1 proteins for degradation and stops unwanted diploidization in fission yeast." Proc Natl Acad Sci U S A **95**(14): 8159-8164.

Jang, Y. K., Y. H. Jin, E. M. Kim, F. Fabre, S. H. Hong and S. D. Park (1994). "Cloning and sequence analysis of *rhp51*$^{+}$, a *Schizosaccharomyces pombe* homolog of the *Saccharomyces cerevisiae RAD51* gene." Gene **142**(2): 207-211.

Jares, P., M. G. Luciani and J. J. Blow (2004). "A *Xenopus* Dbf4 homolog is required for Cdc7 chromatin binding and DNA replication." BMC Mol Biol **5**: 5.

Jee, J., T. Mizuno, K. Kamada, H. Tochio, Y. Chiba, K. Yanagi, G. Yasuda, H. Hiroaki, F. Hanaoka and M. Shirakawa (2010). "Structure and mutagenesis studies of the C-terminal region of licensing factor Cdt1 enable the identification of key residues for binding to replicative helicase Mcm proteins." J Biol Chem **285**(21): 15931-15940.

Jin, J., E. E. Arias, J. Chen, J. W. Harper and J. C. Walter (2006). "A family of diverse Cul4-Ddb1-interacting proteins includes Cdt2, which is required for S phase destruction of the replication factor Cdt1." Mol Cell **23**(5): 709-721.

Johansson, E. and S. A. MacNeill (2010). "The eukaryotic replicative DNA polymerases take shape." Trends Biochem Sci **35**(6): 339-347.

Jones, R. M. and E. Petermann (2012). "Replication fork dynamics and the DNA damage response." Biochem J **443**(1): 13-26.

Jorgensen, S., M. Eskildsen, K. Fugger, L. Hansen, M. S. Larsen, A. N. Kousholt, R. G. Syljuasen, M. B. Trelle, O. N. Jensen, K. Helin, et al. (2011). "SET8 is degraded via PCNA-coupled CRL4^{CDT2} ubiquitylation in S phase and after UV irradiation." J Cell Biol **192**(1): 43-54.

Kalderon, D., B. L. Roberts, W. D. Richardson and A. E. Smith (1984). "A short amino acid sequence able to specify nuclear location." Cell **39**(3 Pt 2): 499-509.

Kamimura, Y., Y. S. Tak, A. Sugino and H. Araki (2001). "Sld3, which interacts with Cdc45 (Sld4), functions for chromosomal DNA replication in *Saccharomyces cerevisiae*." EMBO J **20**(8): 2097-2107.

Karakaidos, P., S. Taraviras, L. V. Vassiliou, P. Zacharatos, N. G. Kastrinakis, D. Kougiou, M. Kouloukoussa, H. Nishitani, A. G. Papavassiliou, Z. Lygerou, et al. (2004). "Overexpression of the replication licensing regulators hCdt1 and hCdc6 characterizes a subset of non-small-cell lung carcinomas: synergistic effect with mutant p53 on tumor growth and chromosomal instability--evidence of E2F-1 transcriptional control over hCdt1." Am J Pathol **165**(4): 1351-1365.

Katayama, S., K. Kitamura, A. Lehmann, O. Nikaido and T. Toda (2002). "Fission yeast F-box protein Pof3 is required for genome integrity and telomere function." Mol Biol Cell **13**(1): 211-224.

Kawasaki, Y., H. D. Kim, A. Kojima, T. Seki and A. Sugino (2006). "Reconstitution of *Saccharomyces cerevisiae* prereplicative complex assembly *in vitro*." Genes Cells **11**(7): 745-756.

Kearsey, S. E. and S. Cotterill (2003). "Enigmatic variations: divergent modes of regulating eukaryotic DNA replication." Mol Cell **12**(5): 1067-1075.

Kearsey, S. E., L. Brimage, M. Namdar, E. Ralph and X. Yang (2005). "*In situ* assay for analyzing the chromatin binding of proteins in fission yeast." Methods Mol Biol **296**: 181-188.

Kelly, T. J., G. S. Martin, S. L. Forsburg, R. J. Stephen, A. Russo and P. Nurse (1993). "The fission yeast *cdc18*$^{+}$ gene product couples S phase to START and mitosis." Cell **74**(2): 371-382.

Kelman, Z. and M. O'Donnell (1995). "Structural and functional similarities of prokaryotic and eukaryotic DNA polymerase sliding clamps." Nucleic Acids Res **23**(18): 3613-3620.

Kim, D. H., V. N. Budhavarapu, C. R. Herrera, H. W. Nam, Y. S. Kim and P. R. Yew (2010a). "The CRL4^{Cdt2} ubiquitin ligase mediates the proteolysis of cyclin-dependent kinase inhibitor Xic1 through a direct association with PCNA." Mol Cell Biol **30**(17): 4120-4133.

Kim, D. U., J. Hayles, D. Kim, V. Wood, H. O. Park, M. Won, H. S. Yoo, T. Duhig, M. Nam, G. Palmer, et al. (2010b). "Analysis of a genome-wide set of gene deletions in the fission yeast *Schizosaccharomyces pombe*." Nat Biotechnol **28**(6): 617-623.

Kim, J., H. Feng and E. T. Kipreos (2007). "*C. elegans* CUL-4 prevents rereplication by promoting the nuclear export of CDC-6 via a CKI-1-dependent pathway." Curr Biol **17**(11): 966-972.

Kim, J. and E. T. Kipreos (2008). "Control of the Cdc6 replication licensing factor in metazoa: the role of nuclear export and the CUL4 ubiquitin ligase." Cell Cycle **7**(2): 146-150.

Kim, S. H. and W. M. Michael (2008). "Regulated proteolysis of DNA polymerase eta during the DNA-damage response in *C. elegans*." Mol Cell **32**(6): 757-766.

Kim, W. J., H. Lee, E. J. Park, J. K. Park and S. D. Park (2001). "Gain- and loss-of-function of Rhp51, a Rad51 homolog in fission yeast, reveals dissimilarities in chromosome integrity." Nucleic Acids Res **29**(8): 1724-1732.

Kim, Y. and E. T. Kipreos (2007). "Cdt1 degradation to prevent DNA re-replication: conserved and non-conserved pathways." Cell Div **2**: 18.

Kim, Y., N. G. Starostina and E. T. Kipreos (2008). "The CRL4^{Cdt2} ubiquitin ligase targets the degradation of p21^{Cip1} to control replication licensing." Genes Dev **22**(18): 2507-2519.

Klemm, R. D., R. J. Austin and S. P. Bell (1997). "Coordinate binding of ATP and origin DNA regulates the ATPase activity of the origin recognition complex." Cell **88**(4): 493-502.

Kochetov, A. V., I. V. Ischenko, D. G. Vorobiev, A. E. Kel, V. N. Babenko, L. L. Kisselev and N. A. Kolchanov (1998). "Eukaryotic mRNAs encoding abundant and scarce proteins are statistically dissimilar in many structural features." FEBS Lett **440**(3): 351-355.

Kochetov, A. V. (2008). "Alternative translation start sites and hidden coding potential of eukaryotic mRNAs." Bioessays **30**(7): 683-691.

Kominami, K. and T. Toda (1997). "Fission yeast WD-repeat protein Pop1 regulates genome ploidy through ubiquitin-proteasome-mediated degradation of the CDK inhibitor Rum1 and the S-phase initiator Cdc18." Genes Dev **11**(12): 1548-1560.

Kozak, M. (1978). "How do eucaryotic ribosomes select initiation regions in messenger RNA?" Cell **15**(4): 1109-1123.

Kozak, M. (1981). "Possible role of flanking nucleotides in recognition of the AUG initiator codon by eukaryotic ribosomes." Nucleic Acids Res **9**(20): 5233-5252.

Kozak, M. (1984). "Compilation and analysis of sequences upstream from the translational start site in eukaryotic mRNAs." Nucleic Acids Res **12**(2): 857-872.

Kozak, M. (1986). "Point mutations define a sequence flanking the AUG initiator codon that modulates translation by eukaryotic ribosomes." Cell **44**(2): 283-292.

Kozak, M. (2005). "Regulation of translation via mRNA structure in prokaryotes and eukaryotes." Gene **361**: 13-37.

Kriegenburg, F., L. Ellgaard and R. Hartmann-Petersen (2012). "Molecular chaperones in targeting misfolded proteins for ubiquitin-dependent degradation." FEBS J **279**(4): 532-542.

Krishna, T. S., X. P. Kong, S. Gary, P. M. Burgers and J. Kuriyan (1994). "Crystal structure of the eukaryotic DNA polymerase processivity factor PCNA." Cell **79**(7): 1233-1243.

Krogh, B. O. and L. S. Symington (2004). "Recombination proteins in yeast." Annu Rev Genet **38**: 233-271.

Kumagai, A., A. Shevchenko, A. Shevchenko and W. G. Dunphy (2010). "Treslin collaborates with TopBP1 in triggering the initiation of DNA replication." Cell **140**(3): 349-359.

Labib, K., J. F. Diffley and S. E. Kearsey (1999). "G1-phase and B-type cyclins exclude the DNA-replication factor Mcm4 from the nucleus." Nat Cell Biol **1**(7): 415-422.

Labib, K. (2010). "How do Cdc7 and cyclin-dependent kinases trigger the initiation of chromosome replication in eukaryotic cells?" Genes Dev **24**(12): 1208-1219.

Lambert, S., A. Watson, D. M. Sheedy, B. Martin and A. M. Carr (2005). "Gross chromosomal rearrangements and elevated recombination at an inducible site-specific replication fork barrier." Cell **121**(5): 689-702.

Lambert, S., B. Froget and A. M. Carr (2007). "Arrested replication fork processing: interplay between checkpoints and recombination." DNA Repair (Amst) **6**(7): 1042-1061.

Lange, A., R. E. Mills, C. J. Lange, M. Stewart, S. E. Devine and A. H. Corbett (2007). "Classical nuclear localization signals: definition, function, and interaction with importin alpha." J Biol Chem **282**(8): 5101-5105.

Langerak, P., E. Mejia-Ramirez, O. Limbo and P. Russell (2011). "Release of Ku and MRN from DNA ends by Mre11 nuclease activity and Ctp1 is required for homologous recombination repair of double-strand breaks." PLoS Genet **7**(9): e1002271.

Lee, C., B. Hong, J. M. Choi, Y. Kim, S. Watanabe, Y. Ishimi, T. Enomoto, S. Tada, Y. Kim and Y. Cho (2004). "Structural basis for inhibition of the replication licensing factor Cdt1 by geminin." Nature **430**(7002): 913-917.

Lee, D. G. and S. P. Bell (1997). "Architecture of the yeast origin recognition complex bound to origins of DNA replication." Mol Cell Biol **17**(12): 7159-7168.

Lee, H. O., S. J. Zacharek, Y. Xiong and R. J. Duronio (2010). "Cell type-dependent requirement for PIP box-regulated Cdt1 destruction during S phase." Mol Biol Cell **21**(21): 3639-3653.

Lee, J. and P. Zhou (2012). "Pathogenic Role of the CRL4 Ubiquitin Ligase in Human Disease." Front Oncol **2**: 21.

Lee, J. K., K. Y. Moon, Y. Jiang and J. Hurwitz (2001). "The *Schizosaccharomyces pombe* origin recognition complex interacts with multiple AT-rich regions of the replication origin DNA by means of the AT-hook domains of the spOrc4 protein." Proc Natl Acad Sci U S A **98**(24): 13589-13594.

Leone, G., J. DeGregori, Z. Yan, L. Jakoi, S. Ishida, R. S. Williams and J. R. Nevins (1998). "E2F3 activity is regulated during the cell cycle and is required for the induction of S phase." Genes Dev **12**(14): 2120-2130.

Li, A. and J. J. Blow (2004). "Non-proteolytic inactivation of geminin requires CDK-dependent ubiquitination." Nat Cell Biol **6**(3): 260-267.

Li, C. J. and M. L. DePamphilis (2002). "Mammalian Orc1 protein is selectively released from chromatin and ubiquitinated during the S-to-M transition in the cell division cycle." Mol Cell Biol **22**(1): 105-116.

Li, J. J., J. Schnick, J. Hayles and S. A. MacNeill (2011). "Purification and functional inactivation of the fission yeast $MCM^{MCM\text{-}BP}$ complex." FEBS Lett **585**(24): 3850-3855.

Li, X., Q. Zhao, R. Liao, P. Sun and X. Wu (2003). "The SCF(Skp2) ubiquitin ligase complex interacts with the human replication licensing factor Cdt1 and regulates Cdt1 degradation." J Biol Chem **278**(33): 30854-30858.

Liku, M. E., V. Q. Nguyen, A. W. Rosales, K. Irie and J. J. Li (2005). "CDK phosphorylation of a novel NLS-NES module distributed between two subunits of the Mcm2-7 complex prevents chromosomal rereplication." Mol Biol Cell **16**(10): 5026-5039.

Limbo, O., C. Chahwan, Y. Yamada, R. A. de Bruin, C. Wittenberg and P. Russell (2007). "Ctp1 is a cell-cycle-regulated protein that functions with Mre11 complex to control double-strand break repair by homologous recombination." Mol Cell **28**(1): 134-146.

Lindsay, H. D., D. J. Griffiths, R. J. Edwards, P. U. Christensen, J. M. Murray, F. Osman, N. Walworth and A. M. Carr (1998). "S-phase-specific activation of Cds1 kinase defines a subpathway of the checkpoint response in *Schizosaccharomyces pombe*." Genes Dev **12**(3): 382-395.

Liu, C., K. A. Powell, K. Mundt, L. Wu, A. M. Carr and T. Caspari (2003). "Cop9/signalosome subunits and Pcu4 regulate ribonucleotide reductase by both checkpoint-dependent and -independent mechanisms." Genes Dev **17**(9): 1130-1140.

Liu, C., M. Poitelea, A. Watson, S. H. Yoshida, C. Shimoda, C. Holmberg, O. Nielsen and A. M. Carr (2005a). "Transactivation of *Schizosaccharomyces pombe cdt2*$^{+}$ stimulates a Pcu4-Ddb1-CSN ubiquitin ligase." EMBO J **24**(22): 3940-3951.

Liu, C., R. Wu, B. Zhou, J. Wang, Z. Wei, B. K. Tye, C. Liang and G. Zhu (2012). "Structural insights into the Cdt1-mediated MCM2-7 chromatin loading." Nucleic Acids Res **40**(7): 3208-3217.

Liu, E., X. Li, F. Yan, Q. Zhao and X. Wu (2004). "Cyclin-dependent kinases phosphorylate human Cdt1 and induce its degradation." J Biol Chem **279**(17): 17283-17288.

Liu, E., A. Y. Lee, T. Chiba, E. Olson, P. Sun and X. Wu (2007). "The ATR-mediated S phase checkpoint prevents rereplication in mammalian cells when licensing control is disrupted." J Cell Biol **179**(4): 643-657.

Liu, X., I. McLeod, S. Anderson, J. R. Yates, 3rd and X. He (2005b). "Molecular analysis of kinetochore architecture in fission yeast." EMBO J **24**(16): 2919-2930.

Liu, Y., T. A. Richards and S. J. Aves (2009). "Ancient diversification of eukaryotic MCM DNA replication proteins." BMC Evol Biol **9**: 60.

Lowndes, N. F., C. J. McInerny, A. L. Johnson, P. A. Fantes and L. H. Johnston (1992). "Control of DNA synthesis genes in fission yeast by the cell-cycle gene *cdc10*$^{+}$." Nature **355**(6359): 449-453.

Lundin, C., N. Schultz, C. Arnaudeau, A. Mohindra, L. T. Hansen and T. Helleday (2003). "RAD51 is involved in repair of damage associated with DNA replication in mammalian cells." J Mol Biol **328**(3): 521-535.

Lutzmann, M., D. Maiorano and M. Mechali (2005). "Identification of full genes and proteins of MCM9, a novel, vertebrate-specific member of the MCM2-8 protein family." Gene **362**: 51-56.

Lutzmann, M., D. Maiorano and M. Mechali (2006). "A Cdt1-geminin complex licenses chromatin for DNA replication and prevents rereplication during S phase in *Xenopus*." EMBO J **25**(24): 5764-5774.

Lutzmann, M. and M. Mechali (2008). "MCM9 binds Cdt1 and is required for the assembly of prereplication complexes." Mol Cell **31**(2): 190-200.

Lutzmann, M., C. Grey, S. Traver, O. Ganier, A. Maya-Mendoza, N. Ranisavljevic, F. Bernex, A. Nishiyama, N. Montel, E. Gavois, et al. (2012). "MCM8- and MCM9-Deficient Mice Reveal Gametogenesis Defects and Genome Instability Due to Impaired Homologous Recombination." Mol Cell **47**(4): 523-534.

Lyapina, S., G. Cope, A. Shevchenko, G. Serino, T. Tsuge, C. Zhou, D. A. Wolf, N. Wei, A. Shevchenko and R. J. Deshaies (2001). "Promotion of NEDD-CUL1 conjugate cleavage by COP9 signalosome." Science **292**(5520): 1382-1385.

Lydeard, J. R., S. Jain, M. Yamaguchi and J. E. Haber (2007). "Break-induced replication and telomerase-independent telomere maintenance require Pol32." Nature **448**(7155): 820-823.

Lydeard, J. R., Z. Lipkin-Moore, Y. J. Sheu, B. Stillman, P. M. Burgers and J. E. Haber (2010). "Break-induced replication requires all essential DNA replication factors except those specific for pre-RC assembly." Genes Dev **24**(11): 1133-1144.

Lygerou, Z. and P. Nurse (1999). "The fission yeast origin recognition complex is constitutively associated with chromatin and is differentially modified through the cell cycle." J Cell Sci **112 (Pt 21)**: 3703-3712.

Maga, G., G. Villani, V. Tillement, M. Stucki, G. A. Locatelli, I. Frouin, S. Spadari and U. Hubscher (2001). "Okazaki fragment processing: modulation of the strand displacement activity of DNA polymerase delta by the concerted action of replication protein A, proliferating cell nuclear antigen, and flap endonuclease-1." Proc Natl Acad Sci U S A **98**(25): 14298-14303.

Maga, G. and U. Hubscher (2003). "Proliferating cell nuclear antigen (PCNA): a dancer with many partners." J Cell Sci **116**(Pt 15): 3051-3060.

Maiorano, D., J. Moreau and M. Mechali (2000). "XCDT1 is required for the assembly of pre-replicative complexes in *Xenopus laevis*." Nature **404**(6778): 622-625.

Maki, K., T. Inoue, A. Onaka, H. Hashizume, N. Somete, Y. Kobayashi, S. Murakami, C. Shigaki, T. S. Takahashi, H. Masukata, et al. (2011). "Abundance of prereplicative complexes (Pre-RCs) facilitates recombinational repair under replication stress in fission yeast." J Biol Chem **286**(48): 41701-41710.

Malumbres, M. and M. Barbacid (2005). "Mammalian cyclin-dependent kinases." Trends Biochem Sci **30**(11): 630-641.

Mandel, C. R., Y. Bai and L. Tong (2008). "Protein factors in pre-mRNA 3'-end processing." Cell Mol Life Sci **65**(7-8): 1099-1122.

Maqbool, Z., P. J. Kersey, P. A. Fantes and C. J. McInerny (2003). "MCB-mediated regulation of cell cycle-specific *cdc22*$^{+}$ transcription in fission yeast." Mol Genet Genomics **269**(6): 765-775.

Marahrens, Y. and B. Stillman (1992). "A yeast chromosomal origin of DNA replication defined by multiple functional elements." Science **255**(5046): 817-823.

Marti, T. M., C. Kunz and O. Fleck (2003). "Repair of damaged and mismatched DNA by the XPC homologues Rhp41 and Rhp42 of fission yeast." Genetics **164**(2): 457-467.

Martin, I. V. and S. A. MacNeill (2004). "Functional analysis of subcellular localization and protein-protein interaction sequences in the essential DNA ligase I protein of fission yeast." Nucleic Acids Res **32**(2): 632-642.

Martin, M. M., M. Ryan, R. Kim, A. L. Zakas, H. Fu, C. M. Lin, W. C. Reinhold, S. R. Davis, S. Bilke, H. Liu, et al. (2011). "Genome-wide depletion of replication initiation events in highly transcribed regions." Genome Res **21**(11): 1822-1832.

Martinho, R. G., H. D. Lindsay, G. Flaggs, A. J. DeMaggio, M. F. Hoekstra, A. M. Carr and N. J. Bentley (1998). "Analysis of Rad3 and Chk1 protein kinases defines different checkpoint responses." EMBO J **17**(24): 7239-7249.

Masai, H., T. Miyake and K. Arai (1995). "*hsk1*$^{+}$, a *Schizosaccharomyces pombe* gene related to *Saccharomyces cerevisiae CDC7*, is required for chromosomal replication." EMBO J **14**(13): 3094-3104.

Masai, H., E. Matsui, Z. You, Y. Ishimi, K. Tamai and K. Arai (2000). "Human Cdc7-related kinase complex. *In vitro* phosphorylation of MCM by concerted actions of Cdks and Cdc7 and that of a criticial threonine residue of Cdc7 by Cdks." J Biol Chem **275**(37): 29042-29052.

Masai, H. and K. Arai (2002). "Cdc7 kinase complex: a key regulator in the initiation of DNA replication." J Cell Physiol **190**(3): 287-296.

Masai, H., C. Taniyama, K. Ogino, E. Matsui, N. Kakusho, S. Matsumoto, J. M. Kim, A. Ishii, T. Tanaka, T. Kobayashi, et al. (2006). "Phosphorylation of MCM4 by Cdc7 kinase facilitates its interaction with Cdc45 on the chromatin." J Biol Chem **281**(51): 39249-39261.

Masai, H., S. Matsumoto, Z. You, N. Yoshizawa-Sugata and M. Oda (2010). "Eukaryotic chromosome DNA replication: where, when, and how?" Annu Rev Biochem **79**: 89-130.

Masumoto, H., S. Muramatsu, Y. Kamimura and H. Araki (2002). "S-Cdk-dependent phosphorylation of Sld2 essential for chromosomal DNA replication in budding yeast." Nature **415**(6872): 651-655.

Matson, D. R. and P. T. Stukenberg (2012). "Cdt1 throws kinetochore-microtubule attachments for a loop." Nat Cell Biol **14**(6): 561-563.

Matsuno, K., M. Kumano, Y. Kubota, Y. Hashimoto and H. Takisawa (2006). "The N-terminal noncatalytic region of *Xenopus* RecQ4 is required for chromatin binding of DNA polymerase alpha in the initiation of DNA replication." Mol Cell Biol **26**(13): 4843-4852.

Matsuyama, A., R. Arai, Y. Yashiroda, A. Shirai, A. Kamata, S. Sekido, Y. Kobayashi, A. Hashimoto, M. Hamamoto, Y. Hiraoka, et al. (2006). "ORFeome cloning and global analysis of protein localization in the fission yeast *Schizosaccharomyces pombe*." Nat Biotechnol **24**(7): 841-847.

McGarry, T. J. and M. W. Kirschner (1998). "Geminin, an inhibitor of DNA replication, is degraded during mitosis." Cell **93**(6): 1043-1053.

Mechali, M. (2010). "Eukaryotic DNA replication origins: many choices for appropriate answers." Nat Rev Mol Cell Biol **11**(10): 728-738.

Meijer, H. A. and A. A. Thomas (2002). "Control of eukaryotic protein synthesis by upstream open reading frames in the 5'-untranslated region of an mRNA." Biochem J **367**(Pt 1): 1-11.

Meister, P., M. Poidevin, S. Francesconi, I. Tratner, P. Zarzov and G. Baldacci (2003). "Nuclear factories for signalling and repairing DNA double strand breaks in living fission yeast." Nucleic Acids Res **31**(17): 5064-5073.

Meister, P., A. Taddei, L. Vernis, M. Poidevin, S. M. Gasser and G. Baldacci (2005). "Temporal separation of replication and recombination requires the intra-S checkpoint." J Cell Biol **168**(4): 537-544.

Melixetian, M., A. Ballabeni, L. Masiero, P. Gasparini, R. Zamponi, J. Bartek, J. Lukas and K. Helin (2004). "Loss of Geminin induces rereplication in the presence of functional p53." J Cell Biol **165**(4): 473-482.

Melo, J. and D. Toczyski (2002). "A unified view of the DNA-damage checkpoint." Curr Opin Cell Biol **14**(2): 237-245.

Mendez, J., X. H. Zou-Yang, S. Y. Kim, M. Hidaka, W. P. Tansey and B. Stillman (2002). "Human origin recognition complex large subunit is degraded by ubiquitin-mediated proteolysis after initiation of DNA replication." Mol Cell **9**(3): 481-491.

Michishita, M., A. Morimoto, T. Ishii, H. Komori, Y. Shiomi, Y. Higuchi and H. Nishitani (2011). "Positively charged residues located downstream of PIP box, together with TD amino acids within PIP box, are important for $CRL4^{Cdt2}$-mediated proteolysis." Genes Cells **16**(1): 12-22.

Mihaylov, I. S., T. Kondo, L. Jones, S. Ryzhikov, J. Tanaka, J. Zheng, L. A. Higa, N. Minamino, L. Cooley and H. Zhang (2002). "Control of DNA replication and chromosome ploidy by geminin and cyclin A." Mol Cell Biol **22**(6): 1868-1880.

Mimitou, E. P. and L. S. Symington (2011). "DNA end resection-unraveling the tail." DNA Repair (Amst) **10**(3): 344-348.

Miotto, B. and K. Struhl (2008). "HBO1 histone acetylase is a coactivator of the replication licensing factor Cdt1." Genes Dev **22**(19): 2633-2638.

Miotto, B. and K. Struhl (2010). "HBO1 histone acetylase activity is essential for DNA replication licensing and inhibited by Geminin." Mol Cell **37**(1): 57-66.

Miotto, B. and K. Struhl (2011). "JNK1 phosphorylation of Cdt1 inhibits recruitment of HBO1 histone acetylase and blocks replication licensing in response to stress." Mol Cell **44**(1): 62-71.

Moldovan, G. L., B. Pfander and S. Jentsch (2007). "PCNA, the maestro of the replication fork." Cell **129**(4): 665-679.

Mondesert, O., C. H. McGowan and P. Russell (1996). "Cig2, a B-type cyclin, promotes the onset of S in *Schizosaccharomyces pombe*." Mol Cell Biol **16**(4): 1527-1533.

Moreno, S., A. Klar and P. Nurse (1991). "Molecular genetic analysis of fission yeast *Schizosaccharomyces pombe*." Methods Enzymol **194**: 795-823.

Moser, B. A. and P. Russell (2000). "Cell cycle regulation in *Schizosaccharomyces pombe*." Curr Opin Microbiol **3**(6): 631-636.

Moss, J., H. Tinline-Purvis, C. A. Walker, L. K. Folkes, M. R. Stratford, J. Hayles, K. L. Hoe, D. U. Kim, H. O. Park, S. E. Kearsey, et al. (2010). "Break-induced ATR and Ddb1-

Cul4^{Cdt2} ubiquitin ligase-dependent nucleotide synthesis promotes homologous recombination repair in fission yeast." Genes Dev **24**(23): 2705-2716.

Moyer, S. E., P. W. Lewis and M. R. Botchan (2006). "Isolation of the Cdc45/Mcm2-7/GINS (CMG) complex, a candidate for the eukaryotic DNA replication fork helicase." Proc Natl Acad Sci U S A **103**(27): 10236-10241.

Mundt, K. E., J. Porte, J. M. Murray, C. Brikos, P. U. Christensen, T. Caspari, I. M. Hagan, J. B. Millar, V. Simanis, K. Hofmann, et al. (1999). "The COP9/signalosome complex is conserved in fission yeast and has a role in S phase." Curr Biol **9**(23): 1427-1430.

Muramatsu, S., K. Hirai, Y. S. Tak, Y. Kamimura and H. Araki (2010). "CDK-dependent complex formation between replication proteins Dpb11, Sld2, Pol epsilon, and GINS in budding yeast." Genes Dev **24**(6): 602-612.

Muris, D. F., K. Vreeken, A. M. Carr, B. C. Broughton, A. R. Lehmann, P. H. Lohman and A. Pastink (1993). "Cloning the RAD51 homologue of *Schizosaccharomyces pombe*." Nucleic Acids Res **21**(19): 4586-4591.

Muris, D. F., K. Vreeken, H. Schmidt, K. Ostermann, B. Clever, P. H. Lohman and A. Pastink (1997). "Homologous recombination in the fission yeast *Schizosaccharomyces pombe*: different requirements for the *rhp51*$^{+}$, *rhp54*$^{+}$ and *rad22*$^{+}$ genes." Curr Genet **31**(3): 248-254.

Nagai, T., K. Ibata, E. S. Park, M. Kubota, K. Mikoshiba and A. Miyawaki (2002). "A variant of yellow fluorescent protein with fast and efficient maturation for cell-biological applications." Nat Biotechnol **20**(1): 87-90.

Nakajima, R. and H. Masukata (2002). "SpSld3 is required for loading and maintenance of SpCdc45 on chromatin in DNA replication in fission yeast." Mol Biol Cell **13**(5): 1462-1472.

Nakashima, N., K. Tanaka, S. Sturm and H. Okayama (1995). "Fission yeast Rep2 is a putative transcriptional activator subunit for the cell cycle 'start' function of Res2-Cdc10." EMBO J **14**(19): 4794-4802.

Nguyen, V. Q., C. Co and J. J. Li (2001). "Cyclin-dependent kinases prevent DNA re-replication through multiple mechanisms." Nature **411**(6841): 1068-1073.

Nick McElhinny, S. A., D. A. Gordenin, C. M. Stith, P. M. Burgers and T. A. Kunkel (2008). "Division of labor at the eukaryotic replication fork." Mol Cell **30**(2): 137-144.

Nieduszynski, C. A., Y. Knox and A. D. Donaldson (2006). "Genome-wide identification of replication origins in yeast by comparative genomics." Genes Dev **20**(14): 1874-1879.

Niimi, S., S. Arakawa-Takeuchi, B. Uranbileg, J. H. Park, S. Jinno and H. Okayama (2012). "Cdc6 protein obstructs apoptosome assembly and consequent cell death by forming stable complexes with activated Apaf-1 molecules." J Biol Chem **287**(22): 18573-18583.

Nishimura, K., M. Ishiai, K. Horikawa, T. Fukagawa, M. Takata, H. Takisawa and M. T. Kanemaki (2012). "Mcm8 and Mcm9 Form a Complex that Functions in Homologous Recombination Repair Induced by DNA Interstrand Crosslinks." Mol Cell **47**(4): 511-522.

Nishitani, H. and P. Nurse (1995). "p65^{cdc18} plays a major role controlling the initiation of DNA replication in fission yeast." Cell **83**(3): 397-405.

Nishitani, H., Z. Lygerou, T. Nishimoto and P. Nurse (2000). "The Cdt1 protein is required to license DNA for replication in fission yeast." Nature **404**(6778): 625-628.

Nishitani, H., S. Taraviras, Z. Lygerou and T. Nishimoto (2001). "The human licensing factor for DNA replication Cdt1 accumulates in G1 and is destabilized after initiation of S-phase." J Biol Chem **276**(48): 44905-44911.

Nishitani, H., Z. Lygerou and T. Nishimoto (2004). "Proteolysis of DNA replication licensing factor Cdt1 in S-phase is performed independently of geminin through its N-terminal region." J Biol Chem **279**(29): 30807-30816.

Nishitani, H., N. Sugimoto, V. Roukos, Y. Nakanishi, M. Saijo, C. Obuse, T. Tsurimoto, K. I. Nakayama, K. Nakayama, M. Fujita, et al. (2006). "Two E3 ubiquitin ligases, SCF-

Skp2 and DDB1-Cul4, target human Cdt1 for proteolysis." EMBO J **25**(5): 1126-1136.

Nishiyama, A., L. Frappier and M. Mechali (2011). "MCM-BP regulates unloading of the MCM2-7 helicase in late S phase." Genes Dev **25**(2): 165-175.

Noguchi, E., P. Shanahan, C. Noguchi and P. Russell (2002). "CDK phosphorylation of Drc1 regulates DNA replication in fission yeast." Curr Biol **12**(7): 599-605.

Noguchi, K., A. Vassilev, S. Ghosh, J. L. Yates and M. L. DePamphilis (2006). "The BAH domain facilitates the ability of human Orc1 protein to activate replication origins *in vivo*." EMBO J **25**(22): 5372-5382.

O'Connell, B. C. and J. W. Harper (2007). "Ubiquitin proteasome system (UPS): what can chromatin do for you?" Curr Opin Cell Biol **19**(2): 206-214.

O'Donnell, M. and J. Kuriyan (2006). "Clamp loaders and replication initiation." Curr Opin Struct Biol **16**(1): 35-41.

Oakley, G. G. and S. M. Patrick (2010). "Replication protein A: directing traffic at the intersection of replication and repair." Front Biosci **15**: 883-900.

Ogawa, Y., T. Takahashi and H. Masukata (1999). "Association of fission yeast Orp1 and Mcm6 proteins with chromosomal replication origins." Mol Cell Biol **19**(10): 7228-7236.

Ohtani, K., J. DeGregori, G. Leone, D. R. Herendeen, T. J. Kelly and J. R. Nevins (1996). "Expression of the *HsOrc1* gene, a human *ORC1* homolog, is regulated by cell proliferation via the E2F transcription factor." Mol Cell Biol **16**(12): 6977-6984.

Ohtani, K., A. Tsujimoto, M. Ikeda and M. Nakamura (1998). "Regulation of cell growth-dependent expression of mammalian CDC6 gene by the cell cycle transcription factor E2F." Oncogene **17**(14): 1777-1785.

Ohtani, K., R. Iwanaga, M. Nakamura, M. Ikeda, N. Yabuta, H. Tsuruga and H. Nojima (1999). "Cell growth-regulated expression of mammalian MCM5 and MCM6 genes mediated by the transcription factor E2F." Oncogene **18**(14): 2299-2309.

Ortega, S., I. Prieto, J. Odajima, A. Martin, P. Dubus, R. Sotillo, J. L. Barbero, M. Malumbres and M. Barbacid (2003). "Cyclin-dependent kinase 2 is essential for meiosis but not for mitotic cell division in mice." Nat Genet **35**(1): 25-31.

Osaka, F., M. Saeki, S. Katayama, N. Aida, E. A. Toh, K. Kominami, T. Toda, T. Suzuki, T. Chiba, K. Tanaka, et al. (2000). "Covalent modifier NEDD8 is essential for SCF ubiquitin-ligase in fission yeast." EMBO J **19**(13): 3475-3484.

Osman, F., M. Bjoras, I. Alseth, I. Morland, S. McCready, E. Seeberg and I. Tsaneva (2003). "A new *Schizosaccharomyces pombe* base excision repair mutant, *nth1*, reveals overlapping pathways for repair of DNA base damage." Mol Microbiol **48**(2): 465-480.

Pacek, M., A. V. Tutter, Y. Kubota, H. Takisawa and J. C. Walter (2006). "Localization of MCM2-7, Cdc45, and GINS to the site of DNA unwinding during eukaryotic DNA replication." Mol Cell **21**(4): 581-587.

Park, S. D., Y. H. Jin and Y. K. Jang (1998). "Regulation of DNA damage inducible *rhp51*$^{+}$ gene, a rec A homolog from *Schizosaccharomyces pombe*." J Toxicol Sci **23 Suppl 2**: 110-116.

Pebernard, S., J. Wohlschlegel, W. H. McDonald, J. R. Yates, 3rd and M. N. Boddy (2006). "The Nse5-Nse6 dimer mediates DNA repair roles of the Smc5-Smc6 complex." Mol Cell Biol **26**(5): 1617-1630.

Petermann, E., M. L. Orta, N. Issaeva, N. Schultz and T. Helleday (2010). "Hydroxyurea-stalled replication forks become progressively inactivated and require two different RAD51-mediated pathways for restart and repair." Mol Cell **37**(4): 492-502.

Piatti, S., C. Lengauer and K. Nasmyth (1995). "Cdc6 is an unstable protein whose *de novo* synthesis in G1 is important for the onset of S phase and for preventing a 'reductional' anaphase in the budding yeast *Saccharomyces cerevisiae*." EMBO J **14**(15): 3788-3799.

Prasanth, S. G., K. V. Prasanth and B. Stillman (2002). "Orc6 involved in DNA replication, chromosome segregation, and cytokinesis." Science **297**(5583): 1026-1031.

Pursell, Z. F., I. Isoz, E. B. Lundstrom, E. Johansson and T. A. Kunkel (2007). "Yeast DNA polymerase epsilon participates in leading-strand DNA replication." Science **317**(5834): 127-130.

Ralph, E., E. Boye and S. E. Kearsey (2006). "DNA damage induces Cdt1 proteolysis in fission yeast through a pathway dependent on Cdt2 and Ddb1." EMBO Rep **7**(11): 1134-1139.

Raman, M., C. G. Havens, J. C. Walter and J. W. Harper (2011). "A genome-wide screen identifies p97 as an essential regulator of DNA damage-dependent CDT1 destruction." Mol Cell **44**(1): 72-84.

Randell, J. C., J. L. Bowers, H. K. Rodriguez and S. P. Bell (2006). "Sequential ATP hydrolysis by Cdc6 and ORC directs loading of the Mcm2-7 helicase." Mol Cell **21**(1): 29-39.

Remus, D., M. Blanchette, D. C. Rio and M. R. Botchan (2005). "CDK phosphorylation inhibits the DNA-binding and ATP-hydrolysis activities of the *Drosophila* origin recognition complex." J Biol Chem **280**(48): 39740-39751.

Remus, D., F. Beuron, G. Tolun, J. D. Griffith, E. P. Morris and J. F. Diffley (2009). "Concerted loading of Mcm2-7 double hexamers around DNA during DNA replication origin licensing." Cell **139**(4): 719-730.

Remus, D. and J. F. Diffley (2009). "Eukaryotic DNA replication control: lock and load, then fire." Curr Opin Cell Biol **21**(6): 771-777.

Reynolds, N., E. Warbrick, P. A. Fantes and S. A. MacNeill (2000). "Essential interaction between the fission yeast DNA polymerase delta subunit Cdc27 and Pcn1 (PCNA) mediated through a C-terminal $p21^{Cip1}$-like PCNA binding motif." EMBO J **19**(5): 1108-1118.

Rhind, N. and P. Russell (1998). "The *Schizosaccharomyces pombe* S-phase checkpoint differentiates between different types of DNA damage." Genetics **149**(4): 1729-1737.

Rhind, N. and P. Russell (2000). "Chk1 and Cds1: linchpins of the DNA damage and replication checkpoint pathways." J Cell Sci **113 (Pt 22)**: 3889-3896.

Ribar, B., T. Izumi and S. Mitra (2004). "The major role of human AP-endonuclease homolog Apn2 in repair of abasic sites in *Schizosaccharomyces pombe*." Nucleic Acids Res **32**(1): 115-126.

Roberts, B. T., C. Y. Ying, J. Gautier and J. L. Maller (1999). "DNA replication in vertebrates requires a homolog of the Cdc7 protein kinase." Proc Natl Acad Sci U S A **96**(6): 2800-2804.

Robinson, P. A. and H. C. Ardley (2004). "Ubiquitin-protein ligases." J Cell Sci **117**(Pt 22): 5191-5194.

Roguev, A., A. Shevchenko, D. Schaft, H. Thomas, A. F. Stewart and A. Shevchenko (2004). "A comparative analysis of an orthologous proteomic environment in the yeasts *Saccharomyces cerevisiae* and *Schizosaccharomyces pombe*." Mol Cell Proteomics **3**(2): 125-132.

Roguev, A., M. Wiren, J. S. Weissman and N. J. Krogan (2007). "High-throughput genetic interaction mapping in the fission yeast *Schizosaccharomyces pombe*." Nat Methods **4**(10): 861-866.

Roukos, V., A. Kinkhabwala, J. Colombelli, P. Kotsantis, S. Taraviras, H. Nishitani, E. Stelzer, P. Bastiaens and Z. Lygerou (2011). "Dynamic recruitment of licensing factor Cdt1 to sites of DNA damage." J Cell Sci **124**(Pt 3): 422-434.

Rowles, A., S. Tada and J. J. Blow (1999). "Changes in association of the *Xenopus* origin recognition complex with chromatin on licensing of replication origins." J Cell Sci **112 (Pt 12)**: 2011-2018.

Sakwe, A. M., T. Nguyen, V. Athanasopoulos, K. Shire and L. Frappier (2007). "Identification and characterization of a novel component of the human minichromosome maintenance complex." Mol Cell Biol **27**(8): 3044-3055.

Salguero, I., E. Guarino, M. E. Shepherd, T. D. Deegan, C. G. Havens, S. A. MacNeill, J. C. Walter and S. E. Kearsey (2012). "Ribonucleotide Reductase Activity Is Coupled to DNA Synthesis via Proliferating Cell Nuclear Antigen." Curr Biol **22**(8): 720-726.

San Filippo, J., P. Sung and H. Klein (2008). "Mechanism of eukaryotic homologous recombination." Annu Rev Biochem **77**: 229-257.

Sancar, A., L. A. Lindsey-Boltz, K. Unsal-Kacmaz and S. Linn (2004). "Molecular mechanisms of mammalian DNA repair and the DNA damage checkpoints." Annu Rev Biochem **73**: 39-85.

Sanchez-Perez, I., S. J. Renwick, K. Crawley, I. Karig, V. Buck, J. C. Meadows, A. Franco-Sanchez, U. Fleig, T. Toda and J. B. Millar (2005). "The DASH complex and Klp5/Klp6 kinesin coordinate bipolar chromosome attachment in fission yeast." EMBO J **24**(16): 2931-2943.

Sangrithi, M. N., J. A. Bernal, M. Madine, A. Philpott, J. Lee, W. G. Dunphy and A. R. Venkitaraman (2005). "Initiation of DNA replication requires the RECQL4 protein mutated in Rothmund-Thomson syndrome." Cell **121**(6): 887-898.

Sansam, C. L., J. L. Shepard, K. Lai, A. Ianari, P. S. Danielian, A. Amsterdam, N. Hopkins and J. A. Lees (2006). "DTL/CDT2 is essential for both CDT1 regulation and the early G2/M checkpoint." Genes Dev **20**(22): 3117-3129.

Sarikas, A., T. Hartmann and Z. Q. Pan (2011). "The cullin protein family." Genome Biol **12**(4): 220.

Sato, N., K. Arai and H. Masai (1997). "Human and *Xenopus* cDNAs encoding budding yeast Cdc7-related kinases: *in vitro* phosphorylation of MCM subunits by a putative human homologue of Cdc7." EMBO J **16**(14): 4340-4351.

Sauvageau, S., A. Z. Stasiak, I. Banville, M. Ploquin, A. Stasiak and J. Y. Masson (2005). "Fission yeast Rad51 and Dmc1, two efficient DNA recombinases forming helical nucleoprotein filaments." Mol Cell Biol **25**(11): 4377-4387.

Saxena, S., P. Yuan, S. K. Dhar, T. Senga, D. Takeda, H. Robinson, S. Kornbluth, K. Swaminathan and A. Dutta (2004). "A dimerized coiled-coil domain and an adjoining part of geminin interact with two sites on Cdt1 for replication inhibition." Mol Cell **15**(2): 245-258.

Schmidt, M. W., P. R. McQuary, S. Wee, K. Hofmann and D. A. Wolf (2009). "F-box-directed CRL complex assembly and regulation by the CSN and CAND1." Mol Cell **35**(5): 586-597.

Schwob, E. and K. Nasmyth (1993). "CLB5 and CLB6, a new pair of B cyclins involved in DNA replication in *Saccharomyces cerevisiae*." Genes Dev **7**(7A): 1160-1175.

Seeberg, E., L. Eide and M. Bjoras (1995). "The base excision repair pathway." Trends Biochem Sci **20**(10): 391-397.

Segurado, M., A. de Luis and F. Antequera (2003). "Genome-wide distribution of DNA replication origins at A+T-rich islands in *Schizosaccharomyces pombe*." EMBO Rep **4**(11): 1048-1053.

Senga, T., U. Sivaprasad, W. Zhu, J. H. Park, E. E. Arias, J. C. Walter and A. Dutta (2006). "PCNA is a cofactor for Cdt1 degradation by CUL4/DDB1-mediated N-terminal ubiquitination." J Biol Chem **281**(10): 6246-6252.

Seo, J., Y. S. Chung, G. G. Sharma, E. Moon, W. R. Burack, T. K. Pandita and K. Choi (2005). "Cdt1 transgenic mice develop lymphoblastic lymphoma in the absence of p53." Oncogene **24**(55): 8176-8186.

Sheu, Y. J. and B. Stillman (2006). "Cdc7-Dbf4 phosphorylates MCM proteins via a docking site-mediated mechanism to promote S phase progression." Mol Cell **24**(1): 101-113.

Sheu, Y. J. and B. Stillman (2010). "The Dbf4-Cdc7 kinase promotes S phase by alleviating an inhibitory activity in Mcm4." Nature **463**(7277): 113-117.

Shibutani, S. T., A. F. de la Cruz, V. Tran, W. J. Turbyfill, 3rd, T. Reis, B. A. Edgar and R. J. Duronio (2008). "Intrinsic negative cell cycle regulation provided by PIP box- and $Cul4^{Cdt2}$-mediated destruction of E2f1 during S phase." Dev Cell **15**(6): 890-900.

Shyu, Y. J., H. Liu, X. Deng and C. D. Hu (2006). "Identification of new fluorescent protein fragments for bimolecular fluorescence complementation analysis under physiological conditions." Biotechniques **40**(1): 61-66.

Slusher, L. B., E. C. Gillman, N. C. Martin and A. K. Hopper (1991). "mRNA leader length and initiation codon context determine alternative AUG selection for the yeast gene *MOD5*." Proc Natl Acad Sci U S A **88**(21): 9789-9793.

Smeets, M. F., S. Francesconi and G. Baldacci (2003). "High dosage Rhp51 suppression of the MMS sensitivity of DNA structure checkpoint mutants reveals a relationship between Crb2 and Rhp51." Genes Cells **8**(7): 573-586.

Sonoda, E., M. S. Sasaki, J. M. Buerstedde, O. Bezzubova, A. Shinohara, H. Ogawa, M. Takata, Y. Yamaguchi-Iwai and S. Takeda (1998). "Rad51-deficient vertebrate cells accumulate chromosomal breaks prior to cell death." EMBO J **17**(2): 598-608.

Soucy, T. A., P. G. Smith, M. A. Milhollen, A. J. Berger, J. M. Gavin, S. Adhikari, J. E. Brownell, K. E. Burke, D. P. Cardin, S. Critchley, et al. (2009). "An inhibitor of NEDD8-activating enzyme as a new approach to treat cancer." Nature **458**(7239): 732-736.

Spahr, H., J. Beve, T. Larsson, J. Bergstrom, K. A. Karlsson and C. M. Gustafsson (2000). "Purification and characterization of RNA polymerase II holoenzyme from *Schizosaccharomyces pombe*." J Biol Chem **275**(2): 1351-1356.

Spahr, H., C. O. Samuelsen, V. Baraznenok, I. Ernest, D. Huylebroeck, J. E. Remacle, T. Samuelsson, T. Kieselbach, S. Holmberg and C. M. Gustafsson (2001). "Analysis of *Schizosaccharomyces pombe* mediator reveals a set of essential subunits conserved between yeast and metazoan cells." Proc Natl Acad Sci U S A **98**(21): 11985-11990.

Stinchcomb, D. T., K. Struhl and R. W. Davis (1979). "Isolation and characterisation of a yeast chromosomal replicator." Nature **282**(5734): 39-43.

Styrkarsdottir, U., R. Egel and O. Nielsen (1992). "Functional conservation between *Schizosaccharomyces pombe ste8*$^{+}$ and *Saccharomyces cerevisiae STE11* protein kinases in yeast signal transduction." Mol Gen Genet **235**(1): 122-130.

Sugimoto, N., Y. Tatsumi, T. Tsurumi, A. Matsukage, T. Kiyono, H. Nishitani and M. Fujita (2004). "Cdt1 phosphorylation by cyclin A-dependent kinases negatively regulates its function without affecting geminin binding." J Biol Chem **279**(19): 19691-19697.

Sugimoto, N., T. Yugawa, M. Iizuka, T. Kiyono and M. Fujita (2011). "Chromatin remodeler sucrose nonfermenting 2 homolog (SNF2H) is recruited onto DNA replication origins through interaction with Cdc10 protein-dependent transcript 1 (Cdt1) and promotes pre-replication complex formation." J Biol Chem **286**(45): 39200-39210.

Sun, W. H., T. R. Coleman and M. L. DePamphilis (2002). "Cell cycle-dependent regulation of the association between origin recognition proteins and somatic cell chromatin." EMBO J **21**(6): 1437-1446.

Szuts, D., L. Kitching, C. Christov, A. Budd, S. Peak-Chew and T. Krude (2003). "RPA is an initiation factor for human chromosomal DNA replication." Nucleic Acids Res **31**(6): 1725-1734.

Tabtiang, R. K. and I. Herskowitz (1998). "Nuclear proteins Nut1p and Nut2p cooperate to negatively regulate a Swi4p-dependent lacZ reporter gene in *Saccharomyces cerevisiae*." Mol Cell Biol **18**(8): 4707-4718.

Tada, S., A. Li, D. Maiorano, M. Mechali and J. J. Blow (2001). "Repression of origin assembly in metaphase depends on inhibition of RLF-B/Cdt1 by geminin." Nat Cell Biol **3**(2): 107-113.

Takahashi, T. S., D. B. Wigley and J. C. Walter (2005). "Pumps, paradoxes and ploughshares: mechanism of the MCM2-7 DNA helicase." Trends Biochem Sci **30**(8): 437-444.

Takara, T. J. and S. P. Bell (2009). "Putting two heads together to unwind DNA." Cell **139**(4): 652-654.

Takara, T. J. and S. P. Bell (2011). "Multiple Cdt1 molecules act at each origin to load replication-competent Mcm2-7 helicases." EMBO J **30**(24): 4885-4896.

Takayama, Y., Y. Kamimura, M. Okawa, S. Muramatsu, A. Sugino and H. Araki (2003). "GINS, a novel multiprotein complex required for chromosomal DNA replication in budding yeast." Genes Dev **17**(9): 1153-1165.

Takayama, Y., Y. M. Mamnun, M. Trickey, S. Dhut, F. Masuda, H. Yamano, T. Toda and S. Saitoh (2010). "Hsk1- and SCF^{Pof3}-dependent proteolysis of *S. pombe* Ams2 ensures histone homeostasis and centromere function." Dev Cell **18**(3): 385-396.

Takeda, D. Y., J. D. Parvin and A. Dutta (2005). "Degradation of Cdt1 during S phase is Skp2-independent and is required for efficient progression of mammalian cells through S phase." J Biol Chem **280**(24): 23416-23423.

Takeda, T., K. Ogino, E. Matsui, M. K. Cho, H. Kumagai, T. Miyake, K. Arai and H. Masai (1999). "A fission yeast gene, $him1^{+}/dfp1^{+}$, encoding a regulatory subunit for Hsk1 kinase, plays essential roles in S-phase initiation as well as in S-phase checkpoint control and recovery from DNA damage." Mol Cell Biol **19**(8): 5535-5547.

Tanaka, S. and J. F. Diffley (2002). "Interdependent nuclear accumulation of budding yeast Cdt1 and Mcm2-7 during G1 phase." Nat Cell Biol **4**(3): 198-207.

Tanaka, S., T. Umemori, K. Hirai, S. Muramatsu, Y. Kamimura and H. Araki (2007). "CDK-dependent phosphorylation of Sld2 and Sld3 initiates DNA replication in budding yeast." Nature **445**(7125): 328-332.

Tanaka, T., D. Knapp and K. Nasmyth (1997). "Loading of an Mcm protein onto DNA replication origins is regulated by Cdc6p and CDKs." Cell **90**(4): 649-660.

Tatsumi, Y., S. Ohta, H. Kimura, T. Tsurimoto and C. Obuse (2003). "The ORC1 cycle in human cells: I. Cell cycle-regulated oscillation of human ORC1." J Biol Chem **278**(42): 41528-41534.

Tatsumi, Y., N. Sugimoto, T. Yugawa, M. Narisawa-Saito, T. Kiyono and M. Fujita (2006). "Deregulation of Cdt1 induces chromosomal damage without rereplication and leads to chromosomal instability." J Cell Sci **119**(Pt 15): 3128-3140.

Tavassoli, M., M. Shayeghi, A. Nasim and F. Z. Watts (1995). "Cloning and characterisation of the *Schizosaccharomyces pombe rad32* gene: a gene required for repair of double strand breaks and recombination." Nucleic Acids Res **23**(3): 383-388.

Terai, K., T. Abbas, A. A. Jazaeri and A. Dutta (2010). "$CRL4^{Cdt2}$ E3 ubiquitin ligase monoubiquitinates PCNA to promote translesion DNA synthesis." Mol Cell **37**(1): 143-149.

Thomae, A. W., D. Pich, J. Brocher, M. P. Spindler, C. Berens, R. Hock, W. Hammerschmidt and A. Schepers (2008). "Interaction between HMGA1a and the origin recognition complex creates site-specific replication origins." Proc Natl Acad Sci U S A **105**(5): 1692-1697.

Thomae, A. W., J. Baltin, D. Pich, M. J. Deutsch, M. Ravasz, K. Zeller, M. Gossen, W. Hammerschmidt and A. Schepers (2011). "Different roles of the human Orc6 protein in the replication initiation process." Cell Mol Life Sci **68**(22): 3741-3756.

Tsuyama, T., S. Tada, S. Watanabe, M. Seki and T. Enomoto (2005). "Licensing for DNA replication requires a strict sequential assembly of Cdc6 and Cdt1 onto chromatin in *Xenopus* egg extracts." Nucleic Acids Res **33**(2): 765-775.

Tsuyama, T., S. Watanabe, A. Aoki, Y. Cho, M. Seki, T. Enomoto and S. Tada (2009). "Repression of nascent strand elongation by deregulated Cdt1 during DNA replication in *Xenopus* egg extracts." Mol Biol Cell **20**(3): 937-947.

Varma, D., S. Chandrasekaran, L. J. Sundin, K. T. Reidy, X. Wan, D. A. Chasse, K. R. Nevis, J. G. DeLuca, E. D. Salmon and J. G. Cook (2012). "Recruitment of the human Cdt1 replication licensing protein by the loop domain of Hec1 is required for stable kinetochore-microtubule attachment." Nat Cell Biol **14**(6): 593-603.

Vas, A., W. Mok and J. Leatherwood (2001). "Control of DNA rereplication via Cdc2 phosphorylation sites in the origin recognition complex." Mol Cell Biol **21**(17): 5767-5777.

Vaziri, C., S. Saxena, Y. Jeon, C. Lee, K. Murata, Y. Machida, N. Wagle, D. S. Hwang and A. Dutta (2003). "A p53-dependent checkpoint pathway prevents rereplication." Mol Cell **11**(4): 997-1008.

Walworth, N., S. Davey and D. Beach (1993). "Fission yeast *chk1* protein kinase links the *rad* checkpoint pathway to *cdc2*." Nature **363**(6427): 368-371.

Walworth, N. C. and R. Bernards (1996). "rad-dependent response of the chk1-encoded protein kinase at the DNA damage checkpoint." Science **271**(5247): 353-356.

Warbrick, E., D. P. Lane, D. M. Glover and L. S. Cox (1997). "Homologous regions of Fen1 and $p21^{Cip1}$ compete for binding to the same site on PCNA: a potential mechanism to co-ordinate DNA replication and repair." Oncogene **14**(19): 2313-2321.

Warbrick, E. (2000). "The puzzle of PCNA's many partners." Bioessays **22**(11): 997-1006.

Waseem, N. H., K. Labib, P. Nurse and D. P. Lane (1992). "Isolation and analysis of the fission yeast gene encoding polymerase delta accessory protein PCNA." EMBO J **11**(13): 5111-5120.

Watson, A., J. Mata, J. Bähler, A. Carr and T. Humphrey (2004). "Global gene expression responses of fission yeast to ionizing radiation." Mol Biol Cell **15**(2): 851-860.

Wee, S., R. K. Geyer, T. Toda and D. A. Wolf (2005). "CSN facilitates Cullin-RING ubiquitin ligase function by counteracting autocatalytic adapter instability." Nat Cell Biol **7**(4): 387-391.

Weinreich, M. and B. Stillman (1999). "Cdc7p-Dbf4p kinase binds to chromatin during S phase and is regulated by both the APC and the RAD53 checkpoint pathway." EMBO J **18**(19): 5334-5346.

Wohlschlegel, J. A., B. T. Dwyer, S. K. Dhar, C. Cvetic, J. C. Walter and A. Dutta (2000). "Inhibition of eukaryotic DNA replication by geminin binding to Cdt1." Science **290**(5500): 2309-2312.

Wold, M. S. (1997). "Replication protein A: a heterotrimeric, single-stranded DNA-binding protein required for eukaryotic DNA metabolism." Annu Rev Biochem **66**: 61-92.

Wood, V., M. A. Harris, M. D. McDowall, K. Rutherford, B. W. Vaughan, D. M. Staines, M. Aslett, A. Lock, J. Bähler, P. J. Kersey, et al. (2012). "PomBase: a comprehensive online resource for fission yeast." Nucleic Acids Res **40**(Database issue): D695-699.

Wu, J. Q. and T. D. Pollard (2005). "Counting cytokinesis proteins globally and locally in fission yeast." Science **310**(5746): 310-314.

Wu, K., A. Chen and Z. Q. Pan (2000). "Conjugation of Nedd8 to CUL1 enhances the ability of the ROC1-CUL1 complex to promote ubiquitin polymerization." J Biol Chem **275**(41): 32317-32324.

Wu, P. Y. and P. Nurse (2009). "Establishing the program of origin firing during S phase in fission Yeast." Cell **136**(5): 852-864.

Wuarin, J., V. Buck, P. Nurse and J. B. Millar (2002). "Stable association of mitotic cyclin B/Cdc2 to replication origins prevents endoreduplication." Cell **111**(3): 419-431.

Xouri, G., Z. Lygerou, H. Nishitani, V. Pachnis, P. Nurse and S. Taraviras (2004). "Cdt1 and geminin are down-regulated upon cell cycle exit and are over-expressed in cancer-derived cell lines." Eur J Biochem **271**(16): 3368-3378.

Xu, H., P. Zhang, L. Liu and M. Y. Lee (2001). "A novel PCNA-binding motif identified by the panning of a random peptide display library." Biochemistry **40**(14): 4512-4520.

Yan, Z., J. DeGregori, R. Shohet, G. Leone, B. Stillman, J. R. Nevins and R. S. Williams (1998). "Cdc6 is regulated by E2F and is essential for DNA replication in mammalian cells." Proc Natl Acad Sci U S A **95**(7): 3603-3608.

Yanagi, K., T. Mizuno, Z. You and F. Hanaoka (2002). "Mouse geminin inhibits not only Cdt1-MCM6 interactions but also a novel intrinsic Cdt1 DNA binding activity." J Biol Chem **277**(43): 40871-40880.

Yanow, S. K., Z. Lygerou and P. Nurse (2001). "Expression of Cdc18/Cdc6 and Cdt1 during G2 phase induces initiation of DNA replication." EMBO J **20**(17): 4648-4656.

Yardimci, H., A. B. Loveland, S. Habuchi, A. M. van Oijen and J. C. Walter (2010). "Uncoupling of sister replisomes during eukaryotic DNA replication." Mol Cell **40**(5): 834-840.

Yasuhira, S. and A. Yasui (2000). "Alternative excision repair pathway of UV-damaged DNA in *Schizosaccharomyces pombe* operates both in nucleus and in mitochondria." J Biol Chem **275**(16): 11824-11828.

Yoshida, K. and I. Inoue (2004). "Regulation of Geminin and Cdt1 expression by E2F transcription factors." Oncogene **23**(21): 3802-3812.

Yoshida, K. (2007). "Geminin organizes the molecular platform to balance cellular proliferation and differentiation." Front Biosci **12**: 2984-2992.

Yoshida, S. H., H. Al-Amodi, T. Nakamura, C. J. McInerny and C. Shimoda (2003). "The *Schizosaccharomyces pombe cdt2*$^{+}$ gene, a target of G1-S phase-specific transcription factor complex DSC1, is required for mitotic and premeiotic DNA replication." Genetics **164**(3): 881-893.

You, Z. and H. Masai (2008). "Cdt1 forms a complex with the minichromosome maintenance protein (MCM) and activates its helicase activity." J Biol Chem **283**(36): 24469-24477.

Yun, D. F., T. M. Laz, J. M. Clements and F. Sherman (1996). "mRNA sequences influencing translation and the selection of AUG initiator codons in the yeast *Saccharomyces cerevisiae*." Mol Microbiol **19**(6): 1225-1239.

Zegerman, P. and J. F. Diffley (2007). "Phosphorylation of Sld2 and Sld3 by cyclin-dependent kinases promotes DNA replication in budding yeast." Nature **445**(7125): 281-285.

Zhang, M. Q. and T. G. Marr (1994). "Fission yeast gene structure and recognition." Nucleic Acids Res **22**(9): 1750-1759.

Zhong, W., H. Feng, F. E. Santiago and E. T. Kipreos (2003). "CUL-4 ubiquitin ligase maintains genome stability by restraining DNA-replication licensing." Nature **423**(6942): 885-889.

Zhou, C., V. Seibert, R. Geyer, E. Rhee, S. Lyapina, G. Cope, R. J. Deshaies and D. A. Wolf (2001). "The fission yeast COP9/signalosome is involved in cullin modification by ubiquitin-related Ned8p." BMC Biochem **2**: 7.

Zhou, C., S. Wee, E. Rhee, M. Naumann, W. Dubiel and D. A. Wolf (2003). "Fission yeast COP9/signalosome suppresses cullin activity through recruitment of the deubiquitylating enzyme Ubp12p." Mol Cell **11**(4): 927-938.

Zhu, J., C. S. Newlon and J. A. Huberman (1992). "Localization of a DNA replication origin and termination zone on chromosome III of *Saccharomyces cerevisiae*." Mol Cell Biol **12**(10): 4733-4741.

APPENDICES

APPENDIX I: MEDIA

Media was made with distilled water (Millipore Elix UV 3 water purification system) and sterilised by autoclaving (Prestige Medical).

LB (Luria-Bertani) medium

10 g/l BD Bacto Tryptone

5 g/l BD Bacto Yeast Extract

10 g/l NaCl

1.5% BD Bacto Agar was added for solid media. Where appropriate, ampicillin was added to a final concentration of 100-150 µg/ml from a stock solution of 50 mg/ml.

YE3S (Yeast extract plus 3 supplements)

5 g/l BD Bacto Yeast Extract

30 g/l glucose

0.75 g/l 3S supplement stock (1:1:1 of adenine, leucine and uracil)

2% BD Agar was added for solid media.

YE3S plus G-418: G-418 was added to a final concentration of 150 µg/ml from a stock solution of 100 mg/ml. YE3S plus hygromycin B: hygromycin B was added to a final concentration of 200 µg/ml from a stock solution of 200 mg/ml. YE3S plus ClonNat (nourseothricin): ClonNat was added to a final concentration of 200 µg/ml from a stock solution of 200 mg/ml.

Where appropriate, additional supplements (L-histidine, arginine and L-lycine) were added to a final concentration of 225 mg/l to make YE6S.

EMM (Edinburgh Minimal Medium)

3 g/l $C_8H_5KO_4$

2.2 g/l Na_2HPO_4

5 g/l NH_4Cl

20 g/l glucose

20 ml/l salts (from a 50x stock)

1 ml/l vitamins (from a 1000x stock)

0.1 ml/l minerals (from a 10000x stock)

0.1 ml/l NaOH (10 M stock)

2% BD Agar was added for solid media.

Note EMM minus nitrogen medium was made as above but without 5 g/l NH_4Cl.

Salts Stock (50x)

52.5 g/l $MgCl_2.6H_2O$, 0.74 g/l $CaCl_2.2H_2O$, 50 g/l KCl, 2 g/l Na_2SO_4

Vitamins Stock (1000x)

1 g/l pantothenic acid, 10 g/l nicotinic acid, 10 g/l inositol, 10 mg/l biotin

Minerals Stock (10000x)

5 g/l H_3BO_3, 4 g/l $MnSO_4$, 4 g/l $ZnSO_4.7H_2O$, 2 g/l $FeCl_2.6H_2O$, 0.4 g/l $H_2MBO_4.H_20$, 1 g/l KI, 0.4 g/l $CuSO_4.5H_2O$, 10 g/l citric acid

Supplements of adenine, leucine and uracil were added to a final concentration of 225 mg/l from stock solutions as required. Adenine and leucine stock solutions were prepared at 7.5 g/l and uracil stock solution was prepared at 3.75 g/l. Thiamine was added to EMM media to repress the *nmt1* promoter. Thiamine was generally added to a final concentration 10 μg/ml from a stock solution of 10 mg/ml. The thiamine stock

solution was filter sterilized and kept in the dark at 4°C.

EMMG (*S. pombe* sporulation medium)

3 g/l $C_8H_5KO_4$

2.2 g/l Na_2HPO_4

1g/l sodium glutamate

20 g/l glucose

20 ml/l salts (from a 50x stock)

1 ml/l vitamins (from a 1000x stock)

0.1 ml/l minerals (from a 10000x stock)

0.5 g/l 3S supplement stock (1:1:1 of adenine, leucine and uracil)

2% BD Agar was added for solid media.

APPENDIX II: PLASMID AND *S. POMBE* STRAIN CONSTRUCTION

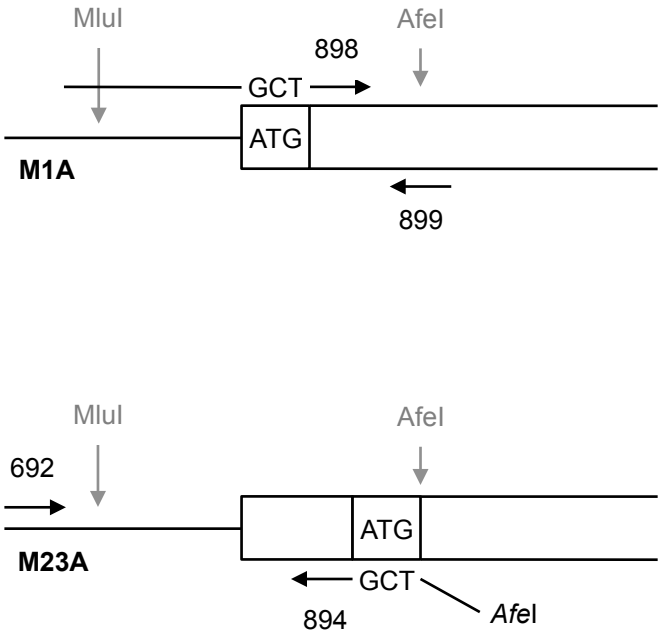
1. *mcm4pr/cdt1(control)-myc* and *mcm4pr/cdt1*Δ100-*myc* plasmids

The *mcm4pr/cdt1(control)-myc* (p780) and *mcm4pr/cdt1*Δ100-*myc* (p808) plasmids were constructed by amplifying *cdt1(control)* and *cdt1*Δ*100* sequences as *Xho*I/*Nhe*I fragments, from plasmid DNA (p776), using oligonucleotide primer pairs 752 + 753 and 754 + 753 respectively. The PCR products were inserted into *Xho*I and *Nhe*I cleaved *mcm4pr/cdt1(WT)-myc* (p776) and each construct was sequenced using primer 792. Note that the sequence AAAATG was included downstream of the *XhoI* site in both the *cdt1(control)* and *cdt1*Δ*100* sequences to optimise utilisation of the initiator codon. The resulting plasmids (p780 and p808) were linearized by *Pac*I digestion and integrated at the endogenous *mcm4* promoter. Correct integration was confirmed by colony PCR, using primers 628 and 452.

2. *cdt1pr/cdt1M1A-YFP* and *cdt1pr/cdt1M23A-YFP* plasmids

The *cdt1pr/cdt1M1A-YFP* (p849) and *cdt1pr/cdt1M23A-YFP* (p846) plasmids were constructed by amplifying the N-terminus of $cdt1^+$ as an *Mlu*I/*Afe*I fragment, using oligonucleotide primers that introduced a mutation at the appropriate methionine residue (see diagram below). The M1A and M23A mutations were introduced using primer pairs 898 + 899 and 692 + 894 respectively, with wildtype *S. pombe* genomic DNA used as a template. The PCR products were inserted into *Mlu*I and *Afe*I cleaved *cdt1pr/cdt1(WT)-YFP* (p818) and each construct was sequenced using primer 896. The resulting plasmids (p849 and p846) were linearized by *Stu*I digestion and integrated at the endogenous $ura4^+$ locus. Correct integration was confirmed by colony PCR, using primers 627 and 626.

Construction of the Cdt1M1A and Cdt1M23A mutations:



3. *cdt1pr/cdt1(WT/M1A/M23A)N-terminus* plasmids

The *cdt1pr/cdt1(WT)N-terminus* (p931), *cdt1pr/cdt1(M1A)N-terminus* (p932) and *cdt1pr/cdt1(M23A)N-terminus* (p933) plasmids were constructed to enable single copy integration of the *cdt1M1A* and *cdt1M23A* sequences. A *Xho*I/*BamH*I fragment consisting of the *cdt1* promoter plus the wildtype or mutated *cdt1* N-terminal sequence was amplified from plasmid DNA (WT, p818; M1A, p849; M23A, p846), using the primer pair 679 + 682. The PCR products were inserted into *Xho*I and *BamH*I cleaved pSMHC2+*mcm2* (p699; the *mcm2* and *CFP* reading frames removed by the restriction enzyme digest). The resulting plasmids (WT, p931; M1A, p932; M23A, p933) were linearized with *Msc*I and integrated at the endogenous *cdt1* promoter of a *cdt1-TAP* strain. Correct integration was confirmed using the primer pair 619 + 685. Plasmid and yeast transformants were sequenced using primer 692.

4. pREP3x-*cdt1-GFP* plasmid

The pREP3x-*cdt1-GFP* plasmid (p934) was constructed in two cloning steps. First, the *cdt1* promoter and reading frame, plus a GA-rich linker sequence, were amplified as a *BamH*I/*Pac*I fragment from wildtype *S. pombe* genomic DNA, using the primer pair 947 + 1115. The PCR product was inserted into *BamH*I and *Pac*I cleaved pFA6a-*GFP* (p319) and the resulting plasmid (p937) was sequenced using primers 896, 527 and 529. Second, the *cdt1-GFP* reading frame was amplified as a *BamH*I/*Pac*I fragment from pFA6a-*cdt1pr/cdt1-GFP* (p937) plasmid DNA, using the primer pair 1114 + 1110. The PCR product was inserted into *BamH*I and *Xma*I cleaved pREP3x (p635) and the resulting plasmid (p934) was sequenced using primers 527, 529, 1111 and 1112 and transformed into a *leu1-32* fission yeast strain.

5. pREP3x-*cdt1M1A-GFP* and pREP3x-*cdt1M23A-GFP* plasmids

The pREP3x-*cdt1M1A-GFP* (p935) and pREP3x-*cdt1M23A-GFP* (p936) plasmids were constructed by amplifying the *cdt1M1A* or *cdt1M23A* N-terminal sequence from plasmid DNA (M1A, p849; M23A, p846) using the primer pairs 1113 + 452 and 1114 + 452 respectively. The PCR products were inserted into *BamH*I and *Spe*I cleaved pREP3x-*cdt1-GFP* (p934). The resulting plasmids (p935 and p936) were sequenced using primers 1111 and 527 and transformed into a *leu1-32* fission yeast strain.

6. *cdt1pr/cdt1(WT)-myc* and *cdt1pr/cdt1Δ26-100-myc* plasmids

The *cdt1pr*/*cdt1(WT)-myc* plasmid (p790) was constructed by amplifying the *cdt1* promoter as an *Apa*I/*Nhe*I fragment, from wildtype *S. pombe* genomic DNA, using the primer pair 815 + 816. The PCR product was inserted into *Apa*I and *Nhe*I cleaved *mcm4pr/cdt1(WT)-myc* (p776). The functionality of the resulting plasmid (p790) was confirmed by *PflF*I digestion and integration at the endogenous *cdt1* promoter of a

*cdt1*Δ [*nmt1-cdt1*$^{+}$] strain (1239), where its ability to relieve the thiamine-sensitivity of the strain was assessed (Figure 4.1B). The *cdt1pr*/*cdt1*Δ*26-100-myc* plasmid (p804) was constructed by amplifying the *cdt1*Δ*26-100* sequence as an *Afe*I/*Nhe*I fragment, from wildtype *S. pombe* genomic DNA, using the primer pair 817 + 753. The PCR product was inserted into *Afe*I and *Nhe*I cleaved *cdt1pr/cdt1(WT)-myc* (p798) and the construct was sequenced using primers 529 and 692. The resulting plasmid (p804) was linearized by *Stu*I digestion and integrated at the endogenous *ura4*$^{+}$ locus. Correct integration was confirmed by colony PCR, using primers 627 and 626.

7. *cdt1pr/cdt1(WT)-YFP* and *cdt1pr/cdt1*Δ*26-100-YFP* plasmids

The *cdt1pr/cdt1(WT)-YFP* (p818) and *cdt1pr/cdt1*Δ*26-100-YFP* (p819) plasmids were constructed by amplifying the C-terminus of *cdt1*$^{+}$ and the full-length *YFP* sequence from a *cdt1-YFP* plasmid (p740), as an *Nhe*I/*Sac*I fragment, using the primer pair 863 + 864. The PCR product was inserted into *Nhe*I and *Sac*I cleaved *cdt1pr/ cdt1(WT)-myc* (p798) and *cdt1pr/ cdt1*Δ*26-100-myc* (p804) and each construct was sequenced using primers 529 and 438. The resulting plasmids (p818 and p819) were linearized by *Stu*I digestion and integrated at the endogenous *ura4*$^{+}$ locus. Correct integration was confirmed by colony PCR, using primers 627 and 626.

8. *cdt1pr/cdt1*Δ*26-100-YFP-2x NLS* plasmid

The *cdt1pr/cdt1*Δ*26-100-YFP-2x NLS* plasmid (p822) was constructed using two complementary oligonucleotides (873 and 874), which were annealed and inserted directly into *BamH*I and *Sac*I cleaved *cdt1pr/cdt1*Δ*26-100-YFP* (p819) to introduce the *2x NLS* sequence. The oligonucleotides were annealed by mixing in equal quantities, boiling for 5 minutes, holding at 65°C for 10 minutes and then cooling to room temperature. The resulting plasmid (p822) was sequenced using primer 438,

linearized by *Stu*I digestion and integrated at the endogenous *ura4*$^{+}$ locus. Correct integration was confirmed by colony PCR, using primers 627 and 626.

9. Large-scale Cdt1 truncation mutants

The large-scale Cdt1 truncation mutants were constructed by amplifying the *cdt1* sequence with the appropriate deletion as an *Afe*I/*Nhe*I fragment from wildtype *S. pombe* genomic DNA and inserting the PCR product into *Afe*I and *Nhe*I cleaved *cdt1pr/cdt1Δ26-100-YFP-2x NLS*. The primers pairs used for each deletion were: *cdt1Δ26-200*, 818 + 753; *cdt1Δ26-300*, 878 + 753; *cdt1Δ26-400*, 879 + 753; *cdt1Δ26-316*, 900 + 753. The *cdt1Δ390-444* sequence was constructed using complementary oligonucleotides 880 and 881, which were annealed and inserted directly into *Mfe*I and *Xma*I cleaved *cdt1pr/cdt1(WT)-YFP* (p818) to introduce the deletion. The resulting *cdt1Δ26-200* (p827) and *cdt1Δ390-444* (p832) plasmids were sequenced using primers 879 and 529 respectively. The resulting *cdt1Δ26-300* (p828), *cdt1Δ26-400* (p829) and *cdt1Δ26-316* (p847) plasmids were sequenced using primer 692. Note that in p829 there was an amino acid substitution (Q to R) at residue 433 in the *cdt1* sequence. The plasmids were linearized by *Stu*I digestion and integrated at the endogenous *ura4*$^{+}$ locus. Correct integration was confirmed by colony PCR, using primers 627 and 626.

10. PIP28^{A8}, PIP301^{A10} and PIP28^{A8} PIP301^{A10} mutants

The PIP28^{A8} and PIP301^{A10} mutations were introduced into the wildtype *cdt1* sequence by site-directed mutagenesis. The original PIP28^{A8} mutant was constructed by Estrella Guarino and is described in Guarino *et al*. (2011). The PIP301^{A10} mutant was constructed using two partially complementary fragments, which were amplified from *S. pombe* genomic DNA using the primer pairs 684 + 903 and 904 + 753, and

which contained the PIP301^{A10} mutation and *Afe*1 or *Nhe*1 restriction sites. The two partially complementary fragments were annealed and amplified to produce the full-length PIP301^{A10} fragment, which was inserted into an *Afe*1 and *Nhe*1 cleaved *cdt1pr/cdt1*-YFP plasmid (p818). The resulting plasmid (p856) was sequenced using primers 692 and 528. The *cdt1pr/cdt1PIP28^{A8}-YFP* (p855) and *cdt1pr/cdt1PIP28^{A8} PIP301^{A10}-YFP* (p857) plasmids were constructed by amplifying the *cdt1PIP28^{A8}* N-terminus as an *Afe*I/*Xba*I fragment, from *S. pombe* genomic DNA extracted from strain 2237, using the primer pair 692 + 749. The PCR product was inserted into *Afe*I and *Xba*I cleaved *cdt1pr/cdt1-YFP* (p818) and *cdt1pr/cdt1PIP301^{A10}-YFP* (p856). The resulting plasmids (p855 and p857) were sequenced using primers 692 and 58. All three plasmids were linearized by *Stu*I digestion, integrated at the endogenous *ura4*$^{+}$ locus and correct integration was confirmed by colony PCR, using primers 627 and 626.

11. BiFC strains

The *VN173-pcn1* (2535) strain was constructed by Israel Salguero and is described in Guarino *et al*. (2011). To construct *cdt1-VC155* wildtype and PIP mutant strains, a *BamH*I/*Pac*I fragment consisting of the *cdt1* promoter plus the wildtype or PIP mutant *cdt1* sequence was amplified from plasmid DNA (WT, p818; PIP28^{A8}, p855; PIP301^{A10}, p856; PIP28^{A8} PIP301^{A10}, p857) using the primer pair 947 + 948. The PCR products were cloned into pFA6a-*VC155* (p841) at *BamH*I and *Pac*I restriction enzyme sites and the resulting plasmids (WT, p883; PIP28^{A8}, p884; PIP301^{A10}, p885; PIP28^{A8} PIP301^{A10}, p886) were linearized by *Nsi*I digestion and integrated as a second copy at the endogenous *cdt1* promoter. Correct integration was confirmed by colony PCR, using the primers 627 and 626. Plasmids and yeast transformants were sequenced using primers 896, 527 and 529.

APPENDIX III: OLIGONUCLEOTIDE PRIMERS USED IN THIS STUDY

Number	Primer	Sequence (5' to 3')
58	3' YFP	ACAGCTCCTCGCCCTTGCTCACCAT
438	5’ YFP	CTCGTGACCACCTTCGGCTACGGCC
452	3’ cdt1	CTCGCGACTTGTTGATTTCTCCAAATTGAG
527	5’ cdt1seqprimer2	CGGCCATTATTGAGCCACCC
528	5’ cdt1seqprimer3	ATGAACTGTCATACCCTCGC
529	5’ cdt1seqprimer4	CCACTTTGTCAAAGTCAGTG
530	5’ cdt1seqprimer5	CTTATCACCTGACCAGTGTG
619	5’ pSMupin	CCGGCTCGTATGTTGTGTGGAATTGTG
626	3’ pSMUinttest	CCTAAAGGGAGCCCCCGATTTAGAGC
627	5’ ura4upin	TGATTCCATACATTAAATGGATAAAACTCCTGAAGC
628	5’ mcm4upin	CTCTAATATTTGAAGCTGATTTATCAAGCCGCA
679	5’ Xho1-cdt1	AAACTCGAGTCGAGTGAGTGAAAACCTTCGAAAATAGAGCTT
682	3’ BamHI-cdt1	AAAGGATCCGGGAGAAGGCTTCAGGAAGATTCGCATTG
684	5’ cdt1wtPIP	TCATGAGCGCTGGATCGCAAACAAAATTG
685	3’ checkCdt1PIP	ATTTTTCTAGTCTCCGTTTAAATTCAATGGAGCG
692	5’ cdt1DELseq	CTAAGTAAGACATAAACTGATTAGTCGG
749	3’ cdt1	GCACGCGATCGAACAGAGAA
752	5’ Xho1-cdt1 (control)	TTTCTCGAGAAAATGAAATGTCGCGCCCTATATAGT
753	3’ Nhe1-cdt1	TTTGCTAGCCTTTGTTTGCAATTCTTCAATTAATTGG
754	5’ XhoI-cdt1Δ100	TTTCTCGAGAAAATGGACATATGTGTAAAATTTCACCTCTCCATC
792	5’ mcm4pr	CTGGTAGCTTGATGATCAATGGAGAATATG
815	5’ ApaI-cdt1pr	TTTGGGCCCTCGAGTGAGTGAAAACCTTCGAAAATAGAGCTT
816	3’ cdt1	GAT GAG GAT CGA GTT TTA CGG ACA GAG
817	5’ AfeI-cdt1Δ26-100	TTTAGCGCTGTCGACATATGTGTAAAATTTCACCTCTCCATC
818	5’ AfeI-cdt1Δ26-200	TTTAGCGCTGAGATTCCTGCTCAACAGTTACAAGCTTTAC
863	5’ cdt1Cterm	GGGAAACCATACTTGCGATCCCAATTAATTG
864	3’ YFP-Sac1	TTTGAGCTCTCAGGATCCGTCGACCTTGTACAG
873	5’ BamH1-NLS-Sac1	GATCCCCTAAGAAAAAACGAAAAGTTGAAGACCCTAAAAAGAAACGAAAAGTTGATTAAGAGCT
874	3’ BamH1-NLS-Sac1	CTTAATCAACTTTTCGTTTCTTTTTAGGGTCTTCAACTTTTCGTTTTTTCTTAGGG
878	5’ AfeI-cdt1Δ26-300	TTTAGCGCTCAGTTAACTTTGAGACAATCTTCTCTGTTCGAT
879	5’ AfeI-cdt1Δ26-400	TTTAGCGCTTGCACTATCAATCTTCTTGGTAATATTCAAGTAGTCA
880	5’ cdt1Δ390-444	AATTGCCGGAGCTGGTGCCGGGGC
881	3’ cdt1Δ390-444	CCGGGCCCCGGCACCAGCTCCGGC
894	3’ cdt1M23A	ATCCAGCGCTAGCGATTTGAACACAAAATCCAAAAATAAGGATATTGTTGTCG

Number	Primer	Sequence (5' to 3')
896	5’ cdt1pr	GCAGAGCAAAGGAGTTATTCAAAATTTATATAACGATG
898	5’ cdt1M1A	ACGCGACGCGTCAACAAACGCGACACGCTCAAATTTAA TATAACCCTCGATATAAGCTAAATGTCGCGCCCTATATA G
899	3’ cdt1Nterm	CAATTTTGTTTGCGATCCAGCGCTCATG
900	5’ cdt1Δ26-316	TTTAGCGCTCAAAAAGCAATGGAAGCAAAAAAAGCTGA AGAATTTAAAAAC
903	3’ MPIP301^{A10}	TGCAGCCGCCACTGCATCGAACAGAGCCGCTGCAGCC GCAGTTAAAGCAGATGATGTTAGCTTACGCGATGAATT TTGAACA
904	5’ MPIP301^{A10}	GCTTTAACTGCGGCTGCAGCGGCTCTGTTCGATGCAG TGGCGGCTGCACAAAAAGCAATGGAAGCAAAAAAAGC TGAAGAATTTAAAAAC
947	5’ BamHI-cdt1pr	TTTGGATCCATCGGTCCTTATAGATATTTGAGTCACATT GTTACT
948	3’ cdt1-PacI	TTTTTAATTAAAGAATTTGAAAGAATAGTGATGCTAGCC TTTGTTTG
1110	3’ GFP-XmaI	TTTCCCGGGCTATTTGTATAGTTCATCCATGCCATGTGT AA
1111	5’ Nmt1pr	GGGGAGAGAAAACAGGGCAAAAGCAAA
1112	5’ GFPseq	GGAGAAGAACTTTTCACTGGAGTTGTCC
1113	5’ BamHI-cdt1M1A	AAAGGATCCTATAAGCTAAATGTCGCGCCCTATATAGT CACGAC
1114	5’ BamHI-cdt1	AAAGGATCCTATAAATGAAATGTCGCGCCCTATATAGT CACGA
1115	3’ cdt1-GA-PacI	TTTTTAATTAAAGCACCAGCACCGGCTCCGGCACCAGC ACCAGAATTTGAAAGAATAGTGATGCTAGCCTTTGTTT G

APPENDIX IV: MATLAB ANALYSIS OF THE *S. POMBE* DELETION LIBRARY IMAGE DATASET

The MATLAB code detailed in this section was developed and employed by Simon Li to detect and quantitate the intensity of nuclear fluorescence per strain in the *S. pombe* deletion library image dataset.

An overview of MATLAB code for the detection and quantitation of *S. pombe* nuclear fluorescence:

1. Read in the three channels of a microscopy image (Phase, YFP and DAPI) to MATLAB.
2. Detect the nuclei in the DAPI image: Gaussian filter the image such that the DAPI stained nuclei are converted to local maxima. Use morphological opening to remove false detections of spots that are smaller than the expected nucleus size. The result of this step is a binary image of potential nuclei.
3. Some false detections of nuclei remain due to variations in background intensity and these are removed by applying an intensity threshold.
4. Specify a fixed mask for the nucleus (radius of 5.5 pixels). Find the centre of each nucleus detected in the previous step and apply the mask, exclude nuclei that are too close to the edge of the image. Note that this code also includes instructions to specify and apply a fixed mask to detect cytoplasmic fluorescence intensity, enabling a nuclear to cytoplasmic ratio of fluorescence intensity to be calculated. However, this ratio was not subsequently used in the analysis of the *S. pombe* deletion library image dataset.
5. Apply the fixed mask to the YFP image and calculate the area and intensity of fluorescence at each nucleus.

6. Estimate the background intensity: threshold the phase image to identify the cell outlines. Create a mask identifying which areas are occupied by cells and apply this mask to the YFP image. This enables identification of the background area not occupied by cells. The mean fluorescence intensity value of this background area can then be used as an estimate of background intensity.
7. Save the program output.
8. A separate code can then be used to compile summary statistics from each image, including the mean nuclear fluorescence intensity and the percentile values of nuclear fluorescence intensity, with or without the background intensity estimate subtracted.

MATLAB code for the detection and quantitation of *S. pombe* nuclear fluorescence:

```
% Process an S. pombe image
%
% $Id: analyse_pombe.m 976 2010-12-21 17:16:03Z simon $
function [marker im mask] = analyse_pombe(filename, save_stem)
%DEBUG = true;
do_save = nargin > 1 && ~isempty(save_stem);

%%
tif = tiffread27(filename);
if length(tif) == 3
   im.phase = tif(1).data;
   im.marker = tif(2).data;
   im.dna = tif(3).data;
elseif length(tif) == 1
   im.dna = tif.data;

   tif = tiffread27(strrep(filename, 'DAPI', 'YFP'));
   assert(length(tif) == 1);
   im.marker = tif.data;

   tif = tiffread27(strrep(filename, 'DAPI', 'Phase'));
   assert(length(tif) == 1);
   im.phase = tif.data;
else
   error('Unexpected number of channels in tif');
end
```

```
im.sz = size(im.dna);
sigma = 5 * 2;
se1 = strel('disk', 5);

% DNA blue, Marker yellow
n01 = @(a)normalise01(double(a));
imagesc(cat(3, n01(im.marker), n01(im.marker), n01(im.dna)));

%% Find the nuclei locations: Gaussian filter, morphologically open, find maxima
%  Use edge replication to handle case where background levels are far from zero
%  (previous images assumed background was near zero so dark edges after filtering weren't
a problem)
im.dnaf = gaussian_filter(im2double(im.dna), sigma * 3, sigma, true);
im.dnaf = normalise01(im.dnaf);
im.imo = imopen(im.dnaf, se1);
im.nuclei1 = imregionalmax(im.imo);

%% Intersect with an Otsu threshold to remove spurious background maxima. Unfortunately
this also removes some valid nuclei
%  Though thresholding the filtered image seems to pick up more
%  If there's a lot of noise Otsu fails (no valley in histogram) so set a minimum of 0.5
[im.level im.em] = graythresh(im.dnaf);
%im.otsu = im2bw(im.dnaf, max(im.level, .5));
im.otsu = im2bw(im.dnaf, im.level);
im.otsuo = imdilate(im.otsu, se1);
im.nuclei2 = im.nuclei1 & im.otsuo;

%% Display the image with nuclei mask in red
imdisp.r = normalise01(double(im.dna));
imdisp.gb = imdisp.r;
imdisp.r(im.nuclei2) = 1;
imdisp.gb(im.nuclei2) = 0;
imdisp.rgb = cat(3, imdisp.r, imdisp.gb, imdisp.gb);
imagesc(imdisp.rgb);

%% Precalculate a fixed mask for a nucleus and cytoplasm (half width)
% The extra .5 makes things more rounded
bodge = 0;
hw = 10 + bodge;
nuc_r = 5.5;
cyto_r1 = 8.5 + bodge;
cyto_r2 = 10.5 + bodge;

[xs ys] = meshgrid(-hw:hw);
rs = xs .^ 2 + ys .^ 2;
mask.nuc = rs < nuc_r ^ 2;
mask.cyto = rs > cyto_r1 ^ 2 & rs < cyto_r2 ^ 2;

mask.area.nuc = sum(mask.nuc(:));
mask.area.cyto = sum(mask.cyto(:));
```

```
%disp([sum(mask.nuc(:)) sum(mask.cyto(:))]);

%% Get the marker intensities for each nucleus
[L nL] = bwlabel(im.nuclei2);

%% Find centers of each nucleus and apply the mask
% If we assume the result from imregionalmax is convex we can use the ultimate erosion

nuclei2_cs = bwulterode(im.nuclei2);
[im.cys im.cxs] = find(nuclei2_cs);
hw2 = -hw:hw;

if length(im.cys) ~= nL
   warning('Pombe:NucleiLocations', ...
      'Discrepancy between labeled nuclei and ultimate erosion');
end
%mask.all_nuc = zeros(im.sz);
%mask.all_cyto = zeros(im.sz);
mask.all_nuc = false(im.sz);
mask.all_cyto = false(im.sz);

% Is this too close to the edge?
marker.valid = false(nL, 1);
% Nuclear and cytoplasmic total intensities and areas
marker.nuc.sums = nan(nL, 1);
marker.nuc.areas = nan(nL, 1);
marker.cyto.sums = nan(nL, 1);
marker.cyto.areas = nan(nL, 1);

im_marker = double(im.marker(:));

for n = 1:nL
   disp(n);
   cx = im.cxs(n);
   cy = im.cys(n);

   %marker.valid is already false so only need to handle the true case
   if cx > hw && cy > hw && cx <= (im.sz(2) - hw) && cy <= (im.sz(1) - hw)
      %mask.all_nuc(cy + hw2, cx + hw2) = mask.nuc * n;
      %mask.all_cyto(cy + hw2, cx + hw2) = mask.cyto * n;
      mask.all_nuc(cy + hw2, cx + hw2) = mask.all_nuc(cy + hw2, cx + hw2) | mask.nuc;
      mask.all_cyto(cy + hw2, cx + hw2) = mask.all_cyto(cy + hw2, cx + hw2) | mask.cyto;

      mn = false(im.sz);
      mc = false(im.sz);

      mn(cy + hw2, cx + hw2) = mask.nuc;
      mc(cy + hw2, cx + hw2) = mask.cyto;

      mn = mn(:);
      mc = mc(:);
```

```
        %marker.nuc.areas(n) = sum(mn);
        marker.nuc.areas(n) = mask.area.nuc;
        marker.nuc.sums(n) = sum(im_marker(mn));

        %marker.cyto.areas(n) = sum(mc);
        marker.cyto.areas(n) = mask.area.cyto;
        marker.cyto.sums(n) = sum(im_marker(mc));

        marker.valid(n) = true;
    end

    drawnow;
end

% Now discard all invalid elements
marker.nuc.areas(~marker.valid) = [];
marker.nuc.sums(~marker.valid) = [];
marker.cyto.areas(~marker.valid) = [];
marker.cyto.sums(~marker.valid) = [];

%display_label_overlay(im.dna, mask.all_nuc + mask.all_cyto * 2);

marker.nuc.means = marker.nuc.sums ./ marker.nuc.areas;
marker.cyto.means = marker.cyto.sums ./ marker.cyto.areas;

%% Estimate the background intensity
se2 = strel('disk', 15);

bg = im2bw(im.phase, graythresh(im.phase)) | mask.all_cyto;
bg = imdilate(bg, se2);
mask.bg = ~imfill(bg, 'holes');

marker.bgavg = mean(im.marker(mask.bg));
marker.bgprc1 = prctile(double(im.marker(:)), 1);


%% Display the image with nuclei and cytoplasm masks overlaid in red,
%  background in blue
imdisp.r = n01(im.dna);
imdisp.g = imdisp.r;
imdisp.b = imdisp.r;
imdisp.r(mask.all_nuc | mask.all_cyto) = 1;
imdisp.b(mask.bg) = .5;
imdisp.rgb1 = cat(3, imdisp.r, imdisp.g, imdisp.b);
imdisp.rgb1 = imresize(imdisp.rgb1, 1 / 3, 'bilinear');
imagesc(imdisp.rgb1);

%%
imdisp.r = n01(im.marker);
imdisp.gb = imdisp.r;
imdisp.r(imdilate(nuclei2_cs, ones(5))) = 1;
imdisp.gb(imdilate(nuclei2_cs, ones(5))) = 0;
```

```
imdisp.rgb2 = cat(3, imdisp.r, imdisp.gb, imdisp.gb);
imdisp.rgb2 = imresize(imdisp.rgb2, 1 / 3, 'bilinear');
imagesc(imdisp.rgb2);

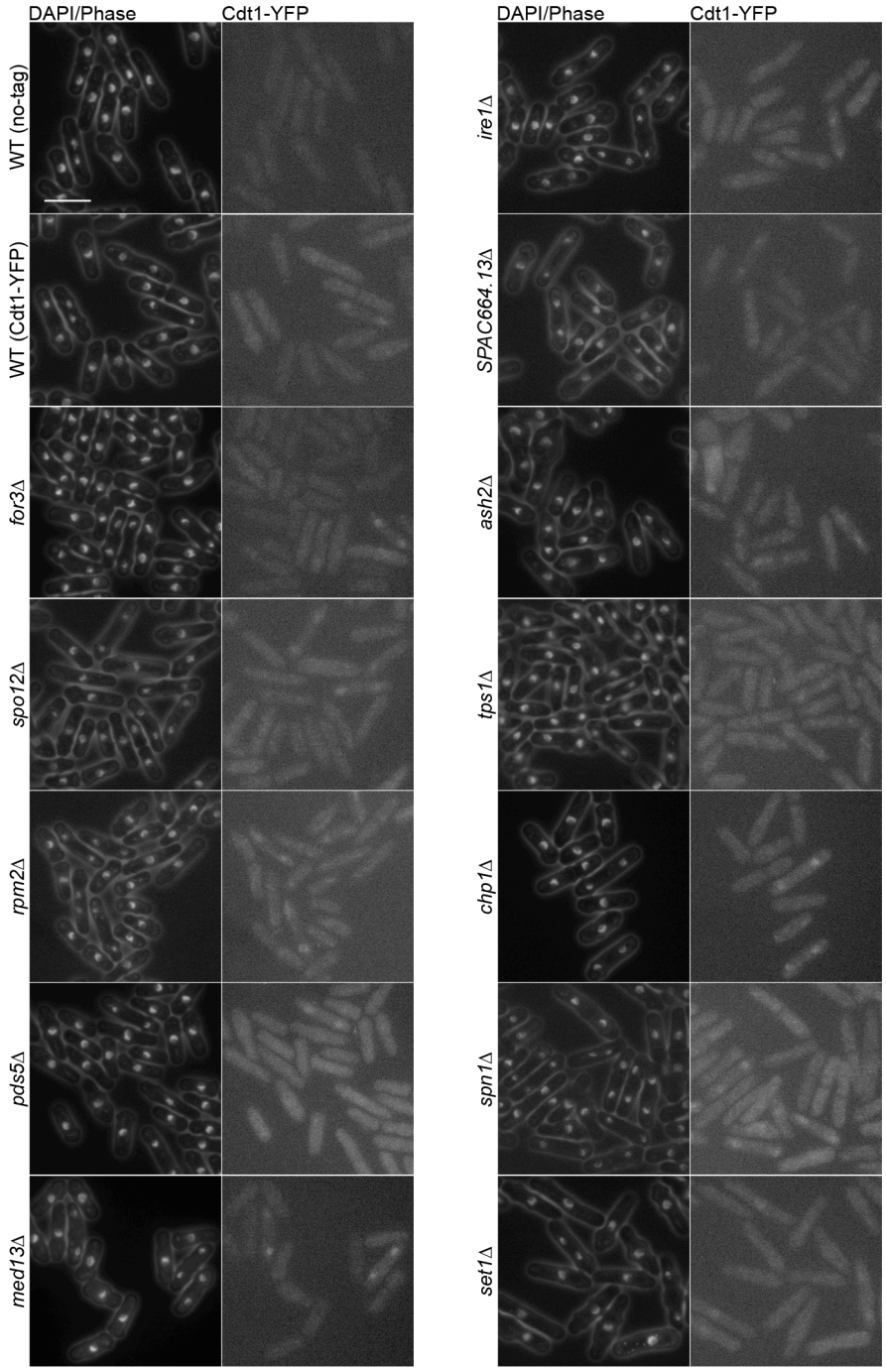

%%
if do_save
    fmt = 'png';
    imwrite(imdisp.rgb1, [save_stem '-nuclei.' fmt], fmt);
    imwrite(imdisp.rgb2, [save_stem '-marker.' fmt], fmt);

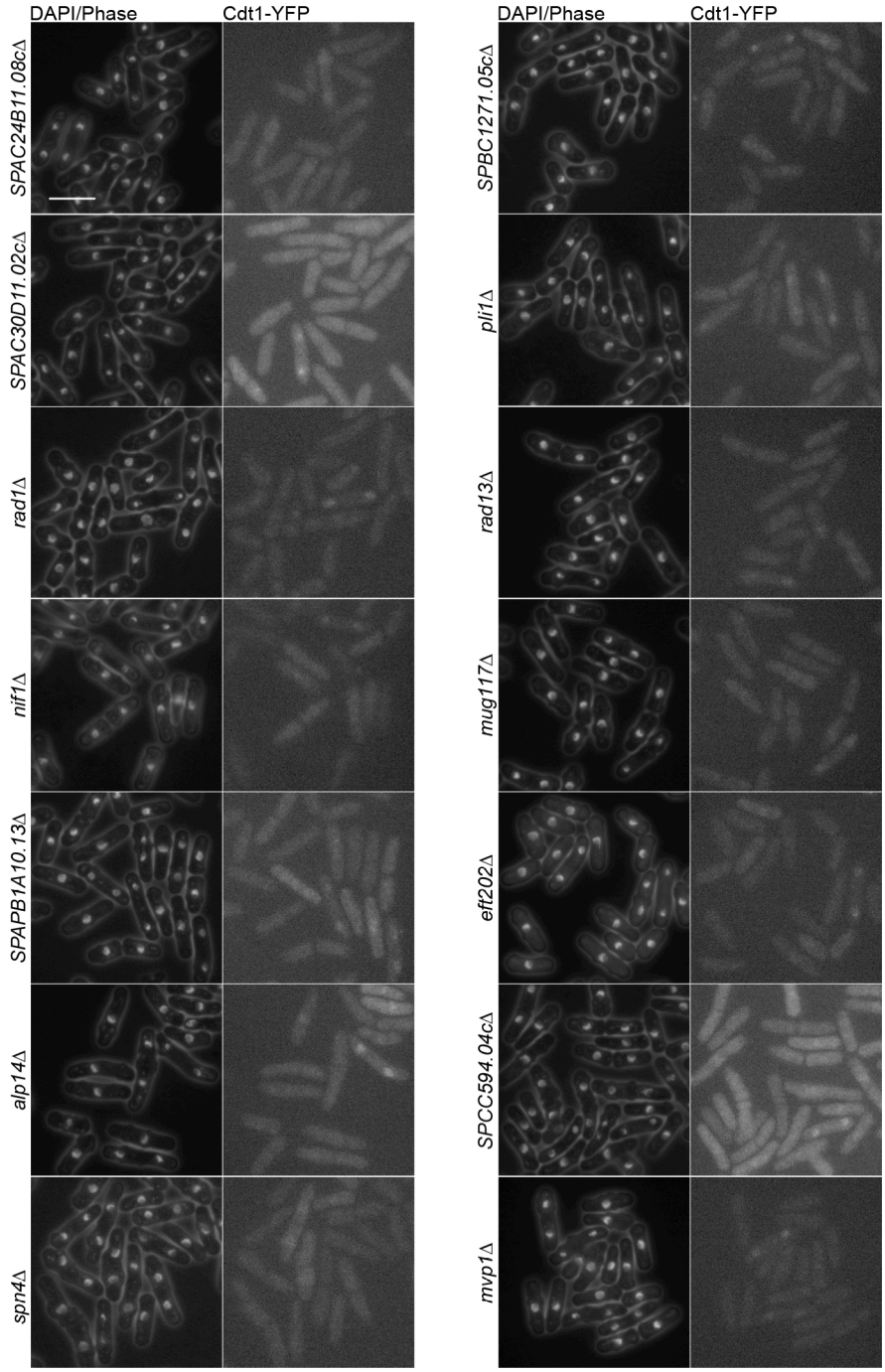
    tosave.filename = filename;
    tosave.marker = marker;
    tosave.mask = mask;
    tosave.im.dna = im.dna;
    tosave.im.marker = im.marker;
    tosave.im.phase = im.phase;
    save([save_stem '.mat'], '-struct', 'tosave');

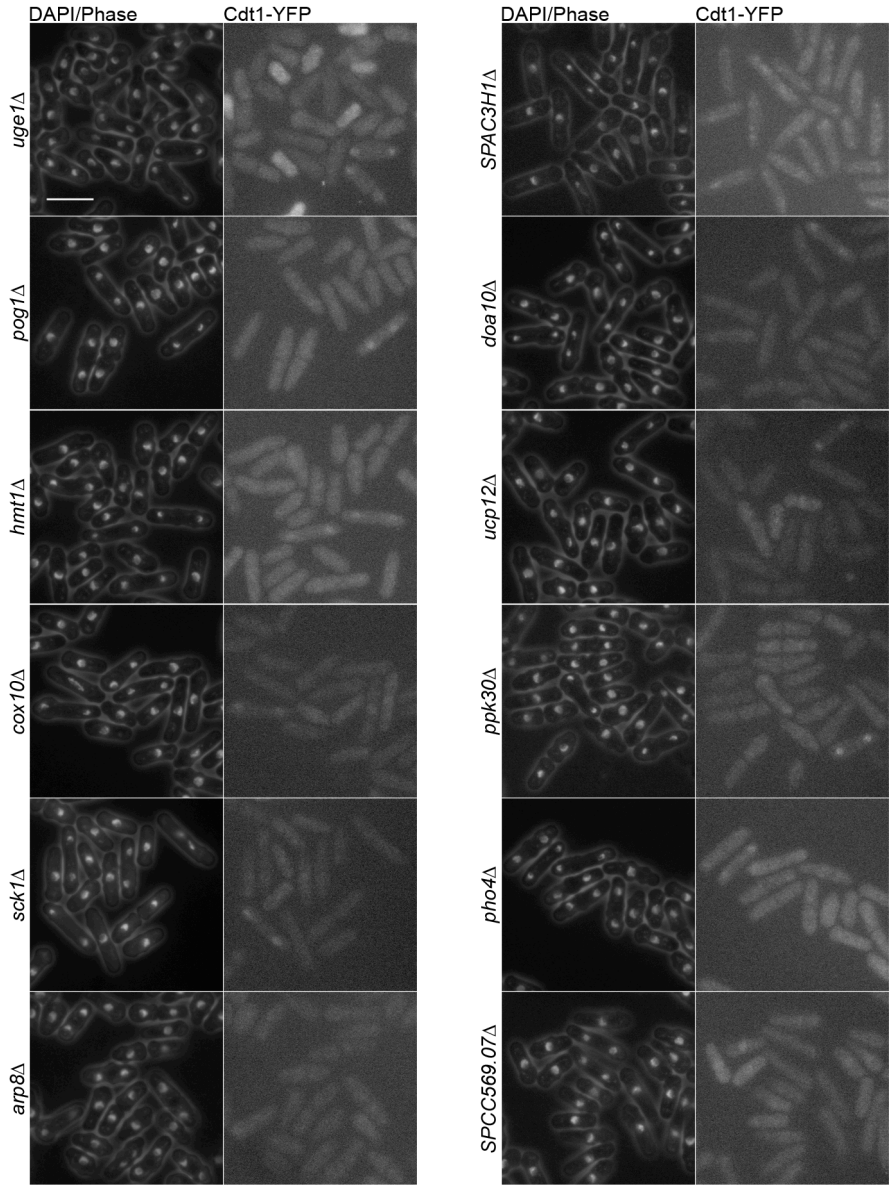
    %dlmwrite([save_dir '/' out_stem '-nuclei.csv'], marker.means, '-append');
    %fid = fopen([save_dir '/' 'means.csv'], 'a');
    %fprintf(fid, '%s,%f\n', strrep(filename, ',', '-'), marker.mean);
    %fclose(fid);
end
```

APPENDIX V: FALSE POSITIVE CANDIDATE GENES

Candidate genes listed in Table 5.1 that exhibited wildtype levels and distributions of Cdt1-YFP when re-examined in liquid culture.




DAPI/Phase
Cdt1-YFP
SPAC24B11.08cΔ
SPAC30D11.02cΔ
rad1Δ
nif1Δ
SPAPB1A10.13Δ
alp14Δ
spn4Δ
DAPI/Phase
Cdt1-YFP
SPBC1271.05cΔ
pli1Δ
rad13Δ
mug117Δ
eft202Δ
SPCC594.04cΔ
mvp1Δ


DAPI/Phase
Cdt1-YFP
uge1Δ
pog1Δ
hmt1Δ
cox10Δ
sck1Δ
arp8Δ
DAPI/Phase
Cdt1-YFP
SPAC3H1Δ
doa10Δ
ucp12Δ
ppk30Δ
pho4Δ
SPCC569.07Δ